Integrated Design and Control with a Focus on Control Structures

By

Mahdi Sharifzadeh

A thesis submitted for the degree of Doctor of Philosophy (PhD)

and for Diploma of Imperial College (DIC)

April 2012

Centre for Process Systems Engineering (CPSE),

Department of Chemical Engineering,

Imperial College London

London SW7 2AZ

Abstract

The common practice is to design chemical processes and their control systems in sequence. However, process design and control share important decisions, and when the process design is fixed there is little room left to improve the control performance. These observations suggest process design and control should be integrated.

The conventional framework for integrated design and control is to optimize the process, its control structure, and controllers, simultaneously. However, there are numerical as well as conceptual complexities associated with optimization of controllers. This research proposes integrated design and control based on perfect control. In the proposed optimization framework, an *inversely controlled process model* replaces the models of process and its controllers. Although the process and its control structure are optimized simultaneously, the complexities associated with controllers are disentangled from the problem formulation.

The thesis starts with introduction of the relevant concepts and review of literature in Chapters 1 and 2. Then, in Chapter 3, the steady-state and dynamic formulations of the proposed framework are presented. A steady-state inversely controlled process model achieves a higher degree of complexity reduction and ensures regulatory steady-state operability. However, at the price of higher modelling efforts, a dynamic inversely controlled process model ensures functional controllability as well. The proposed steady-state and dynamic optimization frameworks are demonstrated using several case studies. The proposed steady-state framework was applied for optimal control structure selection of a distillation train in Chapter 4 and integrated design and control of a reactive distillation column in Chapter 5. The proposed dynamic optimization framework was applied for the case of two heat-integrated series reactors in Chapter 6. The proposed optimization frameworks were successful in establishing the trade-off between control and process objectives. Finally, the thesis concludes with discussions, critical evaluation of the research and suggestions for future research in Chapter 7.

Declaration of originality

The author declares that the present thesis reports the results of his own research and that all else is appropriately referenced. In addition, the presented materials are not submitted elsewhere for another degree.

Acknowledgement

Firstly, I would like to thank my advisor Professor Nina Thornhill for her kind academic advice and academic mentorship. Special thanks go to Professor Nilay Shah, my collaborating academic, for his kind supports and encouragements. In addition, I am grateful to my former advisors, Professor Davood Rashtchian and Dr. Mahmoud Reza Pishvaie for their academic advice and supports. During my PhD studies, I had the opportunities to attend several courses and lectures by Professor Stratos Pistikopoulos, Professor Constantinos Pantelides and other researchers at Centre for Process Systems Engineering (CPSE), for which I am thankful. Furthermore, I would like to thank the members of Centre for Process Systems Engineering (CPSE) and the Department of Chemical Engineering, Imperial College London, for their hospitality.

During my PhD studies, I had the opportunities to present and discuss my research with Professor John Perkins (BIS), Professor Ignacio Grossmann (Carnegie Mellon University), Professor Christos Georgakis (Tufts University) and Dr Richard Burkett (previously BP). I am grateful for their kind and motivating advice. I am also thankful to the members of Center for Advanced Process Decision-making (CAPD) at Carnegie Mellon University for providing the opportunities for me to attend several short courses in optimization and control.

I gratefully acknowledge partial financial supports from the 2010 and 2011 ISA Educational Foundation scholarships, the Burkett Scholarship and the Ure bursary award of the Department of Chemical Engineering, Imperial College London.

Finally and most importantly, I would like to thank my family for their love and supports all through my life. I am forever indebted to them...

Table of contents

Thesis title.. 1

Abstract.. 2

Table of contents.. 5

List of figures 12

List of snips... 17

List of panels.. 18

List of tables 19

Chapter 1 | Introduction 21

1.1. Introduction... 21

1.2. Introduction to the research.. 23

1.2.1. Basic concepts.. 23

1.2.2. Plant-wide versus unit-wise visions.. 25

1.2.3. Integrated design and control versus sequential design and control……....... 26

1.2.4. The conventional problem statement for integrated design and control.. 30

1.2.5. Integrated design and control based on perfect control................................ 33

1.2.6. Research aims and objectives... 37

1.2.7. Research novelty claims and contributions.. 37

1.3. Introduction to the thesis.. 39

1.3.1. Introduction to Chapter 2: Background and context..................................... 39

1.3.2. Introduction to Chapter 3: An optimization framework using an inversely controlled process model... 39

1.3.3. Introduction to Chapter 4: Optimal selection of control structures using a steady-state inversely controlled process model.. 40

1.3.4. Introduction to Chapter 5: Integrated design and control using a steady-state inversely controlled process model.. 40

1.3.5. Introduction to Chapter 6: Integrated design and control using a dynamic inversely controlled process model.. 40

1.3.6. Introduction to Chapter 7: Discussions and suggestions for future research.. 41

1.4. Conclusion…... 41

Chapter 2 | Background and context.. 43

2.1. Introduction.. 43

2.2. Incentives for integrated design and control... 44

2.3. Industrial perspective.. 45

2.4. Overview of research in the field.. 46

2.5. Modelling techniques... 49

2.5.1. Modelling from first principles.. 50

2.5.2. Linear models.. 51

2.5.3.Model reduction techniques... 52

2.5.4. The importance of modelling from first principles.................................. 53

2.6. Process insights and heuristics: decomposition techniques for complexity reduction... 54

2.6.1. Complexity reduction based on process components: a unit-wise approach... 55

2.6.2. Complexity reduction based on temporal decomposition............................ 56

2.6.3. Complexity reduction based on prioritization of control objectives............ 56

2.6.4. Complexity reduction based on the production rate and the inventory control systems.. 58

2.6.5. Complexity reduction based on causality analysis...................................... 60

2.7. Control design: controllers... 61

2.7.1. Degree of decentralization: spatial.. 62

2.7.2. Degree of decentralization: temporal.. 64

2.7.3. Conventional multi-loop controllers.. 66

2.7.4. Model predictive controllers.. 66

2.8. Control design: control structures.. 68

2.8.1. Control structure reconfiguration.. 68

2.8.2. Degree of freedom analysis... 70

2.8.3. Manipulated variables (MVs) 72

2.8.4. Controlled variables (CVs) 73

2.8.4.1. Conventional methods for selection of controlled variables............ 74

2.8.4.2. Setpoint policy.. 75

2.8.4.2.1. Static setpoint policy... 76

2.8.4.2.2. Dynamic setpoint policy.. 79

2.9. Controllability measures.. 80

2.9.1. Flexibility, operability, switchability and controllability............................. 80

2.9.2. Causes of control imperfection... 83

2.9.2.1. Interactions between control loops.. 83
2.9.2.2. Manipulated variable constraints and the effects of disturbances.. 84
2.9.2.3. Delays, right-half-plane zero, and non-minimum-phase behaviour.. 85
2.9.2.4. Model uncertainties.. 86
2.9.2.5. Multi-objective optimization methods based on controllability measures.. 86
2.10. Methods based on passivity/dissipativity... 87
2.11. Multi-objective optimization methods to incorporate controllability measures into the process design... 88
2.12. Methods based on model reduction and robust control measures........................... 89
2.13. Methods based on analysing nonlinear behaviour of chemical processes............... 91
2.14. Geometric operability analysis... 93
2.15. Steady-state and dynamic flexibility optimization.. 96
2.16. Economic optimization based on minimization of the economic losses associated with back-off from active constraints.. 100
2.17. Simultaneous optimization of a process and its controllers............................ 101
2.18. Mathematical optimization 104
2.18.1. MINLP solution algorithms.. 104
2.18.2. Dynamic optimization.. 107
2.18.3. Global optimization... 108
2.18.4. Optimization with implicit constraints: Simulation-optimization programming.. 111
2.18.6. Multi-criteria decision-making.. 112
2.19. Conclusion…... 115
Chapter 3 | An optimization framework using an inversely controlled process model.. 118
3.1. Introduction.. 118
3.2. Mathematical formulation of conventional integrated design and control, Problem 1 120
3.3. Applying an inversely controlled process model for integrated design and control (proposed framework) 122
3.4. A steady-state inversely controlled process model for optimal selection of control structures... 125

3.5. A steady-state inversely controlled process model for integrated design and control........ 127
3.6. A dynamic inversely controlled process model for integrated design and control........ 128
3.7. Steady-state operability versus functional controllability........ 129
3.7.1. Regulatory steady-state operability........ 130
3.7.2. Functional controllability………........ 130
3.8. Conclusion........ 133

Chapter 4 | Optimal selection of control structures using a steady-state inversely controlled process model........ 134

4.1. Introduction........ 134
4.2. Multi-objective function and goal programming........ 135
4.3. Engineering insights and heuristics: dynamic degrees of freedom and design of inventory control systems........ 138
4.4. Case study: optimal control structure selection for a distillation train........ 139
4.4.1. Process description of pyrolysis gasoline hydrogenation (PGH) plant........ 139
4.4.2. Optimization variables........ 140
4.4.3. Optimization constraints........ 141
4.4.3.1. Constraints regarding the available degrees of freedom and the implications of inventory control systems........ 141
4.4.3.2. Constraints regarding inferential temperature control........ 143
4.4.3.3. Constraints regarding disturbance scenarios........ 143
4.4.3.4. Instances of goal programming objective function........ 145
4.5. Implementation software tools 148
4.5.1. Simulation-optimization programming 148
4.5.2. Constructing a steady-state inversely controlled process model........ 149
4.5.3. Simulation-optimization information flow........ 150
4.6. Results of the case study........ 151
4.7. Discussions........ 159
4.7.1. Optimized control structure versus base case........ 159
4.7.2. Sensitivity analyses........ 161
4.7.2.1. Sensitivity analyses with respect to the 5% disturbance scenarios........ 161
4.7.2.2. Sensitivity analyses with respect to the 10% and 20% disturbance scenarios…........ 162
4.8. Conclusion........ 162

Chapter 5 | Integrated design and control using a steady-state inversely controlled process model 164

5.1. Introduction........ 164

5.2. Multi-objective function and goal programming........ 165

5.3. Engineering insights and heuristics: dynamic degrees of freedom and design of inventory control systems........ 167

5.4. Case study: Integrated design and control of an ETBE reactive distillation column........ 168

5.4.1. Process description........ 170

5.4.2. Optimization constraints........ 171

5.4.2.1. Available degrees of freedom and the implications of inventory control systems........ 171

5.4.2.2. Constraints regarding disturbance scenarios........ 172

5.4.2.3. Constraints regarding perfect control........ 173

5.4.2.4. Constraints regarding first principles modelling........ 175

5.4.3. Optimization variables........ 176

5.4.4. Multi-objective function for integrated design and control of an ETBE reactive distillation column........ 178

5.5. Implementation software tools 181

5.6. Treatment of the convergence failure of the equation solver 183

5.7. Comparisons between modelling approaches based on kinetic correlations and the assumption of equilibrium reaction........ 185

5.8. Results of the case study........ 186

5.9. Discussions........ 193

5.9.1. Discussion of the optimization results........ 193

5.9.2. Discussion of Total Annual Profit (TAP) maximization........ 194

5.9.3. The results for the comparisons between modelling approaches based on the kinetic correlations and the assumption of chemical equilibrium........ 195

5.10. Conclusion........ 195

Chapter 6 | Integrated design and control using a dynamic inversely controlled process model 196

6.1. Introduction........ 196

6.2. Multi-objective function and weighting factors.. 197
6.3. Solution strategies for dynamic optimization... 198
6.3.1. Dynamic optimization based on the sequential integration strategy.............. 198
6.3.2. Dynamic optimization based on the full discretization strategy..................... 201
6.4. Case study for the conventional integrated design and control optimization framework.. 203
6.5. Application of the proposed integrated design and control framework using a dynamic inversely controlled process model.. 207
6.5.1. Amendments to the original case study... 207
6.5.2. Inversely controlled process model for the case of two series reactors......... 209
6.5.3. Feasibility constraints.. 210
6.5.4. Multi-objective function for integrated design and control of the two series reactors.. 212
6.5.5. Post-optimization analysis: Designing actual controller.............................. 215
6.6. Implementation tools and considerations.. 216
6.7. Results of the case study... 218
6.8. Discussions.. 224
6.8.1. The results of the proposed dynamic optimization framework...................... 224
6.8.2. Uncontrollable process structures.. 225
6.8.4. The implications of competing process and control objectives...................... 226
6.8.3. Discussions of post-optimization studies.. 227
6.11. Conclusion.. 228

Chapter 7 | Summary, discussions and suggestions for future research.................... 230

7.1. Research summary... 231
7.2. Physical implications of an inversely controlled process model............................... 232
7.2.1. Index reduction.. 232
7.2.2. Limiting factors of controllability... 234
7.3. Critical evaluation of research.. 235
7.4. Suggestions for future research directions... 239
7.4.1. Detailed design of controllers with emphasize on the cases with limited controllability.. 239
7.4.2. Degree of centralization... 239
7.4.3. Inversely controlled process model within the context of self-optimizing control.. 240
7.4.4. Incorporating into commercial software tools.. 240

7.4.5. Developing surrogate inversely controlled process model from rigorous simulations.......... 241

Bibliography.......... 243

Appendix A. Fortran code (used in Chapter 5).......... 266

List of figures

Figure 1.1.a: The temperature control loop for a heat exchanger.................................... 24
Figure 1.1.b: The block diagram for the temperature control loop around heat exchanger shown in Figure 1.1.a. 24
Figure 1.2. Luyben's (1996) solution for the Tennessee Eastman problem. 25
Figure 1.3. The heat exchanger is used for heat recovery from the reactor effluent......... 26
Figure 1.4.a: A bypass stream is added to the reactant effluent stream 27
Figure 1.4.b: A bypass stream is added to the reactor feed stream 27
Figure 1.5.a. A heat exchanger is added on the reactor effluent stream and before the pre-heater 28
Figure 1.5.b. A heat exchanger is added on the reactor effluent stream and after the pre-heater... 28
Figure 1.5.c. A heat exchanger is added on the reactor feed stream and after the pre-heater... 28
Figure 1.5.d. A heat exchanger is added on the reactor feed stream and before the pre-heater... 28
Figure 1.6. The key problems and sub-problem involved in the conventional integrated design and control.. 33
Figure 1.7. The key problems and sub-problem involved in the proposed integrated design and control.. 36
Figure 2.1. Overview of research in the field.. 47
Figure 2.2. The inflows are used for design of the inventory control systems on the upstream of the throughput manipulation point. However, the outflows are used on the downstream of this point.. 59
Figure 2.3. Ethylene glycol flowsheet: (1) Feed tank, (2) preheater, (3) reactor, (4) evaporator, (5) light end columns, (6) mono ethylene glycol column, (7) higher glycol recovery, (Rawlings and Stewart 2008). 63
Figure 2.4. Hierarchy of conventional multi-loop and MPC structures are shown at the left and right respectively. (adapted from Qin and Badgwell 2003)............. 65
Figure 2.5. Automation pyramid (adapted from Harjunkoski et al. 2009) 65
Figure 2.6. The block diagram representation of an MPC system: estimator, target calculator, regulator, (Rawlings 2000)... 67
Figure 2.7. Different configurations of a control structure, (Froisy 1994)........................ 69

Figure 2.8. Setpoint policies; the methods for static and dynamic setpoint policies are shown by the red envelopes. The other classification is according to optimality and feasibility criteria, shown by the grey envelopes, (Chachuat, et al. 2009) 76

Figure 2.9. Maintaining the setpoints at constant values results in economic loss (distance between the re-optimized curve and the actual curve) due to a disturbance. However, the associated costs strongly depend on the selected controlled variable. (Skogestad 2000b).......... 77

Figure 2.10. The algorithm for flexibility optimization, adapted from (Sakizlis, et al 2004).......... 99

Figure 2.11. Optimal steady-state and dynamic economic solutions adapted from Kookos and Perkins (2004).......... 101

Figure 2.12. Different MINLP algorithms represented as a combination of NLP and M-MILP subproblems, (adapted from Grossmann 2002) 105

Figure 2.13. The concept of constructing the convex under-estimator for a non-convex function, adapted from Grossmann and Biegler (2004) 111

Figure 2.14. The feasible region and Pareto front for a bi-objective optimization problem.......... 113

Figure 2.15. Goal programming; a) correct choices of the target levels, b) unbalanced, sub-optimal solution due to incorrect choices of the target levels.......... 114

Figure 3.1. The conventional optimization framework for integrated design and control of chemical processes. 121

Figure 3.2. The proposed optimization framework for integrated design and control using an inversely controlled process model.......... 124

Figure 3.3. The proposed optimization framework for optimal selection of control structures using a steady-state inversely controlled process model.......... 126

Figure 3.4. The proposed optimization framework for integrated design and control using a steady-state inversely controlled process model.......... 128

Figure 4.1. PGH plant; the framed part of the flowsheet is selected for the case study.......... 139

Figure 4.2a. The temperature profiles of the depentanizer column for the base case design.......... 147

Figure 4.2b. The temperature profiles of the dehexanizer column for the base case design.......... 147

Figure 4.2c. The temperature profiles of rerun the column for the base case design.......... 147

Figure 4.3. The base-case control structure.......... 148

Figure 4.4. Information flow of the simulation-optimization programming. 150

Figure 4.5. The selected controlled variables using the proposed optimization framework (dotted circles), and the inventory controlled variables (solid squares) 154
Figure 4.6. The control structure for the distillation train of the PGH process (Tray-numbering is bottom-up) 154
Figure 4.7a. The temperature profiles of depentanizer column for the base-case control structure.. 155
Figure 4.7b. The temperature profiles of dehexanizer column for the base-case control structure.. 155
Figure 4.7c. The temperature profiles of rerun column for the base-case control structure.. 155
Figure 4.8a. The temperature profiles of depentanizer column for 5% disturbances.. 156
Figure 4.8b. The temperature profiles of dehexanizer column for 5% disturbances.. 156
Figure 4.8c. The temperature profiles of rerun column for 5% disturbances.. 156
Figure 4.9a. The temperature profiles of depentanizer column for 10% disturbances.. 157
Figure 4.9b. The temperature profiles of dehexanizer column for 10% disturbances.. 157
Figure 4.9c. The temperature profiles of rerun column for 10% disturbances.. 157
Figure 4.10a. The temperature profiles of depentanizer column for 20% disturbances.. 158
Figure 4.10b. The temperature profiles of dehexanizer column for 20% disturbances.. 158
Figure 4.10c. The temperature profiles of rerun column for 20% disturbances.. 158
Figure 5.1. Process flow diagram of ETBE reactive distillation column. 171
Figure 5.2. The manipulated variables in an ETBE reactive distillation shown by control valves.. 171
Figure 5.3. Information flow of the simulation-optimization programming. 181
Figure 5.4. Optimized process and control structures of the ETBE reactive distillation column.. 189

Figure 5.5a. Temperature profiles of the ETBE reactive distillation column for nine disturbance scenarios.. 190
Figure 5.5b. ETBE composition profiles of the ETBE reactive distillation column for nine disturbance scenarios.. 190
Figure 5.5c. Ethanol composition profiles of the ETBE reactive distillation column for nine disturbance scenarios.. 190
Figure 5.5d. Isobutene composition profiles of the ETBE reactive distillation column for nine disturbance scenarios... 190
Figure 5.5e. N-butene composition profiles of the ETBE reactive distillation column for nine disturbance scenarios. 190
Figure 5.6a. Temperature profiles of the ETBE reactive distillation column for nine disturbance scenarios. This figure is the result of TAP maximization.......... 191
Figure 5.6b. ETBE composition profiles of the ETBE reactive distillation column for nine disturbance scenarios. This figure is the result of TAP maximization... 191
Figure 5.6c. Ethanol composition profiles of the ETBE reactive distillation column for nine disturbance scenarios. This figure is the result of TAP maximization... 191
Figure 5.6d. Isobutene composition profiles of the ETBE reactive distillation column for nine disturbance scenarios. This figure is the result of TAP maximization... 191
Figure 5.6e. N-butene composition profiles of the ETBE reactive distillation column for nine disturbance scenarios. This figure is the result of TAP maximization... 191
Figure 5.7a. The temperature profiles calculated based on the kinetic correlations (blue circles) and the equilibrium reaction assumption (red squares)…................. 192
Figure 5.7b. The composition profiles of ETBE calculated based on the kinetic correlations (blue circles) and the equilibrium reaction assumption (red squares).. 192
Figure 5.7c. The composition profiles of ethanol calculated based on the kinetic correlations (blue circles) and the equilibrium reaction assumption (red squares)…... 192
Figure 5.7d. The composition profiles of isobutene calculated based on the kinetic correlations (blue circles) and the equilibrium reaction assumption (red squares).. 192
Figure 5.7e. The composition profiles of n-butene calculated based on the kinetic correlations (blue circles) and the equilibrium reaction assumption (red squares)…... 192

Figure 6.1. The sequential solution strategy for integrated design and control framework.. 200

Figures 6.2. Different process structures: a) co-current heat exchange b) counter-current heat exchange 203

Figure 6.3. The variations of the controlled variable (T_2) with the manipulated variable (Q_c) 211

Figure 6.4. The time trajectories of the flow rate of the cooling water as the manipulated variable (Q_c) for two identical disturbances with reverse directions. The lower trajectory is infeasible... 211

Figures 6.5. Results for the best solution (Structure 6 in Table 6.5) based on perfect control. The time trajectories of a) the feed temperature as the manipulated variable, b) the temperature of the first reactor as the controlled variable (overlaid on each other), c) the composition in the second reactor. Disturbance scenarios were described in Section 6.5.1................................ 222

Figures 6.6. The variations of the temperature of the first reactor with the flow rate of the cooling water, for a) the co-current structure, b) the counter-current structure... 222

Figure 6.7. The Pareto front for the multi-objective function (6-23) based on the results in Table 6.6.. 223

Figure 6.8. The variations of the composition of the second reactor with the feed temperature for the co-current structure... 223

Figures. 6.9. Results of the first set of post-optimization studies. Trajectories of a) the feed temperature as the manipulated variable, b) the temperature of the first reactor as the controlled variable, c) the composition in the second reactor, for the best solution (Structure 6 in Table 6.5) using an optimized PI controller. Disturbances scenarios are described in Section 6.5.1................. 223

Figures. 6.10. Results of post-optimization analyses. Trajectories of a) the feed temperature as the manipulated variable, b) the temperature of the first reactor as the controlled variable, c) the composition in the second reactor, using an optimized PI controller. The disturbances are step functions from $C_f = 0.6$ to 0.55 (dotted line) and $C_f = 0.6$ to 0.65 (solid line) corresponding to case 5 and case 6 of (Flores-Tlacuahuac and Biegler 2007) respectively.. 223

List of snips

Snip 2.1.1. Research in the field: Decomposition techniques for complexity reduction (Figure 2.1 revisited)........ 54

Snip 2.1.2. Research in the field: Controllers (Figure 2.1 revisited)........ 61

Snip 2.1.3. Research in the field: Control structures (Figure 2.1 revisited)........ 67

Snip 2.1.4. Research in the field: Controllability measures (Figure 2.1 revisited)........ 80

Snip 2.1.5. Research in the field: Methods based on passivity/dissipativity (Figure 2.1 revisited)........ 87

Snip 2.1.6. Research in the field: Multi-objective optimization to incorporate controllability measures into the process design (Figure 2.1 revisited)........ 89

Snip 2.1.7. Research in the field: Methods based on model reduction and robust control measures (Figure 2.1 revisited). 90

Snip 2.1.8. Research in the field: Methods based on analysing nonlinear behaviour of chemical processes (Figure 2.1 revisited)........ 91

Snip 2.1.9. Research in the field: Geometric operability analysis (Figure 2.1 revisited)........ 93

Snip 2.1.10. Research in the field: Steady-state and dynamic flexibility optimization (Figure 2.1 revisited)........ 96

Snip 2.1.11. Research in the field: Minimization of the economic losses associated with back-off from active constraints (Figure 2.1 revisited). 100

Snip 2.1.12. Research in the field: Simultaneous optimization of the process and its controllers (Figure 2.1 revisited)........ 101

List of panels

Panel 7.1. The problem statement the research aims and objectives (from Chapter 1) and the proposed framework for integrated design and control (from Chapter 3) 236

List of tables

Table 4.1. Objective functions for steady-state control structure selection 135

Table 4.2. List of the optimization variables for the PGH case study. 141

Table 4.3. Feed composition.. 144

Table 4.4. The target values for the quality of products. 146

Table 4.5. The nominal values of the manipulated variables, i.e., the targets for the second objective of Table 4.1... 146

Table 4.6. Economic data for calculating the fourth objective of Table 4.1........................ 146

Table 4.7. The average of optimal values of the objective functions................................ 152

Table 4.8. The control structures selected for the three distillation columns, as the results of optimizations and sensitivity analyses... 153

Table 5.1. Objective functions for steady-state integrated design and control................... 165

Table 5.2. Disturbance scenarios: $\pm10\%$ changes in molar fractions of isobutene and n-butene 173

Table 5.3. Candidate controlled and manipulated variables for the ETBE reactive distillation according to equations (5-6a, b)... 175

Table 5.4. Optimization variables; $\alpha_{1,s}$ represents the ratio $F_s^{bottom}/F_s^{Ethanol-Feed}$ for disturbance scenario s. $\alpha_{2,s}$ represents the ratio $F_s^{Ethanol-feed}/F_s^{isobutene-Feed}$ for disturbance scenario s.. 177

Table 5.5.Economic data for calculating Total Annual Profit (Equation 7a-c).................. 180

Table 5.6. The value of objective functions.. 186

Table 5.7. Optimal values of the optimization variables using the proposed optimization framework.. 187

Table 5.8. Optimal values of the optimization variables for the optimization of TOTAL Annual Profit (TAP) discussed in Section 5.4.4............................... 188

Table 6.1. Comparison of the characteristics of two solution strategies for dynamic optimization.. 202

Table 6.2 The parameters and the values of the variables at the base case scenario…..... 206

Table 6.3 The correspondence of the two solution strategies with case study formulation.. 208

Table 6.4 The correspondence of the two solution strategies with case study formulation.. 210

Table 6.5. The results of optimization for different process and control structures using the sequential integration strategy.. 219

Table 6.6. The results of optimization for different weighting factors (w'_1, w'_2) in the multi-objective function using the full discretization strategy......................... 220

Table 6.7. The results of optimization for different process and control structures enumerated by full discretization strategy.. 221

Table 6.8. The results of the first set of post-optimization studies: designing a PI controller for the best structures of Table 6.5.. 221

Table 6.9. The results of the second set of post-optimization studies: designing a PI controller for the best solution and comparison with the results of Flores-Tlacuahuac and Biegler (2007) 222

1 | Introduction

1.1. Introduction

The title of this thesis is *Integrated Design and Control with a Focus on Control Structures*. The purpose of this chapter is to introduce the topic of research and to explain why it is important. This chapter will also introduce the thesis and the organization of the presented materials.

The current industrial practice for design of chemical processes and their control systems is sequential in that control design is deferred until process is designed (Sakizlis, et al. 2010, Downs and Skogestad 2011). However, design of a process and design of its control system share important decisions. When the process design is fixed, there are limited opportunities left to improve the control performance. Furthermore, there are conflicts and competitions between control and process objectives, (Luyben 2004). Therefore, many researchers (e.g., Luyben 2004; Sakizlis, et al. 2004; Seferlis and Georgiadis 2004; Klatt and Marquardt 2008) have suggested that design and control should be integrated.

The integrated design and control is also known as *simultaneous process and control design* or *co-design*. In integrated design and control, the structural and parametric decisions regarding process and its control system are decided simultaneously, leading to economic benefits and improvements in the control performance.

This chapter is organized as follows. The subsequent sections will introduce the PhD research title, *Integrated Design and Control with a Focus on Control Structures* in more detail and will justify the research directions. The discussions start with introducing the basic concepts. Then, there is a discussion about whether the unit-wise vision is sufficient or a plant-wide approach is needed. The necessities for integrated design and control are explained, and the important properties of the problem are concluded. The statements of the key problems and sub-problems involved in integrated design and control are presented and the complexities associated with optimization of controllers are explained. These discussions enable proposing a new framework for integrated design and control which will be formulated and demonstrated in the next chapters. This chapter also presents the research aims and objectives and explains the research contributions. Finally, this chapter introduces the thesis organization. The aim is to explain links between the research objectives and the layout of the thesis.

1.2. Introduction to the research

The subsequent subsections introduce the research and justify its direction. The aim is to provide an overview of the research, its motivations and contributions.

1.2.1. Basic concepts

Generally, a typical chemical plant includes thousands of process variables. The aim of *plant-wide control structure selection* is to select manipulated variables and controlled variables from all candidate process variables. Then, controllers are designed, which close the loop between these variables. *Manipulated variables* (MV) are employed by controllers for inserting the control action into the process. The examples of manipulated variables are the flows of process or utility fluids at a rate determined by the opening of a control valve, or electrical power supply empowering and adjusting the speed of rotors or connecting /disconnecting switches. *Controlled variables* (CV) are those variables, which are fed back to inform controllers of the state of the process. They may be directly measurable or may need to be inferred from other measured variables. Examples of controlled variables are flowrates, temperatures, pressures, and compositions of process streams. The desired value of a controlled variable is called *setpoint*. In the control community, manipulated variables and controlled variables are sometimes called *input* and *output* variables respectively and process variables other than inputs and outputs are called *state variables*. This terminology is originally from state-space presentation of systems.

Figure 1.1.a shows a heat exchanger and its control loop. The aim is to control the temperature of the hot process stream (i.e., the controlled variable) using the cooling medium (i.e., the manipulated variable). The temperature of the hot stream is measured and fed back to the controller. Based on a comparison between the actual and the desired values of the controlled variable, the controller actuates the control valve by changing its opening. The control algorithm might be a proportional plus integral control law, implemented in the process control computer. The block diagram representation of this single control loop is shown in Figure 1.1.b.

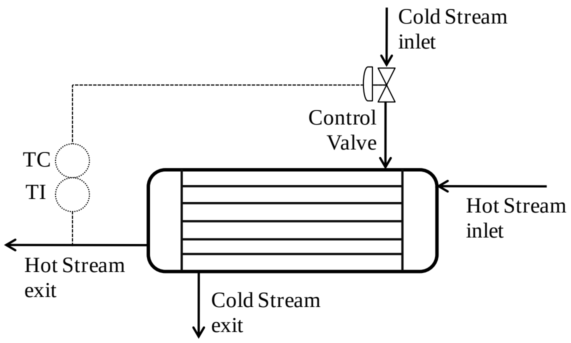

Figure 1.1.a: The temperature control loop for a heat exchanger.

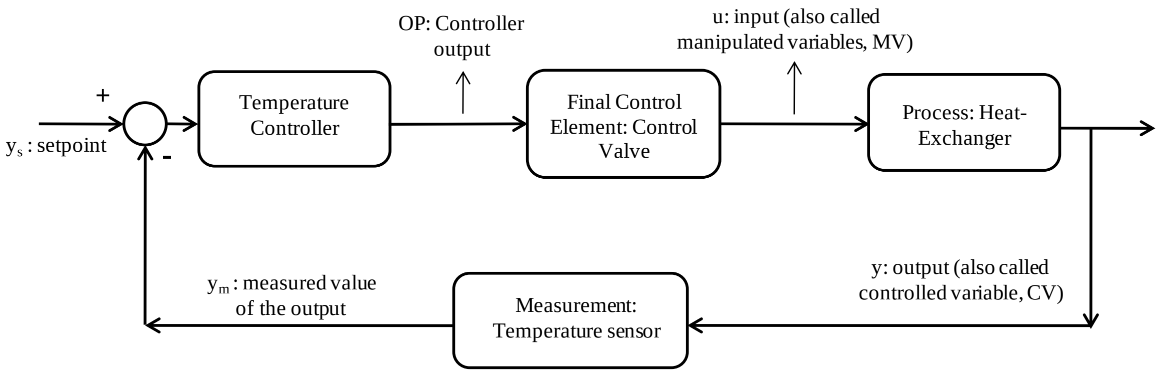

Figure 1.1.b: The block diagram for the temperature control loop around heat exchanger shown in Figure 1.1.a.

As another example, the red envelope in Figure 1.2 shows a condenser, a separator, and a control loop. This figure shows a benchmark problem (Tennessee-Eastman by Downs, and Vogel, 1993) that also has been worked by many other researchers (e.g., Luyben 1996). The letters LC indicate that the control loop is a level controller. In this control structure, the flow of the cooling medium to the condenser is being manipulated in order to control the level of the separator. As the condensation rate changes, the amount of the liquid entering the vessel will change, which in turn, will affect the level of the liquid hold-up. An alternative strategy is to control the liquid level using the flow of the outlet stream of the separator and to use the condensation rate for another purpose (e.g. controlling the pressure of the gaseous recycle loop).

The rationale behind a control structure is called *control strategy* or *control philosophy*. It is the strategy that is adapted to control several items of process equipment together. For example, shown in the blue envelope in Figure 1.2, the throughput is being controlled using the product flow at the bottom of the stripper. The reasoning for this strategy is that minimizing the variations of this flow is critical for operation of the downstream processes.

The typical objectives of a control structure are (i) maintaining optimal operation (ii) meeting the constraints of equipment, (iii) regulating and stabilizing the disturbed conditions, and (iv) tracking the changes of the setpoints.

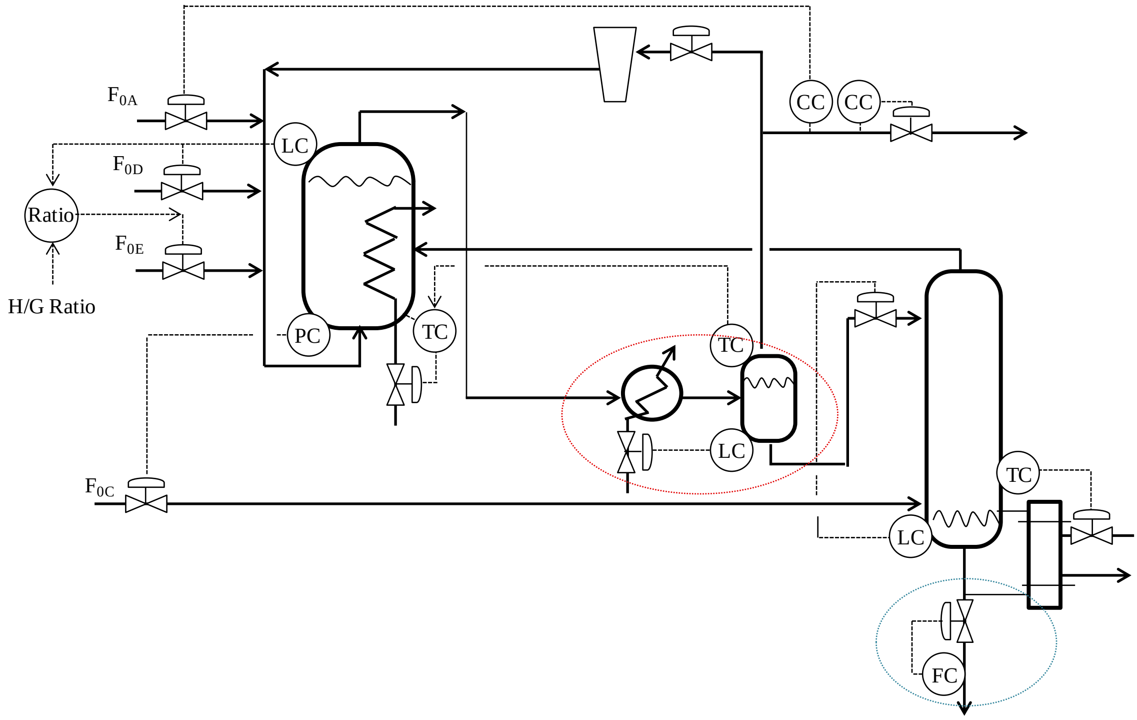

Figure 1.2. Luyben's (1996) solution for the Tennessee Eastman problem.

1.2.2. Plant-wide versus unit-wise visions

The design of a process and its control system can be considered either plant-wide or unit-wise. The implications of these two approaches are profound, for example:

- The superposition of individual process units and control loops does not necessarily form a consistent and unified process and control system.
- The optimality of the designs for individual unit operations does not ensure the optimal plant-wide design.
- In general, individual process units and their control loops are not independent and interact with each other through mass and energy flows, and control signals. For example, the interaction between individual control loops can be quantified using relative gain arrays (RGAs), as will be discussed in Chapter 2.

The motivating example below demonstrates how the control structure of an individual unit operation may be inappropriate in the context of plant-wide control.

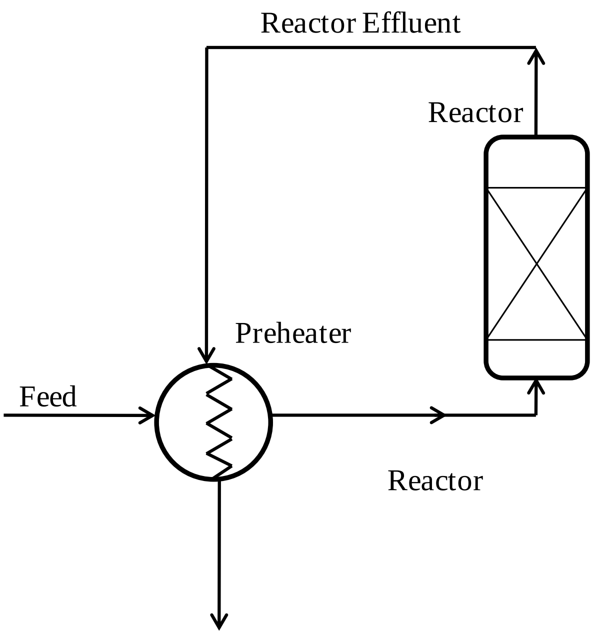

Figure 1.3. The heat exchanger is used for heat recovery from the reactor effluent.

Figures 1.1.a showed a heat exchanger as an individual unit operation. There is one manipulated variable that can be adjusted independently. Figure 1.3 shows the same heat exchanger in a process. It is a common practice to use a heat exchanger for energy recovery from the reactor effluent. The heat exchanger preheats the reactor feed by bringing it into contact with the reactor effluent. However, in the new energy-efficient scheme (assuming the feed as a disturbance) there is no independent manipulated variable because the flows of the hot stream and the cold stream are the same at the steady state, and this structure is not controllable. In the next section, this example is used for explaining interdependency of process design and control design.

1.2.3. Integrated design and control versus sequential design and control

The current industrial practice is to firstly design a process, and then design a control system for that process, which suggests a *sequential* strategy. However, design of a process and design of its control system share important decisions. This section employs the example of Figure 1.3 to illustrate the interactions between process design and control. As discussed earlier, the heat-integrated reactor, shown in Figure 1.3, is rendered uncontrollable. There are two options to resolve the uncontrollability issue. A bypass stream (Figures 1.4.a, b) can partially resolve the loss of controllability. However, if a stronger control action is needed, an auxiliary heat exchanger should be embedded in the flowsheet, as shown in Figures 1.5.a, b, c, d.

In addition to selection between a bypass stream and an auxiliary heat exchanger, there are still other structural decisions to be made. The new manipulated variable (shown by a control valve in Figures 1.4 and 1.5) could be used to control a controlled variable. There are four and five candidate controlled variables for the structures with the bypass and the auxiliary heat exchanger respectively. They are shown using temperature indicators (TIs) in Figures 1.4 and 1.5. Depending on the philosophy of the control, the designer may have preferences for each alternative process and control structure. If the suppression of undesirable reactions is the main challenge, the designer may choose to control the temperature of the reactor effluent and prefer the structures in which the control action is directly inserted to this stream (Figures 1.4.a and 1.5.a, b). However, if maintaining the reactor temperature is an active constraint, the designer may decide to control this variable and select those structures in which the control action is directly inserted to the reactor feed (Figures 1.4.b and 1.5.c, d). Depending on the temperature of the available utility resources, the designer may locate the new heat exchanger before or after the pre-heater in order to minimize the energy requirements. This is because the temperature difference between the heat-exchanging streams is a design variable and affect the required heat transfer area. If the new control action is not sufficient or if there are several constraints and criteria needed to be satisfied simultaneously, then the designer may choose to combine these structures.

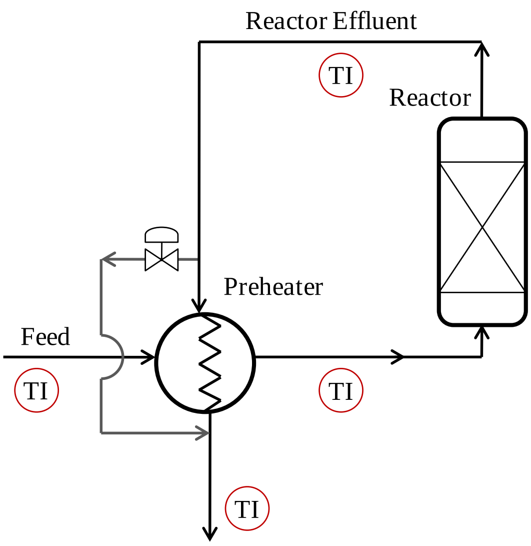

Figure 1.4.a: A bypass stream is added to the reactant effluent stream

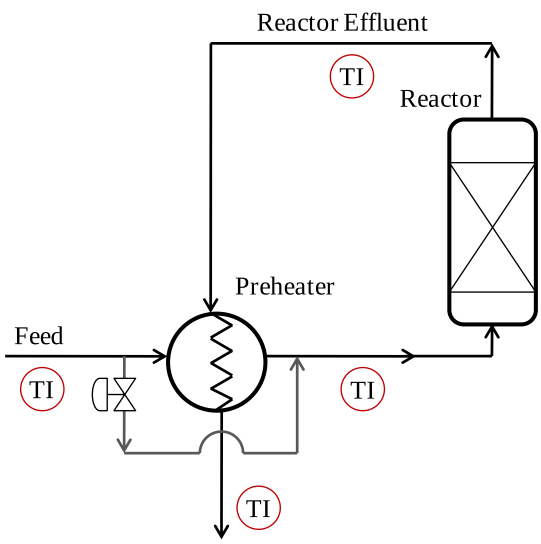

Figure 1.4.b: A bypass stream is added to the reactor feed stream

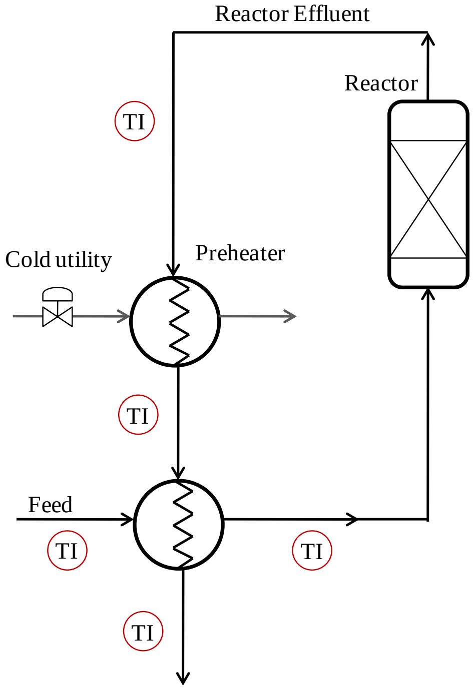

Figure 1.5.a. A heat exchanger is added on the reactor effluent stream and before the pre-heater

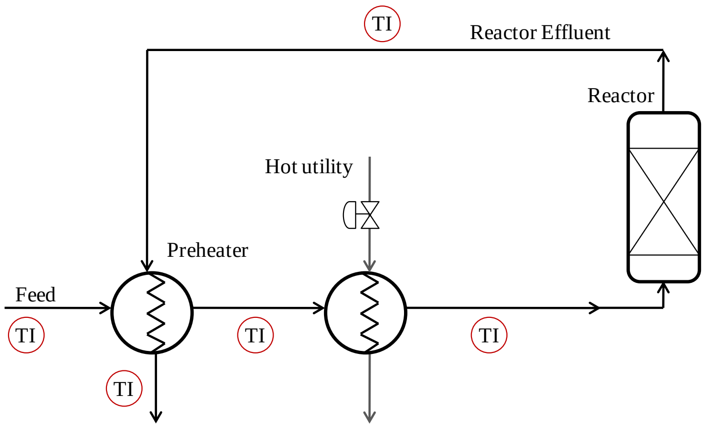

Figure 1.5.c. A heat exchanger is added on the reactor feed stream and after the pre-heater

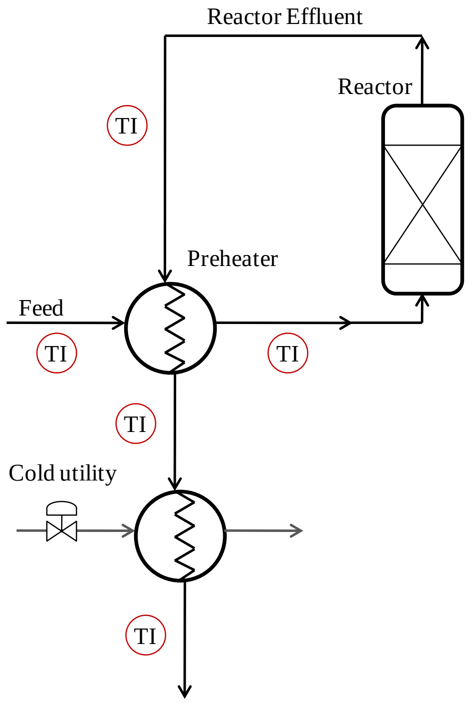

Figure 1.5.b. A heat exchanger is added on the reactor effluent stream and after the pre-heater

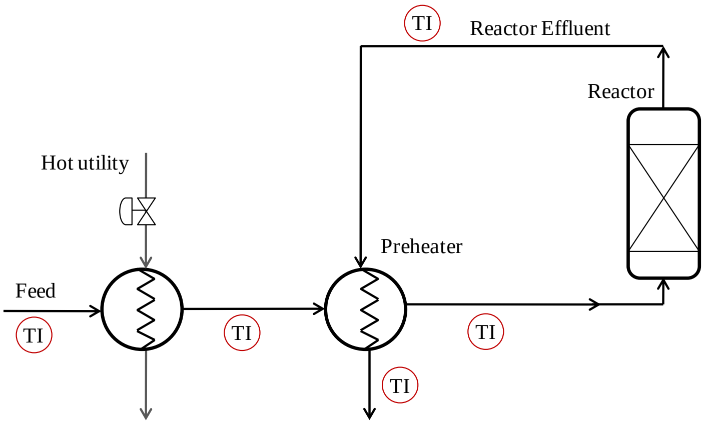

Figure 1.5.d. A heat exchanger is added on the reactor feed stream and before the pre-heater

In addition to the structural decisions described above, capturing the effects of parametric decisions on the economic and control performances is challenging. The value of bypass flowrate (i.e., split ratio) depends on the heat exchange area in the pre-heater and the expected range of the variations in the feed flowrate. In addition, the designer need to decide whether the auxiliary heat exchanger will be used during normal (steady-state) operations or its application is limited to transient and disturbed conditions. This decision influences the sizes of both the pre-heater and the auxiliary heat exchanger. Furthermore, different phenomena in the process may behave at different temporal and spatial scales. For instance, the reactions may act at very different time scales than material inventories. Failure to consider these interactions may result in economic losses, as well as safety concerns (e.g., runaway reactions).

In summary, several interesting conclusions can be derived from the above motivating example:

- Design and control of a chemical process share important structural and parametric decisions. A systematic framework is needed in order to establish a trade-off between the process and control objectives.
- The problem features combinatorial characteristics, i.e., the number of alternative solutions increases with the size of the process and becomes intractable. A systematic framework is needed in order to generate alternative designs and screen them.
- In many cases, the structural and parametric decisions are highly interdependent.
- The involved problems have multi-scale nature.

Further complications arise from the implementation issues and the directions of developments in process and control technologies:

- Increase in energy prices, incentives for waste minimization and safety concerns encourage process integration and reduction of in-plant inventories. However, the new processes are difficult to control and vulnerable to disturbances. This is because in such processes, disturbances propagate in several paths and smaller inventories are less likely to tolerate disturbing conditions.

- The development of control systems is encouraged by industry, demanding for simplicity and conceivability of the process design and operation procedures. However, in practice new control technologies feature more complexities. Any future development should be toward conceptual and numerical complexity reductions.

The next section represents the above problem in a more systematic way, by investigating the involved subproblems and their interrelations, with some hints about the direction of research in the present thesis.

1.2.4. The conventional problem statement for integrated design and control

In this section firstly, the conventional problem statement for integrated design and control is presented. This problem includes other sub-problems namely process design, control structure selection, controllability analysis, and controller design, which are also explained in this section. The phrase *conventional integrated design and control* is used because in the next section, a new problem statement will be presented in which for the sake of numerical and conceptual complexity reductions, controller design is separated from the conventional problem. It is notable that the presented problem statements are to some extent qualitative, and the mathematical notations are not presented in order to avoid unnecessary details. The mathematical formulations will be presented later in Chapter 3.

Problem 1: Integrated design and control (conventional)

Given the specifications of the feedstocks and the products, the desired throughputs and the expected disturbance scenarios, design a process, its control structure and the controllers, which are optimal with respect to the economic and control performance criteria and satisfy all the technical, safety and environmental constraints. Furthermore, ensure that the solution is controllable.

Problem 1 is the most general problem statement and implies that all the elements of the problem be addressed simultaneously. In practice, often Problem 1 is decomposed into Subproblems 1 to 4 below, and is solved in sequence. The statements of the subproblems within Problem 1 are as follows.

Subproblem 1: Process design

Given the specifications of the feedstocks and the products, in addition to the desired throughputs, it is intended to design a process which is optimal with respect to the economic criteria and satisfies all the technical, safety and environmental constraints.

Subproblem 2: Control structure selection

Given the detailed process design, the specifications of the feedstocks and the products, the desired throughputs and the expected disturbance scenarios, it is intended to select the manipulated variables, and the controlled variables, which are optimal with respect to the economic and control performance criteria, and satisfy all the technical, safety and environmental constraints.

Subproblem 3: Controllability analysis

Given the detailed process design, the specifications of the feedstocks and the products, the desired throughputs and the expected disturbance scenarios, the manipulated variables and the controlled variables, it is intended to evaluate whether it is possible at all to maintain the controlled variables at their setpoints by adjusting the manipulated variables and at the same time satisfy all the technical, safety and environmental constraints.

Subproblem 4: Controller design

Given the detailed process design, the specifications of the feedstocks and the products, the desired throughputs, the expected disturbance scenarios, the manipulated variables and the controlled variables, it is intended to decide the degree of centralization (and in the case of a decentralized control system, paring/partitioning between the manipulated and controlled variables), and to design the controllers (i.e., decisions about the control law and its parameters), which are optimal with respect to the economic and control performance criteria and satisfy all the technical, safety and environmental constraints.

Notice that the setpoints and nominal values of the manipulated variables are not within the design decisions of Subproblem 2, *Control structure selection*. This is because these variables are decided and fixed in Subproblem 1, *process design*. For instance, if a linear control valve is designed to pass the flowrate of F when it is 50% open, it is not possible to assign the nominal value of $2F$ to this valve because in that case it would saturate and would be fully opened, which means the loss of control action. Similarly, if the nominal flowrate of this control valve is set to a value corresponding to 25% opening, then the capability of this control valve for addressing the disturbances below its nominal value is halved. Similar argument can be made for controlled variables. The setpoints of controlled variables are constrained by their corresponding physical systems. For instance, the temperature of a reboiler is constrained to the physical properties of the boiling fluid, physical dimension of the reboiler, and even more importantly to the heating media. Therefore, if its setpoint is designed to be T , it is not possible to increase the temperature to $2T$. These observations suggest that the sequential approach in which the process design is fixed in advance may result in suboptimal solutions compared to the problem of integrated design and control in which the shared decision variables of these subproblems are decided simultaneously.

Nevertheless, the problem of control structure selection is an important industrial problem, because the number of old processes which are being re-engineered and new control structures are selected for them are even more than the new processes which are being built from scratch.

The sequential approach to address the above subproblems is unfortunate, because many important decisions are shared between Subproblems 1 to 4. For example as shown by aforementioned examples, when the process design is fixed, there are limited opportunities to improve the control performance and controllability. These observations suggest that process design and control should be integrated and Subproblem 1 to 4 must be addressed simultaneously, (as shown in Figure 1.6). However, there are several conceptual as well as numerical difficulties in the simultaneous approach, which are associated with Subproblem 4, i.e. design of controllers. The next section discusses the motivations for separating controller design (Subproblem 4) from the conventional integrated design and control (Problem 1) and proposes to solve a new integrated design and control problem, (Problem 2).

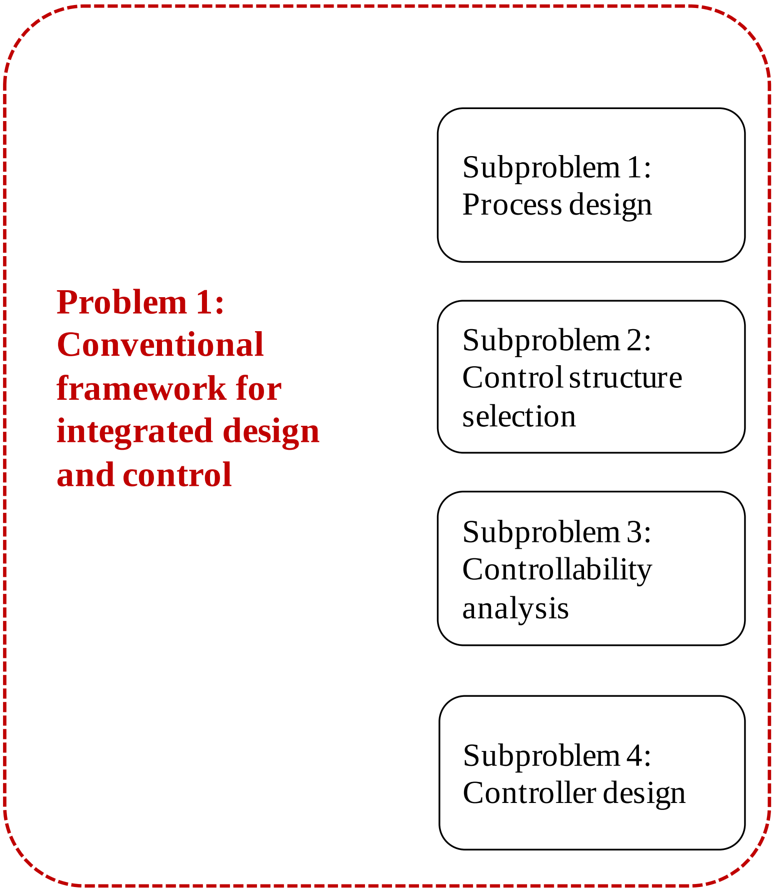

Figure 1.6. The key problems and subproblem involved in the conventional integrated design and control.

1.2.5. Integrated design and control based on perfect control

Unfortunately, the conventional integrated design and control problem (Problem 1) suffers from the curse of dimensionality, i.e. the combinations of alternative design decisions increases sharply with the size of the problem and becomes intractable. A part of this combinatorial characteristic should be attributed to the design of controllers (Subproblem 4). Design of controllers needs decisions on pairing/partitioning of manipulated and controlled variables (i.e. the degree of centralization), the type of controllers (e.g. feedback, feed-forward, or model-based), and the controller parameters.

In addition to the numerical complexity issues, there are other concerns about including controllers in the problem formulation. Morari (1983) was among the earliest researchers who recognised the challenging issues posed by the modelling of controllers in a dynamic simulation:

"*…It is generally necessary that controllers are included in the model. This often leads to arbitrary decisions about the control structure and also requires the engineer to tune these controllers interactively during the simulation, a very time consuming task. The modelled control systems are only those which are based on the experience (or ingenuity!) of the engineer doing the work. It is then impossible to distinguish if an observed poor performance is caused by some inherent plant characteristic or rather by the unfortunate choice of the control system by the engineer."*

The complexities associated with controllers have been the concerns of other researchers too. Perkins and his students introduced the idea of minimizing economic losses associated with back-off from active constraints, as a tool for selecting optimal control structures. The early versions of their methodology were based on frequency domain analysis and perfect control (Narraway and Perkins 1993; Heath, et al. 2000). Later, they extended their methodology by including a generalized formulation for the controllers. However, the proposed formulation was limited to linear time invariant output feedback controllers and did not include the majority of the important classes of nonlinear and model-based controllers, (Kookos and Perkins 2004).

Other researchers also encountered similar difficulties. For example, since static relative gain arrays (RGAs) do not consider dynamic information, dynamic relative gain arrays (DRGAs) were introduced. However, calculating the denominator of a dynamic relative gain array (DRGA) requires detailed design of controllers and *"since the DRGA is most valuable for screening alternate control system designs, the requirement of an extensive controller design tends to defeat the utility of these methods."*, (McAvoy, et al. 2003).

Furthermore, the design of controllers at the process design stage is of limited practicality. This is because there is no general agreement between researchers on the criteria for selection of the controller type. Some researchers (Luyben 2004; Skogestad 2009) emphasize simplicity and robustness of the conventional multi-loop control systems and criticize the reliability and costs of modern types. On the other side of this discussion, other researchers (Stephanopoulos, and Ng 2000; Rawlings and Stewart 2008) argue the economic advantages of model-based control systems and their systematic approach for handling constraint violations. In addition, they criticize the economic disadvantages of the constant-setpoint policy in decentralized control systems. Furthermore, in practice, advanced controllers (e.g. MPCs) are designed using commercial packages, often during process commissioning stages

(Sakizlis, et al. 2010; Qin and Badgwell 2003), which may not be available at the process design stages.

To cut through these arguments, this research proposes a new optimization framework for integrated design and control, based on perfect control. The implication of perfect control is that the best achievable control performance can be determined by the inverse solution of the process model, (Garcia and Morari1982; Morari and Zafiriou 1989; Yuan, et al. 2011), in which manipulated variables taking account of disturbances such that the controlled variables are precisely at their specified setpoints. This is a well-known concept that has resulted in development of a class of controllers which use the inverse of the process model as an internal element, (Skogestad and Postlethwaite 2005). Furthermore, based on this concept, a variety of controllability measures has been developed in order to quantify the causes of control imperfection, as discussed by Yuan, at al. (2011). However, no attempt has been made to incorporate the concept of perfect control into integrated design and control using first principles modelling. This research addresses this opportunity and proposes a methodology in which Subproblem 4 is removed from the formulation of Problem 1, but still the process and its control structure are optimized simultaneously and their controllability is ensured. Therefore, in this research, Problem 1 is distinguished as *conventional integrated design and control*, and a new problem statement is proposed:

Problem 2: Integrated design and control (proposed)

Given the specifications of the feedstocks and the products, the desired throughputs and the expected disturbance scenarios, it is intended to design a process, and its control structure, which are optimal with respect to the economic and control performance criteria and satisfy all the technical, safety and environmental constraints. Furthermore, ensure that the designed process and its control structure are controllable.

Figure 1.7 compares the two key problems, i.e., the conventional and proposed integrated design and control problems. While the conventional framework for integrated design and control (Problem 1) considers all Subproblems 1 to 4, simultaneously, in the proposed integrated design and control (Problem 2), the complexities associated with controllers are removed from the problem formulation and the design of controllers (Subproblem 4) is delegated to control practitioners.

The proposed framework for integrated design and control (Problem 2) makes no assumption about the controllers. However, it provides a benchmark for the best achievable control performance. It is left for the control engineer to devise practical controllers which most closely meets the benchmark performance, from the range of controller types available to him or her. Such a design philosophy is consistent with the current industrial practice developed over the last 20 years (Jelali 2006; Qin 1998) in which the fitness for the purpose of a control loop is assessed against the best achievable performance.

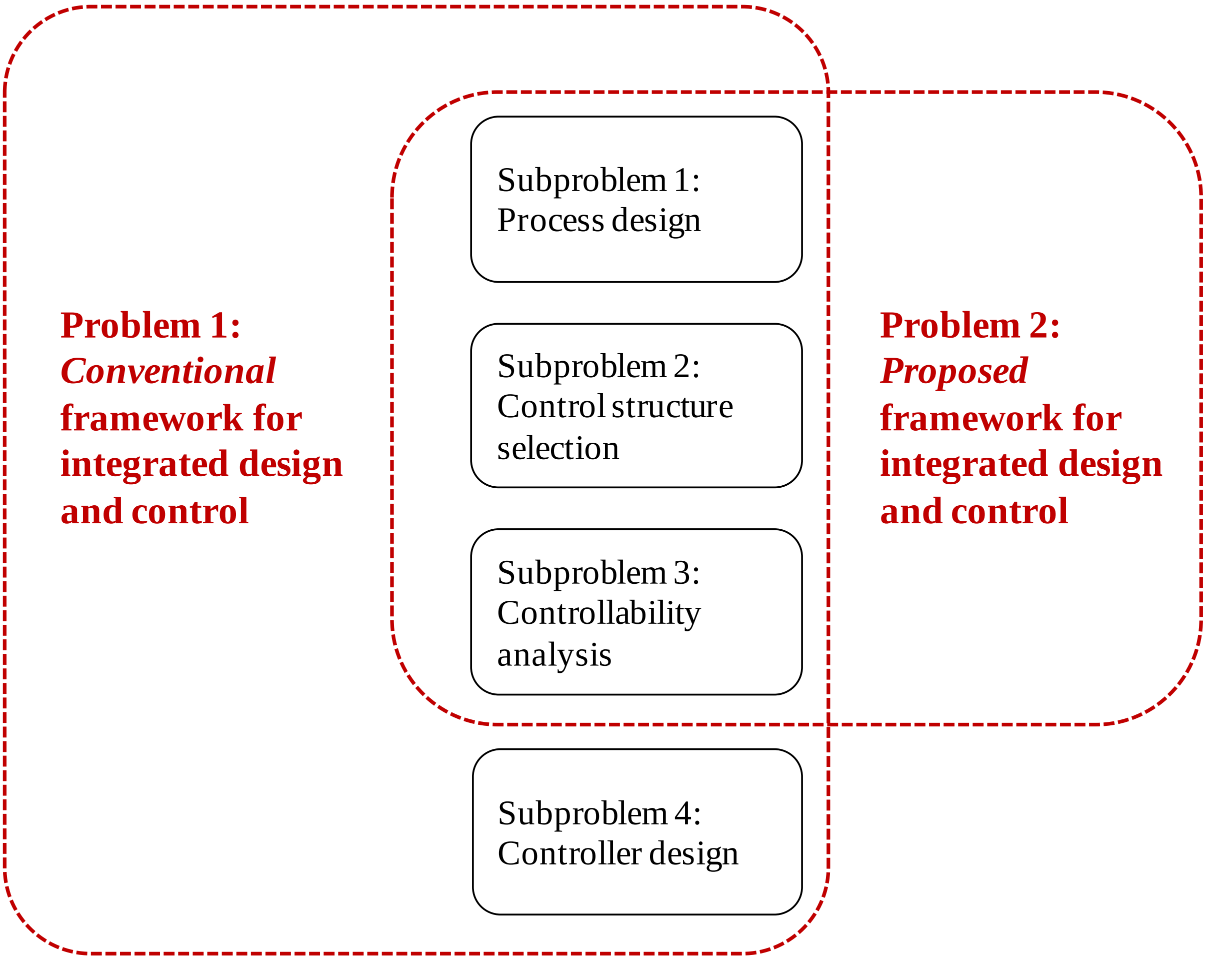

Figure 1.7. The key problems and subproblem involved in the proposed integrated design and control

1.2.6. Research aims and objectives

This research aims at developing a new framework for addressing Problem 2. The developed framework will feature the following characteristics:

1. **A systematic approach**

   The developed framework systematically generates and screen alternative decisions regarding process and its control structure based on economic and control performance criteria.
2. **Complexity reduction**

   The developed framework reduces the problem complexities.
3. **Controllability**

   The developed framework should be able to ensure some desirable properties of the process and its control structure such as steady-state operability or functional controllability.
4. **First principles modelling**

   The developed framework can be implement using first principles models and is not necessarily limited to any simplifying assumption.

1.2.7. Research novelty claims and contributions

The novelty claim of present research is to develop a new optimization framework for addressing Problem 2 that features the characteristics mentioned in the research aims (last section). The results of this research are published or under review/preparation as follows:

- Sharifzadeh M., Thornhill N.F., (2012a). Optimal selection of control structures using a steady-state inversely controlled process model. *Computers & Chemical Engineering,* 38, 126-138. DOI: 10.1016/j.compchemeng.2011.12.007.
- Sharifzadeh M., Thornhill N.F., (2012b). Integrated design and control using a dynamic inversely controlled process model, accepted for publication at *Computers & Chemical Engineering*. DOI: 10.1016/j.compchemeng.2012.08.009.
- Two other papers under review and preparation/submission.

In addition, research was presented in the following conferences and meetings:

- Sharifzadeh, M., Thornhill, N.F., (2011). Optimal controlled variable selection using a nonlinear simulation-optimization framework. *21st European Symposium on Computer Aided Process Engineering, May 21- June 1, Porto Carras, Greece*. Book series: *Computer-Aided Chemical Engineering*, 29, 597-601.
- Sharifzadeh, M., (2012). Integrated design and control with a focus on control structures. Oral presentation at Departmental Symposium, 30th March 2012, Department of Chemical Engineering, Imperial College London.

It should be emphasized that although the proposed methods make use of optimization algorithms and solvers, developing a new optimization algorithm is not within the novelty claims of this research. The author attempted to present the formulations in such a way that they can be conveniently addressed using available modelling and optimization tools.

Disclaimer: The models used in present research are for demonstration purpose only and were not validated using actual plant data.

1.3. Introduction to the thesis

This section introduces the PhD thesis. As discussed earlier, the aim of this thesis is developing a new optimization framework for integrated design and control. To this end firstly, the research activities in the field are reviewed in Chapter 2 and the merits and limitations of each method are explained. Then, in chapter 3, a new optimization framework for integrated design and control is proposed, which is based on the concept of perfect control. Several steady-state and dynamic versions of the proposed framework are demonstrated using the case studies of Chapters 4, 5 and 6, for optimal selection of control structures and integrated design and control. Chapter 7 discusses the implications of perfect control and presents a critical evaluation of the research, as well as suggestions for future research.

The layout of the thesis is explained in more detail in the following subsections. It is intended to justify the organization of the thesis as well as illustrating the interrelations of the presented materials.

1.3.1. Introduction to Chapter 2: Background and context

Chapter 2 reviews the relevant research activities in the field. Different methods for addressing the problem and subproblems of Section 1.2.4 are discussed. As will be seen, these methods can be classified into the methods for sequential design and control, and the methods for integrated design and control. The aim is to put research in the context and provide a solid background for the proposed methodology in the next chapters.

1.3.2. Introduction to Chapter 3: An optimization framework using an inversely controlled process model

Chapter 3 presents the theory of the present research. The mathematical formulation of the proposed optimization framework for integrated design and control (Problem 2) is developed by modifying the mathematical formulation of the conventional optimization framework (Problem 1). In conventional integrated design and control, a model is used which is the combination of the process and controllers models. In the new framework for integrated design and control, the combined process-controller model is replaced by an *inversely controlled process model*. Here, the treatment is based on the notion of perfect control. Several steady-state and dynamic versions of the proposed optimization framework will be formulated for optimal selection of control structures and integrated design and control. Finally, this chapter explains that the application of a steady-state inversely controlled process model ensures regulatory steady-state operability, and the application of a dynamic inversely controlled process model ensures functional controllability. The proposed frameworks in Chapter 3 will be demonstrated using three case studies in the subsequent Chapters 4, 5 and 6.

1.3.3. Introduction to Chapter 4: Optimal selection of control structures using a steady-state inversely controlled process model

Chapter 4 illustrates the application of a steady-state inversely controlled process model for optimal selection of control structures (Sub-problem 2) by studying a distillation train. The mathematical formulation of the problem is presented and the implementation considerations and optimization programming are explained. Finally, the results are presented and discussed.

1.3.4. Introduction to Chapter 5: Integrated design and control using a steady-state inversely controlled process model

Chapter 5 illustrates the application of a steady-state inversely controlled process model for integrated design and control (Problem 2). This chapter extends the results from the previous chapter by including the structural and parametric process variables. The mathematical formulation of the problem is presented and the methodology is illustrated by studying the case of a reactive distillation column. The applied software tools are explained and the results are discussed.

1.3.5. Introduction to Chapter 6: Integrated design and control using a dynamic inversely controlled process model

Chapter 6 extends the results from the last chapters by applying a dynamic analysis and considering transient conditions. This chapter illustrates the application of a dynamic inversely controlled process model for integrated design and control (Problem 2) of two series reactors. Two solution strategies are applied. They are dynamic optimization based on (i) sequential integration and (ii) full discretization. The first solution strategy is the classic strategy for dynamic optimization in which discrete variables are enumerated and continuous sub-problems are optimized. However, the first strategy is limited to problems in which the number of the discrete variables is small and enumeration of continuous sub-problems is possible. For this reason, the second strategy is presented in which all the time-dependent variables are discretized and the underlying discretized formulation is posed as a mixed integer nonlinear programming (MINLP) problem. As explained earlier, there are often competitions and conflicts between process objectives and control objectives. The other advantage of the second strategy is that its execution time is shorter. This provides the opportunity to explore the trade-off between these competing objectives by constructing a Pareto front as will be discussed. Finally, several post-optimization analyses are performed and a PI controller is designed for the optimized process and control structure. This will provide the opportunity for comparison of the proposed and conventional optimization frameworks.

1.3.6. Introduction to Chapter 7: Discussions and suggestions for future research

Chapter 7 provides the discussions and comparisons of the methods presented in the thesis. Since, the dynamic formulation may include high index differential algebraic equations, the implications of the index of a dynamic inversely controlled process model for disturbance rejection and setpoint tracking are explained. In addition, the implications of the causes of control imperfection for the proposed optimization framework are discussed. The discussions go on with critical evaluation of the research contributions and achievements. Finally, Chapter 7 provides suggestions for the future research directions.

1.4. Conclusion

This chapter presented an introduction to the research title as well as the thesis. It was discussed that due to the interactions between individual unit operations, and their implications for feasibility and optimality of process operation, a plant-wide approach to process design and control is required. Furthermore, it was explained that the problems of process design and control design share important decisions and should be integrated. Nevertheless, the integrated problem is highly complex and may become intractable.

This chapter identified that a part of these complexities and combinatorial features of integrated design and control should be attributed to the controller design. The design of controllers requires decision-making regarding the type of controllers, pairing/partitioning of manipulated and controlled variables, and tuning the parameters of controllers. In addition, controllability is the inherent property of the process and does not depend on the controller design, and should be considered independently. Finally, the modern control systems are designed during the commissioning stages and using commercial packages which may not be available during the process design stage. Therefore, this chapter proposed a new optimization framework for integrated design and control based on the notion of perfect control. In the new framework, the process and its control structure are optimized simultaneously, while design of controllers are disentangles and delegated to control practitioners.

The discussions in this chapter justified the research directions and will provide opportunities for further developments and contributions as will be presented in Chapter 3 and will be demonstrated using the case studies in Chapters 4, 5 and 6. In addition to introducing the research title, this chapter also introduced the thesis structure. The organizations of the presented materials were explained, and the merits of the each contribution were highlighted.

2 | Background and context

2.1. Introduction

This chapter presents a thematic review of the relevant topics for process design and control. Firstly, the industrial perspective and the incentives for integrated design and control are discussed. Then, an overview of research in the field is presented. There are two categories of the methods. The methods in the first category have a sequential approach in which the process is designed first, and then the design of its control system is decided. In the second category, however, the process design and control are to some extent integrated. Since most of the methods in both categories employ a model in their analyses, different methods for modelling chemical processes are reviewed first and their relationships to the problem of integrated design and control are established.

Then, the review starts by exploring the methods in the first category. The methods based on applying engineering insights in order to decompose the problem into smaller sub-problems are reviewed. Controllers and control structures are also discussed, and the causes of imperfect control are explained. The methods based on passivity analysis are also discussed briefly.

The methods in the second category, however, consider the interactions between process design and control. The geometric methods for operability analysis, the multi-objective optimization methods based on controllability measures, the methods using robust control measures, the methods for steady-state and dynamic flexibility optimization, the methods based on minimization of the economic losses associated with back-off from active constraints and simultaneous process and controller optimization are reviewed and discussed. Finally, the chapter briefly reviews the solution algorithms for the optimization-based methods. These discussions serve as the introductions to the next chapter where the theory of research is presented.

2.2. Incentives for integrated design and control

The common perception is that steady-state economy dominates profitability of a chemical process, (Downs and Skogestad 2011). However, there is no guarantee that optimizing a process based on a steady-state economic criterion will also ensure desirable controllability properties. In fact, Luyben (2004) recognized that in many processes steady-state process economic objectives and dynamic control performance objectives are inherently competing and conflicting. He mentioned that in order to achieve a high energy efficiency, thermodynamically reversible processes are favourable. This is because in these processes no entropy is created (i.e., no energy wasted) and therefore, the required energy is minimized. Such an economic optimal process employs very negligible driving forces, i.e., small temperature, pressure, and concentration differences. However, these driving forces are crucial for control systems to be able to reject disturbances or switch between steady states. The examples of situations in which process and control objectives compete and conflict are, (Luyben 2004):

1. Sizing a small control valve, as the resulted small pressure drop improves energy efficiencies due to the reduction in the power requirements of compressors and pumps, but at the same time increases the likelihood of valve saturation and loss of control action.
2. Designing a small heat transfer area, which reduces the required capital costs but at the same time implies that at normal operating conditions, a lager temperature difference is used, and a small potential temperature difference is reserved for disturbed operating conditions.

3. Designing large reflux and boil-up ratios in distillation columns, which may imply a higher energy requirement, but will act better in the presence of disturbances.
4. Designing a limiting reactant; in the case of a reaction with two reactants, steady-state economy favours the reactants to be fed equimolar to maximize the reaction rate and minimize the reactor volume, hence reduce the costs. However, if the reaction is exothermic, the high inventories of the reactants increase the risk of a runaway reaction. Designing for a limiting reactant will self-regulate the process, as the limiting reactant will deplete in the case of a runaway reaction. However, such a design requires a larger reactor and a larger recycle stream to return unreacted materials and therefore increases the capital investment and the operating costs.

These observations encouraged process systems engineers to integrate process design and control, because isolated decision-making for process design and control design would result in, if not infeasible, a sub-optimal solution. Reviews of the research activities regarding integrated design and control is presented by Sakizlis, et al. (2004), Seferlis and Georgiadis (2004), Ricardez-Sandoval, et al. (2009a) , Yuan et al. (2011) and Yuan et al. (2012).

2.3. Industrial perspective

Due to depletion of worldwide energy resources, stringent safety regulations, and environmental concerns, new chemical processes tend to employ less in-plant inventories, and a higher degree of material and energy integrations. In addition, they feature higher yields incorporating recycle streams in complex flowsheets. These processes operate closer to operational constraints (Luyben 2004), and produce a larger variety of products with different specifications. Furthermore, due to current economic climate and high costs of building new facilities, optimization and retrofit of old processes in order to produce new products add to the problem complexities, (Downs and Skogestad 2011).

Downs and Skogestad (2011) emphasized that despite the large variety of methods developed for designing plant-wide control systems, the industry has conservatively maintained its traditional practice to design control systems for individual unit operations. For example, in Eastman Chemical Company, the procedure for designing a control system is still to set the throughput by the feed flowrate and then design the control systems for individual units, sequentially. This is because unit-wise control systems are simple and understandable to operators and plant engineers, and any malfunctioning unit operation can be treated without a need for intervention of control experts, (Downs and Skogestad 2011).

Page Buckley (1964) was among the pioneer industrial engineers who recognized the importance of integrated design and control. He achieved this integration by transferring to Design Division of DuPont's Engineering department and coordinating the efforts of process and instrumentation engineers. However, despite the long history of integrated design and control, there are several practical barriers to commercialize the integrated approach:

1. Developing rigorous models and controllability analysis during the design stage can be time-consuming and expensive and requires a high level of expertise, (Chachuat 2010; Downs and Skogestad 2011).
2. Economic objectives and control objectives are incommensurable and establishing sensible links between business derivers and control objectives is an elusive task, (Edgar 2004).
3. In addition, control engineers and process engineers usually have different mindsets and for cultural reasons it is difficult to encourage the integrated approach, (Downs and Skogestad 2011).
4. Industrial incentives for simplicity and conceivability of control systems discourage the application of highly complex control systems such as real-time optimizations, (Downs and Skogestad 2011).

Therefore, systematic methodologies are needed that capture the interactions between process design and control and be able to manage the conceptual as well as numerical complexities of the problem.

2.4. Overview of research in the field

The subsequent sections present a thematic review of the relevant topics for process design and control. The hierarchical tree in Figure 2.1 gives an overview of research in the field, and serves as a roadmap for this chapter. It consists of two main branches. The left branch has a sequential/iterative approach in which Subproblems regarding control structure selection (Subproblem 2), controllability analysis (Subproblem 3), and controller design (Subproblem 4) are solved in sequence and after the process design (Subproblem 1) is fixed. However, the methods in the right branch have a simultaneous approach in which process design and control (Problems 1) are integrated to some extents.

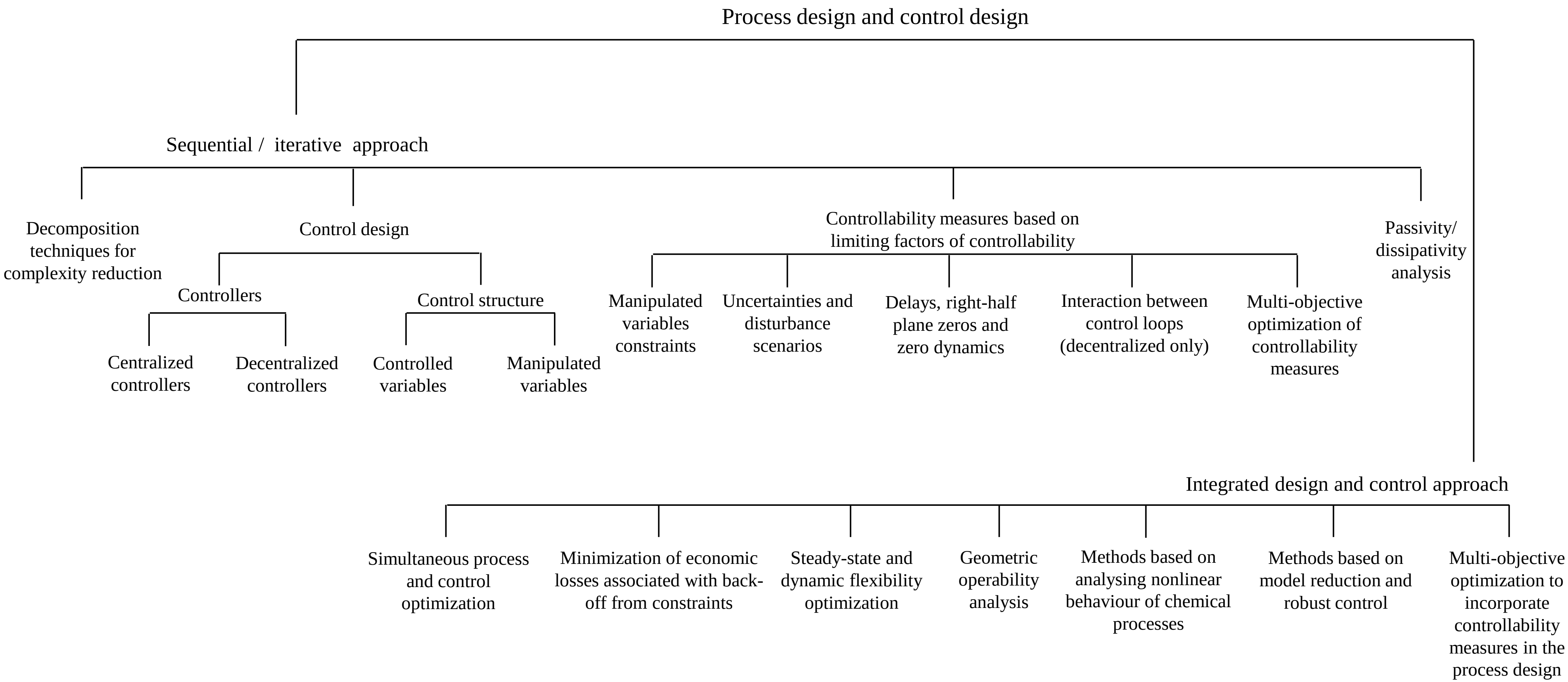

Figure 2.1. Overview of research in the field

Since different methods for process modelling have had crucial roles in developments of the methods in Figure 2.1, different types of process models are reviewed first. The sequential approach (left branch in Figure 2.1) consists of a variety of methods which address the key sub-problems of Section 1.2.4 in sequence. The review starts with the methods based on process insights and heuristics, developed over decades of engineering practice, which enable conceptual as well as temporal and spatial decomposition of the problem. Moreover, understanding the elements of control systems is crucial. The reviews of controllers and control structures are presented in this chapter. The focus is on the degree of centralization, the economic implication of set-point policies and self-optimizing control, in addition to the desired properties of controlled and manipulated variables. The causes of control imperfection also limit process controllability. They are (1) interactions between control loops for decentralized controllers, (2) constraints on the manipulated variables, (3) model uncertainties and disturbance scenarios, (4) right-half-plane zeros, and (5) time delays. Based on the causes of control imperfection, a variety of methods is developed, which characterize process controllability from different perspectives. Different definitions of operability, flexibility, and controllability are presented and methods for quantification of control imperfection are reviewed briefly. In parallel, as will be discussed, the methods based on passivity/dissipativity investigate the interactions of individual control systems and controllability of the whole network.

The disadvantage of the methods in the sequential approach is that they consider only individual subproblems of Section 1.2.4 (control structure selection, controllability analysis and controller design) and do not consider the interactions between them. Some of the sequential methods have a qualitative approach and some others have yes/no or evaluation/ranking attitudes. However, controllability characteristics are the inherent properties of the process and depend on the structural and parametric process variables as well. The incentives to integrate controllability and control performance criteria into process design have motivated new studies which are shown on the right branch of Figure 2.1. One way forward is to employ multi-objective optimization and incorporate controllability measures into an economic multi-objective function. Other researchers focused on reducing the first principles model of a process to a linear model and applying the measures that conventionally are used for robust control. In addition, the process model can be applied in order to map the available inputs into the output space and determine if the process operation remains feasible, which resulted in the geometrical methods for operability analysis.

Alternatively, flexibility analysis can be conducted using optimization. The early versions of flexibility optimization were based on a steady-state formulation and identifies whether for a range of the values of uncertain variables, the process operation is feasible or not. This formulation had no implication for the control system. Later, flexibility optimization was extended to consider the transient conditions using a dynamic formulation. Other researchers suggested economic optimization of the losses associated with disturbances. These losses were formulated in terms of the required back-off from active constraints to ensure a feasible operation. In addition, advancement of computational tools and optimization algorithms encouraged the researchers to optimize the process and controllers simultaneously. However, the resulted mathematical formulation is very large and limited to a certain type of controllers.

2.5. Modelling techniques

This section provides an overview of the modelling techniques used by the control community. With some exceptions in the heuristic methods, all the methods shown by the end nodes of the hierarchical tree in Figure 2.1 use process modelling for understanding the underlying physical and chemical phenomena. The aim is to explain the characteristics of different modelling approaches and establish their relationships to the problem of integrated design and control. The applied models can be classified according to:

1. Source of information: empirical or from first principles,
2. Mathematical presentation: linear or nonlinear,
3. The treatment of time-dependent variables; discretized or continuous,
4. Importance of transient conditions: steady state or dynamic,
5. Spatial details: lumped or distributed, and
6. Degree of uncertainty: deterministic or stochastic.

Different combinations of the abovementioned properties result in different modelling approaches. The most common approaches are linear dynamic models, discrete time models, stochastic linear models, input-output models, distributed models, and first principles models, (Rawlings and Mayne 2008). It is crucial to understand the implications of the modelling approaches. This is because if a model has a poor relationship to the original underlying physical and chemical phenomena, its application for integrated design and control is of limited practicality. In the following subsection, different modelling approaches are reviewed and the importance of first principles modelling is emphasized.

2.5.1. Modelling from first principles

First principles models are based on the constitutive and phenomenological laws such as mass and heat balances, laws of thermodynamics, reaction kinetics and heat, mass and momentum transfer phenomena. Often the first principles models can be represented accurately enough by the following differential algebraic formulation:

$$\frac{d\boldsymbol{x}(t)}{dt} = \boldsymbol{f}(\boldsymbol{x}(t), \boldsymbol{u}(t), t) \qquad (2-1a)$$

$$\boldsymbol{y}(t) = \boldsymbol{h}(\boldsymbol{x}(t), \boldsymbol{u}(t), t) \qquad (2-1b)$$

$$\boldsymbol{x}(t_o) = \boldsymbol{x}_o \qquad (2-1c)$$

In above, $\boldsymbol{x}(t)$ is the vector of state variables, $\boldsymbol{u}(t)$ is the vector of manipulated variables, $\boldsymbol{y}(t)$ is the vector of controlled variables, and t represents the time. In addition, $\boldsymbol{f}[\,]$ is the vector of differential equations, and $\boldsymbol{h}[\,]$ is the vector of algebraic equations. $\boldsymbol{x}_o$ is the vector of the values for state variables at the initial time t_o.

If in addition to time, other variations such as spatial variations or particle size distributions are also important, the resulted formulation may involve partial differential equations. For example, a multi-component mixture including a chemical reaction and convection can be represented as (Rawlings and Mayne 2008):

$$\frac{\partial C_A}{\partial t} = \nabla.(C_A\, v_A) - R_A = 0 \qquad (2-2)$$

in which, C_A represents concentration, v_A is the velocity, and R_A is the reaction rate of component A. The operator ∇ in (2-2) is defined as:

$$\nabla = \delta_x \frac{\partial}{\partial x} + \delta_y \frac{\partial}{\partial y} + \delta_z \frac{\partial}{\partial z}$$

where δ_x, δ_y and δ_z are unit vectors.

By increasing interests in nanotechnology and molecular systems engineering, a variety of models for describing the random behaviour of molecular systems has evolved. However, the focus of control theory is mostly macroscopic properties of chemical processes in which systems of small numbers of molecules are not considered.

2.5.2. Linear models

Due to numerical difficulties and motivated by solid linear control theories, linearization of equations (2-1) is often performed and the corresponding linear model is used instead. However, the resulted reduced model is only valid locally and around the linearization point. The most general time-varying linear dynamic model is represented as:

$$\frac{d\boldsymbol{x}(t)}{dt} = \mathbf{A}(t)\boldsymbol{x}(t) + \mathbf{B}(t)\boldsymbol{u}(t) \qquad (2-3a)$$

$$\boldsymbol{y}(t) = \mathbf{C}(t)\boldsymbol{x}(t) + \mathbf{D}(t)\boldsymbol{u}(t) \qquad (2-3b)$$

$$\boldsymbol{x}(t_o) = \boldsymbol{x_o} \qquad (2-3c)$$

The time-invariant equivalent formulation of (2-3) can be derived by making **A**, **B**, **C** and **D** constant. In addition, the stochastic equivalent formulation of (2-3) is

$$\frac{d\boldsymbol{x}(t)}{dt} = \mathbf{A}(t)\boldsymbol{x}(t) + \mathbf{B}(t)\boldsymbol{u}(t) + \mathbf{H}(t)\boldsymbol{w}(t) \qquad (2-4a)$$

$$\boldsymbol{y}(t) = \mathbf{C}(t)\boldsymbol{x}(t) + \mathbf{D}(t)\boldsymbol{u}(t) + \boldsymbol{v}(t) \qquad (2-4b)$$

$$\boldsymbol{x}(t_o) = \boldsymbol{x}_o \qquad (2-4c)$$

where $\boldsymbol{w}(t)$ is the vector of random variables acting on the state transitions and $\boldsymbol{v}(t)$ is the vector of random variables acting on the measurable output variables. In the context of control theory, these random variables represent the unmodelled behaviour of the environment, i.e., disturbances.

The discretized version of formulation (2-3) is of interest when the measurable output variables are sampled at discrete times:

$$\boldsymbol{x}(k+1) = \mathbf{A}\boldsymbol{x}(k) + \mathbf{B}\boldsymbol{x}(k) \qquad (2-5a)$$

$$\boldsymbol{y}(k) = \mathbf{C}\boldsymbol{x}(k) + \mathbf{D}\boldsymbol{u}(k) \qquad (2-5b)$$

$$\boldsymbol{x}(t_o) = \boldsymbol{x}_o \qquad (2-5c)$$

where k is a nonnegative integer number. If the internal structure of a system is unimportant or not completely understood, input-output modelling can be used instead. Such a model can also be the result of system identification in which inputs are manipulated and a linear model is developed based on the measured outputs. In such an input-output approach, the process internal elements are considered as a black box. The input-output representation of formulation (2-3) using the notations of Laplace transform, can be represented as:

$$\overline{\boldsymbol{y}}(s) = \mathbf{G}(s)\overline{\boldsymbol{u}}(s) \qquad (2-6)$$

The formulation (2-6) can be derived directly from state space representation (2-3) as follows:

$$\mathbf{G}(s) = \mathbf{C}(s\mathbf{I} - \mathbf{A})^{-1}\mathbf{B} \qquad (2-7)$$

Different methods in Laplace domain, z domain and frequency domain are developed based on the properties of linear models, which their details are available in literature (e.g. Ogunnaike and Ray 1994; Skogestad and Postlethwaite 2005).

2.5.3. Model reduction techniques

Mathematical models in chemical and petroleum engineering consist of thousands of algebraic and differential equations. Simultaneous solution of all these equations may pose a numerical challenge. The other motivations for reducing the mathematical models are for storage and retrieval of the optimal solutions, getting insights about the model structure, and degree of freedom analysis. Marquardt (2001) presented a review of the conventional methods for model reduction. In general, these methods can be classified into two categories, i.e. model simplification and model-order reduction.

Model simplification can be performed by linearization (Antoulas et al. 2000) around a nominal operating point, or simplifying kinetic and/or physical property models and approximation of model equations with simpler functional (e.g., explicit) expressions (Dormeanu 2009). The other simplifying method is model lumping (Ranzi et al. 2001) in which thermodynamic models and components are simplified to lumped species and pseudo-phases. However, this type of model reduction may introduce more complexities to the functional expressions in the remaining equations, (Dormeanu et al. 2009).

Model-order reduction methods can be classified into linear and nonlinear methods. The linear methods can be classified into projection-based and non-projection-based methods. The projection-based methods decompose the original space S^0 (of dimension n) into the reduced space S^1 (of dimension k) and the residue space S^2 (of dimension $n-k$). Krylov-subspace or momentum matching methods, balanced realization-based methods and proper orthogonal decomposition (POD)-based methods are in this category (Skogestad and Postlethwaite, 2005; Antoulas et al. 2000; Rathinam and Petzold, 2003; Penzl, 2006). In the non-projection methods, the states of the approximate model have no connection to the original model states. The examples of techniques in this category are Hankel optimal model reduction method, and singular perturbation method (Mäkilä, 1991; Marquardt, 2001).

Each of the above methods has advantages and disadvantages. For example, the Krylov-subspace-based methods can be applied for a high-order system, but they have robustness, stability and efficiency issues (Bai, 2002). In the case of balanced realization methods, very low-rank approximations are possible and will result in accurate low-order models. However, the solution requires dense computations and can be carried out only for low-dimension (a few hundreds of equations) models (Antoulas, et al. 2000). The proper orthogonal decomposition (POD)-based methods strongly depend on the initial excitation, but these methods can be applied for high-complexity systems. The nonlinear methods are mostly the extended application of linear methods to nonlinear models, using linearization of model nonlinearities. As a result, the reduced model is only valid locally. The methods based on the application of neural networks (Prasad and Bequette, 2003) or hybrid models (Nagy and Braatz 2007; Nagy et al. 2010) are the other class of the nonlinear methods. However, the resulted reduced model can be even more difficult to solve than the original model, (Marquardt, 2001).

Since the philosophy behind all these techniques is to eliminate those state variables or their derivatives (i.e., balanced truncation or balanced residualization) which have the minimum effects on the input-output behaviour of systems, most of these methods destroy the structure of the problem and result in the loss of physical significance of the model parameters and variables. Moreover, understanding the effects of the uncertainties on the precision of the reduced model is another challenge, (Nagy and Braatz 2007). In addition, an important drawback of model reduction approaches such as balanced covariance matrices and proper orthogonal decomposition is that they only reduce the number of differential variables and not algebraic variable, which are not efficient because often the algebraic variables outnumber the differential variables.

2.5.4. The importance of modelling from first principles

As discussed earlier, it is crucial that the applied model for integrated design and control establishes strong links to the physical and chemical properties of the process and is able to give rigorous evaluations of the control performance criteria as well as process objectives. Therefore, despite the numeral easing, the methods which destroy the internal structure of the underlying first principles models (such as abovementioned model reduction techniques) or the methods which are only locally valid (e.g. linearization methods) are not appropriate for integrated design and control. This is one of the reasons that most of the methods developed on the left branch of Figure 2.1 can only be used in sequence (i.e., after process design fixes nominal operating point) and have yes/no or evaluation/ranking attitudes. By contrast, most of the methods on the right branch of Figure 2.1 have strong links to the underlying first principles models.

2.6. Process insights and heuristics: decomposition techniques for complexity reduction

The following subsections discuss the methods in the first node of the left branch in Snip 2.1.1 (Figure 2.1 revisited) which concerns decomposition techniques for complexity reduction.

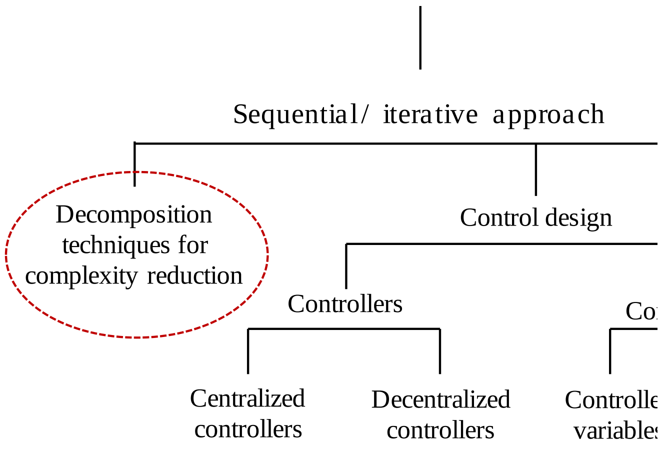

Snip[1] 2.1.1. Research in the field: Decomposition techniques for complexity reduction, (Figure 2.1 revisited).

The fact that the subproblem of process design needs to be resolved and decomposed into more manageable subproblems is not new in the area of process systems engineering. For example, Douglas (1988) presented a hierarchical view of a plant to make the problem of process design tractable. The methodology of Douglas employs different resolutions of the plant details, for example evaluation of the interactions of the plant and surroundings and then evaluation of the interactions of process components with each other inside the plant and so on. The same is true for the control design and many authors suggested a hierarchical approach or a decomposition technique in order to reduce the problem complexities.

The focus here is on control structures. Control structures feature different complexities. They have multi-scale multi-layer structures and work in different time scales. While

[1] In this thesis, snips refer to small pieces of figures which are revisited to facilitate the discussion.

business planning is performed in the time scale of days and weeks, the regulatory control layer which stabilizes the process, acts in seconds. In addition, control structures have different objectives, such as stabilizing controlled variables, avoiding technical limitations, respecting environmental and safety constraints, and following the optimal economic operation. Furthermore, the problem complexities increase with the process efficiency and integration, because in highly integrated processes, there are significant interactions between different parts of the process. For example, the propagation of disturbances in a highly integrated process is not only along the main production path, but also through recycle streams and/or between process streams which exchange materials and energy, (Luyben et al, 1999). These complicated characteristics require a systematic approach for complexity reduction. Therefore, handling the problem complexities is the key characteristic of the desirable methodology. A variety of decomposition techniques is developed over the decades of engineering practice, as discussed in the following.

2.6.1. Complexity reduction based on process components: a unit-wise approach

The early attempts to reduce the complexities of control structures involved design of control structures for individual unit operations such as heat exchangers, reactors, and distillation columns and then interconnecting them in order to develop the overall plant-wide control structure. Here, engineering insights have to be employed to resolve the conflicts (e.g. two control valves on the same stream) that arise by adding individual control structures. The inspiration for this approach is that comprehensive knowledge and experiences are available for controlling the major unit operations.

A criticism about the unit-wise approach is that combining the optimal control structures of individual unit operations does not guarantee the optimality of the overall plant-wide control structure. In addition, the heuristic methods used for eliminating the conflicts become more and more complicated and inapplicable as the number of process components increases, (Kookos 2001; Ng 1997).

Although combining unit-wise control structures ignores the plant-wide effects, still this method has wide applications. The reason for its popularity is the simplicity of the developed control structures, which makes them more conceivable to the operation people. Downs and Skogestad (2011) also attributed this practice to the "*overriding issues of reliable operation*".

Control design for special unit operations has been the subject of academic and industrial research, (Ward, et al. 2007; Ward, et al. 2010; Skogestad 1988, 2007).

2.6.2. Complexity reduction based on temporal decomposition

Temporal decomposition is another strategy in order to reduce complexities of control structures. It employs differences in the time scales in which the control structure is performing.

Buckley (1964) recognized that control systems have a high frequency control layer for quantity control (material balance) and a low frequency control layer for quality control (e.g. specifications of products). As another example, it is well-known that in multi-loop traditional control systems, interactive loops with a significant difference in their time constant may demonstrate a decoupled performance, and can operate separately, (Ogunnaike and Ray 1994).

In addition, Morari (1980a; 1980b; 1980c) categorized process control objectives into regulatory and optimizing objectives. Those control systems which are responsible for regulation of the process, handle fast disturbances that have a zero expected value in long-term. However, longstanding disturbances with significant economic effects are treated by optimizing control systems.

2.6.3. Complexity reduction based on prioritization of control objectives

Several researchers have attempted to reduce the complexities of the problem by prioritizing control objectives in order to decompose control structures into smaller parts, so each part pursues an individual objective.

McAvoy (1994) suggested considering the overall mass balance through control of the flowrates, first. Then, the energy balance must be regulated by controlling temperatures and pressures. Later, the product quality and component mass balances are considered. Finally, the remaining degrees of freedom and setpoints of the regulatory control layer are employed for optimizing the operational costs.

The tiered framework approach suggested by Price, et al. (1993, 1994) firstly meet the targets of the overall inventory and throughput regulations, then product specifications are treated, later operational constraints are considered, leaving the optimal operation to be the last target. They called their methodology a “*direct descendant*” of Buckley’s method.

Ponton and Laing (1993) recommended developing the control structure for controlling the flowrates of products and feed first. Then, recycle flow must be regulated and the compositions of intermediate streams should be treated. Energy and temperature stabilization are the next targets and finally inventory control will be addressed.

Luyben, et al. (1997) suggested a framework for control structure selection in which firstly the decisions regarding control of the production flowrate are made. Secondly, the product quality specifications and constraint satisfaction must be considered. Then, inventory control is designed. It must be checked that the overall mass balance will be met for all the components. Finally, the remaining manipulated variables are assigned for optimizing the economic objective.

Larsson and Skogestad (2000) and Skogestad (2004a) developed an iterative top-down/bottom-up algorithm for control structure selection. The design approach in the top-down direction is steady-state economic analysis such as meeting the operational objectives, optimizing the process variables for important disturbances and determining active constraints such as throughput/efficiency constraints. However, the bottom-up design is concerned with dynamic issues such as designing the control structure for the regulatory layer, paring/partitioning the manipulated and controlled variables, and designing the supervisory control layer.

Luyben (1996) presented a survey of the control structures developed for the Tennessee Eastman problem. He discussed the pros and cons of his own solution in addition to a list of other schemes such as those presented by Lyman and Georgakis (1995), McAvoy and Ye (1994), and Ricker (1996). Luyben (1996) argued that different control structures developed for the Tennessee Eastman problem are the results of different rankings of the control objectives: "*...diversity of structures is a very nice example of one of the basic process control principles that says that the "best" control structure depends on the control objectives*".

As discussed also by Edgar (2004), in evolution of the above methods, the priorities of the objectives have been reversed. In the former approaches, the control system was simply a tool to achieve the predetermined goals of production, which were set in the process design stage. The operation personnel did not think of the control system as an optimization tool to improve profitability of the process. Therefore, economic optimization had the lowest priority. However nowadays, business planning of process industries has become online and much less limited by the early decisions at the design stage. Consequently, the new control systems have also inputs from economic parameters and translate them into operational decisions. This has encouraged designers to consider the highest priority to economic objectives and the roles of other control tasks (e.g. inventory control in the next section) are to realize the targeted economic objectives.

2.6.4. Complexity reduction based on the production rate and the inventory control systems

Since inventory control systems have a dynamic nature and do not appear in a steady-state analysis, they need to be treated separately. Therefore, inventory control has received special attentions in literature. The following discussions about inventory control and dynamic degrees of freedom are also of interest to the steady-state methods of Chapters 4 and 5 as will be discussed later.

The process mass inventories refer to the gaseous, liquid, and solid materials accumulated within the process. Inventory control has a priority in control structure design, because many instability modes such as emptying/overflowing of a vessel or flooding/weeping of a distillation column are related to inconsistency or failure of inventory control systems. In addition, modern process plants tend to have less material inventories due to efficiency, safety, and environmental considerations, which makes the control of their inventories more challenging. Therefore, developing general rules that enable design of inventory control systems without the aid of costly rigorous dynamic models would be highly desirable. The necessity of developing a consistent and efficient plant-wide inventory control structure has led to a range of heuristics and judgement-based methods. In the following, a brief review of these methods is presented.

Buckley (1964) emphasized the requirement for consistency of the flow controls, upstream and downstream of the throughput manipulation point (TMP). He suggested that in order to develop a consistent control structure, flows must be controlled in the opposite direction at the upstream of the throughput manipulation point and in the same direction at the downstream of this point.

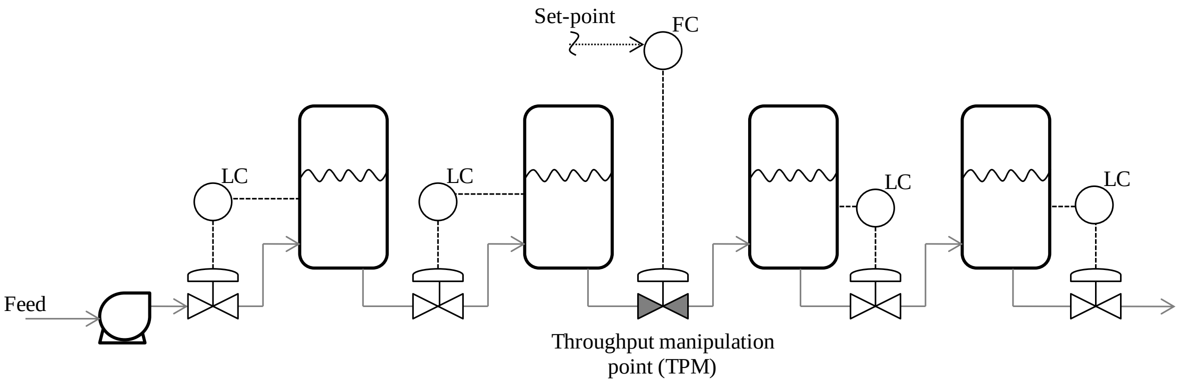

Figure 2.2. The inflows are used for design of the inventory control systems on the upstream of the throughput manipulation point. However, the outflows are used on the downstream of this point.

Later, Price, et al. (1993, 1994) emphasized the existence of a primary path from the feed to the product in most chemical processes. They suggested that the inventory control should be designed in the direction of the flow if the feed flowrate is chosen to be the throughput manipulation point, and in the opposite direction of the flow if the product flowrate is chosen as the throughput manipulation point and in general radiates from the throughput manipulation point. This requirement is shown in Figure 2.2 for a series of liquid inventories with throughput located inside the process.

Luyben and his coworkers (Luyben 1993a,b,c; Tyreus and Luyben 1993; Luyben 1994; Luyben, M. L., and Luyben, W. L., 1995) in a series of articles, using examples of reaction-separation processes, explained how reaction kinetics and economic factors might result in different control structures. They concluded a general rule that a flow control must be included in each recycle stream. Luyben, et al. (1997) recommended one flow control in the liquid recycle loop, but setting gas recycle at the maximum circulation rate. It is notable that the effects of recycle streams are not limited to material inventories, and energy inventories are also important. Luyben, et al. (1999) using the example of an exothermic reactor, showed that positive feedback of energy could lead to the loss of control action and may pose the risk of runaway reactions.

Aske and Skogestad (2009a,b) investigated the consistency requirements for inventory control systems. Their suggested rules can be summarized to firstly assign an inflow or outflow controller to each inventory and secondly to check whether inventory of each component is consistently regulated by at least a degree of freedom or a chemical reaction.

Each phase inventory also needed to be controlled by the inflow or outflow or via phase change.

Recent studies (Skogestad 2004a; Aske 2009a,b,c; Downs and Skogestad 2011) focus on the relation of inventory control and profitability. Chemical processes can be classified according to which constraints become active earlier, during economic optimization: (i) throughput constraints or (ii) efficiency constraints. In the case of new plants, economic objectives are often driven by optimizing the efficiencies regarding reaction yields, waste treatment requirements, and energy consumptions. Therefore, after the optimal production rate is reached, any change in the throughput will result in economic losses and is treated as a disturbance. Conversely, when there are economic incentives to increase the production rate, for example because of high demand or high price of the products, the throughput constraints become active before the efficiency constraints. Therefore, in the second scenario, the process operation will be constrained by the throughput bottleneck. The instances of these capacity constraints at the bottleneck are limitations in the liquid flow to a vessel, the pressure difference of a distillation column or the temperature constraint of a reactor.

While dynamic degrees of freedom are assumed to have less economic importance, it has been shown that they are critical when process economy is constrained by the maximum throughput. In this case, the loss of process throughput can be avoided by temporary reduction in the in-plant material inventory. Aske (2009c) studied two cases of a coordinated MPC and a ratio control structure to show how dynamic degrees of freedom (which apparently have no steady-state economic significance) can be employed to increase the economic profitability.

2.6.5. Complexity reduction based on causality analysis

Causality analysis using graph theory is a recently developed mathematical tool, which reduces the first principles model to a *signed directed graph* (SDG). Signed directed graphs are directed graphs, which represent the causal relationship between variables of a system. Often a sign or a weighting factor is added to an arc to represent of the direction or the intensity of that causality relation. The advantage of this methodology is that it extracts only the necessary data for the process modelling and makes the model interrogation easier than the equivalent first principles model.

Application of this method for fault detection in process industries has gained great interests. Maurya, et al. (2003a, 2003b, 2004) presented the review, including detailed evaluations of the advantages and disadvantages of the application of these graphs for representation of dynamic models. Yim, et al. (2006) and Thambirajah, et al. (2009) applied the methods of signed directed graphs and connectivity matrices to extract causality relation from process topology. Then, they used these data for evaluation of the performance of control loops and disturbance propagation. Also transfer entropy is applied by Bauer (2007, 2004) as a probabilistic tool to extract causal relationship between process variables from plant data. Hangos and Tuza (2001) applied the signed directed graphs for developing an optimal control structure selection in a decentralized control system. They demonstrated a one to one correspondence between linearized state space model and the weighted digraph. They use a method based on maximum weight matching for determining the best control structure.

2.7. Control design: controllers

This section discusses the different types of controllers. The corresponding node in the hierarchical tree of Figure 2.1 is shown in Snip 2.1.2. Temporal and spatial decentralizations of controllers are discussed. In addition, conventional multi-loop controllers and their counterparts, i.e., model predictive controllers are described. This section will provide supporting arguments for the following sections where the properties of control structures, implications of setpoint policies and interactions between control loops are discussed.

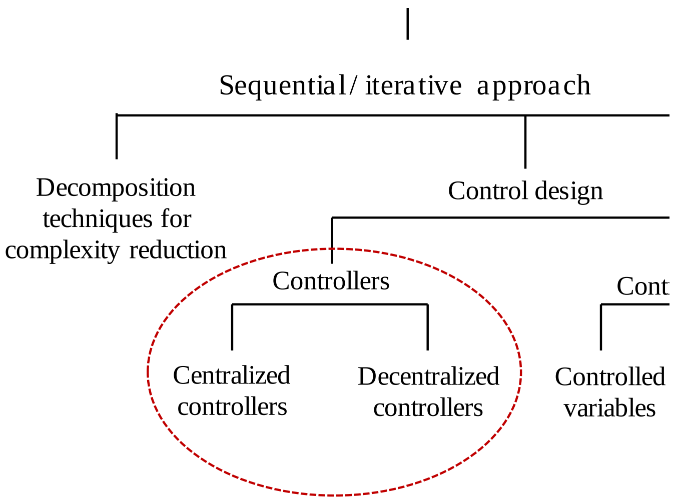

Snip 2.1.2. Research in the field: Controllers, (Figure 2.1 revisited).

2.7.1. Degree of decentralization: spatial

The degree of centralization can be defined as the level of independence of individual controllers within a control structure. Rawlings and Stewart (2008) classified the control structures into four groups:

1. Centralized control structures in which a centralized controller employs a single objective function and a single model of the whole system for decision-making,
2. Decentralized control structures in which the controllers are distributed and the interactions between subsystems are totally ignored,
3. Communication-based control structures in which each distributed controller employs a model for its sub-process and an interaction model for communicating with other sub-systems. However, the distributed controllers have their own objective functions. The disadvantage of communication-based structures is that controllers with individual objective functions may compete rather than cooperate with each other and make the whole system unstable.
4. Cooperative control structures in which the distributed subsystems employ an objective function for the whole system, and the predictions of each controller are available to other controllers. The improvement is not in awareness of the local controllers from each other, but in the same objective function that is employed by all of them. This framework is plant-wide stable with no offset and by convergence of the control calculations provides centralized optimal decision.

The decision regarding the degree of centralization significantly influences the design of control structures. In conventional multi-loop control systems (examples of decentralized controllers), the designer examines the alternative pairings between manipulated variables and controlled variables, often based on analysis of the interactions between corresponding control loops. However, in model predictive control (MPC) systems (examples of centralized controllers) these interactions are of no concern, because all manipulated and controlled variables are interconnected to each other through the control algorithm.

However, neither an entirely decentralized control structure nor a fully centralized one is desirable, and it is often favourable to employ some degree of decentralization which locates the control structure between these two extremes. The reason is that while a pure decentralized control structure does not necessarily ensures an optimal operation, there are many concerns regarding computational load, reliability, and the cost of implementation and maintenance of a large-scale centralized control structure.

Rawlings and Stewart (2008) also discussed that a fully connected communication strategy is unnecessary at least with respect to plant stability. However, the penalty of reducing communications is the synchronization of state calculations. In addition, reduction in communication between local MPCs causes problems in the systems with recycle streams (e.g. systems 1 and 2 in Figure 2.3), because it requires iterative calculation or one subsystem must do the calculations for the others. Therefore, a hybrid communication strategy is needed, in which a total communication scheme is considered for each recycle loop and a reduced communication scheme is considered for the rest of the process, (Rawlings and Stewart 2008). More details on the hierarchical and temporal coordination of distributed MPCs can be found in (Scattolini, 2009).

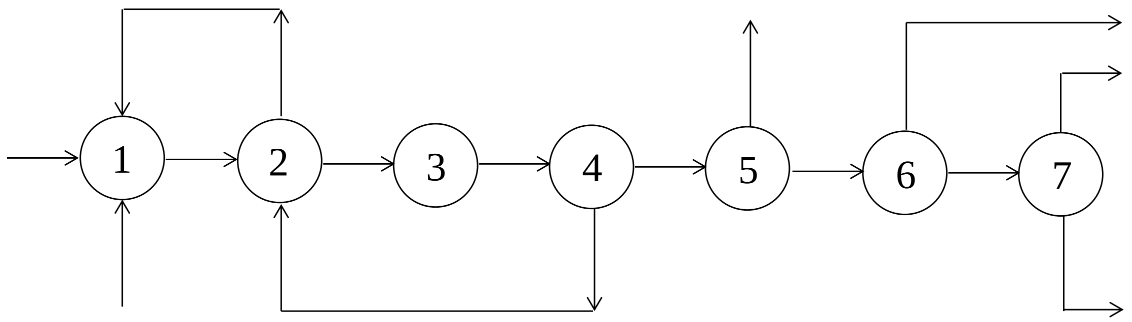

Figure 2.3. Ethylene glycol flowsheet: (1) Feed tank, (2) preheater, (3) reactor, (4) evaporator, (5) light end columns, (6) mono ethylene glycol column, (7) higher glycol recovery, (Rawlings and Stewart 2008).

2.7.2. Degree of decentralization: temporal

The above classification suggests a spatial decentralization. However, decentralization of controllers can be temporal, as shown in Figure 2.4 (adapted from Qin and Badgwell 2003). In the shown control structures, the decision-making process is decentralized vertically (top-down) through different time scales from days and weeks in the highest optimizing layer to seconds in the lower regulating layer. While the left structure shows a decentralized control structure, the right structure suggests a higher degree of centralization.

The top layer often employs a steady-state optimization for determining the setpoints. This information will be sent to the localized optimizers which may employ more detailed models and run more frequently. Detailed information will be sent to the constraint control system which is responsible for moving the process from one constrained steady-state to another one while minimizing the violation of the constraints. In the right control structure, a model predictive controller is responsible for constraint handling, while in the left control structure, a combination of PIDs, lead-lag (L/L) blocks and logic-based elements are responsible for constraint handling. The regulatory layer which runs at much higher frequency, is responsible for maintaining the controlled variables at their setpoints, (Qin and Badgwell 2003).

Figure 2.5 adapted from Harjunkoski et al. (2009) shows the control system in a broader context which conforms to the *automation* paradigm. The lowest layer is responsible for process control including regulatory control systems, as well as monitoring and fault diagnosing systems. The middle layer is responsible for production scheduling, quality assurance and more advanced control algorithms. On the top layer, the long-term production strategies are decides and the whole supply-chain including feedstock procurements, product warehousing, distributions and sales are coordinated. More details on automation can be found in ANSI/ISA-95 (2000, 2001, and 2005) standards which provide guidelines for the communication and information exchange between different sections of an enterprise and are not in the scope of the present research.

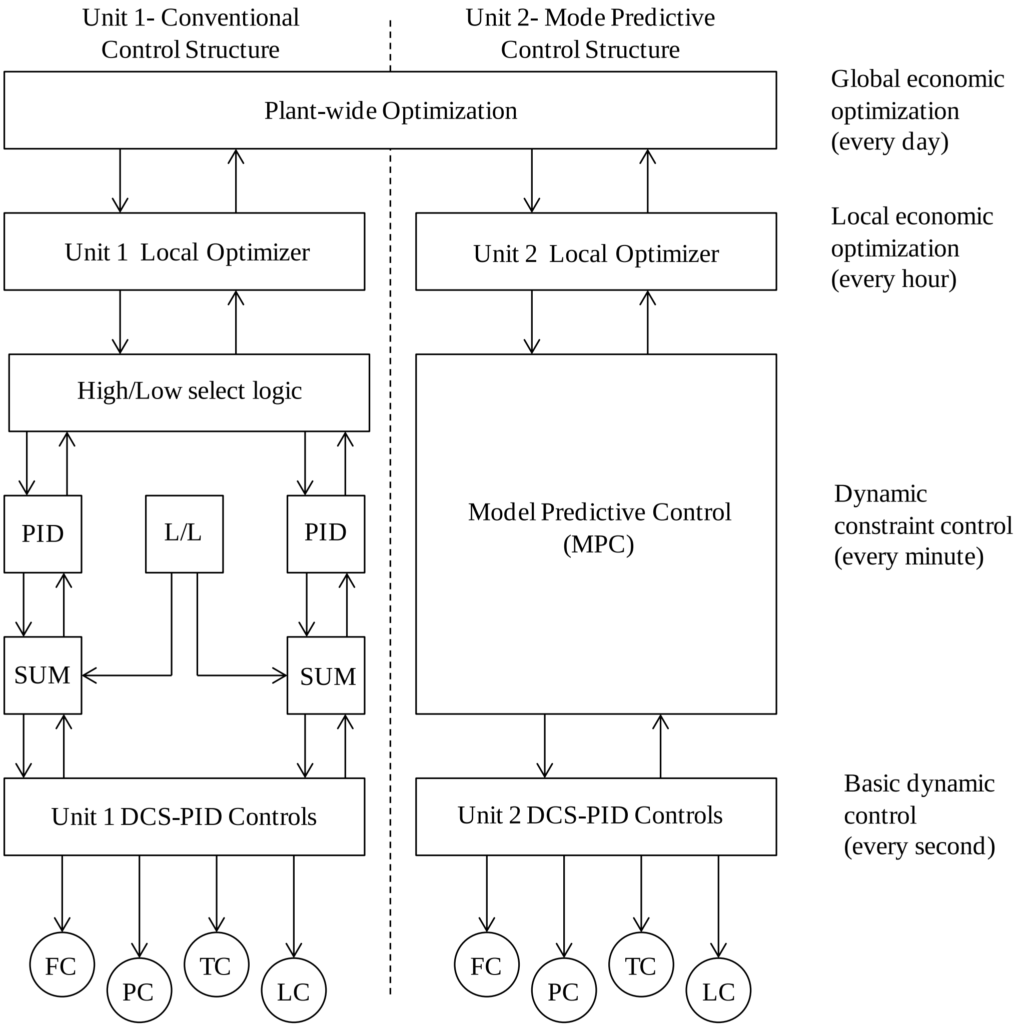

Figure 2.4. Hierarchy of conventional multi-loop and MPC structures are shown at the left and right respectively. (adapted from Qin and Badgwell 2003).

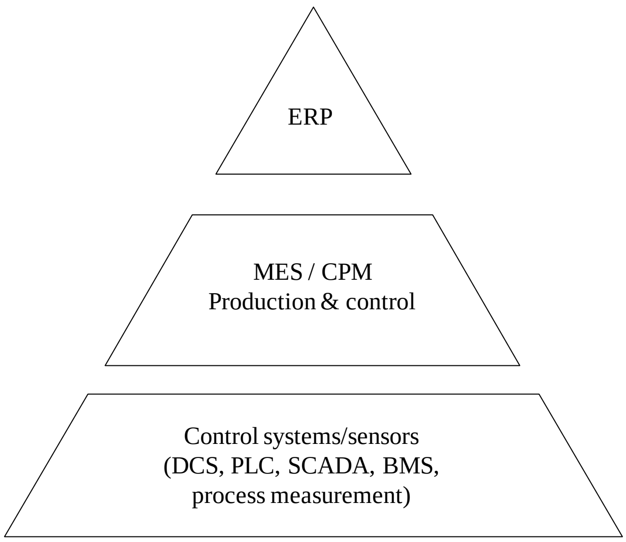

Figure 2.5. Automation pyramid (adapted from Harjunkoski et al. 2009)

2.7.3. Conventional multi-loop controllers

Chemical processes have some characteristics which make their control difficult. For example, when Qin and Badgwell (2003) were explaining the reasons for little impact of the linear quadratic Gaussian (LQG)-based technologies in process industries (despite their success in electronics and aerospace areas), they emphasized that chemical processes are nonlinear, constrained, and multivariable systems and their behaviours change over the time (e.g. ageing of catalysts). By contrast, conventional multi-loop controllers are proved to be efficient in controlling chemical processes. They have reliable operations and are understandable to operation people, (Downs and Skogestad 2011). In addition, there are efficient methods for off-line or on-line determination of their tuning parameters.

However, conventional multi-loop controllers have a significant drawback; leaving setpoints at constant values is a poor economic policy, because disturbances and the changes in economic parameters can change the desirable setpoints and even in some cases (e.g. moving bottleneck) require control structure reconfiguration, (Downs and Skogestad 2011). The treatment of economic losses due to constant setpoint policy will be discussed later in this chapter.

2.7.4. Model predictive controllers

This section discusses model predictive controllers (MPCs) briefly. A detailed review of the common MPC technologies and their characteristics is presented by Qin and Badgwell, (2003).

The concept is shown in Figure 2.6 adapted from Rawlings, (2000). The estimator block enquires the statuses and values of the manipulated and controlled variables and then using a model estimates the unmeasured states. Then, the target calculator calculates the target values of the manipulated and controlled variables. Finally, this information is used by a dynamic model (shown by the regulator block) to bring the process from the current state to the targeted state. The outcomes of these calculations are the decisions regarding adjustment of the manipulated variables. Richalet, et al. (1978) emphasized that the economic advantages of model predictive control systems derive from manipulation of the setpoints, which allows to operate closer to active constraints, and should not be merely attributed to application of the dynamic model used for minimizing the variations of the controlled variables (i.e. control error).

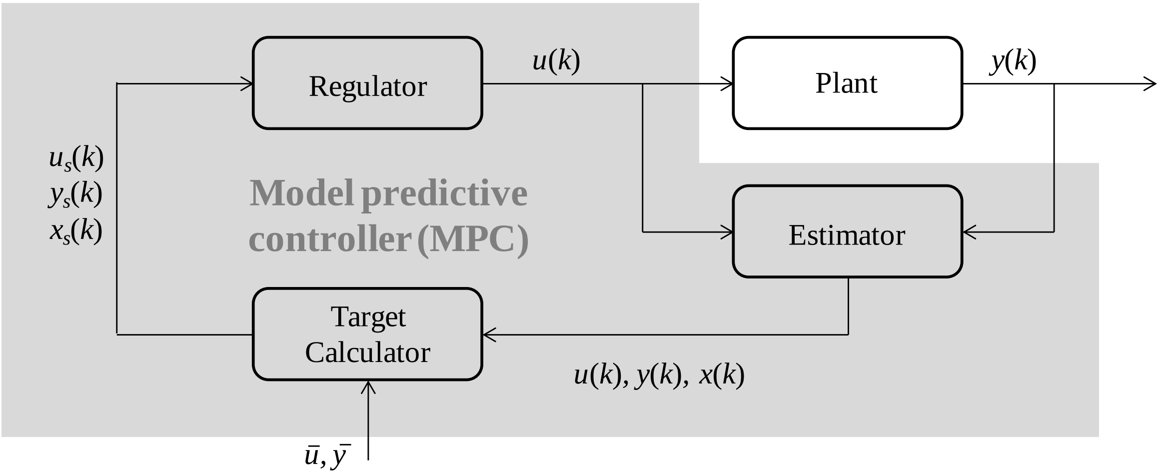

Figure 2.6. The block diagram representation of an MPC system: estimator, target calculator, regulator, (Rawlings 2000).

The capability for systematic constraint handling is another important advantage of MPC systems over multi-loop control systems. The modern MPC systems apply three types of constraint-handling methods. They are hard, soft and setpoint approximation constraint-handling methods. The hard constraints are those which are not allowed to be violated such as the constraints on the maximum, minimum, and the rate of the changes of manipulated variables. The soft constraints (e.g. the constraints on the controlled variables) are permitted to be violated to some extent and their violations will be minimized by penalizing the objective function. Another way of handling soft constraints is the setpoint approximation method. In this method, a setpoint is assigned to a soft constraint and the deviations on both sides of the constraint are penalized. However, the penalty weights are assigned dynamically so the penalty function becomes significant only when the constraint is likely to be violated, (Qin and Badgwell 2003).

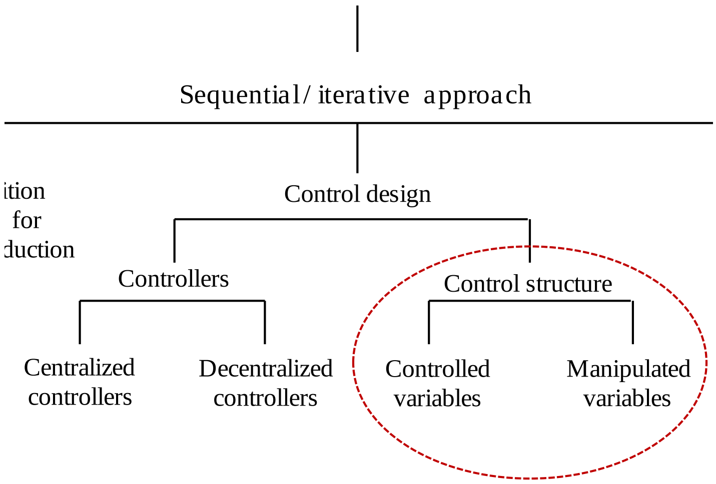

Snip 2.1.3. Research in the field: Control structures, (Figure 2.1 revisited).

2.8. Control design: control structures

This section discusses control structures. The corresponding node in the hierarchical tree of Figure 2.1 is shown in Snip 2.1.3. A control structure consists of controlled variables (CVs) and manipulated variables (MVs). Manipulated variables, also known as process inputs, are selected from the available degrees of freedom with desired properties for performing control actions. Controlled variables are those process variables which are selected to be maintained constant at their desired setpoints (or trajectories) by controllers. If direct measurement of a controlled variable is not possible then its value must be *inferred* or estimated from other process variables, (Qin and Badgwell 2003). These *inferential* controlled variables together with direct controlled variables are known as the measured variables. Selection of manipulated variables is the subject of degree of freedom analysis, as will be discussed later. However, selection of controlled variables should be conducted based on the process profitability.

The following subsections explore the characteristics of control structures and desirable properties of manipulated variables and controlled variables. The methods for degree of freedom analysis are reviewed and the implications of controlled variables and setpoint policy for process profitability are also discussed.

2.8.1. Control structure reconfiguration

A comparison between the populations of manipulated variables and controlled variables provides insights about feasibility of the control problem. Figure 2.7, adapted from Froisy (1994), depicts the alternative scenarios. In the design stage, the population of manipulated variables often exceeds the population of controlled variables and the plant control structure is underdetermined (right-hand side of Figure 2.7). In this case, extra manipulated variables are available for economic optimization. During the process operation, the population of the manipulated variables may decrease for example because of activation of constraints, saturation of control valves, or failures of control signals, which make the control structure over-determined (left-hand side of Figure 2.7), and consequently the control problem becomes infeasible. The middle control problem in Figure 2.7 represents a square problem with a deterministic solution. All these three scenarios may happen in the same control system. However, still the control system is expected to perform the best possible control action.

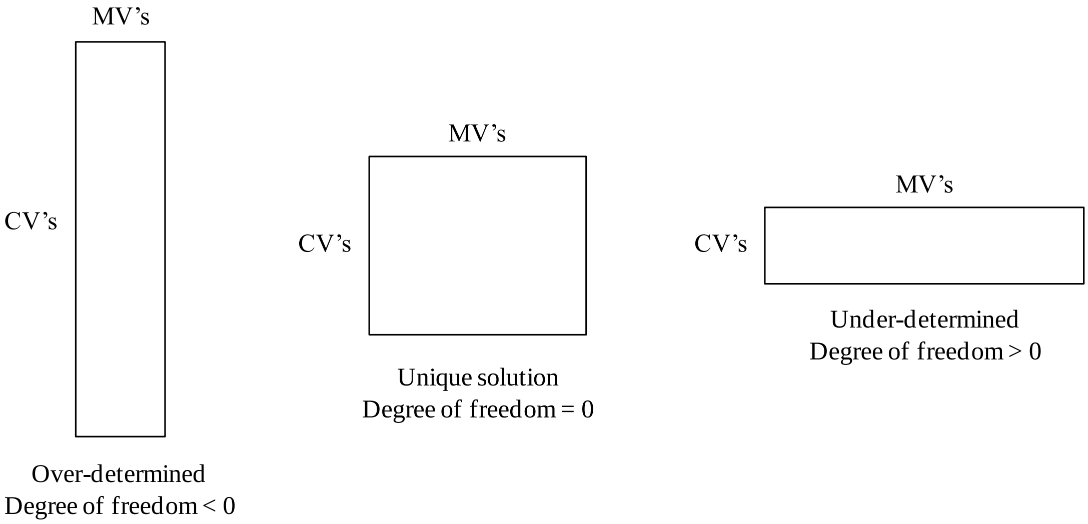

Figure 2.7. Different configurations of a control structure, (Froisy 1994).

For the case of conventional multi-loop control structures, drastic changes in economic parameters may enforce control structure reconfiguration. These scenarios are mostly concerned with the movements in active constraints. An example of necessary control reconfiguration is when the inventory control structure and throughput manipulation point must be reconfigured due to the movement of economic bottleneck(s), (Aske 2009c).

However, MPC systems are subject to dynamic changes in the dimension of the control problem during control execution. The reason is that the manipulated and controlled variables may disappear due to valve saturations, signal failures, or operator interventions in each control execution and return on the next one. These changes sometimes make the control configuration underdetermined and therefore perfect control (i.e., maintaining controlled variables at their desired values) would be infeasible. However, it is still desirable to have the best possible control action through the remaining manipulated variables. Unfortunately, depending on the size of the system, it may not be possible to evaluate all of the alternative subspaces of a control problem at the design stage. Therefore, MPC systems have an online monitoring agent that is responsible for subproblem conditioning. The strategy is to meet the control objectives based on their priorities, (Qin and Badgwell 2003). In MPC systems in order to avoid saturation of the manipulated variables, their nominal values are treated as additional controlled variables with low priorities. In addition, when a manipulated variable disappears from the control structure (e.g. because of operator intervention), it may be treated as a measured disturbance. Similarly, saturated valves are treated as one-directional manipulated variables. By contrast to manipulated variables, when a controlled variable is lost for instance because of signal failure or delay in measurements, the practical approach is to use the predicted value for it. However, if the faulty situation persists for an unreasonable number of execution steps, in some MPC algorithms the contribution of the missing controlled variable will be omitted from the objective function, (Qin and Badgwell 2003).

2.8.2. Degree of freedom analysis

Konada and Rangaiah (2012) presented a recent review of the methods for degree of freedom (DOF) analysis. Degrees of freedom can be evaluated as:

$$\text{DOF} = \text{number of unknown variables} - \text{number of independent equations} \quad (2-8)$$

However, in the context of control engineering, external variables such as disturbances also need to be considered, (Stephanopoulos 2003):

$$\text{CDOF} = \text{number of unknown variables} - (\text{number of independent equations} + \text{number of external variables}) \quad (2-9)$$

In which CDOF stands for control degrees of freedom and concerns the number of manipulated variables. The above approach has been applied by Seider, et al (2010) for a number of processes. However, for large processes, counting all the equations and variables may not be practical and is prone to mistakes. In addition, the focus of CDOF is mostly extensive variables. This is because manipulated variables are in principle defined as the flowrates of energy and materials (e.g., control valve openings, pump speeds, electricity streams). Therefore, researchers tried to develop methodologies which do not require first principles modelling and still are able to accurately determine the available degrees of freedom. Dixon (1972) introduced the notion of boundary variables. These are the variables which cross the predefined boundaries of a system. Furthermore, steady-state control degrees of freedom, CDOF_{ss} , were distinguished from dynamic control degrees of freedom.

$$\text{CDOF}_{\text{ss}} = N_{\text{bv}} - N_{\text{bes}} \quad (2-10a)$$

$$\text{CDOF} = \text{CDOF}_{\text{ss}} + N_0 \quad (2-10b)$$

N_{bes} represents boundary equations and N_{bv} represents boundary variables. N_0 is the number of independent holdups. Equation (2-10*b*) suggests that CDOF_{ss} is a subset of CDOF. Later, Pham (1994) introduced the concept of output control degrees of freedom:

$$\text{CDOF}_{\text{ss,out}} = \sum_k (P_k\, S_k) + M + E - N \quad (2-11)$$

where k is the number of circuits (a circuit is a set of streams connected inside the process), S is the number of stream split, P is the number of phases in the output stream of a circuit, M is the number of influential variables (e.g. a control valve), E is the number of energy streams, N is the number of phase constraints. The focus of Pham's method was the operational degrees of freedom that are the variables available for control when the process is built and is in operation. Konada and Rangaiah (2012) showed that Pham's method may result in wrong results because it assumes that the place of control valves are known in advance. However, Pham's method was a step forward because it recognized that in order to evaluate the correct number of degrees of freedom, it is not necessary to write all the equations. In an independent study, Ponton (1994) derived the general equations:

$$\mathrm{CDOF_{ss}} = n_i + n_o + n_e - P + 1 \qquad (2-12a)$$

$$\mathrm{CDOF} = n_i + n_o + n_e \qquad (2-12b)$$

where n_i is the number of inlet material streams, n_o is the number of outlet material streams, n_e is the number of energy streams and P is the number of phases. An interesting result from (2-12b) is that CDOF is independent of the number of phases. This is because in practice each phase is associated with an outlet stream and is considered implicitly. However, equation (2-12b) is of limited practicality because it is not possible to manipulate all streams simultaneously. This issue has been addressed by Konda, et al. (2006) and Vasudevan, et al. (2008) who recently proposed and examined a method which is flowsheet-oriented, and requires only the information of process flow diagrams and general knowledge of important unit operations. The idea is to identify the streams that are redundant or restrained from being manipulated. Then, this number can be subtracted from the overall number of streams to identify the available degrees of freedom. They argued that the restraining streams are mostly the characteristics of individual unit operations and not the process flowsheet and therefore, once they are calculated, they can be used in any complicated process flowsheet. They proposed the following correlation:

$$\mathrm{CDOF} = N_{\mathrm{streams}} - \sum_{1}^{\text{all the units}} (N_{\mathrm{restraining}}) - N_{\mathrm{redundant}} \qquad (2-13)$$

In above, N_{streams} is the total number of material and energy streams, $N_{\mathrm{restraining}}$ is the number of streams that cannot be controlled, and $N_{\mathrm{redundant}}$ is the number of streams that are not efficient to be manipulated (e.g., a material stream with small pressure drop). They further classified restraining streams based on the units with and without material holdups.

The number of restraining streams is equal to total independent and overall mass balances in units without holdups. This is because each mass balance imposes a constraint and reduces one degree of freedom. However, in the case of unit operations with material inventories, there is additional flexibility and all the streams can be manipulated provided that not all of them are used for controlling extensive variables. Therefore, the number of restraining streams is equal to the number of independent material balances which are not associated with any mass inventory. Since the number of restraining streams is the inherent characteristics of a unit operation and is constant regardless of the flowsheet configuration, Konda, et al. (2006) presented a table for the restraining variables of major unit operations. They also demonstrated their method for distillation columns and several complex flowsheets. Example of redundant streams in a distillation column is the stream connecting the column top to the condenser, the stream returning vapours from reboiler to the column and the column bottom sump which is sending liquids to the reboiler. They showed that in (total or partial reflux) distillation columns with total number of twelve streams, the number of restrained streams is three and the number of redundant streams is three and therefore the number of control degrees of freedom, CDOF , based on equation (2-13) is

$$\mathrm{CDOF} = 12 - 3 - 3 = 6 \qquad (2-14)$$

Details of their methods and analyses can be found in Konda, et al. (2006) or Konada and Rangaiah (2012).

2.8.3. Manipulated variables (MVs)

Manipulated variables are those degrees of freedom which are used for inserting the control action to the system. Although the degree of freedom is defined as the difference between the number of the variables and the number of the equations in the mathematical model, one must be careful, because each model represents the actual system in a range of scales and consequently resolution of the model may mislead the designer, (Stephanopoulos 1984). For instance, the molecular simulation cannot be used for degree of freedom analysis of a control system. In practice, degrees of freedom are interpreted from the number of manipulation devices (e.g. valves, electrical or mechanical equipment) which are able to modify the mass or energy flows into or from the process efficiently and consistently.

The manipulated variables can be classified into two categories of steady-state and dynamic degrees of freedom. Manipulated variables used for controlling material inventories are in the category of dynamic degrees of freedom (Skogestad 2004a). The steady state degrees of freedom affect the ultimate state of the process and have more economic significance than dynamic degrees of freedom.

The desired properties of manipulated variables are to be (i) consistent with each other, (ii) far from saturation, (iii) reliable. Two manipulated variables may be inconsistent when they cannot be adjusted simultaneously. The example of inconsistency is when two control valves adjust the flowrate of the same material stream. Reliability is defined as the probability of failure to perform the desired action. Reliability of manipulated variables is important because it is not desirable to select a manipulated variable which is likely to fail for example due to corrosion or erosion.

If the available degrees of freedom are not sufficient to meet the controllability requirements, there are some limited opportunities for adding degrees of freedom to the process for example by inserting bypass streams, heat exchangers or buffer tanks into the process flowsheet, (Skogestad 2004a). As discussed earlier, dynamic degree of freedom and inventory control can influence the economic profitability, when the throughput is an active constraint and limits the process profitability, (Aske 2009c).

2.8.4. Controlled variables (CVs)

Selection of controlled variables is more complicated compared to manipulated variables. This is because controlled variables can be categorized based on two different tasks. Firstly, these variables are responsible for detection of disturbances and stabilizing the process within its feasible operational boundaries. Secondly, selection of controlled variables and their setpoints provide opportunities to optimize profitability. The first category of controlled variables is selected for treatment of instability modes such as snowball effects (i.e., an instability mode concerned with materials inventories inside a recycle loop), or emptying/overflowing liquid holdups. The second category of controlled variables should be selected employing economic analysis.

In the subsequent sections, the conventional methods for selection of controlled variables are discussed and the effects of controlled variables and their setpoints on process profitability are explained. Here, the focus is on optimizing controlled variables.

2.8.4.1. Conventional methods for selection of controlled variables

The controlled variables can be selected by engineering insights and heuristics, especially when the control structure is developed for a single unit operation. In addition, controllability measures, to be discussed later, can be applied for selecting controlled variables. For instance, Luyben (2005; 2006) listed five methods for selecting the location of the temperature sensors (measured variables) within a distillation column, i.e., controlling the temperature of which tray inferentially ensures the desired compositions of the product streams. They are:

1. Slope criterion. In this method, a tray is selected, which has the largest temperature difference, compared to the neighbour trays.
2. Sensitivity criterion. In this method, a tray is selected, which its temperature changes the most for a change in a manipulated variable.
3. Singular value decomposition (SVD) criterion. This method is based on calculating the process gain matrix and its singular values as described by Moor, (1992).
4. Invariant temperature criterion. In this method, a tray is selected which its temperature does not change when the feed composition is changed and the compositions of the products are fixed.
5. Minimum product variability criterion. In this method, a tray is selected which if maintained constant results in least variability in the compositions of the products.

The other common approach for selection of controlled variables, in particular for decentralized control systems is to minimize the interactions between control loops using relative gain arrays (RGAs), as will be discussed later in this chapter. However, none of the abovementioned methods ensures minimum economic losses in the presence of disturbances. The subsequent sections explain that optimal selection of controlled variables can ensure profitability.

2.8.4.2. Setpoint policy

When a control structure is designed for a process, the objectives for controlling that process such as stabilizing, safety concerns, environmental constraints, and profitability will be translated to maintaining a specific set of controlled variables at their setpoints. However, some of targets of the abovementioned objectives may need to be updated after the design stage. This can be due to disturbances, the changes in environmental or safety policies, the changes in the specifications of products or feedstocks, or even because of changing the process model over time (e.g. ageing of catalysts). The ability of the control structure to keep pace with these changes is crucial for feasibility and profitability of that process.

As will be discussed in the subsequent subsections and shown in Figure 2.8 adapted from Chachuat, et al. (2009), two strategies are possible for ensuring process feasibility and profitability. They are (i) static setpoint policy: off-line optimization and (ii) dynamic setpoint policy: on-line optimization. These are shown by red vertical envelopes in Figure 2.8. The methods for dynamic setpoint policy may apply two approaches. In the first approach, the measurements are used to update the model parameters (shown by model parameter adaptation) and in the second approach, the measurements are used for updating modifier terms which are added to the objective function of the online optimizer, (shown by modifier adaptation).

The other classification, shown by grey horizontal envelopes, is according to (a) feasibility and (b) optimality criteria. Chachuat, et al. (2008) showed that the results of variational analysis in the presence of small parametric errors conform to the common sense that feasibility is of a higher priority than optimality. The references in the figure highlight the active researchers in the area. The dynamic and static setpoint policies are discussed in the subsequent subsections.

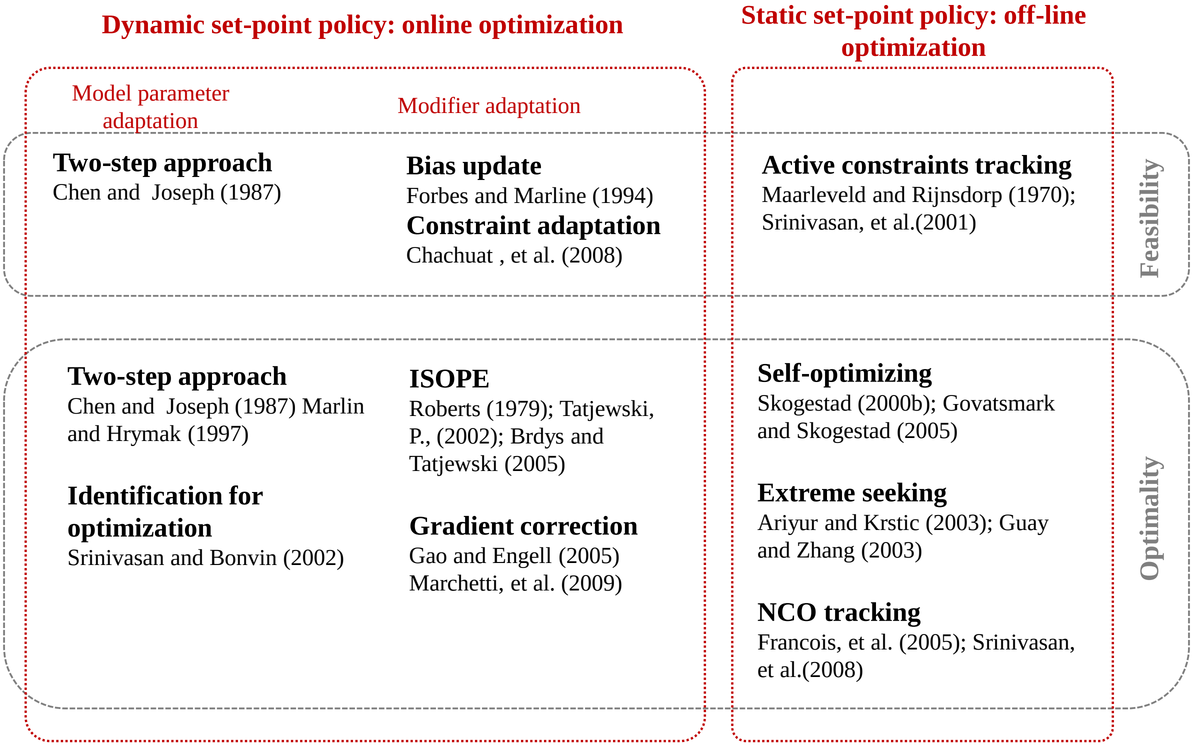

Figure 2.8. Setpoint policies; the methods for static and dynamic setpoint policies are shown by the red envelopes. The other classification is according to optimality and feasibility criteria, shown by the grey envelopes, (Chachuat, et al. 2009).

2.8.4.2.1. Static setpoint policy

The motivation for the static setpoint policy is that, while the costs of the development and maintenance of a model-based online optimizer are relatively high, selection of the controlled variables that guarantee a feasible and near optimal operation is by no means trivial. Static setpoint policy has a direct relation to the optimal selection of controlled variables. In this approach, online optimization of setpoints is substituted by maintaining optimal controlled variables constant. This approach is also consistent with the culture of industrial practitioners who would like to counteract model mismatches and the effects of disturbances by feedback control, (Chachuat, et al. 2009). Similarly, Engell (2007) emphasized that feedback control is indispensable for handling uncertainties during design stage and for utilizing the full capacity of equipment.

Morari, et al. (1980a) introduced the idea of optimal selection of controlled variables:

"In attempting to synthesize a feedback optimizing control structure, our main objective is to translate the economic objective into process control objectives. In other words we want to find a function c of the process variables [...] which when held constant, leads automatically to the optimal adjustment of the manipulated variables, and with it, the optimal operating conditions."

Later, researchers (e.g. Skogestad 2000a, 2000b, 2004b; Kariwala 2007) investigated the possibility of optimal selection of controlled variables. Figure 2.9, adapted from Skogestad (2000b), shows that the costs (i.e. the losses or decreases in profitability) associated with disturbances, are not the same for two different controlled variables. These controlled variables were maintained constant at their corresponding setpoints and the corresponding losses are compared to the scenario in which the objective function is re-optimized.

As can be seen from the figure, in the presence of disturbance d, the loss associated with maintaining $C_{1,s}$ at its setpoint is significantly lower than $C_{2,s}$. This observation suggests that selection of controlled variables can be employed as a method for off-line optimization of process profitability.

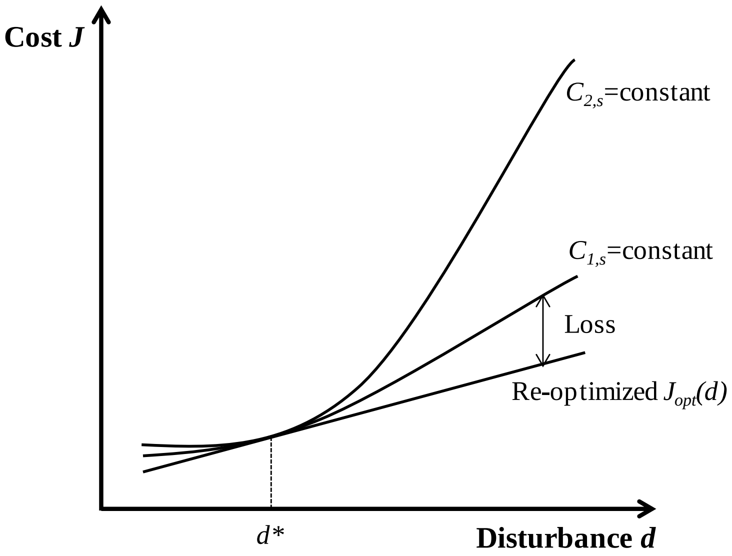

Figure 2.9. Maintaining the setpoints at constant values results in economic loss (distance between the re-optimized curve and the actual curve) due to a disturbance. However, the associated costs strongly depend on the selected controlled variable, (Skogestad 2000b).

Optimal controlled variables can be selected using *brute-force* optimization and direct calculations of the losses for different sets of controlled variables. Halvorsen, et al. (2003) presented a local method for optimal selection of controlled variables based on maximization of the minimum singular value. In that method, it was assumed that the setpoint error of different controlled variables (i.e., the difference between the selected setpoint and the re-optimized setpoint) are independent of each other, which does not often hold. Later, Alstad, et al. (2009) showed that an optimal linear combination of controlled variables is more likely to minimize the losses. This local method, called *null space* method, is based on the idea that the setpoints of optimal controlled variables must be insensitive to disturbances. This method ignores the measurement error. The work of Alstad, et al. (2009) also extends the methodology to the cases in which measurements are in excess or are fewer than the available inputs and the expected disturbances. The above methods are based on a quadratic objective function and linearization of the model. Therefore, the results are local and must be checked by a nonlinear model.

Kariwala (2007) proposed a computationally efficient method using singular value decomposition and Eigen-values for selection of optimal controlled variables. Later, this method was extended (Kariwala, et al. 2008) to use *average losses* instead of *worst-case losses*. The justification for using average losses instead of worst-case losses is that the latter may not happen frequently and would result in unreasonable loss of the control performance. Kariwala, et al. (2008) also showed that minimization of average losses also had already minimized worst-case losses and was superior when the actual disturbance differs significantly from the average value.

Although maintaining controlled variables or a linear combination of them is convenient, there is no guarantee that the optimal operation is reached by the convergence. The reason is that in the presence of disturbances, the gradient of the cost function may changes from zero. In addition, the gradient of the cost function may have a nonzero value for a constrained solution. Therefore, Cao, (2005) suggested that the sensitivity of the reduced gradient function to disturbances and implementation errors is a reliable method for selection of controlled variables. Alternatively, some researchers chose to directly control the elements of the necessary condition for optimality. It can be shown (Chachuat, et al. 2009) that by determining the set of active constraints, the elements of the necessary condition for optimality can be decomposed into two categories. The first category ensure that the process operation remains feasible (i.e., constraints are satisfied). The second category ensures an optimal operation (i.e., reduced gradient is equal to zero).

However, the main difficulty associated with the methods based on static setpoint policy, is that active constraints may change. The methods for constraint handling proposed by researchers are split-range control (for the constraints on manipulated variables), parametric programming, cascade control approach, and explicit constraint handling. Details of these methods can be found in literature (e.g., Umara, et al. 2012).

2.8.4.2.2. Dynamic setpoint policy

The methods in the second category (shown by the left red envelope in Figure 2.8) apply an online optimizer to update the setpoints. The main challenge in the application of online optimizing control systems is the inability to develop accurate and reliable models with a manageable degree of complexity and uncertainty. The reason is that online optimization using an inaccurate model may result in a suboptimal or even infeasible operation, (Chachuat, et al. 2009). The two main approaches are (i) the methods for model parameter adaptation, in which the available measurements are used to refine the process model parameters; then this model is used for optimization, (Chen and Joseph, 1987; Marlin and Hrymak, 1997), and (ii) the methods for modifier adaptation in which modifier terms are added to the objective function and constrains and these modifiers are updated using available measurements, (Forbes and Marlin, 1994; Gao and Engell, 2005; Roberts, 1979; Tatjewski, 2002). The details and comparison of these methods are available in literature, (e.g., Chachuat, et al. 2009).

Recently, integration of economic optimizing layer and lower regulatory control layers (Figure 2.4) has been the focus of several research activities. The motivation for this integration is that operating the optimization layer intermittently, and at a slow sampling rate may incur economic penalties. In the new integrated scheme, referred to as the *direct approach*, the available degrees of freedom are directly used to optimize an economic objective function, over a prediction horizon and using a nonlinear rigorous process model. The review of these methods can be found in literature, (e.g., Engell, 2007, Kadam and Marquardt, 2007).

2.9. Controllability measures

Significant research activities have been devoted to understanding the controllability characteristics of chemical processes. In this section, firstly the definitions of operability and controllability are presented. Later the limiting factors of controllability are reviewed. The corresponding nodes in the hierarchical tree of Figure 2.1 are shown in Snip 2.1.4. They are discussed in the following subsections.

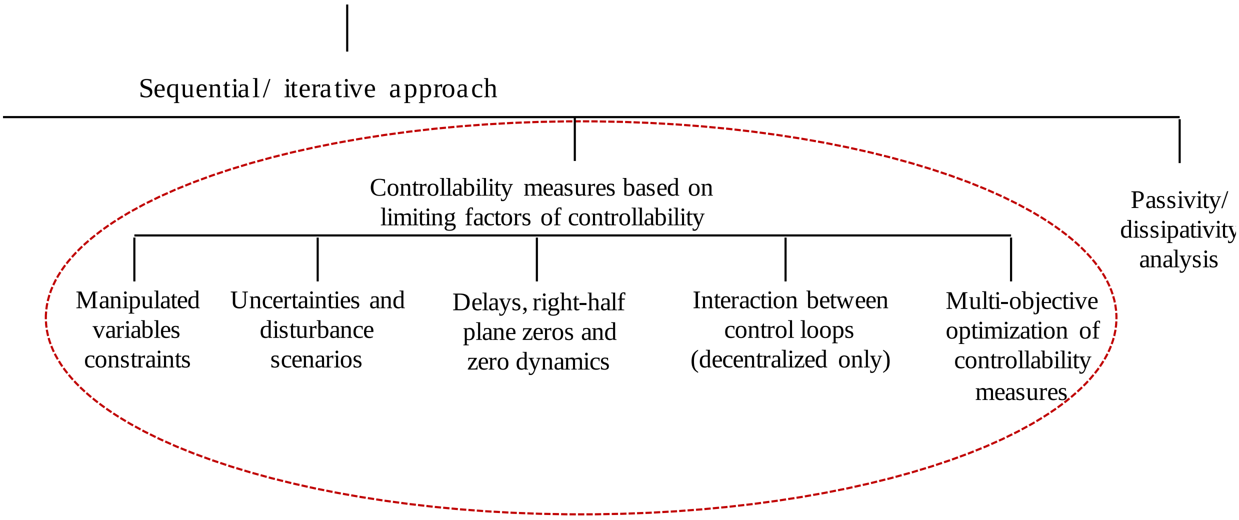

Snip 2.1.4. Research in the field: Controllability measures, (Figure 2.1 revisited).

2.9.1. Flexibility, operability, switchability and controllability

The operability of a chemical process strongly depends on its operational mode, i.e. whether it deals with a constant load, or the load is time-dependent. A continuous operation implies that the process spends most of its life cycle within a narrow envelope of steady states. Therefore, the control task is posed as regulation (i.e., disturbance rejection). By contrast, shutdowns, start-ups, and the operations of semi-continuous or periodic processes involve transient conditions along the desired time trajectories, and servo control is needed, (Pedersen, Jørgensen, and Skogestad 1999).

Operability is defined as the ability of input (manipulated) variables to meet the desired steady-state and dynamic performance criteria defined in the design stage, in the presence of expected disturbances, without violating any constraint, (Georgakis, et al. 2004). The mathematical descriptions of dynamic operability and steady-state operability are presented in Section 2.14. The implication of steady-state operability for the methods proposed in this research will be discussed in Chapter 3.

Flexibility is defined as the ability to achieve a feasible operation over a range of uncertainties, (Dimitriadis and Pistikopoulos 1995). The mathematical programming of steady-state and dynamic flexibility optimizations are presented in Section 2.15.

Switchability is define as the ability to move between operating points, (Pedersen, Jørgensen, and Skogestad 1999).

A comparison between the definitions of operability and flexibility reveals some similarities and some differences. Both criteria emphasize the importance of ensuring a feasible operation by avoiding constraint violation. However, the criteria for flexibility also include the uncertainties in the model parameters, while in evaluating operability the focus is on disturbance scenarios.

In addition, a variety of qualitative and quantitative definitions is available in literature for *controllability*, which reflects the experience of researchers. From the early studies, Ziegler, Nichols and Rochester (1942) suggested that their proposed test for finding tuning parameters can be used for classification of processes. Morari (1983) introduced the term *resiliency* that includes both switchability and controllability and is defined as the ability to move smoothly and rapidly between operating conditions and to effectively reject disturbances. He recognized that controllability is the inherent property of the process and does not depend on the controller design.

Kalman (1960) introduced the concept of *state controllability*. A state x is controllable, if for an initial condition $x_0 = x(t_0)$ and a final state x_1, there exist a manipulated variable $u_1(t)$ and a final time t_1 , $0 < t < t_1$, such that $x_1 = x(t_1)$. In other words, the state controllability is the ability to bring the system from the initial state to the final state in a finite time.

Another important concept is *input-output controllability*. It is the ability to maintain the controlled variables $\boldsymbol{y}(t)$, within their desired bounds or displacements from their setpoints $\boldsymbol{r}$, in the presence of unknown but bounded disturbances d, using the available manipulated variables u, (Skogestad and Postlethwaite 2005).

A process is *functionally controllable* if for the desired trajectories of the output variables, $\boldsymbol{y}(t)$, defined for $t > 0$, there exist some trajectories of the input variables, $\boldsymbol{u}(t)$, defined for $t > 0$, which generates the desired controlled variables from the initial states $\boldsymbol{x}(t_0)$, (Rosenbrock 1970).

In is notable that functional controllability depends on the structural properties of the system, i.e., a system that is functionally controllable with respect to a particular set of controlled variables may be rendered uncontrollable for another set, (similar to the situation for structural identifiability). Furthermore, functional controllability is defined with respect to a set of the desired trajectories of controlled variables. Therefore, a system may be functional controllable for a set of controlled variable trajectories and become uncontrollable for another set. Furthermore, functional controllability has a clear relationship with perfect control, i.e., the controlled variables are maintained constant at their setpoints (or the desired trajectories) and the manipulated variables are adjusted accordingly, which is also recognized by other researchers. For example, Russel and Perkins (1987) applied the concept of functional controllability and process inversion for discussing the causes of control imperfection in linear systems. The necessary and sufficient condition for functional controllability and the characteristics of the desired controlled variable trajectories will be discussed later in Chapter 3.

In addition, a comparison between the definitions of different controllability criteria suggests that functional controllability is more constraining compared to input-output controllability. This is because for a system to be functionally controllable the controlled variables should take the values of the desired trajectories. Therefore, their values are necessarily bounded, and the system features input-output controllability. However, the reverse is not true, because in the case of input-output controllability, although the system is required to have bounded outputs, it is not necessarily capable of following a certain desired trajectories of the controlled variables.

Functional controllability and input-output controllability concern only manipulated and controlled variables. On the other hand, state controllability additionally considers the initial and final conditions of the internal states. However, there is not a requirement for the controlled variables to follow a certain set of trajectories and a system which is state controllable may not be functionally controllable. However, a state controllable system has bounded inputs and outputs and is input-output controllable. Finally it is notable that a system which is functional or input-output controllable is not necessarily capable of ensuring certain initial and final values for the internal states because functional controllability and input-output controllability do not consider internal states. Therefore, functional controllability and input-output controllability do not ensure state controllability.

2.9.2. Causes of control imperfection

Early studies in this research field had an *evaluation* attitude, i.e. *"if the process is controllable at all?"* Later, the viewpoint of these studies evolved to address the question of *"how controllable the process is?"*, (Downs and Skogestad 2011). Several measures were introduced based on understanding of what limits process controllability. Moaveni and Khaki-Sedigh (2009) presented a recent review of these methods.

The idea is to apply the controllability measures iteratively in the process design stage in order to screen and eliminate solutions with undesirable properties. The limiting factors of process controllability can be classified as:

1. Interactions between control loops,
2. Manipulated variable constraints,
3. Delays and right-half-plane zeros,
4. Model uncertainties, and
5. Effects of disturbances.

A variety of methods for quantifications of these deficiencies is available in literature, which with exception of few, all of them rely on linear models, as discussed in the following.

2.9.2.1. Interactions between control loops

Bristol (1966) introduced relative gain arrays (RGAs) as the measure for the interactions between control loops, which has received significant industrial and academic attentions and is applied for pairing controlled and manipulated variables. An element of a relative gain array, $\mathbf{\Lambda} = [\lambda_{ij}]$, represents the ratio of the open loop gain from the manipulated variable j to the controlled variable i, in which all the control loops are open, to the closed-loop gain in which all control loops, except the loop $i - j$, are perfectly controlled (Ogunnaike and Ray 1994):

$$\lambda_{ij} = \frac{\left(\partial y_i / \partial m_j\right)_{\text{all loops open}}}{\left(\partial y_i / \partial m_j\right)_{\text{loop } m_j \text{ open; all other loops closed with perfect control}}} \qquad (2-14)$$

Since then, the Bristol's method has been extended by many researchers in order to capture the different characteristics of the interactions in decentralized control structures. Since static RGA methods do not consider dynamic information, dynamic relative gain arrays (DRGAs) were introduced, in which transfer functions replace steady-state gains. The numerator is open loop transfer function but denominator is perfectly controlled for all frequencies. The DRGAs rely on *a priori* decision about the type of controllers (McAvoy, et al. 2003). The applications of RGA methods are not limited to single-input single-output (SISO) control systems. Manousiouthakis and Nikolaou (1989) introduced static nonlinear block relative gain arrays (NBGA) and dynamic nonlinear block relative gain arrays (DNBGA) as measures for the interactions between different blocks of a decentralized control structure.

Another relevant criterion is the *integrity* of a decentralized control structure, which ensures that system remains stable while individual control loops are brought in and out. Niederlinski (1971) presented the integrity measure as:

$$NI = \det[\mathbf{G}(0)] \Big/ \prod_{i=1}^{n} g_{ii}(0) \qquad (2-15)$$

where $\mathbf{G}[g_{ij}]_{n\times n}$ is the transfer matrix of a process. It is proved that if under closed loop condition the Niederlinski Index is negative, ($NI < 0$), the multi-loop control structure will be unstable for all values of the controller tuning parameters. This result is necessary and sufficient for 2×2 systems. However, for higher order systems it is a sufficient condition, i.e., if $NI < 0$, the system will be unstable, (Ogunnaike and Ray 1994)

It is notable that the interactions between control loops limit controllability of decentralized control systems and is not of concern for centralized control systems, (Ogunnaike and Ray 1994).

2.9.2.2. Manipulated variable constraints and the effects of disturbances

The effects of manipulated variable constraints can be measured using the methods for singular value decomposition (SVD). Consider the linear transfer function model below:

$$\mathbf{Y}(s) = \mathbf{G}(s)\mathbf{u}(s) + \mathbf{G_d}(s)\mathbf{d}(s) \qquad (2-16)$$

The gain matrix, $\mathbf{G}$, should be firstly scaled as $\mathbf{G}'(s) = S_1\mathbf{G}(s)\,S_2$ in which S_1 and S_2 are output and input scaling vectors respectively. The importance of input scaling is sometimes neglected. However, Hori and Skogestad (2008) showed that for ill-conditioned processes such as distillation columns, input scaling is crucial. Then, the scaled gain matrix, $\mathbf{G}'(s)$, is decomposed into the products of two rotational matrices and a diagonal matrix of singular values. The smallest and largest singular values (σ_{min} and σ_{max} respectively) and their ratio (called condition number, γ) have implications for the constraints on the manipulated variables and hence process controllability. The singular value decomposition method relies on the property that the bounds on the reproducible output region depend on the minimum and maximum singular values and their ratio, (Cao, Biss and Perkins 1996):

$$\sigma_{min}(\omega)\|\mathbf{u}(j\omega)\|_2 \leq \|\mathbf{y}(j\omega)\|_2 \leq \sigma_{max}(\omega)\|\mathbf{u}(j\omega)\|_2 \qquad (2-17)$$

$$\gamma = \sigma_{min}/\sigma_{max} \qquad (2-18)$$

Therefore, it is desirable that σ_{min} and σ_{max} have large values to minimize the influence of manipulated variable constraints. However, the ratio of them, i.e., the condition number (CN), is also important because large γ implies strong dependency of output amplitude on the direction of input amplitude (Morari and Zafiriou 1989), therefore, γ close to one is desirable. Furthermore, a large minimum singular value, σ_{min}, is desirable because it ensures that larger disturbances can be handled by the manipulated variables. In other words, the magnitudes of the disturbances that can be rejected depend on the manipulated variable constraints.

2.9.2.3. Delays, right-half-plane zero, and non-minimum-phase behaviour

Delays, right-half-plane zeros, and non-minimum phase behaviours have implications for closed loop performances, as discussed in the following.

Holt and Morari (1985) showed that in a multi-variable closed loop system, the minimum bound on the settling time for a controlled variable i is $\tau_i = min\, p_{ij}$, where p_{ij} is time delay in the numerator of element g_{ij} in the transfer function matrix, $\mathbf{G}(s)$. In addition, based on functional controllability, Perkins and Wong (1985) characterized a multi-variable system based on parameter Δ_{min}, which is the period that must be waited before the output trajectory can be specified independently, otherwise perfect control is not achievable. This period is bounded by the smallest and largest time delays in the process transfer function.

When process model is inverted, right-half-plane zeros become poles. It is well understood that right-half-plane zeros cannot be moved by any feedback controller and similar to time delays, they are the characteristics of the process (Yuan, et al. 2011). In particular, right-half-plane zeros limit the control performance of feedback controllers, (Skogestad and Postlewaithe 2005).

Zero dynamics are defined to be the internal dynamics of a nonlinear system when the deviations of the controlled variables (process outputs) are maintained at zero using the manipulated variables (process inputs). Unstable zero dynamics are the nonlinear analogues of right-half-plane zeros, and imply instability of process inversion, called non-minimum phase behaviour (Isidori 1989, Slotine 1991). The effects of input multiplicity on degrading switchability due to non-minimum phase behaviour are also studies by Kuhlmann and Bogle (2001; 2004).

2.9.2.4. Model uncertainties

Skogestad and Morari (1987) studied the effects of model uncertainties on control performances. Uncertainties in the process model require that the actual controller be detuned and hence degrade the control performance. In the case that the relative errors of transfer matrix elements are independent and have similar magnitude bounds, they concluded that the relative gain array can be an indicator of closed loop sensitivity to uncertainties. Other contributions to quantify the effects of uncertainties, which are not limited to linear models, have been made by optimization-based methods, namely back-off (Narraway and Perkins 1991) and flexibility optimization (Swaney and Grossmann 1985) methods, as will be discussed later in this chapter.

2.9.2.5. Multi-objective optimization methods based on controllability measures

One of disadvantages of controllability measures is that each measure only considers a single cause of control imperfection. To address this issue, Cao and Yang (2004) proposed a multi-objective framework based on linear matrix inequalities (LMIs), which considers different controllability measures such as control error and control input effort.

The other issue about methods based on controllability measures is that enumeration and evaluation of all possible alternative solutions can lead to an intractable problem. In order to overcome this difficulty, researchers (Cao and Kariwala 2008; Kariwala and Cao 2009, 2010a, 2010b) proposed an optimization framework based on a bi-directional branch and bound algorithm for screening alternative solutions, in which the nodes that do not lead to the optimal solution are eliminated faster and a smaller number of nodes need to be evaluated.

2.10. Methods based on passivity/dissipativity

The focus of the methods based on passivity/dissipativity analysis, is stability of decentralized control systems. The corresponding node in the hierarchical tree of Figure 2.1 is shown in Snip 2.1.5.

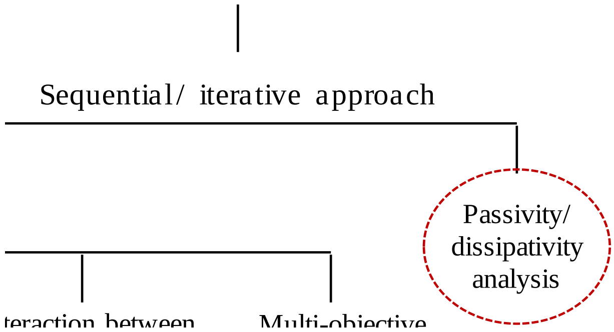

Snip 2.1.5. Research in the field: Methods based on passivity/dissipativity, (Figure 2.1 revisited).

A comprehensive review of the methods for passivity analysis is presented in a book written by Bao and Lee (2007), for which a review is also provided by Ydstie, (2010). By definition, a dissipative system cannot deliver energy more than stored in it. This can be formulated by the following equation:

$$W(t_1) \leq W(t_0) + \int_{to}^{t1} \varphi(\boldsymbol{y}(t), \boldsymbol{u}(t))dt \qquad (2-19)$$

in which, $\varphi(\boldsymbol{y}(t), \boldsymbol{u}(t))$ is energy supply rate (energy/time), and $W(t) \geq 0$ is the stored energy at time t. The above correlation is called dissipation inequality. $W(t_1)$ can be any generalized energy function and $\varphi(\boldsymbol{y}(t), \boldsymbol{u}(t))$ can be any abstract power function. In the following, three functions for energy supply rate are discussed, (Rojas, et al. 2009).

A system is called passive if $\varphi(\boldsymbol{y}(t), \boldsymbol{u}(t)) = \boldsymbol{y}(t)^{\boldsymbol{T}}\boldsymbol{u}(t)$. Then, for $\mathbf{y}(t) = -k\boldsymbol{u}(t)$:

$$k\int_{to}^{t1} \boldsymbol{y}^2(t)dt \leq W(t_0) \qquad (2-20)$$

where $k > 0$ is the gain. Therefore by choosing an appropriate value for k, any passive system can be controlled using proportional controllers. Furthermore, it is possible to prove that two passive systems connected by feedback control are also passive. The other systems of interest are *input feedforward passive* (IFP) systems in which:

$$\varphi(\boldsymbol{y}(t), \boldsymbol{u}(t)) = \boldsymbol{y}(t)^{\boldsymbol{T}}\boldsymbol{u}(t) - v\boldsymbol{u}(t)^{\boldsymbol{T}}\boldsymbol{u}(t), \ \ v > 0 \qquad (2-21)$$

and *output feedback passive* (OFP) systems in which:

$$\varphi\big(\boldsymbol{y}(t),\boldsymbol{u}(t)\big) = \boldsymbol{y}(t)^{\boldsymbol{T}}\boldsymbol{u}(t) - \rho\boldsymbol{y}(t)^{\boldsymbol{T}}\boldsymbol{y}(t), \;\; \rho > 0 \qquad (2-22)$$

A nonlinear input feedforward passive system is minimum phase (i.e., it has stable zero dynamics) and an output feedback passive system has bounded gains (i.e., it is input-output stable). If the dissipative inequality holds but with $\rho < 0$ or $\upsilon < 0$, then it is in shortage of IFP or OFP, respectively. The shortage of IFP (or OFP) of a subsystem can be compensated with the excess of IFP (or OFP) of another subsystem in the same process network.

These properties serve as the foundations for studying stability of process networks and evaluation of controllability of decentralized and block-decentralized multivariable systems. The methodology is also extended to analyse the system integrity, i.e. whether the system remains stable if a control loop fails, and what back-up control loops are required in order to design a fault tolerant system. The advantage of passivity methods is that their representations are not limited to linear models. However, the required modelling efforts have limited their application to small problems, (Yuan, et al. 2011). Furthermore, the focus of these methods is feasibility rather than optimality of operation and control. However, establishing a trade-off between competing control and process objectives is the key requirement for integrated design and control. In addition, these methods are based on input-output representation of subsystems of a process network and ignore the underlying first principles that link these inputs and outputs, which suggests an iterative approach to the problem of integrated design and control.

2.11. Multi-objective optimization methods to incorporate controllability measures into the process design

The methods using controllability measures suffer from several disadvantages. They have a yes/no attitude and each of these measures only concerns a certain limiting factor of controllability and at most can be used for highlighting the situations in which process controllability is lost. Acknowledging these limitations, some research activities have focused on defining multi-objective criteria to incorporate controllability measures into the process design. The corresponding node in the hierarchical tree of Figure 2.1 is shown in Snip 2.1.6.

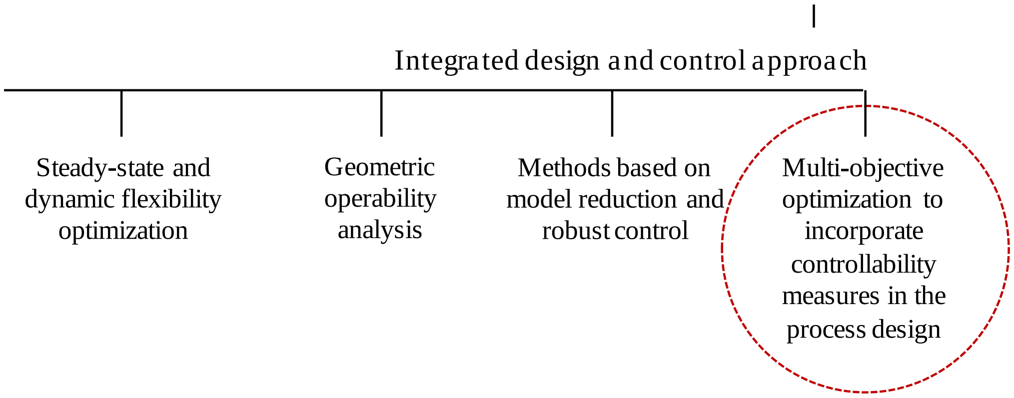

Snip 2.1.6. Research in the field: Multi-objective optimization to incorporate controllability measures into the process design, (Figure 2.1 revisited).

Luyben and Floudas (1994) employed a multi-objective function for incorporating controllability measures and economic objectives. The economic objectives such as capital costs and operating costs were calculated using a steady-state model while bounds on controllability objectives were calculated using measures such as relative gain array, minimum singular value, condition number, and disturbance condition number. The resulting MINLP formulation was solved using generalized benders decomposition (GBD) algorithm. Similarly, Chacon-Mondragon and Himmelblau (1996) proposed a bi-objective optimization in which costs and flexibility were optimized simultaneously. Later, Alhammad and Romagnoli (2004) proposed an optimization framework in which process economy, controllability and environmental measures were incorporated into a multi-objective function.

2.12. Methods based on model reduction and robust control measures

In order to reduce the numerical complexities of underlying mixed integer nonlinear dynamic optimization problem, Douglas and co-workers proposed a method based on model reduction (Chawanku, et al. 2005; Ricardez-Sandoval, et al, 2008, 2009a, 2009b). The corresponding node in the hierarchical tree of Figure 2.1 is shown in Snip 2.1.7.

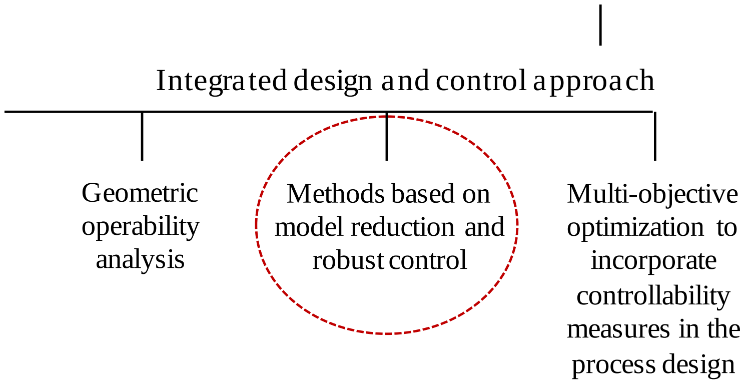

Snip 2.1.7. Research in the field: Methods based on model reduction and robust control measures, (Figure 2.1 revisited).

The idea is to perform process identification on the nonlinear first principles model. The results of identification are a linear model and a model for uncertainties, which represents the difference between the full nonlinear model and the linear model. Then, the measures commonly used in robust control (e.g., structured singular value) are used to estimate the bounds on process variables and to evaluate flexibility, stability and controllability of the process. These bounds give evaluations of the worst variability and violations of constraints. For this reason, this methodology is termed *bound worst-case approach*. The advantage of bound worst-case approach is that the application of the reduced model avoids the requirement of computationally expensive dynamic optimization. The disadvantage of this method is that it is based on a worst-case scenario which is not necessarily the most common scenario, and the method could be too conservative resulting in unnecessarily degradation of the objective function. To overcome this difficulty, Ricardez-Sandoval, et. al, (2011) suggested to calculate the worst disturbance scenario using structured singular value but the process variability should be calculated using a closed loop first principles model, resulting in a less conservative solution. They called the new method *hybrid worst-case approach*, because in the new method both linear and first principles models are involved.

Malcolm, et al. (2007), Moon, et al. (2011), and Patel, et al. (2008) pursued similar idea. However, they decomposed the problem into a bi-level optimization, in which control design was performed using a reduced (adaptive state-space) model, and process design was performed using the original first principles model. The linear state-space model was used for deciding control action in each optimization iteration, in order to disentangle the numerical complexities of feedback control. Malcolm, et al. (2007) applied sequential least square method for identification of the state-space model. Their method employed three layers (identifier/observer/regulator) at the control optimization level. In addition, the process optimization level consisted of two optimization loops for steady-state and dynamic flexibility tests. The justification is that if the steady-state process operation is infeasible, further investigation of dynamic flexibility is not needed. Patel, et al. (2008) applied similar idea with modified linear quadratic regulator (mLQR). The applied mLQR method incorporated an additional penalty term on the movement of the manipulated variables in order to add integrating action to the controller. They considered the corners of a hyper-rectangular disturbance space rather than dynamic flexibility test.

The advantage of the aforementioned methods is that the linear model benefits from analytical solutions and the computationally expensive dynamic nonlinear optimization is avoided. The disadvantage of these methods is that due to application of a linear model, the solution is local. In addition, in the case of highly nonlinear processes, application of nonlinear identification and observation methods may further augment the required computation expenses, (Yuan 2012).

2.13. Methods based on analysing nonlinear behaviour of chemical processes

Chemical processes may demonstrate nonlinear behaviour in term of steady-state multiplicity. The corresponding node in the hierarchical tree of Figure 2.1 is shown in Snip 2.1.8.

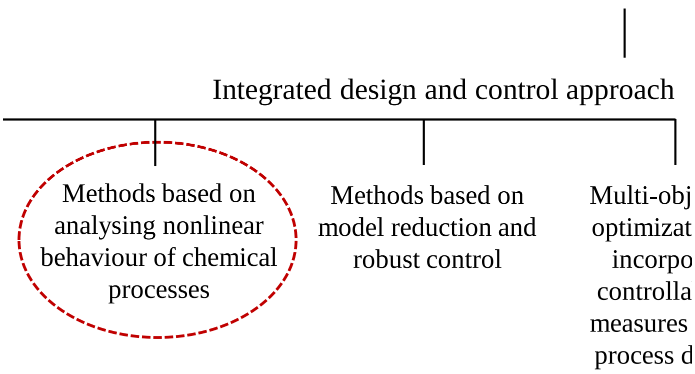

Snip 2.1.8. Research in the field: Methods based on analysing nonlinear behaviour of chemical processes, (Figure 2.1 revisited).

In order to determine steady-state multiplicities, the mathematical model of the process should be condensed into an algebraic equation (Silva-Beard and Flores-Tlacuahuac, 1999):

$$F(x,p) = 0 \qquad (2-23)$$

where x is the state variables and p is the vector of design parameters. Then the necessary condition of input-multiplicity is given by the implicit function theorem (Poston and Stewart 1996):

$$F(x,\varphi) = \frac{\partial F(x,\varphi)}{\partial \varphi} = 0 \qquad (2-24)$$

in which $\varphi \in p$. Therefore, the maximum number of multiplicity points, k, is given by:

$$\frac{\partial F^k(x,\varphi)}{\partial \varphi^k} = 0, \;\; and \quad \frac{\partial F^{k+1}(x,\varphi)}{\partial \varphi^{k+1}} \neq 0 \qquad (2-25)$$

Similarly, the necessary condition for output-multiplicity is given by:

$$F(x,\varphi) = \frac{\partial F(x,\varphi)}{\partial x} = 0 \qquad (2-26)$$

Then, *isolas*, i.e., the points where isolated solutions originate and disappear, can be found by:

$$F(x,\varphi) = \frac{\partial F(x,\varphi)}{\partial \varphi} = \frac{\partial F(x,\varphi)}{\partial x} = 0 \qquad (2-27)$$

In the following, several interesting results for integration of process design and control are reviewed. Silva-Beard and Flores-Tlacuahuac (1999) studied the regions of nonlinear behaviour of a free-radical CSTR polymerization reactor using continuation algorithm and global multiplicity diagrams. They showed that closed loop control in the optimal point of operation could be difficult because steady-state multiplicities would introduce positive zeros into the transfer function and limit the speed of closed loop control. Pavan Kumar and Kaistha (2008a, b) showed, depending on the control structure, input steady-state multiplicity might cause state transition and wrong control action in a generic ideal reactive distillation column. They recommended a three-point temperature control structure for addressing large deviations in the throughput. The effects of input multiplicity on degrading switchability due to non-minimum phase behaviour are also studied by Kuhlmann and Bogle (2001; 2004).

Kiss, et al. (2002, 2003, 2007) studied the effects of recycle streams on product selectivity and steady-state multiplicity of a reactor-separator process. They identified two types of inventory control; *self-regulatory inventory control* in which the reactants are fed according to stoichiometry of reactions and is characterized by a minimum reactor volume required to avoid snowball effects, and *regulation by feedback inventory control* in which the inventories of the reactants are controlled by manipulating fresh feed. They argued that although the latter method is more difficult to implement, it eliminates the risk of instability and state multiplicity.

The early methods for analysing the nonlinear behaviour of chemical process rely extensively on the analytical solution of the process model. Marquardt and Mönnigmann (2005) applied the underlying theory for synthesis rather than analysis. They defined a critical manifold as the stability boundary which separates the design parameter space of feasible steady states from unstable oscillatory states. Then, an operational point should back-off from the critical manifolds in order to ensure a safe operation due to uncertainties and disturbances. A signal function was applied for testing if the manifold is crossed. This function enabled identifying unknown critical manifolds. Then, the constraints for maintaining distance from these new critical manifolds were added and the optimization was repeated until no new critical manifold is found. This method has been successfully applied to the systems consisting of hundreds of equations.

2.14. Geometric operability analysis

The definition of operability was mentioned earlier in Section 2.9.1. The geometric measures for steady-state and dynamic operability were introduced in order to quantify the area in which the process remains operable, (Vinson and Georgakis 2000; Uztürk and Georgakis 2002) The corresponding node in the hierarchical tree of Figure 2.1 is shown in Snip 2.1.9 and is discussed in the following.

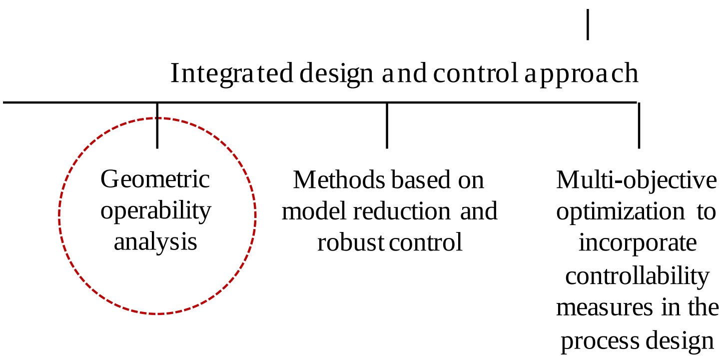

Snip 2.1.9. Research in the field: Geometric operability analysis, (Figure 2.1 revisited).

The discussion is based on the following state-space representation of the process model (Georgakis, et al. 2004):

$$\text{M:} \quad \dot{\boldsymbol{x}} = f(\boldsymbol{x}, \boldsymbol{u}, \boldsymbol{d}) \qquad \text{Processs model}$$

$$\boldsymbol{y} = g(\boldsymbol{x}, \boldsymbol{u}, \boldsymbol{d})$$

$$\boldsymbol{h}_1(\dot{\boldsymbol{x}}, \boldsymbol{x}, \boldsymbol{y}, \dot{\boldsymbol{u}}, \boldsymbol{u}, \boldsymbol{d}) = 0$$

$$\boldsymbol{h}_2(\dot{\boldsymbol{x}}, \boldsymbol{x}, \boldsymbol{y}, \dot{\boldsymbol{u}}, \boldsymbol{u}, \boldsymbol{d}) \leq 0$$

In the above, $x \in R^{n_x}$ is the vector of state variables, $u \in R^{n_u}$ is the vector of input (manipulated) variables, $d \in R^{n_d}$ is the vector of disturbance variables, and $y \in R^{n_y}$ is the vector of output (controlled) variables. The method for steady-state operability analysis utilizes a steady-state process model that maps process inputs to process outputs. The process inputs are able to take the values in the available input set (AIS). Using the process model and AIS, it is possible to calculate the achievable output set (AOS). Notice that AOS is a function of u and d. A comparison between the desired output set (DOS) and the achievable output set (AOS) can be quantified as the operability index (OI):

$$\mathrm{OI} = \frac{\mu(\mathrm{DOS} \cap \mathrm{AOS})}{\mu(\mathrm{DOS})} \qquad (2-28)$$

where μ is a measure of the size of each set, e.g., in a two-dimensional space, it represents the area and in a three-dimensional space, it represents the volume, (Georgakis and Li 2010). However, there are different definitions for operability index depending on whether the setpoints are constant or they are controlled in intervals (i.e., equivalent to setpoint tracking).

The achievable output set (AOS) can be calculated for a given available input set (AIS) and by fixing disturbances at their nominal values d^N. Then a comparison between the desired output set (DOS) and the achievable output set (AOS) leads to quantification of the steady-state servo-operability index, as follows:

$$\mathrm{s-OI} = \frac{\mu(\mathrm{AOS}_u(d^N) \cap \mathrm{DOS})}{\mu(\mathrm{DOS})} \qquad (2-29)$$

in which

$$\mathrm{AOS}_u(d^N) = \{y |\, M(\dot{x} = 0, \dot{u} = 0, d = d^N); \forall u \in \mathrm{AIS}\} \qquad (2-30)$$

Similarly the regulatory steady-state operability index will be:

$$\mathrm{r-OI} = \frac{\mu\big(\mathrm{AIS} \cap \mathrm{DIS}_d(y^N)\big)}{\mu\big(\mathrm{DIS}_d(y^N)\big)} \qquad (2-31)$$

in which the desired input set is defined as:

$$\mathrm{DIS}_d(y^N) = \{u|\ M(\dot{x} = 0, \dot{u} = 0, y = y^N); \forall d \in \mathrm{EDS}\} \qquad (2-32)$$

where EDS is the expected disturbance space. Later this method was developed to include dynamic operability (Uztürk and Georgakis 2002; Georgakis, et al. 2003). The set of values over which inputs can move is called dynamic available input space (dAIS). The dynamic desired operating space (dDOpS) is a function of desired output set (DOS), expected disturbance space (EDS) and the maximum allowable response time ${t^d}_f$ as follows:

$$\mathrm{dDOpS} = \left\{(t_f, y_{sp}, d)\middle|\ t_f \ \leq {t^d}_f, \forall y_{sp} \in \mathrm{DOS}, \forall d \in \mathrm{EDS}\right\} \qquad (2-33)$$

Similarly, the dynamic achievable operating space (dAOpS) is defined as

$$\mathrm{dAOpS} = \left\{(t_f, y_{sp}, d)\middle|\ t_f \ \geq {t^*}_f, \forall y_{sp} \in \mathrm{DOS}, \forall d \in \mathrm{EDS}, \forall u \in \mathrm{dAIS}, \right\} \qquad (2-34)$$

${t^*}_f$ is the minimum time that is required for optimal control and its value can be calculated using dynamic optimization, (Georgakis, et al. 2003). In order to define the dynamic operability two other spaces are needed:

$$\mathrm{S}_1 = \left\{(y_{sp}, d)\middle|\ \forall y_{sp} \in \mathrm{DOS}, \forall d \in \mathrm{EDS}\right\} \qquad (2-35)$$

$$\mathrm{S}_2 = \left\{(y_{sp}, d)\middle|\ {t^*}_f \ \leq {t^d}_f, \forall y_{sp} \in \mathrm{DOS}, \forall d \in \mathrm{EDS}\right\} \qquad (2-36)$$

Then

$$\mathrm{dOI} = \frac{\mu(\mathrm{S}_2)}{\mu(\mathrm{S}_1)} \qquad (2-37)$$

The first operating space, S_1, is the combination of the setpoints (DOS) and disturbances (EDS). The second space, S_2, is the projection of intersection of dDOpS and dAOpS, and represents the operating space that can be achieved. Therefore, the dynamic operability index represents the fraction of operating space that can be achieved by the available inputs during the desirable response time. More details on these methods can be found in (Georgakis, et al. 2004).

It is notable that in the case of input multiplicity, additional interior points of AIS also need to be imaged in order to calculate the complete boundaries of AOS, (Subramanian and Georgakis 2001). The geometric methods for operability analysis are nonlinear and multi-variable. However, they have no implication for the regulatory control structure or inventory control systems, (Vinson and Georgakis 2000). In addition, the problem suffers from the curse of dimensionality, i.e., the dimensions of the abovementioned sets increase sharply and the problem becomes intractable. To overcome this difficulty, Georgakis and Li (2010) introduced a method based on the techniques used in *design of experience* (Montgomery 2005) which selects a finite number of points to perform the input-output mapping.

2.15. Steady-state and dynamic flexibility optimization

A variety of methods for steady-state and dynamic flexibility optimization has been proposed by the researchers (e.g., Swaney and Grossman 1985a; Grossmann and Floudas 1987; Dimitriadis and Pistikopoulos 1995). The corresponding node in the hierarchical tree of Figure 2.1 is shown in Snip 2.1.10 and is discussed in the following.

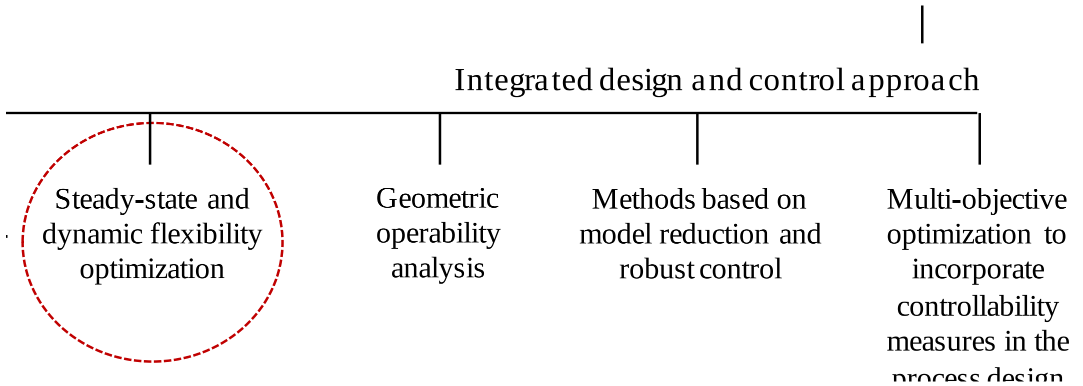

Snip 2.1.10. Research in the field: Steady-state and dynamic flexibility optimization, (Figure 2.1 revisited).

The steady-state process model can be represented by the following equations, (Dimitriadis and Pistikopoulos 1995):

$$\boldsymbol{h}(\boldsymbol{d},\boldsymbol{x},\boldsymbol{z},\boldsymbol{\theta}) = 0 \qquad (2-38)$$

$$\boldsymbol{g}(\boldsymbol{d},\boldsymbol{x},\boldsymbol{z},\boldsymbol{\theta}) \le 0 \qquad (2-39)$$

$$\boldsymbol{\theta} \in T = \{\boldsymbol{\theta}|\boldsymbol{\theta}^L \le \boldsymbol{\theta} \le \boldsymbol{\theta}^U\} \qquad (2-40)$$

$$\boldsymbol{z} \in Z = \{\boldsymbol{z}|\boldsymbol{z}^L \le \boldsymbol{z} \le \boldsymbol{z}^U\} \qquad (2-41)$$

where $dim\,\{\boldsymbol{h}\} = dim\,\{\boldsymbol{x}\}$. In above, $\boldsymbol{x}$ is the vector of the state variables, $\boldsymbol{z}$ is the vector the control (input) variables, $\boldsymbol{\theta}$ is the vector of the uncertain parameters, $\boldsymbol{d}$ is the vector of the design variables. The design variables are decided during the process design stage and remain unchanged during the process operation. In the above set of equations, the state variables can be eliminated between equations (2-38) and (2-39), resulting in the following concise representation of the process model:

$$\boldsymbol{g}(\boldsymbol{d},\boldsymbol{x}(\boldsymbol{d},\boldsymbol{z},\boldsymbol{\theta}),\boldsymbol{z},\boldsymbol{\theta}) = \boldsymbol{f}(\boldsymbol{d},\boldsymbol{z},\boldsymbol{\theta}) \le 0 \qquad (2-42)$$

As shown by Halemane and Grossman (1983), for evaluating the steady-state flexibility the following optimization problem need to be solved:

$$\boldsymbol{\mathcal{X}}(\boldsymbol{d}) = \max_{\boldsymbol{\theta}\in \boldsymbol{T}} \min_{\boldsymbol{z}\in \boldsymbol{Z}} \max_{\boldsymbol{j}\in \boldsymbol{J}} f_j(\boldsymbol{d}, \boldsymbol{z}, \boldsymbol{\theta}) \qquad (2-43)$$

where j is the index of inequalities of equation (2-42). If $\boldsymbol{\mathcal{X}}(\boldsymbol{d}) \leq 0$, the design is feasible for all $\boldsymbol{\theta} \in T$, otherwise a set of critical values for uncertain parameters $\boldsymbol{\theta^c}$ is determined which causes the worst violation of constraints.

Swaney and Grossman (1985a), proposed a scalar flexibility index, F, in order to quantify the area in which the process operation remains feasible, under uncertain conditions.

$$\boldsymbol{F} = \max \ \delta \qquad \text{steady} - \text{state flexibility optimization}$$

Subject to

$$\max_{\boldsymbol{\theta}\in \boldsymbol{T}(\delta)} \min_{\boldsymbol{z}\in \boldsymbol{Z}} \max_{\boldsymbol{j}\in \boldsymbol{J}} f_j(\boldsymbol{d}, \boldsymbol{z}, \boldsymbol{\theta}) \leq 0$$

$$\delta \geq 0$$

$$\boldsymbol{T}(\delta) = \{\boldsymbol{\theta} | \boldsymbol{\theta}^N - \delta\Delta\boldsymbol{\theta}^- \leq \boldsymbol{\theta} \leq \boldsymbol{\theta}^N + \delta\Delta\boldsymbol{\theta}^+\}$$

In above θ^N is the nominal value of uncertain parameters. In addition, $\Delta\theta^+$ and $\Delta\theta^-$ are the expected deviations from this value. The implication of the above formulation is that F is the largest scaled deviation of the uncertain parameters that can be accommodated by the process before the operation is rendered infeasible. In addition, Swaney and Grossman, (1985a) showed that under certain convexity conditions, the causes of infeasibility lie on the vertices of the uncertainty space and the problem simplifies to identifying the active constraints whose intersections limit feasible operation.

The early versions of flexibility optimization employed a steady-state formulation. The optimization variables were process design parameters and process inputs which could be optimized to compensate the losses associated with realization of uncertainties. The steady-state version of flexibility analysis did not have any implication for control design and do not consider transient states. However, in some important applications such as batch processes, shutdown and start-up procedures, disturbance rejection, or product changeover, the dynamic operability of the process is of vital importance. Therefore, Dimitriadis and Pistikopoulos (1995) extended this method to consider dynamic process optimization under time-varying uncertainties. In the dynamic formulation, the following system consisting of ordinary differential equations was considered to describe the process model:

$$\boldsymbol{h}(\boldsymbol{d}, \dot{\boldsymbol{x}}(\boldsymbol{t}), \boldsymbol{x}(\boldsymbol{t}), \boldsymbol{z}(\boldsymbol{t}), \boldsymbol{\theta}(\boldsymbol{t}), \boldsymbol{t}) = 0; \boldsymbol{x}(0) = \boldsymbol{x_0} \qquad (2-44)$$

$$\boldsymbol{g^{path}}(\boldsymbol{d}, \boldsymbol{x}(\boldsymbol{t}), \boldsymbol{z}(\boldsymbol{t}), \boldsymbol{\theta}(\boldsymbol{t}), \boldsymbol{t}) \leq 0 \qquad (2-45)$$

$$\boldsymbol{g_k}^{\boldsymbol{point}}(\boldsymbol{d}, \boldsymbol{x}(\boldsymbol{t^k}), \boldsymbol{z}(\boldsymbol{t^k}), \boldsymbol{\theta}(\boldsymbol{t^k}), \boldsymbol{t^k}) \leq 0, \ \ k = 1, \ldots, NP \qquad (2-46)$$

Compared to the steady-state formulation, in the above states, inputs and uncertain parameters are time-dependent. The constraints $\boldsymbol{g}^{\boldsymbol{path}}$ and $\boldsymbol{g_k}^{\boldsymbol{point}}$ represent path and point constraints respectively. Then, the dynamic flexibility can be tested by solving the following optimization problem:

$$\boldsymbol{\mathcal{X}}(\boldsymbol{d}) = \max_{\boldsymbol{\theta}(\boldsymbol{t})\in \boldsymbol{T}(\boldsymbol{t})} \min_{\boldsymbol{z}(\boldsymbol{t})\in \boldsymbol{Z}(\boldsymbol{t})} \max_{\boldsymbol{j}\in \boldsymbol{J}, \boldsymbol{t}\in [\boldsymbol{0},\boldsymbol{H}]} g_j(\boldsymbol{d}, \boldsymbol{x}(\boldsymbol{t}), \boldsymbol{z}(\boldsymbol{t}), \boldsymbol{\theta}(\boldsymbol{t}), \boldsymbol{t}) \qquad (2-47)$$

Subject to

$$\boldsymbol{h}(\boldsymbol{d}, \dot{\boldsymbol{x}}(\boldsymbol{t}), \boldsymbol{x}(\boldsymbol{t}), \boldsymbol{z}(\boldsymbol{t}), \boldsymbol{\theta}(\boldsymbol{t}), \boldsymbol{t}) = 0; \;\; \boldsymbol{x}(0) = \boldsymbol{x_0} \qquad (2-48)$$

$$T(t) = \{\boldsymbol{\theta}(\boldsymbol{t}) | \boldsymbol{\theta}^L(t) \leq \boldsymbol{\theta}(t) \leq \boldsymbol{\theta}^U(t)\} \qquad (2-49)$$

$$Z(t) = \{\boldsymbol{z}(t) | \boldsymbol{z}^L(t) \leq \boldsymbol{z}(t) \leq \boldsymbol{z}^U(t)\} \qquad (2-50)$$

where $\boldsymbol{H}$ is the maximum time over which the flexibility of the dynamic system is considered. Similar to steady-state test, if $\boldsymbol{\mathcal{X}}(\boldsymbol{d}) \leq 0$, the system is flexible. Otherwise, at least for one $\boldsymbol{\theta}(t)$, there is no control action which can make the process operation feasible over the considered time horizon.

Similar to the steady-state case, the dynamic operability index problem can be formulated as follows:

$$\boldsymbol{DF} = \max \; \delta \qquad \text{dynamic flexibility optimization}$$

Subject to

$$\boldsymbol{\mathcal{X}}(\boldsymbol{d}) = \max_{\boldsymbol{\theta}(\boldsymbol{t})\in \boldsymbol{T}(\boldsymbol{t})} \min_{\boldsymbol{z}(\boldsymbol{t})\in \boldsymbol{Z}(\boldsymbol{t})} \max_{\boldsymbol{j}\in \boldsymbol{J}, \boldsymbol{t}\in [\boldsymbol{0},\boldsymbol{H}]} g_j(\boldsymbol{d}, \boldsymbol{x}(\boldsymbol{t}), \boldsymbol{z}(\boldsymbol{t}), \boldsymbol{\theta}(\boldsymbol{t}), \boldsymbol{t}) \leq 0$$

$$\boldsymbol{h}(\boldsymbol{d}, \dot{\boldsymbol{x}}(\boldsymbol{t}), \boldsymbol{x}(\boldsymbol{t}), \boldsymbol{z}(\boldsymbol{t}), \boldsymbol{\theta}(\boldsymbol{t}), \boldsymbol{t}) = 0; \;\; \boldsymbol{x}(0) = \boldsymbol{x_0}$$

$$\delta \geq 0$$

$$\boldsymbol{T}(\delta, t) = \{\boldsymbol{\theta}(t) | \boldsymbol{\theta}^N(t) - \delta\Delta\boldsymbol{\theta}(t)^- \leq \boldsymbol{\theta}(t) \leq \boldsymbol{\theta}^N(t) + \delta\Delta\boldsymbol{\theta}(t)^+\}$$

$$Z(t) = \{\boldsymbol{z}(t) | \boldsymbol{z}^L(t) \leq \boldsymbol{z}(t) \leq \boldsymbol{z}^U(t)\}$$

It is notable that dynamic flexibility optimization can be used as an outer optimization loop in order to ensure that process operation remains feasible over the range of uncertain parameters.

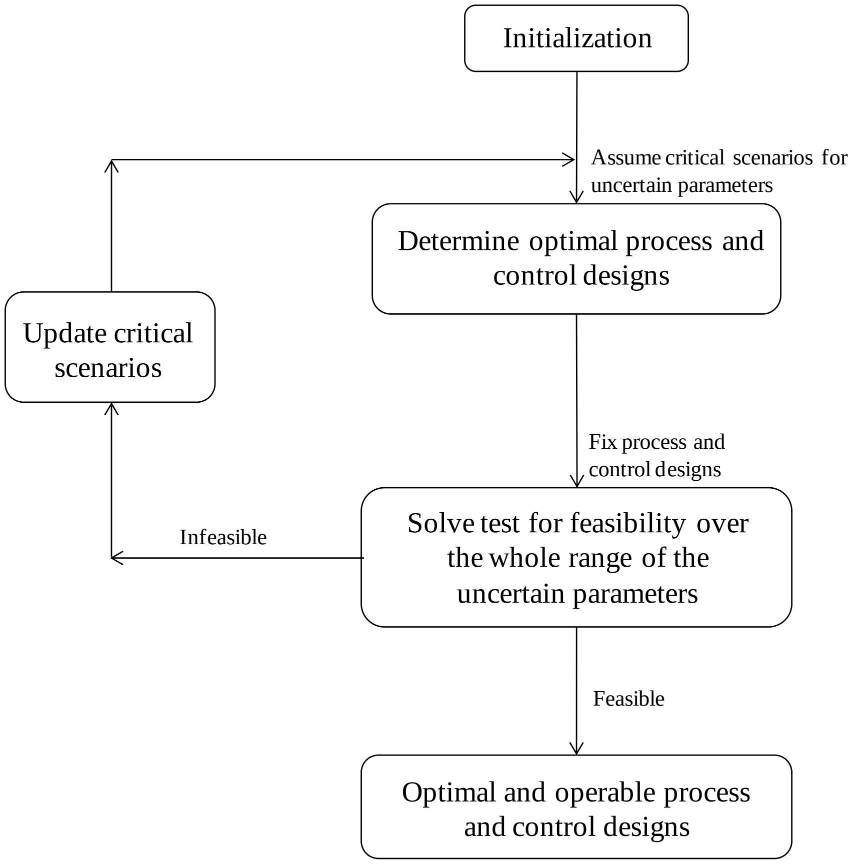

Figure 2.10. The algorithm for flexibility optimization, adapted from (Sakizlis, et al 2004).

The concept is shown in Figure 2.10, (adapted from Sakizlis, et al. 2004). In this method, firstly multi-period optimization is performed for an initial set of uncertain scenarios. This gives intermediate values for the design variables. Then, a feasibility test (another optimization) is performed in which the design variables are fixed and the violations of the constraints are maximized using the uncertain parameters. This gives a critical scenario of the uncertain parameters with worst violation of constraints. The current set of the uncertain scenarios is updated and the two optimization problems are solved iteratively, until the second optimization fails to find a realization of the uncertain parameters, which violates the constraints and therefore, the design is feasible for the whole range of uncertain parameters.

2.16. Economic optimization based on minimization of the economic losses associated with back-off from active constraints

Perkins (Narraway, et al. 1991; Narraway and Perkins 1993) proposed a method based on minimization of economic penalties associated with back-off from active constraints. The corresponding node in the hierarchical tree of Figure 2.1 is shown in Snip 2.1.11.

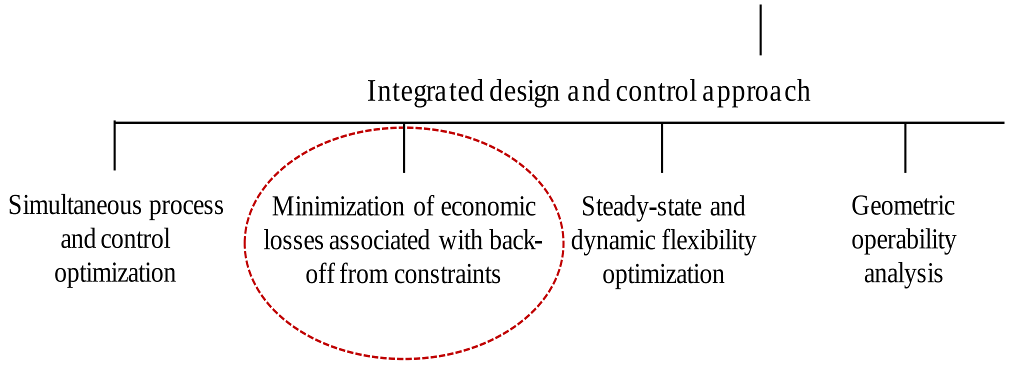

Snip 2.1.11. Research in the field: Minimization of the economic losses associated with back-off from active constraints, (Figure 2.1 revisited).

The importance of this contribution was the recognition and integration of economic objectives into the problem formulation. The idea is shown in Figure 2.11. In many processes, the optimal steady-state economic solution lies on the intersection of constraints. However, these constraints may be violated due to disturbances. Therefore, in order to ensure a safe and feasible operation, the nominal operating point must be moved away from the active constraints. Minimization of economic penalties associated with *back-off* from active constraints leads to identification of the optimal dynamic economic solution, shown in Figure 2.11.

The early versions of the back-off method were based on frequency analysis and perfect control (Narraway, et al. 1991; Narraway and Perkins 1993). Later, this method was extended to time domain by considering decentralized (Heath, et al. 2000) and centralized (Kookos and Perkins 2001) proportional integral controllers. They also developed a general formulation which included any linear time-invariant output feedback controller, (Kookos and Perkins 2004).

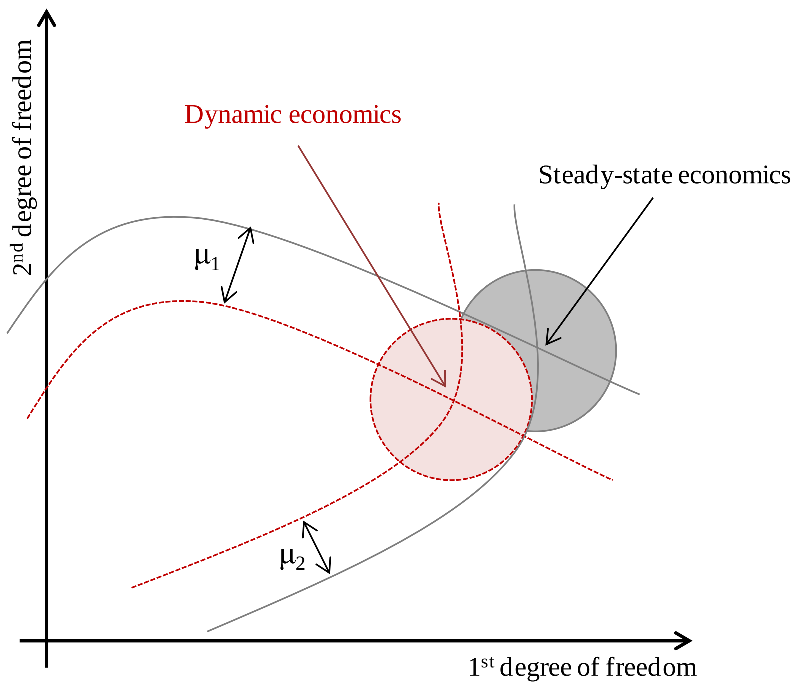

Figure 2.11. Optimal steady-state and dynamic economic solutions adapted from Kookos and Perkins (2004)

2.17. Simultaneous optimization of a process and its controllers

The simultaneous approach to integrated design and control employs a stochastic mixed integer nonlinear dynamic formulation to optimize a superstructure of the process, its control structure and controllers. However, solving the resulted mathematical formulation can be a formidable task. The corresponding node in the hierarchical tree of Figure 2.1 is shown in Snip 2.1.12.

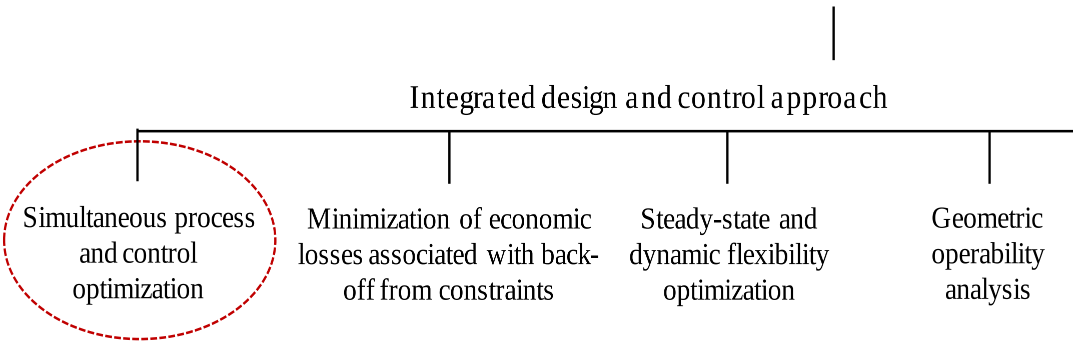

Snip 2.1.12. Research in the field: Simultaneous optimization of the process and its controllers, (Figure 2.1 revisited).

Since the underlying mathematical formulation for simultaneous optimization of a process and its controllers may result in large-scale MIDO problems, several research activities were devoted to develop new solution strategies in order to reduce the computational costs.

Samsatli, et al. (1998) proposed an smooth approximation of binary variables to reformulate the MIDO problem using continues variables, as follows:

$$Y = \frac{1}{2} \times \ [tanh\,\{\xi(z)\} + 1] \qquad (2-51)$$

Here ξ is a large number, then $Y = 1$ when $z \gg 0$ and $Y = 0$ when $z \ll 0$. However, the proposed approximating function results in errors when $z \approx 0$, because $Y = 0.5$.

Several research activities investigated decomposition of the problem into a primal subproblem and a master subproblem, with of the aim of reducing the computational costs. In all these methods, the primal subproblem is performed in a reduced space in which the binary variables are fixed. The primal subproblem gives an upper bound on the solution. However, as discussed in the following, different methods are used to formulate the master subproblem which determines the new realizations for the binary variables and gives lower bound on the solution. These two subproblems are solved iteratively until the difference of the upper and lower bounds lies within the desirable tolerance. Avraam, et al. (1998, 1999) and Sharif, et al. (1998) applied linearization to construct an MILP master subproblem which was solved using outer approximation (OA) method. By comparison, Mohideen, et al. (1997), Schweiger and Floudas, (1997) and Bansal, et al. (2000a, 2003) applied dual information and generalized benders decomposition (GBD) algorithm (Geoffrion 1972) to construct the master subproblem. The former method based on outer approximation requires less evaluation of the primal subproblem because its master subproblem gives tighter lower bounds. However, the application of outer approximation algorithms required that the binary variables appear linearly and separated in the objective function and constraints. It is notable that new OA algorithms (e.g., applied by the recent versions of DICOPT) are extened to overcome this deficiency.

The method of full discretization based on orthogonal collocation was also applied by Cervantes and Biegler (2000b; 2002), and Flores-Tlacuahuac and Biegler (2005; 2007; 2008). Flores-Tlacuahuac and Biegler (2007) also studied the effects of the convexities of the problem formulation on the results. In that study, firstly the problem formulation was presented using generalized disjunctive programming (GDP) method (Biegler, et al. 1997) and then it was translated into several equivalent mixed integer formulations such as Big M, disaggregation or nonconvex formulations.

From the application point of view, these methods are applied to a number of case studies: a double effect distillation column (Bansal, et al. 2000b), a high purity distillation column (Ross, et al. 2001), and a multi-component distillation column (Bansal, et al. 2002). Later, Sakizlis, et al. (2003; 2004) and Khajuria and Pistikopoulos (2010) extended this method by including multi-parametric model predictive controllers. Asteasuain, et al. (2006) studeid simultaneouse process and control system design of styrene polymerization CSTR reactor. They considered a superstructure of feedback and forward controllers, and the optimization included the determination of optimal initial and final steady states and the time trajectories between them. Recently, Terrazas-Moreno, et al. (2008) studied a methyl-methacrylate continuous polymerization reactor. In this research, the design decisions (equipment size and steady-state operating conditions), the scheduling decisions (grade productions sequence, cycle duration, production quantities, inventory levels) and the optimal control decisions (grade transition time and profile) were made simultaneously. Different methods for solving MINLP and MIDO problems will be discussed next.

2.18. Mathematical optimization

This section reviews the relevant methods for addressing optimization-based algorithms of the last sections. The features of interest are the methods for solving MINLP problems, the methods for dynamic optimization, the methods for global optimization, simulation-optimization programming, and multi-criteria decision-making.

2.18.1. MINLP solution algorithms

As discussed earlier, in design and control of chemical processes, two categories of variables are involved, structural variables and parametric variables. Structural variables are discrete and are represented as binary or integer variables. If the latter take large values, often it is approximated as a continuous variable, (Biegler and Grossmann 2004). The main MINLP algorithms can be explained using four subproblems. They are:

Subproblem NLP 1: the relaxation subproblem.

In this subproblem, the discrete variables are relaxed to have non-integer values. In general, the solution of Subproblem NLP1 results in non-integer values for discrete variables and gives a lower bound on the objective function of the main MINLP problem.

Subproblem NLP2: the subproblem with fixed discrete variables.

The solution of this subproblem gives an upper bound on the objective function of the main MINLP problem.

Subproblem NLPF: the feasibility subproblem with fixed discrete variables.

The Subproblem NLPF can be thought as minimization of infeasibilities of the corresponding NLP2 subproblem.

Subproblem M-MILP: the cutting planes subproblem

The Subproblem M-MILP exploits the convexity of the objective function and the constraints, as they are replaced by the corresponding supporting hyper-planes. Due to the convexity of the feasible region, these hyper-planes are outer approximations of the nonlinear feasible region. Subproblem M-MILP may include linearization of all the constraints or only the violated constraints. The hyper-planes in Subproblem M-MILP provide new values for discrete variables, and a non-decreasing lower bound for the objective function. In other words, Subproblem M-MILP over estimates the feasible region and underestimates the objective function.

The mathematical formulation of the above subproblems can be found in (Grossmann 2002). The main MINLP algorithms are branch and bound (BB), outer approximation (OA), generalized benders decomposition (GBD), and extended cutting planes (ECP) which can be explained using the above sub-problems NPL1, NP2, NLPF, and M-MILP, as explained in the following, and shown in Figure 2.12, (adapted from Grossmann 2002).

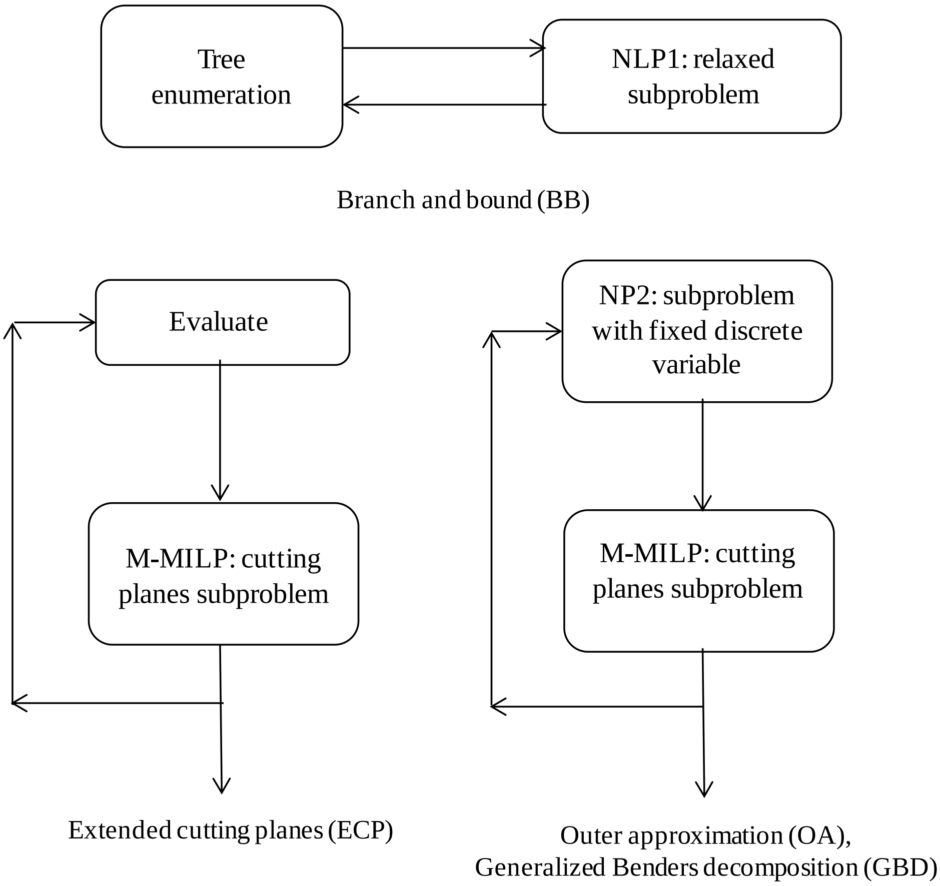

Figure 2.12. Different MINLP algorithms represented as a combination of NLP and M-MILP subproblems, (adapted from Grossmann 2002).

Branch and bound (BB)

The branch and bound algorithm successively enumerates the nodes of the tree (constructed according to integer variables) by fixing the discrete variables corresponding to the current node, and solving the relaxed Subproblem NLP1 for the rest of discrete variables. If all the discrete variables take integer values, the algorithm stops. Otherwise, the nodes of the tree are enumerated. The relaxed Subproblem NLP1 gives a lower bound for the subproblems in the descendant nodes. Fathoming is performed when the lower bound exceeds the current upper bound, when the Subproblem is infeasible, or when all discrete variables take integer values.

Outer approximation (OA)

In outer approximation algorithm, NLP2 (subproblem with fixed discrete variables) and M-MILP (subproblem with cutting planes) are solved iteratively. If the solution of NLP2 is feasible, it is used for constructing the cutting planes in M-MILP. Otherwise, the feasibility Subproblem, NLPF, is solved to generate the corresponding feasible solution. NLP2 and M-MILP subproblems give the upper and lower bounds respectively. The iterations continue until the difference of the lower and upper bounds lies within the allowable tolerance.

Generalized Benders decomposition (GBD)

Generalized benders decomposition (GBD) is similar to outer approximation (OA) in that subproblems M-MILP and NLP2 are solved iteratively. However, in GBD only active constraints are linearized for constructing the cutting planes.

Extended cutting planes (ECP)

The extended cutting planes algorithm does not require the abovementioned NLP sub-problems. M-MILP Subproblem is solved iteratively by adding the linearization of the most violated constraints. The algorithm converges when the violation of constraints lies within the allowable tolerance.

The algorithms based on branch and bound are only attractive when NLP subproblems are not computationally expensive or when due to the small dimension of discrete variables, the number of NLP subproblems is small. In general, outer approximation (OA) methods converge in fewer iterations. It can be shown that in extreme when the objective function and the constraints are linear, OA finds the solution in one iteration. In fact, as explained by Grossmann (2002), the M-MILP Subproblem does not even need to be solved to optimality. The generalized benders decomposition (GBD) algorithm can be thought as a special case of OA algorithm. Since the lower bounds of the GBD algorithm are weaker than OA algorithms, a larger number of iterations is required. For the case of extended cutting planes (ECP), since the discrete and continuous variables are treated simultaneously, a larger number of iterations is required. There are other variants and extensions of the above-mentioned algorithms such as branch and cut, LP/NLP branch and bound, and so on, which are not the focus of this discussion. The interested reader may refer to literature, (e.g., Biegler and Grossmann 2004). In general, branch and bound methods perform well when relaxation of MINLP is tight. Outer approximation methods are better when the NLP subproblems are computationally expensive. GDB methods are more favourable for problems with a large number of discrete variables and ECP methods are preferred for linear problems, (Biegler and Grossmann 2004).

The off-shelf commercial solvers for mixed integer nonlinear problems are available within modelling systems such as GAMS and AMPL. The common computer codes for nonlinearly constrained MINLPs are DICOPT, SBB, α-ECP and BARON. DICOPT is developed by Viswanathan and Grossmann (1990) at Carnegie Mellon University, based on OA. According to the recent manual of software, the algorithm is extended to include integer variables which appear nonlinearly in the problem formulation, (DICOPT documentation 2012). BARON is developed by Sahinidis (1996) and implements a global optimization method. This solver is based on a branch and reduce algorithm. SBB applies a branch and bound method and α-ECP is based on an extended cutting plane method. Comparison of these algorithms is not the focus of this research. DICOPT and SBB are used in Chapter 6 for optimization of the discretized formulation of a MIDO problem. All these methods are based on the assumption of convexity of the objective function and constraints and may converge to a local solution in the presence of non-convexities. The methods for global optimization will be discussed later.

2.18.2. Dynamic optimization

In general, the solution algorithms for dynamic optimization problems can be classified into variational, sequential, full discretization and multiple-shooting methods. These methods are discussed in the following.

The *variational methods* use the first order optimality necessary conditions based on Pontryagin's Maximum Principle (Cervantes and Biegler 2000a). The resulted formulation conforms to a boundary value problem which can be solved using methods such as single shooting, and invariant embedding. If the analytical solution is found, these methods have the advantage that the solution is achieved in the original infinite dimensional space. However, analytical solution is often not possible and numerical solution features combinatorial characteristics in the presence of constraints. Therefore, the application of variational methods is limited to small problems.

In the *sequential integration* methods, also called *partial discretization* or *control vector parameterization*, only the control input variables (i.e., manipulated variables) are discretized. When initial conditions, time-independent variables and the parameters of the input variables are fixed, the resulted differential algebraic equations (DAEs) can be solved using a DAE solver. This produces the required objective function and gradients for an NLP solver. The NLP solver determines the optimal values for the time-independent variables and the parameters of the control inputs. The special feature of sequential methods is that it generates a feasible solution in each iteration, (Biegler and Grossmann 2004).

In *full discretization* methods, also called *simultaneous methods*, all time-dependent variables are discretized which results in a large-scale nonlinear problem. The main technique for discretization is collocation based on finite elements, in which the profiles of the time-dependent variables are approximated by a family of polynomials. These methods follow an infeasible path and the differential algebraic equations are solved at the optimum point, only. Therefore, the execution time is significantly shorter than the sequential method. The full discretization methods are advantageous when state variables are (path) constrained or unstable modes exists, (Biegler and Grossmann 2004). In addition, the control input (manipulated) variables are discretized at the same level of accuracy as the state variables and the output (controlled) variables. However, the reformulated discretized problem could be very large which requires careful initialization of the optimization algorithm.

A method that should be categorized between the two extremes of the sequential methods and the full discretization methods, is called *multiple shooting*. In this method, the time horizon is divided into several stages and in each stage a partial discretization problem, based on sequential approach is solved. The continuities between stages are established using additional equality constraints. The main advantage of the multiple-shooting methods over the sequential methods is that the (path) constraints on state variables can be imposed at the points between stages.

2.18.3. Global optimization

The motivation for the research into global optimization is that the nonlinear optimization methods do not guarantee to find the global solution in the case of non-convex problems. The methods for global optimization can be classified into stochastic methods and deterministic methods. The stochastic optimization methods, often apply an algorithm in analogy to physical systems (e.g. evolution in genetic algorithm) in order to generate trial points which approach an equilibrium point. The common examples of stochastic optimization methods are genetic, simulated annealing, and Tabu search algorithms. Stochastic optimization methods are widely applied in chemical engineering. For example Low and Sorensen, (2003a-b, 2005), and Wongrat, and Younes (2011) applied genetic algorithms and Exler, et al. (2008) applied Tabu Search for mixed integer dynamic optimization. Furthermore, these methods do not require calculation of gradients and can be applied for simulation-optimization programming. Genetic algorithm (GA) is an important derivative free algorithms which is discussed in the following, briefly.

The main characteristic of GA is that it mimics the process of natural evolution. GA employs a population of solutions for optimization and applies two main operators for improving the fitness (i.e., the value of the objective function) of individual solutions. The first operator combines two individuals (parents) to create a new individual (offspring). This operation is called *crossover*. The other operation for improving the fitness of individuals is to randomly change their characteristics. The corresponding operator is called *mutation*. Mutation has an exploration attitude that is, it explores new areas in the search space (i.e., the space in which optimization variables are defined). However, crossover has an interpolative attitude, as it tries to combine the best characteristics of the current individuals to create a better individual in the next generation. Both mutation and crossover operations may have destructive effects, because an offspring may not be as good as its parents. In order to avoid increasing the value of the objective function, the best individual of each population is copies directly to the next generation, which is known as *elitism*. In this research, MATLAB® GA Toolbox is applied in Chapters 4 and 5. More details about genetic algorithm are available in literature (e.g., Edgar, et al. 2001; Mitchell, M. 1998).

Recently, a variety of methods for deterministic global optimization is proposed by researchers. In summary, the main idea is to use convex envelopes or under-estimators in order to construct the equivalent lower bounding convex problem. Consider the following mixed integer programming (MIP) problem:

$$\min Z = \boldsymbol{f}(\boldsymbol{x}, \boldsymbol{y}) \qquad \text{(MIP)}$$

Subject to

$$\boldsymbol{g}(\boldsymbol{x}, \boldsymbol{y}) \leq 0$$

In which $\boldsymbol{x}$ and $\boldsymbol{y}$ are continuous and discrete variables respectively. In addition, $\boldsymbol{f}(\boldsymbol{x}, \boldsymbol{y})$ and $\boldsymbol{g}(\boldsymbol{x}, \boldsymbol{y})$ are generally non-convex. The equivalent lower bounding mixed integer programming (LBMIP) problem has the general form of:

$$\min\ Z = \overline{\boldsymbol{f}}(\boldsymbol{x}, \boldsymbol{y}) \qquad \text{(LBMIP)}$$

Subject to

$$\overline{\boldsymbol{g}}(\boldsymbol{x}, \boldsymbol{y}) \leq 0$$

where, $\bar{\boldsymbol{f}}$ and $\bar{\boldsymbol{g}}$, are valid convex under-estimator, $\bar{\boldsymbol{f}}(\boldsymbol{x},\boldsymbol{y}) \leq \boldsymbol{f}(\boldsymbol{x},\boldsymbol{y})$ and $\bar{\boldsymbol{g}}(\boldsymbol{x},\boldsymbol{y}) \leq 0$ holds if $\boldsymbol{g}(\boldsymbol{x},\boldsymbol{y}) \leq 0$. As discussed by Grossmann and Biegler (2004), the differences between the methods for deterministic global optimization are based on the way that the above lower bounding problem is constructed and the way that branching is performed on discrete and continuous variables. The spatial tree enumeration can be done for both continuous and discrete variables. Alternatively, the spatial branch and bound can be performed on continuous variables and the resulted LBMIP can be solved by conventional MIP methods at each node. Branching on continuous variables is performed by diving the feasible region, and comparing the upper and lower bound for fathoming each sub-region, (Figure 2.13).The sub-region which contains the global optimal solution is found by eliminating the sub-regions which are proved not to contained the global optimal solution. Finally, some methods branch on discrete variables of LBMIP problem and switch on spatial branch and bound on the nodes where feasible values for discrete variables are found. For constructing the under-estimator some special structures such as bilinear, linear fractional, or concave separable structures may be assumed for continuous variables. Alternatively, in some methods a quadratic large term is added to the original function. Nevertheless, in all these methods the quality of the under-estimator depends on the method for tightening the upper and lower bounds. The details of these methods and the way that the convex envelopes and under-estimators are constructed are reviewed by Grossmann and Biegler (2004), Tawarmalani and Sahinidis (2004), and Floudas, et al. (2005). Recently researchers have extended the global optimization methods for dynamic optimization. Barton and Lee, (2004) solved MIDO problems with embedded linear time-varying dynamic systems to global optimality. Later Chachuat, et al. (2005; 2006) proposed a decomposition method based on outer approximation, which is able to address a wider range of problems with embedded ordinary differential equations (ODEs) without enumerating the discrete variables.

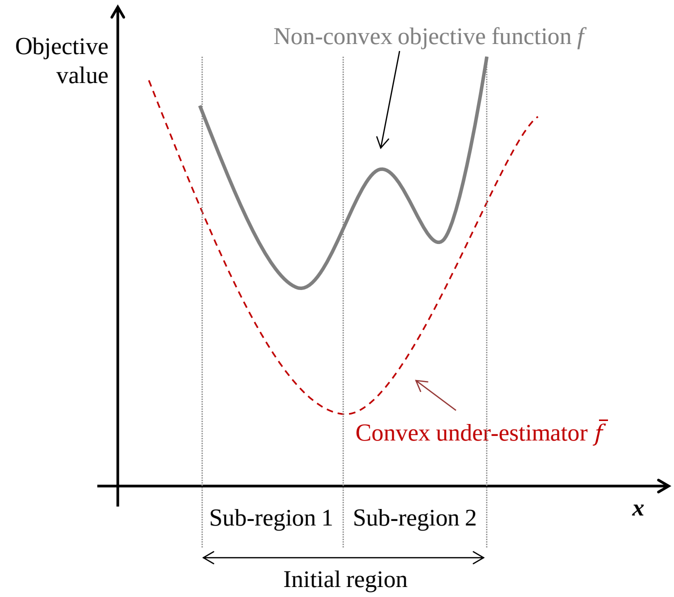

Figure 2.13. The concept of constructing the convex under-estimator for a non-convex function, adapted from Grossmann and Biegler (2004).

2.18.4. Optimization with implicit constraints: Simulation-optimization programming

The simulation-optimization programming techniques (which will be used in Chapters 4 and 5) conform to optimization with implicit constraints and have proved efficient in process optimization using simulators (Sharifzadeh et al, 2011; Caballero et al 2007; Odjo et al, 2011). In simulation-optimization programming, the simulator has an input-output black-box relationship to the optimizer. Optimization is performed in the outer loop and the simulation is solved in the inner loop. The advantage of this method is that it provides an opportunity to apply off-the-shelf simulation software tools with advanced thermodynamic property packages. In addition, the number of optimization variables is limited to the required specifications of the simulation program, (i.e., the variables which should be specified independently to run the simulator). For fixed values of the optimization variables, the equation solver of the simulator is able to calculate the remaining variables. By convergence of the equation solver, the value of the objective function is evaluated and reported to the optimizer. The disadvantage of this method is that evaluation of the objective function is computationally expensive and time-consuming because for each evaluation, the equation solver needs to converge.

2.18.5. Multi-criteria decision-making

As discussed by many researchers, (e.g., Luyben 2004; Alhammadi and Romagnoli 2004), there are conflicts and competitions between control and process objectives. The requirement to establish a trade-off between these objectives conforms to the concept of multi-criteria decision-making (MCDM) (also known as multi-objective programming). If the objectives were not competing with each other, optimizing them separately would result in the overall optimal solution. However, in the case of competing and conflicting objectives, all the objectives need to be optimized, simultaneously.

The mathematical formulation of multi-objective optimization can be presented as:

$$\min \{J_1(X,Y), J_2(X,Y), \ldots, J_N(X,Y)\} \qquad \text{MCDM}$$

Subject to:

$$h_j(X,Y) = 0$$

$$g_{j'}(X,Y) \leq 0$$

$$X \in S_1 \,, \qquad Y \in S_2$$

in which J_i is an objective function. The variables X and Y are discrete and continuous respectively and $N \geq 2$ represents the total number of objectives. The notations $h_j(\,)$ and $g_{j'}(\,)$ represent equality and inequality constraints respectively. In addition, S_1 and S_2 are the feasible domains of the discrete and continuous variables respectively.

Figure 2.14 (adapted from Jones and Tamiz 2010) shows the concept for a bi-objective function. The feasible region is the area in which it is possible to satisfy the constraints. Outside this region, the constraints are violated. Some points in the feasible region feature a better fitness regarding the objective functions. The solution of a multi-objective optimization problem is not unique, and is a set of Pareto optimal solutions. A Pareto optimal (also called Pareto efficient) solution is a non-inferior solution (i.e., not inside the feasible region, as shown in Figure 2.14) for which no other feasible solution exists, which can improve the value of an objective without sacrificing the other objectives. The Pareto front (also called Pareto frontier) is the set of all Pareto optimal solutions. In Figure 2.14, by moving a Pareto optimal solution on the Pareto front to the right and left, the values of the first and second objective function improves respectively. At the same time by improving the value of an objective function, the value of the other objective function deteriorates.

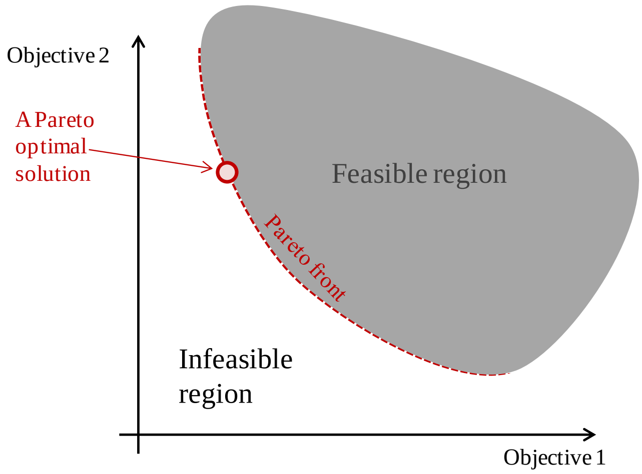

Figure 2.14. The feasible region and Pareto front for a bi-objective optimization problem.

One way of constructing a Pareto front is to calculate an aggregated objective value by assigning weighting factors, w_i , to different objectives, J_i. Then, by varying the ratios of the weighing factors, the Pareto front is constructed.

$$\text{Aggregated Objective} = \sum_{i=1}^{N} w_i J_i(X, Y) \qquad (2-52)$$

The main disadvantage of the above approach is that it is computationally expensive. The alternative approach is to use goal programming. In goal programming, for each objective, a target level is assigned and the deviation from that target is minimized. Since, meeting the goals as closely as possible is the main aim of goal programming, the underlying philosophy of goal programming is satisfying and sufficiency of the achieved levels of the targets. The extensive and recent discussions of the methods for goal programming are presented by Jones and Tamiz (2010).

It is notable that constraints are interpreted differently from goals and their deviational variables. Unmet constraints render the solution infeasible and unimplementable. However, a nonzero deviational variable can represent a feasible or even a Pareto optimal solution, as shown in Figure 2.15a. In fact, for conflicting and competing objectives, a solution by which all the goals are achieved and all the deviational variables are zero is often infeasible, and nonzero deviational variables represent the level of disagreement between competing objectives. Therefore, goal programming aims at establishing a trade-off between the achieved levels of goals, by finding reasonable values for deviational variables.

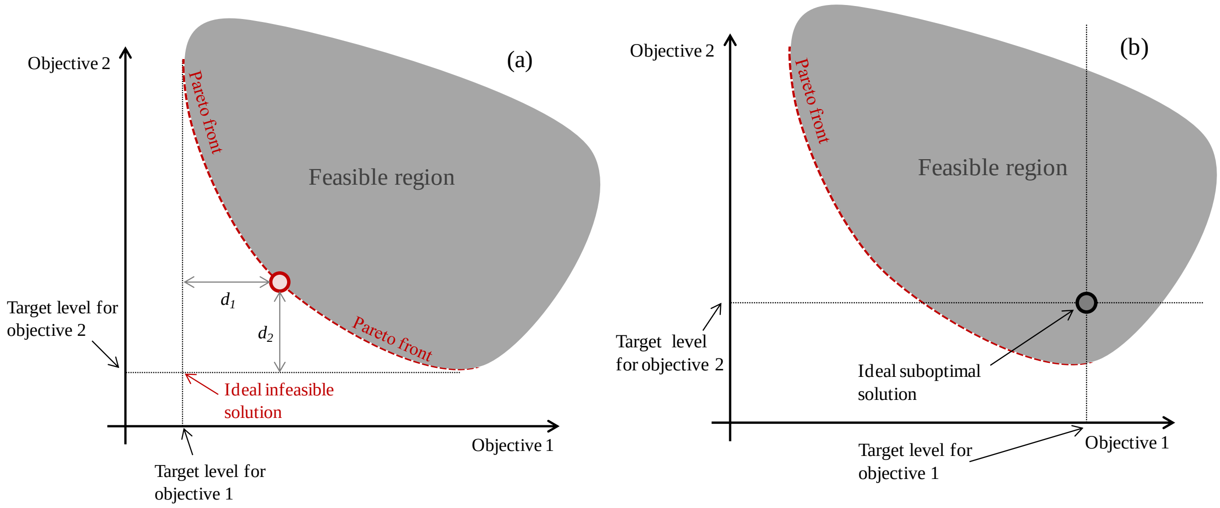

Figure 2.15. Goal programming; a) correct choices of the target levels, b) unbalanced, sub-optimal solution due to incorrect choices of the target levels.

Figures 2.15 show the concept; two target levels are specified for the two objective functions and the corresponding deviational variable d_1 and d_2 are minimized. These figures also reveal the importance of the target values. In Figure 2.15a, target levels are set optimistically and the ideal solution is infeasible, but the goal program found a Pareto optimal solution. In Figure 2.15b, pessimistic choices of the target values resulted in an inferior suboptimal solution. Jones and Tamiz (2010) argued that if the goals are set optimistically, goal programming and optimization coincide. However, if the goals are set pessimistically, the solution of goal programming could be sub-optimal (as shown in Figure 2.15b), i.e., another feasible solution exists that improves at least one of the objectives without worsening the other objectives.

The other important aspect of goal programming is that in most cases, it is not sufficient to solely rely on the average of deviational variables for constructing the aggregated objective:

$$\min \frac{1}{N}\sum_{i=1}^{N}(J_i(X,Y) - J_i^{target}) \qquad (2-53)$$

If balancing between the achieved level of goals is also important, a min-max metric (also known as Chebyshev distance metric) is added, in which the worst level of the achieved goals is also minimized. This method is known as efficiency-equity trade-off method (Gonzales-Pachon and Romero, 1999):

$$\min \left(\frac{1}{N}\sum_{i=1}^{N}(f_i(X,Y) - f_i^{target}) + Maximum\{J_i(X,Y) - J_i^{target}\}\right) \qquad (2-54)$$

It is notable that the method of weighting factor may not explore the entire Pareto front in the case of non-convexities. Other alternatives for constructing Pareto fronts are evolutionary and Ɛ-constraint methods. The details of these methods are available in literature (e.g., Alhammadi and Romagnoli 2004). Comparison of these methods is not the focus of the present research.

2.19. Conclusion

In this chapter, a thematic review of literature regarding process design and control was presented. Figure 2.1 gave a snapshot of research in the field. The main approaches for process design and control can be classified into sequential methods and integrated design and control methods. The sequential methods have a yes/no attitude to the problem while the integrated design and control methods incorporate some aspects of control design into the process design. All the above methods use mathematical modelling. However, the methods using first principles modelling are more successful in integrating design and control.

Due to high dimensionality of the problem, a variety of methods addresses the problem by decomposing it to several smaller subproblems. Decomposition can be based on individual unit operations, different time-scales, prioritization of control objectives, or heuristics for the design of inventory control systems.

This chapter also reviewed the characteristics and desired properties of the elements of control systems. Spatial and temporal decentralizations of control systems were explained and conventional multi-loop controllers and centralized model predictive controllers were discussed. This chapter also discussed the desirable properties of manipulated and controlled variables. The economic implications of static and dynamic setpoint policies were discussed and the importance of selection of controlled variables for process profitability was emphasized.

The causes of control imperfection, also limit process controllability. Different definitions for operability, flexibility, and controllability were presented and the causes of control imperfection namely the interactions between control loops, delays and right-half-plane zeros, manipulated variable constraints and model uncertainties were discussed in this chapter. Moreover, it was explained that the methods based on passivity, exploit the process model to evaluate the stability and integrity of decentralized control structures.

Then, the discussions moved to the methods in which process design and control are integrated to some extents. A category of optimization-based methods uses a multi-objective function for screening alternative solutions. This also provides the opportunity for incorporating controllability measures into economic optimization. These methods were reviewed in this chapter.

A variety of methods is devoted to flexibility analysis, i.e., whether for a range of uncertain scenarios, the process operation remains feasible. As discussed in this chapter, the optimization methods for steady-state and dynamic operability analyses are developed by researchers. In addition, it is possible to evaluate the feasibility of the process operation by mapping the bounds of the input variables into the output spaces. This idea resulted in the geometric methods for operability analysis.

It was also discussed that minimizing the economic losses associated with disturbances, in terms of back-off from active constraints, can be applied as an economic measure for integrated design and control.

By development of computational capabilities, some researchers optimized the process and its controllers simultaneously. However, the underlying formulation features combinatorial nature and is limited to smaller problems. In addition as discussed in the first chapter, due to conceptual complexity issues, including controllers in the optimization is of limited practicality.

The comparisons between the methods on the right branch of Figure 2.1 are illustrative. All these methods try to establish criteria for evaluating and screening the performances of alternative decisions in designing process and control systems. Some methods employ the controllability measures, and incorporate them into a multi-objective function. In the methods based on model reduction, robust control measures were used instead. In the methods for analysing the nonlinear behaviour of chemical processes, the aim is to avoid undesirable characteristics such as steady-state multiplicity. The geometric methods for operability analysis are trying to ensure that for all disturbance scenarios, the desired outputs are achievable, using available inputs. Similarly, the methods for flexibility optimization, try to evaluate and quantify the effects of uncertain parameters on feasibility of process operation. In some research, the decision-making criterion is the economic losses associated with retreat from active constraints. Finally, the methods for simultaneous optimization of process and its controllers measure directly the controller error and incorporate it to a multi-objective function.

Furthermore, investigating the evolution path of the methods for integrated design and control suggests that the methods which have a direct link to the underlying first principles are more successful in integrating process design and control. This is the reason that almost all of the methods on the right branch of Figure 2.1 are nonlinear. Furthermore, simultaneous optimization of process and controllers pose a tough challenge for the current optimization methods, and requires efficient complexity reduction methods. The requirement for complexity reduction should address both numerical and conceptual complexities, in terms of the required computational costs, reliability of the solution and the desirable properties such as controllability, operability and flexibility. Finally, as discussed in this chapter, the problem of integrated design and control need to address the interactions between competing and conflicting process design and control objectives. Therefore, the desirable method should feature multi-criteria decision-making capabilities in order to be able to establish a trade-off between different objectives.

The presented materials in this chapter will serve as basis for theoretical developments in the next chapter, which present a new optimization framework for integrated design and control.

3 | An optimization framework using an inversely controlled process model

3.1. Introduction

The conventional approach for integrated design and control is to optimize a combined model of the process and its controllers. However, as discussed earlier, optimizing controllers poses conceptual as well as numerical challenges. This chapter introduces a new optimization framework using an *inversely controlled process model*, in which the model of controllers is replaced by perfect control equations. The complexities associated with controllers are removed from the problem formulation, while the process and its control structure are still optimized, simultaneously. This chapter presents the steady-state as well as the dynamic mathematical formulations of the proposed optimization framework for optimal control structure selection and integrated design and control.

In the subsequent sections, firstly the mathematical formulation of the new optimization framework for integrated design and control (Problem 2) is developed as the mathematical formulation of the conventional optimization framework (Problem 1) is modified and perfect control equations are included. These modifications enable formulation and proposition of a new optimization framework using *an inversely controlled process model*. Two versions of the proposed optimization framework are presented for steady-state and dynamic analyses. These optimization frameworks will be applied to three case studies in the subsequent Chapters 4, 5, and 6. They are:

- Subproblem 2.stst: *Optimal selection of control structures* using a *steady-state* inversely controlled process model will be studied on the case of a distillation train in Chapter 4.
- Problem 2.stst: *Integrated design and control* using a *steady-state* inversely controlled process model will be studied on the case of a reactive distillation column in Chapter 5.
- Problem 2.dyn: *Integrated design and control* using a *dynamic* inversely controlled process model will be studied on the case of two heat-integrated series reactors in Chapter 6.

This chapter presents the mathematical formulations of the above problems and subproblem and serves as the theoretical basis for the subsequent chapters in which the proposed frameworks will be applied to several cased studies.

The statements of the conventional framework for integrated design and control (Problem 1) and the proposed framework for integrated design and control (Problem 2) were presented in Chapter 1. Furthermore, the motivations for numerical and conceptual complexity reductions by separating the controller design were discussed in that chapter. In the subsequent sections, firstly the mathematical formulation of the conventional integrated design and control framework is presented. Then, this formulation is modified and the mathematical formulation for the new optimization framework based on perfect control is developed.

3.2. Mathematical formulation of conventional integrated design and control, Problem 1

The conventional approach to integrated design and control can be formulated as a stochastic mixed integer dynamic optimization problem as follows:

$$\min E\{J_s[\boldsymbol{Y_p}, \boldsymbol{Y_{cv}}, \boldsymbol{Y_{mv}}, \boldsymbol{p}, \boldsymbol{\vartheta}, \boldsymbol{u}(t)]\} \qquad \text{Problem 1}$$

Subject to:

$$\boldsymbol{f}[\dot{\boldsymbol{z}}(t), \boldsymbol{z}(t), \boldsymbol{x}(t), \boldsymbol{u}(t), \boldsymbol{y}(t), \boldsymbol{Y_p}, \boldsymbol{p}, \boldsymbol{\mu}(t)] = 0$$

$$\boldsymbol{h}[\boldsymbol{z}(t), \boldsymbol{x}(t), \boldsymbol{u}(t), \boldsymbol{y}(t), \boldsymbol{Y_p}, \boldsymbol{p}, \boldsymbol{\mu}(t)] = 0$$

$$\boldsymbol{g}[\boldsymbol{z}(t), \boldsymbol{x}(t), \boldsymbol{u}(t), \boldsymbol{y}(t), \boldsymbol{Y_p}, \boldsymbol{p}, \boldsymbol{\mu}(t)] \leq 0$$

$$\boldsymbol{\theta}[\dot{\zeta}(t), \zeta(t), \boldsymbol{\gamma}(t), \boldsymbol{x}(t), \boldsymbol{z}(t), \boldsymbol{y}(t), \boldsymbol{u}(t), \boldsymbol{Y_{cv}}, \boldsymbol{Y_{mv}}, \boldsymbol{\vartheta}] = 0$$

$$\boldsymbol{\varphi}[\boldsymbol{x}(t), \boldsymbol{u}(t), \boldsymbol{y}(t), \zeta(t), \boldsymbol{\gamma}(t), \boldsymbol{Y_{cv}}, \boldsymbol{Y_{mv}}, \boldsymbol{\vartheta}] = 0$$

$$\Omega_s[\boldsymbol{\mu}(t)] = 0$$

In above, $\boldsymbol{z}(t)$ is the vector of process differential variables, $\boldsymbol{x}(t)$ is the vector of process algebraic variables, $\boldsymbol{u}(t)$ is the vector of candidate manipulated variables, $\boldsymbol{y}(t)$ is the vector of candidate controlled variables, $\boldsymbol{p}$ is the vector of process parameters, $\zeta(t)$ is the vector of control differential variables, $\boldsymbol{\gamma}(t)$ is the vector of control algebraic variables, $\boldsymbol{\vartheta}$ is the vector of control parameters, $\boldsymbol{\mu}(t)$ is the vector of disturbance parameters. s is the index of disturbance scenario. $\boldsymbol{Y_p}$ is the vector of structural process variables. $\boldsymbol{Y_{cv}}$ and $\boldsymbol{Y_{mv}}$ are the vectors of structural variables for selection of controlled and manipulated variables respectively. While $\boldsymbol{Y_p}$, $\boldsymbol{Y_{cv}}$ and $\boldsymbol{Y_{cv}}$ are vectors of integer variables, the rest of the variables are continuous.

In addition, $\boldsymbol{f}[\,] = 0$ is the vector of process differential equations, $\boldsymbol{h}[\,] = 0$ is the vector of process algebraic equations, $\boldsymbol{g}[\,] \leq 0$ is the vector of inequality constraints, $\boldsymbol{\theta}[\,] = 0$ is the vector of control differential equations, $\boldsymbol{\varphi}[\,] = 0$ is the vector of control algebraic equations, $\Omega_s[\,] = 0$ is the vector of equations for disturbances. The expected value $E\{\,\}$ of the objective function $J_s[\,]$ should be minimized.

The above mathematical formulation applies a combined modelling approach in which the models of the process and its controllers are included and linked together. This combined model includes optimization variables which are structural (integer) or parametric (continuous). While structural decisions concern choices between alterative process configurations and alternative control structures, the parametric decisions concern the values of process variables such as flows, temperatures or pressures, the design parameters of process equipment and also controller parameters.

The concept of the conventional optimization framework for integrated design and control is shown in Figure 3.1. It shows the trial values of the optimization variables being exported by the optimization algorithm to the combined process-controller model. By setting the values of the optimization variables, the combined model is fixed and its performance is tested against different disturbance scenarios. Then the values of the objective function and the violations of constraints are reported to the optimization algorithm. The optimization algorithm evaluates the termination criteria and decides on improvement of the optimization variables.

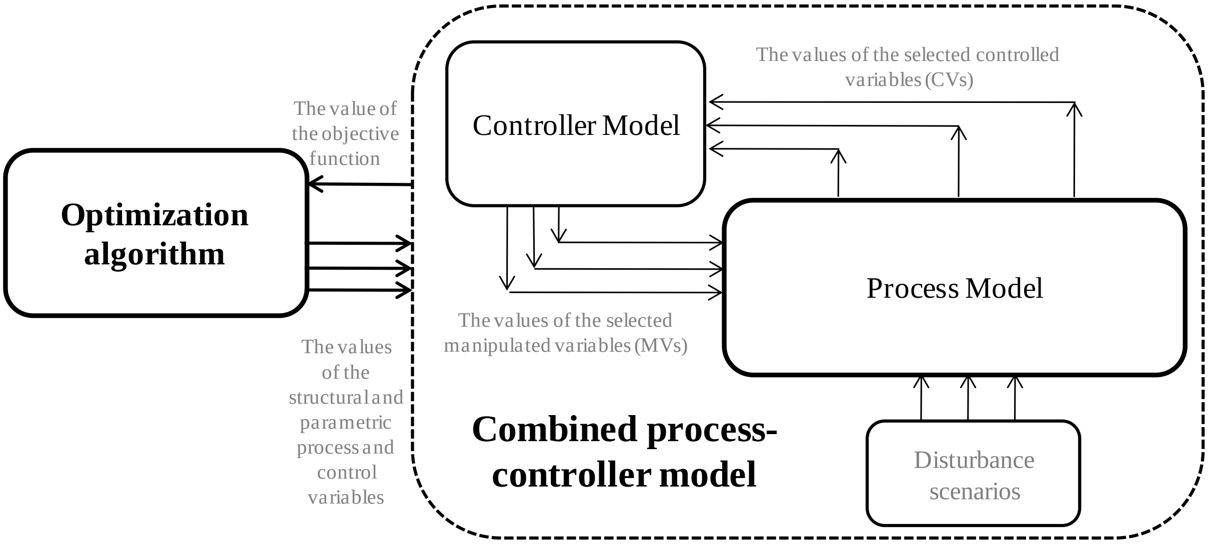

Figure 3.1. The conventional optimization framework for integrated design and control of chemical processes.

A comparison between the mathematical formulation, Problem 1, and the graphical representation in Figure 3.1 is illustrative. The constraints $\boldsymbol{f}[\,]$, $\boldsymbol{h}[\,]$ and $\boldsymbol{g}[\,]$ represent the process model. The constraints $\boldsymbol{\theta}[\,]$, and $\boldsymbol{\varphi}[\,]$ represent the controller models. The equality constraints $\Omega_s[\,] = 0$ represent disturbance scenario s. $\boldsymbol{\mu}(t)$, disturbance variables, represent those exogenous variables over which we have no control, (Ogunnaike and Ray, 1994). The examples of disturbances include the fluctuations in immediate upstream processes, sudden changes in the ambient conditions or measurement noises. The disturbance scenarios can be extracted from plant operating data. In addition, in Chapter 2, it was explained that the flexibility analysis method or the methods base on model reduction and robust control can be used to identify the worst disturbance scenario. In this research, it is assumed that expected disturbance scenarios are known in advance. As shown in Figure 3.1, disturbances affect the process model, and therefore, $\boldsymbol{\mu}(t)$ appear in the arguments of the constraints representing the process model. Then, the effects of the disturbances are detected by the controllers through the controlled variables and are counteracted by adjusting the manipulated variables. For each disturbance scenario, a value for the objective function is calculated $J_s[\,]$. Therefore, the multi-objective function depends on the expected disturbance scenarios. The optimization variables are the structural process variables $\boldsymbol{Y_p}$ (such as process configuration), the structural variables $\boldsymbol{Y_{cv}}$ and $\boldsymbol{Y_{mv}}$ for selection of controlled and manipulated variables, the process parameters $\boldsymbol{p}$ (such as the size of process equipment, nominal operating conditions), the controller parameters $\boldsymbol{\vartheta}$ (such as gain and integral constants in a proportional integral controller) and the optimal trajectories of the manipulated variables, $\boldsymbol{u}(t)$. The overall objective value is calculated for all disturbances and then reported to the optimization algorithm for decision-making.

3.3. Applying an inversely controlled process model for integrated design and control (proposed framework)

The aim of this section is to remove the complexities associated with controllers from the conventional optimization framework presented in the last section. The modification is firstly explained by considering the troublesome element in Figure 3.1, i.e., the controller model. Then, the mathematical formulation of Problem 1 is modified to include perfect control equations and to eliminate the need for modelling controllers.

In order to disentangle the design of controllers, their algebraic and differential equations ($\boldsymbol{\theta}[\,] = 0$ and $\boldsymbol{\varphi}[\,] = 0$) must be replaced by perfect control equations which ensure that the selected controlled variables are maintained at their desired values:

$$y_i(t) = y_{i,setpoint} \qquad (3-1a)$$

$$u_{j'}(t) = u_{j',nominal} \qquad (3-1b)$$

where $y_i(t)$ is the selected controlled variable and $y_{i,setpoint}$ is the corresponding setpoint. However, $u_{j'}(t)$ represents the manipulated variable which is not selected and $u_{j',nominal}$ is the corresponding nominal value. The implication of equation $(3-1b)$ is that if a manipulated variable is not selected, it will be left unadjusted at its nominal value.

In principle, $y_{i,setpoint}$, can be time-dependent. However, in optimization of a continuous process it would normally be constant, equivalent to disturbance rejection which is the focus of this research.

In general, there will be several alternatives for perfect control because it is possible to select different sets of controlled variables and manipulated variables. In addition, perfect control equations consume degrees of freedom and their consistency with the available degrees of freedom must be ensured. These considerations can be formulated using mixed integer nonlinear programming:

$$\min E\{J_s[\boldsymbol{Y_p}, \boldsymbol{Y_{cv}}, \boldsymbol{Y_{mv}}, \boldsymbol{p}, \boldsymbol{\vartheta}, \boldsymbol{y_{i,setpoint}}, \boldsymbol{u_{j,nominal}}]\} \qquad \text{Problem 2}$$

subject to:

$$\boldsymbol{f}[\dot{\boldsymbol{z}}(t), \boldsymbol{z}(t), \boldsymbol{x}(t), \boldsymbol{u}(t), \boldsymbol{y}(t), \boldsymbol{Y_p}, \boldsymbol{p}, \boldsymbol{\mu}(t)] = 0$$

$$\boldsymbol{h}[\boldsymbol{z}(t), \boldsymbol{x}(t), \boldsymbol{u}(t), \boldsymbol{y}(t), \boldsymbol{Y_p}, \boldsymbol{p}, \boldsymbol{\mu}(t)] = 0$$

$$\boldsymbol{g}[\boldsymbol{z}(t), \boldsymbol{x}(t), \boldsymbol{u}(t), \boldsymbol{y}(t), \boldsymbol{Y_p}, \boldsymbol{p}, \boldsymbol{\mu}(t)] \leq 0$$

$$\Omega_s[\boldsymbol{\mu}(t)] = 0$$

$$\boldsymbol{Y_{cv,i}}\left(\boldsymbol{y_i}(t) - \boldsymbol{y_{i,setpoint}}\right) = 0 \qquad i \in I_{kcv}$$

$$(\boldsymbol{1} - \boldsymbol{Y_{mv,j}})\left(\boldsymbol{u_j}(t) - \boldsymbol{u_{j,nominal}}\right) = 0 \qquad j \in I_{kmv}$$

$$\boldsymbol{\Psi}(\boldsymbol{Y_{cv,i}}, \boldsymbol{Y_{mv,j}}) \geq 0$$

In above, the mathematical notations are similar to Problem 1. In addition, the controller differential and algebraic equations (i.e., $\boldsymbol{\theta}[\,] = 0$ and $\boldsymbol{\varphi}[\,] = 0$) are replaced by perfect control equations. The perfect control equations are shown by the dotted envelope. $\boldsymbol{Y_{cv,i}}$ and $\boldsymbol{Y_{mv,j}}$ are the binary variables which indicate whether a controlled variable or a manipulated variable is selected respectively. The multiplier of the manipulated variables in the second to the last equation encloses the complement of the corresponding binary variables, i.e. $(\boldsymbol{1} - \boldsymbol{Y_{mv,j}})$. The implication is that if a manipulated variable is not selected, it is left at its nominal value, while the required value of the selected manipulated variables are calculated. The last set of constraints, $\boldsymbol{\Psi}(\,)$, are the results of degree of freedom analysis and represent the constraints needed to ensure that the selected manipulated and controlled variables are consistent. Examples of these constraints and the required analysis are presented in Section 4.4.3.1 and Section 5.4.2.1. The options for a controlled variable or a manipulated variable are represented by I_{kcv} and I_{kmv} respectively. Notice that in the proposed framework using a dynamic inversely controlled process model, the setpoints of the controlled variables are the optimization variables, compared to the conventional framework in which the trajectories of manipulated variables are optimized. It is also important to note that in both conventional and proposed optimization framework, the results strongly depend on the expected disturbances.

Figure 3.2 shows the concept. The model of controllers is replaced with equations representing perfect control, which enable the directions of the information flows to be reversed from the controlled variables (CVs) to the manipulated variables (MVs).

Firstly, the optimization algorithm decides the trial values of the parametric and structural optimization variables. These variables include the design parameters of process equipment and the operating conditions such as temperatures, pressures and flowrates as well as the process structure and the control structure. Then, the fitness of these trial values must be tested against disturbance scenarios. In an inversely controlled process model, the values of the controlled variables are maintained constant by the perfect control equations while the time trajectories of the manipulated variables are adjusted in order to reject the disturbances. Then, the values of the objective function and the violations of constraints are evaluated and reported to the optimization algorithm. The optimization algorithm evaluates the termination criteria and decides on improvement of the optimization variables.

The following sections develop and discuss several variants of Problem 2 in which steady-state and dynamic inversely controlled process models are applied for optimal selection of control structures and integrated design and control.

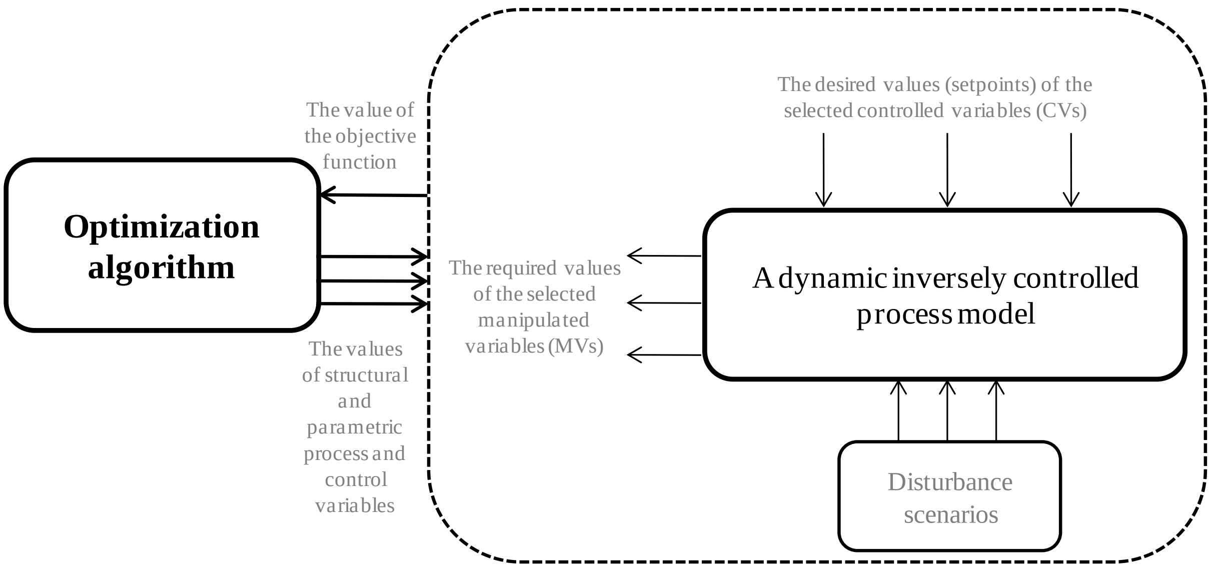

Figure 3.2. The proposed optimization framework for integrated design and control using an inversely controlled process model

3.4. A steady-state inversely controlled process model for optimal selection of control structures

The problem statement for optimal selection of control structures was presented in Section 1.2.4. The mathematical formulation for optimal selection of control structures using a steady-state inversely controlled process model (Subproblem 2.stst) can be derived directly from the formulation of Problem 2. Due to the steady-state assumption, the time dependencies of the variables are ignored and the time-derivatives are set equal to zero. Therefore, the mathematical formulation of Subproblem 2.stst consists of only algebraic equations (AEs). Since the control structure is being decided, different controlled variables or manipulated variables may be selected during optimization search, which represent different perfect controls. Therefore, each candidate control structure generates a different set of AEs. In addition, a set of constraints should be implemented in order to ensure that the selected degrees of freedom are consistent. Therefore, the mathematical formulation of the proposed steady-state optimization framework for optimal selection of control structures can be presented as follows:

$$\min E\{J_s[\boldsymbol{Y_{cv}}, \boldsymbol{Y_{mv}}]\} \qquad \text{Subproblem 2.stst}$$

subject to:

$$\boldsymbol{h}'[\boldsymbol{x}', \boldsymbol{u}, \boldsymbol{y}, \boldsymbol{\mu}] = 0$$

$$\boldsymbol{g}[\boldsymbol{x}', \boldsymbol{u}, \boldsymbol{y}, \boldsymbol{\mu}] \leq 0$$

$$\Omega_s[\boldsymbol{\mu}] = 0$$

$$\boldsymbol{Y_{cv,i}}(\boldsymbol{y_i} - \boldsymbol{y_{i,setpoint}}) = 0 \qquad i \in I_{kcv}$$

$$(\boldsymbol{1} - \boldsymbol{Y_{mv,j}})(\boldsymbol{u_j} - \boldsymbol{u_{j,nominal}}) = 0 \qquad j \in I_{kmv}$$

$$\boldsymbol{\Psi}(\boldsymbol{Y_{cv,i}}, \boldsymbol{Y_{mv,j}}) \geq 0$$

The notation Subproblem 2.stst refers to a subproblem (proposed control structure selection) within a larger problem (proposed integrated design and control) using a steady-state inversely controlled process model. Since, the steady-state assumption implies that the time-derivatives are equal to zero, the differential equations (i.e., $\boldsymbol{f}[\ ]$) in Problem 2 become algebraic equations in Subproblem 2.stst and their union with other algebraic equations (i.e., $\boldsymbol{h}[\ ]$) is represented by $\boldsymbol{h}' = \begin{bmatrix} \boldsymbol{f} \\ \boldsymbol{h} \end{bmatrix}$. Similarly, the new vector of algebraic variables is $\boldsymbol{x}' =$

$\begin{bmatrix} z \\ x \end{bmatrix}$. The complexity reduction described above limited the optimization variables to the structural (integer) control variables $Y_{cv,i}$ and $Y_{cv,i}$. All the continuous variables are implied in the optimization constraints. The above formulation can be addressed using the methods for mixed integer nonlinear programming (MINLP).

The equality constraints in Subproblem 2.stst represent a time-independent mathematical model in which the values of the manipulated variables are calculated from the desired values (i.e., setpoints) of the controlled variables, hence the process model is inverted.

Figure 3.3 shows the concept of the steady-state inversely controlled process model for optimal selection of control structures. The information flow is similar to Figure 3.2. However, the optimization variables are limited to structural control variables (i.e. selection of manipulated and controlled variables) as discussed earlier.

In the new framework, the controlled variables, the expected disturbance scenarios, and the manipulated variables used to reject the disturbances are the primary decisions that need to be considered. Later in this chapter, it will be discussed that the application of a steady-state inversely controlled process model ensures regulatory steady-state operability.

The application of the proposed optimization framework of Subproblem 2.ststs, shown in Figure 3.3, will be demonstrated using a case study of a distillation train, in Chapter 4. The optimization programming and employed software tools will be explained and the results will be discussed.

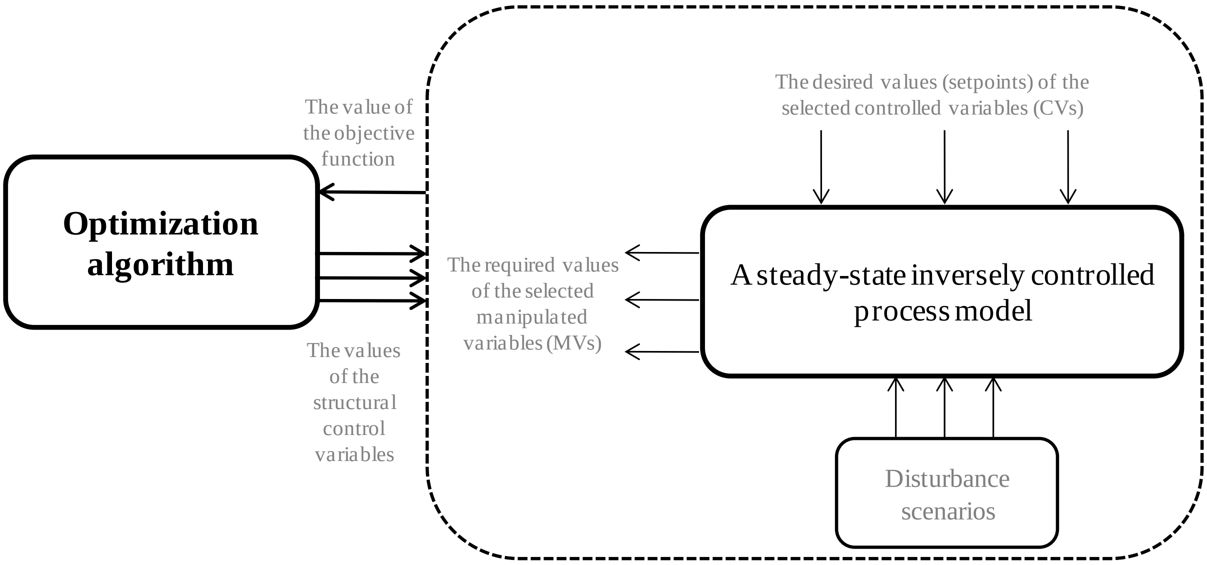

Figure 3.3. The proposed optimization framework for optimal selection of control structures using a steady-state inversely controlled process model

3.5. A steady-state inversely controlled process model for integrated design and control

This section now extends the formulation of the last section to enable design of the process in addition to selection of the control structure. Similar to the last section, the application of a steady-state inversely controlled process model limits the constraints to algebraic equations (AEs). However, both the process and its control structure are being optimized simultaneously. The problem has a mixed integer nonlinear programming (MINLP) formulation, as follows:

$$\min E\{J_s[\boldsymbol{Y_p}, \boldsymbol{Y_{cv}}, \boldsymbol{Y_{mv}}, \boldsymbol{p}, \boldsymbol{y_{i,setpoint}}, \boldsymbol{u_{j,nominal}}]\} \qquad \text{Problem 2.stst}$$

subject to:

$$\boldsymbol{h}'[\boldsymbol{x}', \boldsymbol{u}, \boldsymbol{y}, \boldsymbol{Y_p}, \boldsymbol{p}, \boldsymbol{\mu}] = 0$$

$$\boldsymbol{g}[\boldsymbol{x}', \boldsymbol{u}, \boldsymbol{y}, \boldsymbol{Y_p}, \boldsymbol{p}, \boldsymbol{\mu}] \leq 0$$

$$\Omega_s[\boldsymbol{\mu}] = 0$$

$$\boldsymbol{Y_{cv,i}}(\boldsymbol{y_i} - \boldsymbol{y_{i,setpoint}}) = 0 \qquad i \in I_{kcv}$$

$$(\boldsymbol{1} - \boldsymbol{Y_{mv,j}})(\boldsymbol{u_j} - \boldsymbol{u_{j,nominal}}) = 0 \qquad j \in I_{kmv}$$

$$\boldsymbol{\Psi}(\boldsymbol{Y_{cv,i}}, \boldsymbol{Y_{mv,j}}) \geq 0$$

The notation Problem 2.stst implies that Problem 2 (the proposed integrated design and control) is presented using a steady-state formulation. The other mathematical notations are the same as the last problems and subproblem.

The concept is shown in Figure 3.4. The information flow is similar to Figure 3.3. However, the optimization variables include also the structural and parametric process variables.

In the new steady-state framework for integrated design and control, the process configuration and design, the controlled variables, the expected disturbance scenarios, and the manipulated variables used to reject the disturbances are the primary decisions that need to be considered. The application of the proposed optimization framework of Problem 2.stst will be demonstrated using a case study of a reactive distillation column, in Chapter 5.

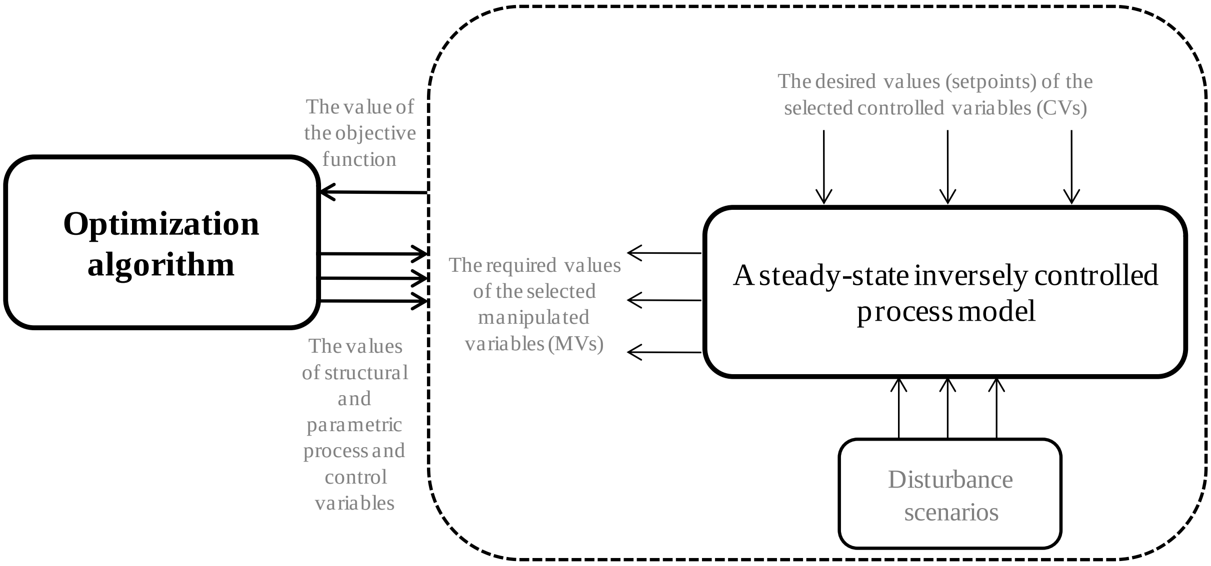

Figure 3.4. The proposed optimization framework for integrated design and control using a steady-state inversely controlled process model.

3.6. A dynamic inversely controlled process model for integrated design and control

The mathematical formulation for integrated design and control using a dynamic inversely controlled process model, Problem 2.dyn, is identical to the mathematical formulation of Problem 2:

$$\text{Problem 2.dyn} \equiv \text{Problem 2} \qquad (3-2)$$

Therefore, Problem 2.dyn consists of differential algebraic equations (DAEs). Since both structural and parametric variables of the process and its control structure are being optimized, the problem conforms to a nonlinear mixed integer dynamic optimization (MIDO) problem.

The concept was shown in Figure 3.2 and the information flow of the proposed dynamic optimization framework for integrated design and control was discussed in Section 3.3.

Compared to the last section, the formulation of Problem 2.dyn requires higher modelling and computational efforts because this formulation consists of differential algebraic equations. However, as will be discussed in Chapter 7, the application of a dynamic inversely controlled process model ensures that the controlled variables are maintained at their desired trajectories while the manipulated variables are adjusted accordingly, which conforms to the notion of *functional controllability*, (Rosenbrock 1970). Furthermore, incorporating functional controllability into the optimization framework for integrated design and control will ensure that such transient trajectories are optimal with respect to the process and control objectives.

In the proposed dynamic framework for integrated design and control, the process configuration and design, selection of controlled variables, the expected disturbance scenarios, and the manipulated variables used to reject the disturbances are the primary decisions that need to be considered. The application of the proposed optimization framework of Problem 2.dyn will be demonstrated using a case study of two series reactors in Chapter 7. The optimization programming will be explained and the results will be discussed.

3.7. Steady-state operability versus functional controllability

This chapter proposed a steady-state inversely controlled process models that consists of a set of nonlinear algebraic equations in which process inversion is made by fixing the controlled variables at their setpoints and calculating the required values of the manipulated variables for disturbance rejection. In addition, a dynamic inversely controlled process model was proposed that consists of a set of differential algebraic equations (DAEs), in which perfect control equations replace the model of controllers. In the dynamic inversely controlled process model, the controlled variables are maintained constant by the perfect control equations, while the time trajectories of the manipulated variables are adjusted in order to perfectly reject the disturbances.

However, there is a trade-off between the precision of controllability analysis and the required modelling efforts and computational expenses of the two steady-state and dynamic formulations. While a steady-state inversely controlled process model features a higher degree of complexity reduction, the efforts of developing a dynamic inversely controlled process model are rewarded by a higher confidence about process controllability. The differences of the two modelling approaches can be explained based on *regulatory steady-state operability* and *functional controllability* as follows.

3.7.1. Regulatory steady-state operability

As discussed in Chapter 2, the regulatory steady-state operability index is:

$$\mathrm{r-OI} = \frac{\mu\left(\mathrm{AIS} \cap \mathrm{DIS}_d(y^N)\right)}{\mu\left(\mathrm{DIS}_d(y^N)\right)} \qquad (2-17)$$

in which desired input set, $\mathrm{DIS}_d(y^N)$, is defined as:

$$\mathrm{DIS}_d(y^N) = \{u \mid M(\dot{x} = 0, \dot{u} = 0, y = y^N); \forall d \in \mathrm{EDS}\} \qquad (2-18)$$

In equation (2-17), AIS represents the available input set which are the values that the process inputs are able to take and EDS represents the expected disturbance space.

A comparison between the information flow in the proposed steady-state framework and the above definition of regulatory steady-state operability is illustrative. Figure 3.3 showed the information flow of the steady-state framework. In each iteration of the optimization framework, for each disturbance $\forall d \in \mathrm{EDS}$ and the nominal setpoints y^N, the desired input set $\mathrm{DIS}_d(y^N)$ is calculated by the steady-state inversely controlled process model. If no constraint on the input (manipulated) variables is violated, the whole set of $\mathrm{DIS}_d(y^N)$ will be achievable and this set is identical with AIS. Therefore, the regulatory steady-state operability will be equal to one. Otherwise, if any constraint on input variables is violated, the proposed optimization framework will encounter an infeasible solution and will be redirected to the feasible solutions for which the regulatory steady-state operability is equal to one.

3.7.2. Functional controllability

The following discussion concerns the implications of a dynamic inversely controlled process model for functional controllability of the solution. The discussion is mostly based on the results from Hirschorn, (1979). The relevance to the present research is to identify when the process inversion is possible and what characteristics the desired output trajectories should have to ensure functional controllability. It is notable that functional controllability has other names such as right-invertibility[2], output realizability, output controllability, and functional reproducibility, (Skogestad and Postlethwaite 2005; Singh 1982a-c). Consider the state-space representation below:

[2] Notice that right and left invertibility are identical for a square system (Daoutidis and Kravaris, 1991).

$x^o(t) = \mathbf{A}\big(x(t)\big) + u(t)\mathbf{B}\big(x(t)\big); \quad \boldsymbol{x}(t_0) = \boldsymbol{x_0} \epsilon\, M$ Nonlinear System (1)

$y(t) = \mathbf{C}\big(x(t)\big)$

In above $x(t)$ is the vector of state variables, $u(t)$ is the vector of input variables, $y(t)$ is the vector of output variables, M is a connected real analytical manifold. Here, the definition of functional controllability is restate from Chapter 2:

Definition: A process is functionally controllable if for the desired trajectories of the output variables, $\boldsymbol{y}(t)$, defined for $t > 0$, there exist some trajectories of the input variables, $\boldsymbol{u}(t)$, defined for $t > 0$, which generates the desired controlled variables from the initial states $\boldsymbol{x}(t_0)$, (Rosenbrock 1970).

According to the above definition, a dynamic system features functional controllability if it is invertible, (see also Hirschorn, 1979; Singh, 1982a-c; Daoutidis and Kravaris, 1991). A system is called invertible, if for an initial state x_0, and distinct inputs u^1, u^2, different outputs $\boldsymbol{y}(t; u^1, x_0) \neq \boldsymbol{y}(t; u^2, x_0)$ are calculated. Therefore, in principle, the required values of the inputs can be calculated from the desired values of the outputs, (Daoutidis and Kravaris, 1991). In order to present the necessary and sufficient condition for invertibility of a nonlinear dynamic system, the concept of *relative order* needs to be defined.

Definition: The relative order of Nonlinear System (1) is α such that $(adj_{\mathbf{A}}{}^{\alpha-1}\mathbf{B}\,)\big(c_j\big) \neq 0$ where c_j is a component of output mapping $\mathbf{C}$ and adj is *Lie bracket* operator.

Theorem 3.1: Nonlinear System (1) is invertible if and only if $\alpha < \infty$.

The proof is provided by Hirschorn, (1979).

Theorem 3.2: Consider Nonlinear System (1) with relative order α. If $\alpha < \infty$, $\boldsymbol{x}(t_0)\ \epsilon\ M$, then $\exists \boldsymbol{u}(t) \in \boldsymbol{U}$ such that $\boldsymbol{y}(t) = \boldsymbol{f}(t)$, if and only if $\boldsymbol{f}^{(\boldsymbol{k})}(t_0) = \boldsymbol{y}^{(\boldsymbol{k})}(t_0) = (\mathbf{A}^k\mathbf{C})(x_0)$ for $k = 0,1, \dots, \alpha - 1$.

The proof is provided by Hirschorn, (1979).

The definition of the rlative order, α, should be interpreted as the least number of times that an output need to be differentiated before an explicit relation to the manipulated variable can be generated. Therfore, Theorem 3.1 has an intuitive implication and that is the process model is invertible if and only if an explicit relationsship between the selcted inputs and the selcted outputs exists. It was explained earlier that a dynamic inversely controlled process model is constructed as the controller model is subtituted by the perfect control equations. The impliciation of Theorem 3.1 for the proposed integrated design and control framework is that it has a feasible solution if and only if the ouptuts corresponding to the included perfect control equations have a finite relative order with respect to the selected inputs.

Theorem 3.2 is known as *functional controllability conditions* in the context of nonlinear control (McLellan 1994) and implies that in order for function $\boldsymbol{f}(t)$ to be selected as the desired ouput trajectory, its initial value and the initial values of its first $\alpha - 1$ derivitives should be equal to the corresponding values of the outputs trajectories. In this research, the problem of disturbance rejection (i.e., setpoints are constant) was studied in which $\boldsymbol{f}^{(\boldsymbol{k})}(t_0) = 0$. The implication is that since for disturbance rejection the controlled variables remain constant at their setpoints (i.e.,$\boldsymbol{y}^{(\boldsymbol{k})}(t) = 0$), the functional controllability conditions in Theorem 3.2 will be always satisfied. Therefore, the application of a dynamic inversely controlled process model for disturbance rejection ensures functional controllability.

For linear systems, the above necessary and sufficient condition of functional controllability translates into the requirement that the process transfer matrix must feature full row rank, (Skogestad and Postlethwaite 2005). However, unlike linear systems, the invertibility of nonlinear systems depends on the initial states too, (Hirschorn, 1979). Since, in a dynamic inversely controlled process model, the required values of the inputs are calculated from the desired values of the outputs, the initial conditions depend on the disturbance scenarios. In other words, the solution is functionally controllable for the selected disturbance scenarios and may or may not be controllable for other disturbances.

It is notable that the concept of relative order has been also applied by researchers (Daoutidis and Kravaris, 1992b) for control structure selection as a measure of sluggishness of initial response and influence of the manipulated variables on the controlled variables,.

3.8. Conclusion

In this chapter, a new optimization framework using an inversely controlled process model was proposed. It was discussed that the proposed steady-state framework consists of nonlinear algebraic equations. The process inversion is performed by fixing the selected controlled variables or unselected manipulated variables at their setpoints and nominal values, respectively. However, the mathematical formulation of the proposed dynamic framework consists of algebraic-differential equations. Here, the process inversion is performed as perfect control equations replace the model of controllers. The outlined method will address the need for disentangling the numerical and conceptual complexities associated with controllers from the problem formulation. Several variants of the proposed optimization framework were formulated and discussed. They are:

- Subproblem 2.stst: *Optimal control structure selection* using a *steady-state* inversely controlled process model
- Problem 2.stst: *Integrated design and control* using a *steady-state* inversely controlled process model
- Problem 2.dyn: *Integrated design and control* using a *dynamic* inversely controlled process model

The mathematical formulation for optimization of the above problems and subproblem were presented and the achieved levels of complexity reduction were explained. It was shown that while the proposed steady-state framework ensures regulatory steady-state operability, a higher confidence regarding controllability can be gained by applying a dynamic inversely controlled process model, which ensures that solution features also functional controllability. The application of the proposed optimization frameworks will be later demonstrated using the case studies in Chapters 4, 5, and 6.

4 | Optimal selection of control structures using a steady-state inversely controlled process model

4.1. Introduction

Profitability of chemical processes strongly depends on their control systems. The design of a control system includes selection of controlled and manipulated variables, known as *control structure selection.* Systematic generation and screening alternative control structures require optimization. However, the size of such an optimization problem is much larger when controllers and their parameters are included and it rapidly becomes intractable.

With the aim of complexity reduction, Chapter 3 proposed an optimization framework for optimal selection of control structures using a steady-state inversely controlled process model. The mathematical formulation of the proposed framework and its characteristics were presented and discussed in Chapter 3. In the present chapter, this framework is applied to the case of a distillation train. A goal-driven multi-objective function is formulated to establish the trade-off between the competing objectives for control structure selection. It is also discussed that inventory control systems do not appear in a steady-state model and should be addressed separately. Then, the process description of the case study is presented and the optimization variables and constraints are discussed. The optimization programming and the employed software tools are also explained. Finally, the results are presented and discussed and the sensitivity of the solution is evaluated.

4.2. Multi-objective function and goal programming

As discussed earlier, there are alternative perfect control systems because it is possible to choose alternative sets of manipulated and controlled variables. Establishing the criteria for selection between these alternatives is an elusive task. In this chapter, a multi-objective function based on goal programming is applied. The proposed objective functions are listed in Table 4.1.

Table 4.1.
Objective functions for steady-state control structure selection

Obj_1 = the deviations in the quality and quantity of products
Obj_2 = the deviations in the manipulated variables
Obj_3 = the deviations in the state variables
Obj_4 = the economic losses due to disturbances

The first objective, Obj_1 , should be included when the quality (e.g., composition, conversion extent) of the products are being inferentially controlled by other measurements (e.g. inferential temperature control in a distillation column). This objective concerns feasibility of process operation, because low quality products are not marketable. Therefore, it has the highest priority.

The second objective, Obj_2 , aims at minimizing the changes in manipulated variables. The suppression of the excessive changes in manipulated variables is desirable:

- *To preserve control action from saturation;* this is because if excessive changes of manipulated variables are allowed for the expected disturbances, unexpected disturbances and uncertain conditions will influence the process even more and may result in the loss of control action (e.g., valve saturation).
- *To minimize the consumption of the resources associated with manipulated variables;* excessive utilization of manipulated variables incurs maintenance costs and may affect reliability of the process.
- *To reduce the interactions between controllers;* this is because changes in a manipulated variable does not solely affect the associated controlled variable, but also may influence the other process variables and may invoke other control loops, (Qin and Badgwell 2003; McAvoy 1999). Nevertheless, if the required changes in the manipulated variables are lessened, consequently the required time for disturbance rejection will be reduced.

The second objective has a lower priority compared to the first and fourth objectives.

The third objective, Obj_3 , is considered to make the intermediate state variables which are not controlled directly, insensitive to the disturbances. If the consequences of the disturbances on the state variables are less, the transition time needed to move from the initial steady state (before the disturbance) to the final steady state (after the disturbance) is shorter. However, in practice, it is not possible to consider all the state variables and the choice of the states for this objective function is subjective. An example of this objective is the changes in the temperature profile of a distillation column when flow or composition of the feed is disturbed. The third objective has a lower priority compared to other objectives.

The fourth objective, Obj_4, concerns the steady-state economic losses, i.e. decrease in profitability due to the disturbances. There is a similarity between this objective and the notion of self-optimizing control. As discussed in Chapter 2, the implication of self-optimizing control is that maintaining optimal controlled variables at their setpoints should minimize the economic losses in the presence of disturbances. This objective has a higher priority than the second and third objectives.

In chapter 3, it was explained that the solutions of multi-objective optimization is a set of Pareto optimal solutions which are located on a Pareto front. Since constructing a Pareto front is computationally expensive, in this chapter a goal programming multi-objective function is formulated. In goal programming, each objective function is given a goal or a target value.

The deviations from these target values are used to construct the aggregated objective value to be minimized as follows:

$$J_s = \left(\frac{1}{4} \sum_{w=1}^{4} \alpha_w \left(Obj_{w,s} - Obj_w{}^{target} \right) + Maximum\left\{ \alpha_w \left(Obj_{w,s} - Obj_w{}^{target} \right) \right\} \right)$$

$$w = 1 \dots 4 \qquad (4-1)$$

where s is the index of disturbances and α_w is the weighting factor of the objective function, $Obj_{w,s}$. These weighting factors are needed because, the four objective functions of Table 4.1 are not equally important, and higher weights should be given to the first and fourth objectives. The values of α_w depends on the problem and sometimes it is needed to refine them during the optimization. Therefore, the goal programming method applied in this thesis can be thought as a method for scaling and identifying the appropriate weights for the multi-objective function.

Selection of target values for the objective functions of Table 4.1 is straightforward because these targets have ideally the values of zero:

$$Obj_w{}^{target} = 0 \quad , \qquad w = 1 \dots 4 \qquad (4-2)$$

The target values of zero imply an optimistic ideal solution which is infeasible, i.e., it is not possible to ensure the quality and quantity of products, maintain the controlled variables constant, do not change the manipulated variables and incur no economic penalty. However, as discussed in Chapter 2, the advantage of the optimistic targets for goals is that the optimized solution will be Pareto optimal and not an inferior sub-optimal solution.

The aggregated objective, J_s , is calculated for each disturbance scenario, s. Then, the expected value of the aggregated objective for different disturbance scenarios must be minimized. This expected value can be constructed by summing up the objective values weighted by the likelihood of each disturbance scenario, L_s , (Sahinidis 2004):

$$\min \sum_{s=1}^{n_s} L_s J_s [\boldsymbol{Y}_{cv}, \boldsymbol{Y}_{mv}] \qquad \text{Subproblem 2.stst.gp}$$

subject to:

$$\boldsymbol{h}'[\boldsymbol{z}, \boldsymbol{x}, \boldsymbol{u}, \boldsymbol{y}, \boldsymbol{\mu}] = 0$$

$$\boldsymbol{g}[\boldsymbol{z}, \boldsymbol{x}, \boldsymbol{u}, \boldsymbol{y}, \boldsymbol{\mu}] \leq 0$$

$$\Omega_s[\boldsymbol{\mu}] = 0$$

$$\boldsymbol{Y}_{cv,i}\left(\boldsymbol{y}_i - \boldsymbol{y}_{i,setpoint}\right) = 0 \qquad i \in I_{kcv}$$

$$(\mathbf{1} - \boldsymbol{Y}_{mv,j})\left(\boldsymbol{u}_j - \boldsymbol{u}_{j,nominal}\right) = 0 \qquad j \in I_{kmv}$$

$$\boldsymbol{\Psi}(\boldsymbol{Y}_{cv,i}, \boldsymbol{Y}_{mv,j}) \geq 0$$

The notation Subproblem 2.stst.gp refers to the steady-state formulation of the proposed control structure selection with a goal programming multi-objective function. The optimization variables are structural variables (i.e., $\boldsymbol{Y}_{cv}$ and $\boldsymbol{Y}_{mv}$). All the continuous variables are implicit and included in the constraints which can be handled using an algebraic equation solver as will be discussed later.

4.3. Engineering insights and heuristics: dynamic degrees of freedom and design of inventory control systems

Since liquid hold-ups and gas inventories do not appear in a steady-state model, these variables must be considered separately. The application of a steady-state inversely controlled process model decomposes the subproblem of control structure selection into two smaller subproblems. One subproblem addresses the task of designing inventory controls, and the other subproblem optimizes the rest of the control structure. A question may arise about whether these subproblems can be addressed independently. The answer is to some extent negative. The reason is that the candidate manipulated variables are shared between steady-state controlled variables and inventory controlled variables. Therefore, the set of candidate steady-state controlled variables must be arranged in such a way that if the optimization algorithm selects any of them, the required manipulated variables is available and none of inventory controlled variables is left uncontrolled. Otherwise, the infeasible solution must be forbidden from the set of candidate controlled variables and the optimization program should be run again. Therefore, in this chapter (and later in Chapter 5) the available manipulated variables are analysed before optimization to ensure the consistency of the optimization formulation.

4.4. Case study: optimal control structure selection for a distillation train

In this chapter, the proposed optimization framework is applied to the case of a distillation train. The aim of the subsequent subsection is to map the case study into the proposed steady-state optimization framework. In the subsequent sections, the process description is presented. The optimization variables are explained and the optimization constraints are discussed.

4.4.1. Process description of pyrolysis gasoline hydrogenation (PGH) plant

The process description for the overall olefin process is available in literature (e.g., Kroschwitz and Seidel 2004). A section of this process concerns the treatment of pyrolysis gasoline from which the case study of this chapter is selected. This part of the process is called pyrolysis gasoline hydrogenation (PGH) section and is shown in Figure 4.1.

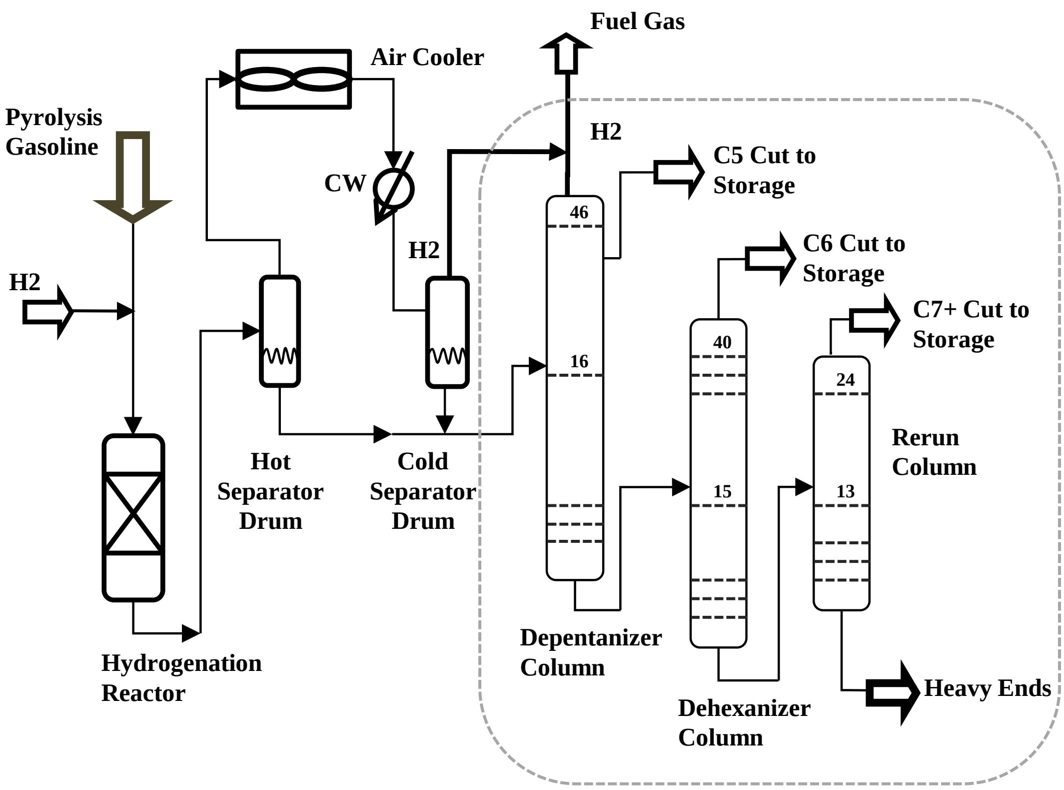

Figure 4.1. PGH plant; the framed part of the flowsheet is selected for the case study.

In olefin processes, the products of the cracking reactions of liquid feedstocks include a blend with properties very similar to gasoline. The disadvantage of this product is that the dissolved light olefins are highly reactive with the risk of polymerization stored untreated. Therefore, this blend must be saturated by hydrogenation reactions. The reaction conditions are 24bar and 140^{o}C. The incondensable components that mostly consist of hydrogen are separated in a series of two separator drums which are operated in hot and cold conditions. The overhead vapours of the first separator are cooled using an air-cooler and a cooling water heat-exchanger in order to minimize the hydrocarbon losses in the fuel gas stream. Then, the condensates from the bottom of these two separator drums will be resolved in a distillation train into C_5 , C_6 , C_7^+ and heavy-ends products. In this chapter, this distillation train is studied and its schematic is shown by the dotted envelope on the right hand side of Figure 4.1.

The first distillation column is depentanizer column. This column has a partial reflux configuration and the gaseous overhead product is mostly hydrogen. The main product is the C_5 cut, and is withdrawn as the side stream. The bottom stream is fed to dehexanizer column. The C_6 cut is produced in the top of dehexanizer column and the bottom stream is fed to rerun column which is operated under vacuum conditions. This column resolves its feed to C_7^+ and heavy-ends streams.

4.4.2. Optimization variables

As discussed earlier, the new optimization framework limits the optimization variables to structural variables $\boldsymbol{Y_{cv}}$ and $\boldsymbol{Y_{mv}}$ regarding selection of controlled and manipulated variables. Table 4.2 lists the optimization variables. The rational choice of these candidate variables is based on the available measurements. The index $j = 5, 6, 7$ represents depentanizer, dehexanizer and rerun columns respectively. The notation $\boldsymbol{Y_{Colj,Trayt}}$ refers to the temperature of tray number t in the column number j. The notation $\boldsymbol{Y_{j,Flow}}$ refers to a flowrate in column j . The notations R, D, B, S represent reflux, distillate, bottom, and side streams respectively. Q_H refers to a reboiler heat duty. These notations also hold for flow ratios, for example $Y_{Col6,B/F}$ represents the ratio of bottom flowrate to feed flowrate in dehexanizer column. R, D, B, S and Q_H are candidate manipulated variables and the rest of variables in Table 4.2 are candidate controlled variables.

Table 4.2.
List of the optimization variables for the PGH case study.

	$Y_{Colj,Trayt}$: a binary variable which represents selection of the temperature of a tray as a controlled variable	$Y_{Colj,Flow}$: a binary variable which represents selection of a flow, a flow-ratio or a heat duty as a controlled variable
Depentanizer: $C5$	$\{Y_{Col5,Tray1} \dots Y_{Col5,Tray46}\}$	$Y_{Col5,B}, Y_{Col5,S}, Y_{Col5,R}, Y_{Col5,Q_H}$, $Y_{Col5,D/F}, Y_{Col5,B/F}, Y_{Col5,S/F}, Y_{Col5,R/F}, Y_{Col5,R/D}$
Dehexanizer: $C6$	$\{Y_{Col6,Tray1} \dots Y_{Col6,Tray40}\}$	$Y_{Col6,D}, Y_{Col6,B}, Y_{Col6,R}, Y_{Col6,Q_H}$, $Y_{Col6,D/F}, Y_{Col6,B/F}, Y_{Col6,R/F}, Y_{Col6,R/D}$
Rerun: $C7$	$\{Y_{Col7,Tray1} \dots Y_{Col7,Tray24}\}$	$Y_{Col7,D}, Y_{Col7,B}, Y_{Col7,R}, Y_{Col7,Q_H}$, $Y_{Col7,D/F}, Y_{Col7,B/F}, Y_{Col7,R/F}, Y_{Col7,R/D}$

4.4.3. Optimization constraints

The following subsections explain the optimization constraints regarding the available degrees of freedom, inferential temperature control and disturbance scenarios.

4.4.3.1. Constraints regarding the available degrees of freedom and the implications of inventory control systems

In the present case study, the first distillation column (depentanizer) is a partial reflux column with a side stream and the second (dehexanizer) and third (rerun) distillation columns are total reflux columns (Figure 4.1). In Chapter 2, the methods for inventory control and degree of freedom analysis were reviewed. In addition, using a flowsheet-oriented method (Konda, et al. 2006), it was shown that the number of control degrees of freedom for a total reflux or a partial reflux distillation column is six. However, for the case of the first distillation column, due to the side stream, there is an extra degree of freedom. Substituting in equation (2-13):

$$\text{CDOF} = 13 - 3 - 3 = 7 \qquad (4-3)$$

In addition, since the feed of the distillation train is assumed as the disturbance source and the inventory control is designed in the direction of flows, one degree of freedom is consumed in each distillation column by the feed and the degrees of freedom for the first, second and third distillation columns are six, five, and five, respectively. In the following, the constraints required for consistency of the manipulated variables are introduced to the problem formulation.

In the first distillation column, due to the presence of the incondensable components, the application of a partial condenser is inevitable. The flow of the overhead vapour is used for controlling the column pressure representing the vapour inventory. The condenser duty is used for the overhead liquid inventory. These are the common engineering practices. Controlling the overhead and bottom liquid inventories, and the column pressure consume three manipulated variables, and three manipulated variables are left for steady-state optimization of the control structure of the first column:

$$Y_{Col5,Tray1} + \cdots + Y_{Col5,Tray46} + Y_{Col5,B} + Y_{Col5,S} + Y_{Col5,R} + Y_{Col5,\frac{D}{F}} + Y_{Col5,\frac{B}{F}}$$
$$+ Y_{Col5,\frac{S}{F}} + Y_{Col5,\frac{R}{F}} + Y_{Col5,\frac{R}{D}} + Y_{Col5,Q_H} = 3 \qquad (4-4a)$$

The column bottom inventory can be controlled by adjusting either the reboiler duty or the bottom flowrate of the first column:

$$Y_{Col5,B} + Y_{Col5,Q_H} \leq 1 \qquad (4-4b)$$

The second (dehexanizer) and third (rerun) distillation columns are total reflux columns and there are five potential manipulated variables in each of them. Controlling the overhead and bottom liquid inventories, and the column pressure consume three manipulated variables, and two manipulated variables are left for steady-state optimization of the control structures:

$$Y_{Col6,Tray1} + \cdots + Y_{Col6,Tray40} + Y_{Col6,D} + Y_{Col6,B} + Y_{Col6,R} + Y_{Col6,D/F} + Y_{Col6,B/F}$$
$$+ Y_{Col6,R/F} + Y_{Col6,R/D} + Y_{Col6,Q_H} = 2 \qquad (4-4c)$$

$$Y_{Col7,Tray1} + \cdots + Y_{Col7,Tray24} + Y_{Col7,D} + Y_{Col7,B} + Y_{Col7,R} + Y_{Col7,D/F}$$
$$+ Y_{Col7,B/F} + Y_{Col7,R/F} + Y_{Col7,R/D} + Y_{Col7,Q_H} = 2 \qquad (4-4d)$$

The following constraints ensure that either reflux or distillate will be available for controlling the overhead mass inventory of the second and third columns:

$$Y_{Col6,D} + Y_{Col6,R} \leq 1 \qquad (4-4e)$$

$$Y_{Col7,D} + Y_{Col7,R} \leq 1 \qquad (4-4f)$$

The following constraints ensure that either reboiler or bottom flowrate will be available for controlling the bottom mass inventory:

$$Y_{Col6,B} + Y_{Col6,Q_H} \leq 1 \qquad (4-4g)$$

$$Y_{Col7,B} + Y_{Col7,Q_H} \leq 1 \qquad (4-4h)$$

Constraints (4-4a to h) ensure that the selected manipulated variables for each distillation column are consistent.

4.4.3.2. Constraints regarding inferential temperature control

With the liquid levels and column pressure under closed loop control, a distillation column is still unstable due to composition drift (Hori and Skogestad 2007; Skogestad 2007). Ideally, composition should be measured and controlled directly. However, composition measurements can be expensive and slow. An alternative is to design inferential temperature controllers, (Luyben 2006). The idea behind this strategy is that the changes in the selected temperature controlled variables should represent the changes in the composition of the products. The instability issues make the composition or inferential temperature control a top priority. Therefore, in this case study, a set of constraints ensured the selection of at least a temperature as a controlled variable in each column:

$$Y_{Col5,Tray1} + Y_{Col5,Tray2} + \cdots + Y_{Col5,Tray45} + Y_{Col5,Tray46} \geq 1 \qquad (4-5a)$$

$$Y_{Col6,Tray1} + Y_{Col6,Tray2} + \cdots + Y_{Col6,Tray39} + Y_{Col6,Tray40} \geq 1 \qquad (4-5b)$$

$$Y_{Col7,Tray1} + Y_{Col7,Tray2} + \cdots + Y_{Col7,Tray23} + Y_{Col7,Tray24} \geq 1 \qquad (4-5c)$$

The implication of selecting at least one temperature as a controlled variable by including constraints (4-5a to c) is to maintain the energy balance of the column. The setpoint of such a temperature controlled variable influence the products composition.

4.4.3.3. Constraints regarding disturbance scenarios

The feed stream to depentanizer column is assumed a disturbance. Table 4.3 presents the feed composition and flowrate. The feed can be represented as the mixture of four cuts of hydrocarbons: C_5, C_6, C_7^+ and heavy-ends cuts, shown in the last column of this table. In each disturbance scenario, the amount of each of these cuts in the feed stream is changed by $\pm 5\%$. The combinations of these changes result in sixteen disturbance scenarios, which represent the operational region. These disturbance scenarios are assumed equally likely. Later in a set of sensitivity analyses, the scenarios in which disturbances are increased to 10% and 20% will be studied too.

Table 4.3.
Feed composition

#	Component	Mass flowrate (kg/h)	Group
1	Hydrogen	5	Flue gas
2	Isobutene	6	C5 cut
3	Isobutane	1	C5 cut
4	1-Butane	33	C5 cut
5	n-Butane	8	C5 cut
6	Cyclopentene	398	C5 cut
7	Cyclopentane	538	C5 cut
8	Isopentene	265	C5 cut
9	Isopentane	52	C5 cut
10	1-Pentene	431	C5 cut
11	n-Pentene	388	C5 cut
12	ME-cyclopentene	252	C6 cut
13	Cyclohexane	112	C6 cut
14	1-hexene	100	C6 cut
15	n-Hexane	70	C6 cut
16	Benzene	6240	C6 cut
17	ME-cyclohexene	39	C7 cut
18	ME-cyclohexane	8	C7 cut
19	Toluene	1898	C7 cut
20	ET-Benzene	1136	Heavy ends
21	P-Xylene	83	Heavy ends
22	M-Xylene	182	Heavy ends
23	O-Xylene	109	Heavy ends
24	C9+	860	Heavy ends
		13214	Total

4.4.3.4. Instances of goal programming objective function

In Subproblem 2, control structure selection, the process design is fixed and the role of control system is to realize the targets set at the process design stage (Subproblem 1). These targets include the process profitability and quality of the products and the nominal operating conditions. In the following, the base-case design (i.e., the result of Subproblem 1) is presented. In addition, the instances of goal programming multi-objective function (4-1) and their target values are discussed.

The instance of the first objective function in Table 4.1 is the quality of the products expressed in terms of their average molecular weights and standard densities. The target values for this objective are reported in Table 4.4 for each product. The instances of the second objective function in Table 4.1 are condenser duty, reboiler duty and reflux rate. The nominal values for these manipulated variables are reported in Table 4.5. The instances of the third objective function in Table 4.1 are chosen to be the temperatures of the trays. The targets (i.e., setpoints of temperature trays) for this objective are reported in Figures 4.2a-c. The fourth objective concerns the economic losses due to disturbances. The net profit is defined as:

$$\text{Total Annual Profit} = \text{Revenues} - \text{Operational costs} \qquad (4-6)$$

The economic losses were defined in term of decrease in Total Annual Profit (TAP). The economic data used for calculating the economic objective function are shown in Table 4.6. The prices of the products were quoted from a petrochemical company in 2008. The utility costs were from Ulrich (2006). The TAP was calculated to be 6.67×10^6 ($\$.year^{-1}$) for the base case design. The values of α_w, the weighting factors of the goal programming objective function (4-1) were $\alpha_1 = 10$, $\alpha_2 = 0.1$, $\alpha_3 = 10$, $\alpha_4 = 100$.

The control structure of the base case design is shown in Figure 4.3. In this research, this control structure is presented for demonstrating the benefits that may be gained by the proposed optimization framework. The result of imposing the 5% disturbances, discussed in the last section, to the base-case control structure will be presented and discussed later in this chapter. Please notice that in the figures of this chapter, the first tray corresponds to the reboiler and the last tray is the condenser.

Table 4.4.
The target values for the quality of products.

	$MW_{average}$	Standard density ($kg.m^{-3}$)
C5 Cut	70.047	685
C6 Cut	78.467	864
C7 Cut	89.939	869
Heavy Ends	136.673	747

Table 4.5.
The nominal values of the manipulated variables, i.e., the targets for the second objective of Table 4.1.

Manipulated variable	Nominal design value	
Condenser heat duty (Depentanizer column)	-5.792×10^{6}	kJ/h
Condenser heat duty (Dehexanizer column)	-4.727×10^{6}	kJ/h
Condenser heat duty (Rerun column)	-3.121×10^{6}	kJ/h
Reboiler heat duty (Depentanizer column)	6.217×10^{6}	kJ/h
Reboiler heat duty (Dehexanizer column)	3.981×10^{6}	kJ/h
Reboiler heat duty (Rerun column)	2.401×10^{6}	kJ/h
Reflux rate (Depentanizer column)	1.34×10^{4}	kg/h
Reflux rate (Dehexanizer column)	7.77×10^{3}	kg/h
Reflux rate (Rerun column)	2.51×10^{3}	kg/h

Table 4.6.
Economic data for calculating the fourth objective of Table 4.1.

C5cut ($\$.kg^{-1}$)	0.36
C6cut ($\$.kg^{-1}$)	0.39
C7cut ($\$.kg^{-1}$)	0.4
heavy end ($\$.kg^{-1}$)	0.424
Medium Pressure (MP) Steam (P=15.5 bar, T=464 K) ($\$.kg^{-1}$)	0.0078
Cooling Water (P=7 bar, T^{supply}=30 oC) ($\$.m^{-3}$)	0.03398

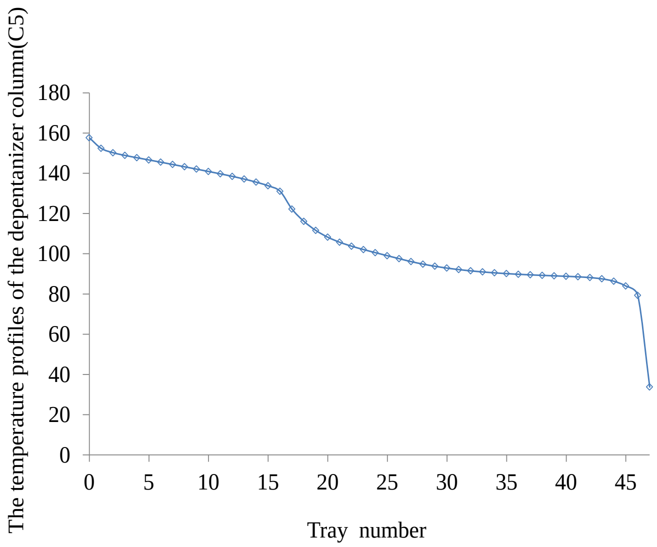

Figure 4.2a. The temperature profiles of the depentanizer column for the base case design

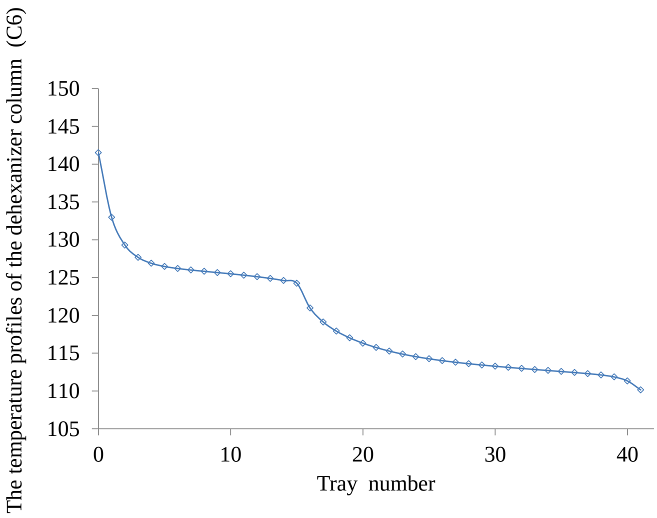

Figure 4.2b. The temperature profiles of the dehexanizer column for the base case design

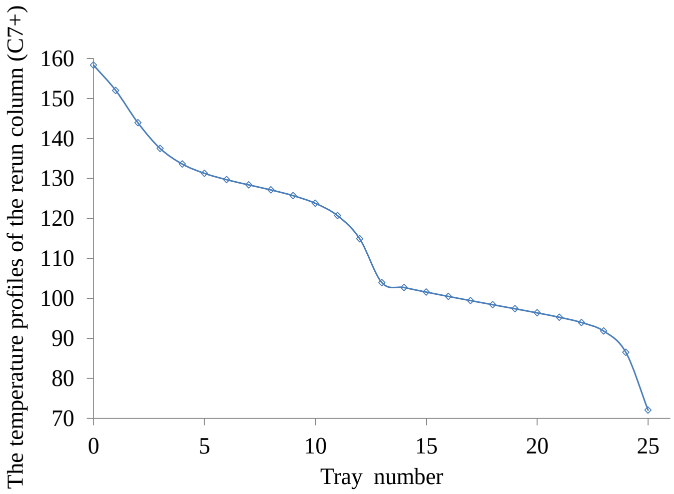

Figure 4.2c. The temperature profiles of rerun the column for the base case design

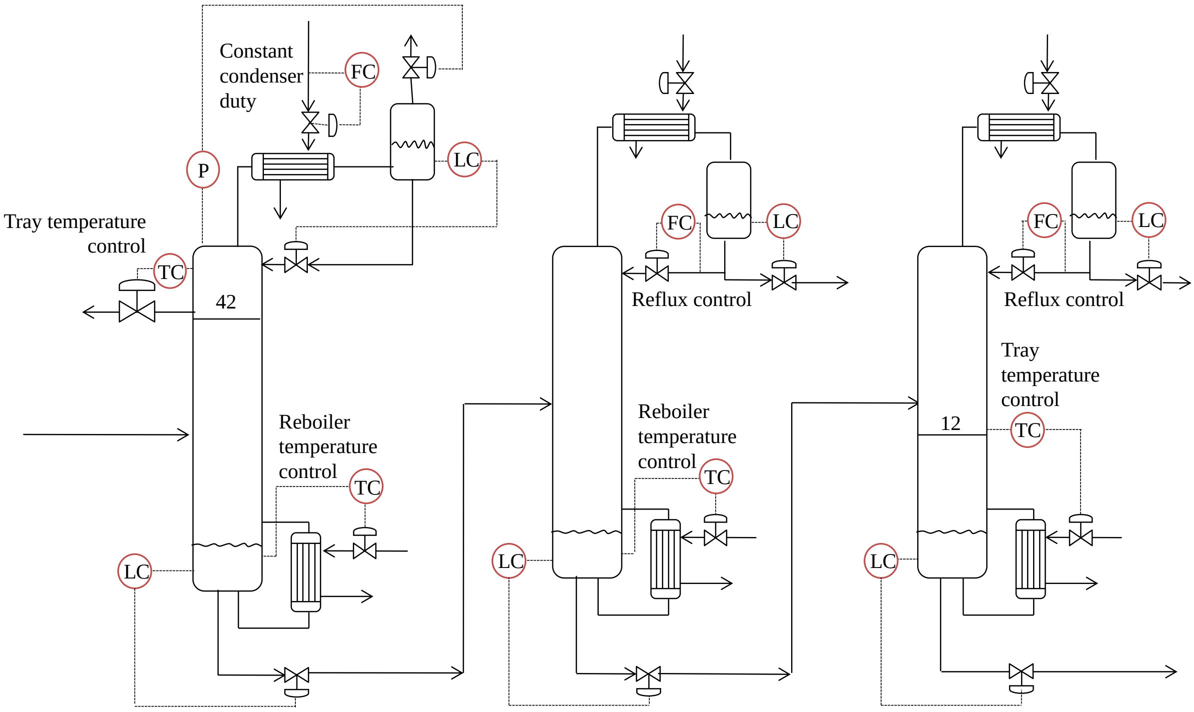

Figure 4.3. The base-case control structure

4.5. Implementation software tools

The following sections explain the employed simulation and optimization software tools. Constructing a steady-state inversely controlled process model is discussed and information flow within the optimization framework is illustrated

4.5.1. Simulation-optimization programming

In Chapter 2, it was explained that simulation-optimization programming conforms to optimization with implicit constraints. Simulation was performed using Aspen-HYSYS® and the optimization algorithm was Genetic Algorithm (GA®) toolbox of MATLAB®. The two software tools were integrated using COM® automation interface. The mathematical modelling was performed using the distillation block of the Aspen-HYSYS simulator. The underlying equations can be found in Aspen-HYSYS (document 2009a). The pyrolysis gasoline was estimated by 24 real components. The modified Peng-Robinson equation of state was employed for thermodynamic calculations (Aspen-HYSYS document 2009b). In the case that the simulation solver failed to converge, the objective function was set to a value ten times larger than an ordinary objective value. There were sixteen disturbance scenarios. Therefore, for each function recall (i.e., one evaluation of the objective function) the simulation program needed to be executed sixteen times. This normally took around 5-7 minutes. That was significantly longer for solutions for which the simulation solver failed to converge. There were twenty individuals in each population, and between 30-50 generations were needed to find a reasonable solution. The simulation run was around a week. The author observation was that in a good evolution, the diversity of the population should be maintained until the midway, i.e., 20^{th} -30^{th} generations. If the individuals become similar in few generations, the solution was assumed pre-matured and the optimization procedure was restarted. In this research in order to generate a good initial population, firstly, the optimization procedure was performed from random populations (generated by the GA Toolbox) several times for a few generations and then, the best individuals were combined to generate a good initial population. The accuracy of the results depends on the applied modelling and optimization methods. The developed model featured a high degree of rigour because the built-in distillation blocks and the high fidelity property package from the simulator library were used for modelling. Furthermore, Genetic Algorithm is a stochastic optimization method based on a population of solutions and is less likely to become entrapped in local optima. However, the stochastic optimization methods do not construct any proof that the solution is globally optimal.

4.5.2. Constructing a steady-state inversely controlled process model

The distillation block in Aspen-HYSYS provides the option for defining column specifications. These are the specifications that the equation-solver tries to meet during simulation. The number of these specifications is the difference between the number of unknown variables and the number of equations in the simulation. In this case study, in order to construct a steady-state inversely controlled process model, all the candidate controlled and manipulated variables in Table 4.2 were defined as the deactivated column specifications. For each specification, a desired value was set according to the operating conditions of the base-case process. Activating and deactivating these specifications provided the opportunity to add and remove perfect control equations and to construct the corresponding steady-state inversely controlled process models.

4.5.3. Simulation-optimization information flow

Figure 4.4 shows the information flow of the simulation-optimization program. The block on the left is GA and the block on the right is Aspen-HYSYS simulator. The middle block is an m-file coded in MATLAB, which integrates the two software tools.

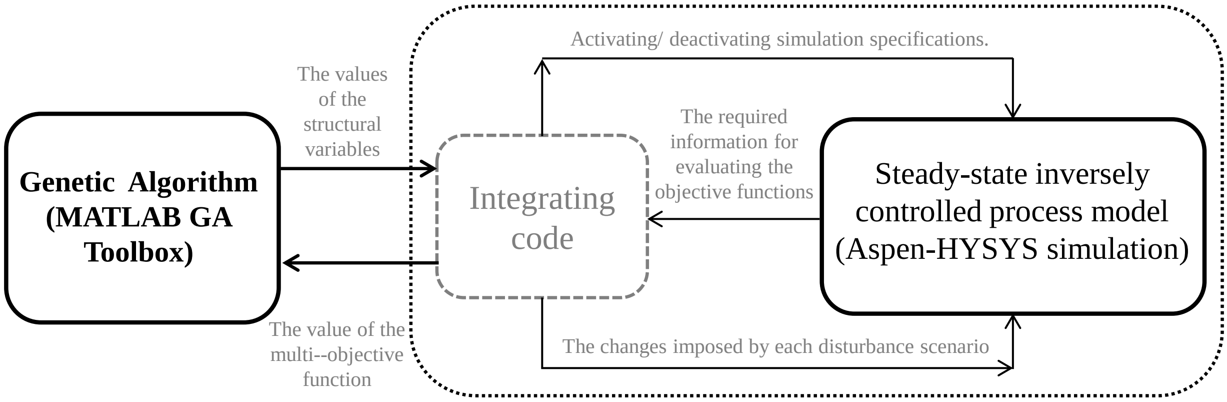

Figure 4.4. Information flow of the simulation-optimization programming.

The steps in each optimization iteration are as follows:

Step 1. The GA decides on the values of the optimization variables (Table 4.2).

Step 2. The integrating code receives the values of the optimization variables, activates the corresponding column specifications, and constructs the corresponding steady-state inversely controlled process model as described earlier.

Step 3. The trial values of the optimization variables must be benchmarked against the expected disturbance scenarios. The integrating code imposes the disturbances to the inversely controlled process model by changing the feed flowrate and composition.

Step 4. By convergence of the simulator for each disturbance scenario, the corresponding values of the objective functions (shown in Table 4.1) are calculated and the aggregated value of the multi-objective function (equation 4-1) is constructed. Since the disturbances are assumed equally likely, the expected value of the multi-objective function is the average of them, which is reported to the GA.

Step 5. The GA evaluates the termination criteria and decides on improving the optimization variables.

4.6. Results of the case study

This section presents the results. Firstly, the effects of the 5% disturbance scenarios are evaluated on the base-case design (explained in Sections 4.4.3.3 and 4.4.3.4). Then, the results of the proposed optimization framework with respect to the 5% disturbance scenarios are presented and compared to the base-case design. The aim was to establish the benefits that can be gained from the proposed optimization framework. Finally, two sets of sensitivity analyses were performed. The first set of sensitivity analyses includes controlling one tray up and down and excluding the reflux of the last column from the controlled variable options. In the second set, the results of the proposed framework for larger disturbances (10% and 20%) are presented. The results are presented in tables and figures in this section and then discussed in the next section. They are:

- Table 4.7 shows the objective values for the abovementioned optimizations and sensitivity analyses.
- Table 4.8 shows the selected controlled and manipulated variables for the abovementioned optimizations and sensitivity analyses.
- Figure 4.5 shows the selected controlled and manipulated variables with respect to the 5% disturbance scenarios.
- Figure 4.6 shows a decentralized control structure for the results with respect to the 5% disturbance scenarios.
- Figures 4.7 show the results for the base case control structure.
- Figures 4.8 show the results with respect to the 5% disturbance scenarios.
- Figures 4.9 show the results with respect to the 10% disturbance scenarios.
- Figures 4.10 show the results with respect to the 20% disturbance scenarios.

Table 4.7.
The optimal values of the objective functions.

	Average changes in product molecular weight [%]	Average changes in the product density [%]	Average changes in manipulated variables [%]	Average changes in the tempreature of trays [oC]	Average changes in net profit [%]	Aggregated Objective Function
5% Disturbances	0.450	0.353	1.474	0.177	-0.041	11.331
Base case	2.368	1.045	0.728	1.169	-0.223	51.486
No reflux (5%)	0.430	0.342	1.562	0.171	-0.043	11.387
(+1) Tray	0.415	0.336	1.478	0.194	-0.045	11.724
(-1) Tray	0.457	0.353	1.445	0.178	-0.046	11.853
10% Disturbances	0.525	0.349	2.893	0.338	-0.062	16.796
20% Disturbances	0.629	0.324	6.367	0.662	-0.104	28.118

Table 4.8.
The control structures selected for the three distillation columns, as the results of optimizations and sensitivity analyses

	First (Depentanizer) Column	Second (Dehexanizer) Column	Third (Rerun) column	Type of the controlled variable
All structures	Column pressure	Column pressure	Column pressure	Inventory
	Overhead liquid level	Overhead liquid level	Overhead liquid level	Inventory
	Bottom liquid level	Bottom liquid level	Bottom liquid level	Inventory
Base case	Temperature of the 42nd tray	Temperature of the reboiler	Temperature of the 12th tray	Steady-state
	Condenser cooling duty	Reflux flowrate	Reflux flowrate	Steady-state
	Temperature of the reboiler	none	none	Steady-state
5% Disturbances	Temperature of the 45th tray	Temperature of the 24th tray	Temperature of the 6th tray	Steady-state
	Temperature of the 33rd tray	Reflux/Feed flow ratio	Reflux flowrate	Steady-state
	Temperature of the 10th tray	none	none	Steady-state
10% Disturbances	Temperature of the 45th tray	Temperature of the 21th tray	Temperature of the 5th tray	Steady-state
	Temperature of the 33rd tray	Reflux/Feed flow ratio	Reflux flowrate	Steady-state
	Temperature of the 10th tray	none	none	Steady-state
20% Disturbances	Temperature of the 44th tray	Temperature of the 19th tray	Temperature of the 5th tray	Steady-state
	Temperature of the 31st tray	Reflux/Feed flow ratio	Reflux flowrate	Steady-state
	Temperature of the 10th tray	none	none	Steady-state
No reflux (5%)	Temperature of the 45th tray	Temperature of the 24th tray	Temperature of the 5th tray	Steady-state
	Temperature of the 33rd tray	Reflux/Feed flow ratio	Reflux/Feed flow ratio	Steady-state
	Temperature of the 11th tray	none	none	Steady-state
(+1) Tray (5%)	Temperature of the 46th tray	Temperature of the 25th tray	Temperature of the 7th tray	Steady-state
	Temperature of the 34th tray	Reflux/Feed flow ratio	Reflux flowrate	Steady-state
	Temperature of the 11th tray	none	none	Steady-state
(-1) Tray (5%)	Temperature of the 44th tray	Temperature of the 24th tray	Temperature of the 5th tray	Steady-state
	Temperature of the 32nd tray	Reflux/Feed flow ratio	Reflux flowrate	Steady-state
	Temperature of the 9th tray	none	none	Steady-state

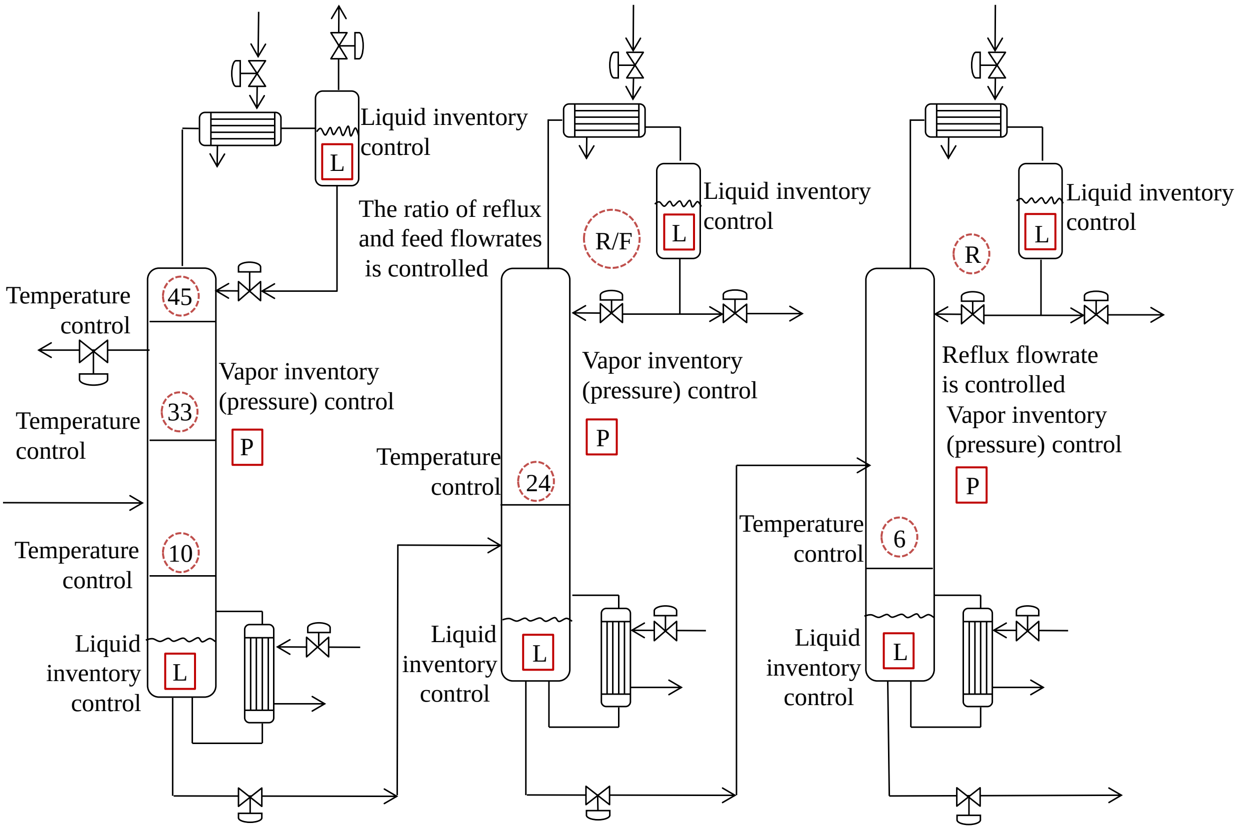

Figure 4.5. The selected controlled variables using the proposed optimization framework (dotted circles), and the inventory controlled variables (solid squares)

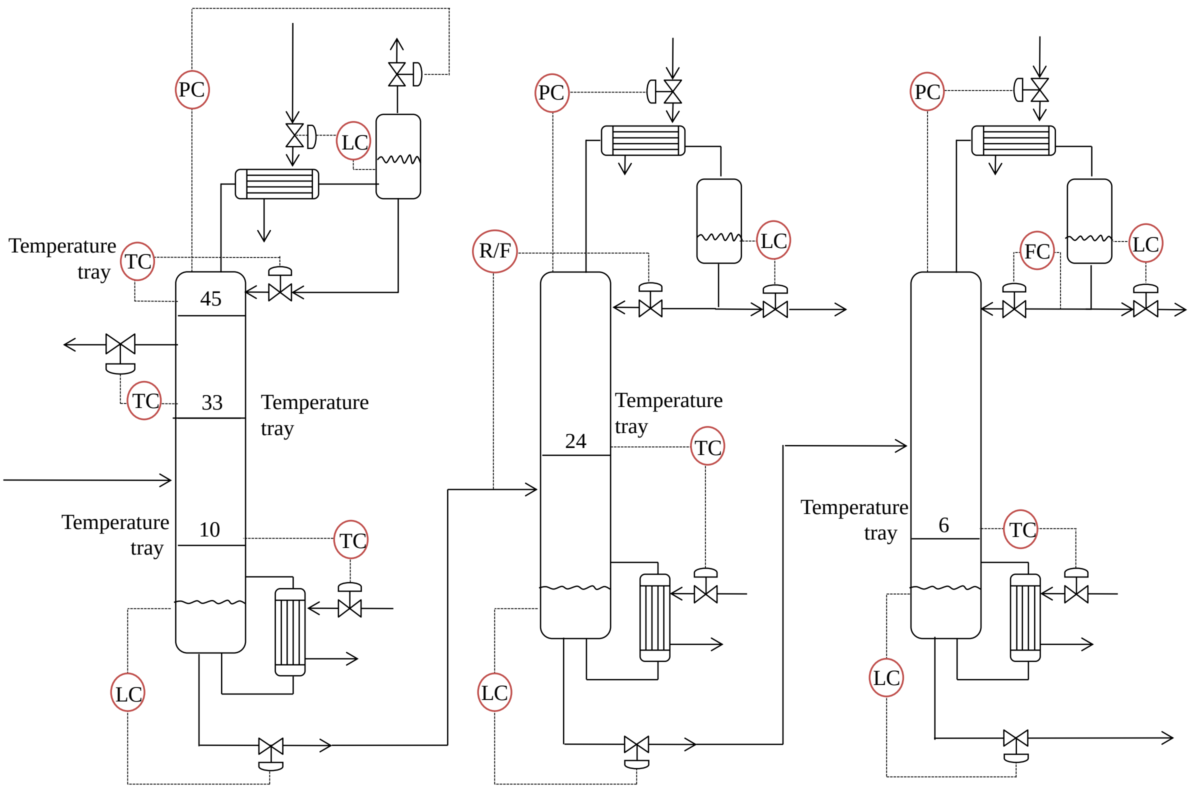

Figure 4.6. The control structure for the distillation train of the PGH process (Tray-numbering is bottom-up)

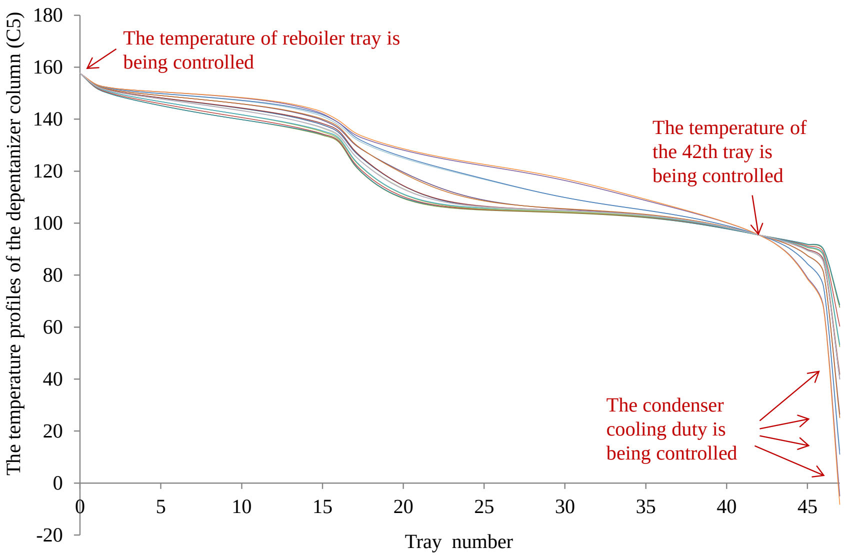

Figure 4.7a. The temperature profiles of depentanizer column for the base-case control structure.

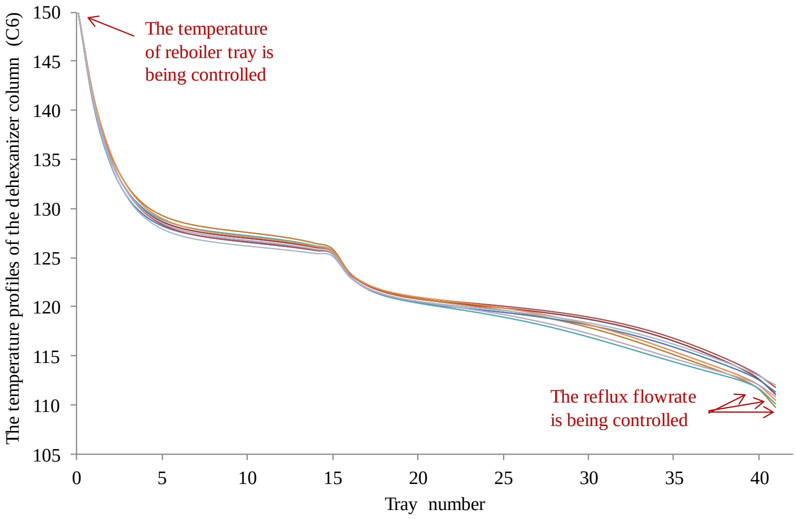

Figure 4.7b. The temperature profiles of dehexanizer column for the base-case control structure.

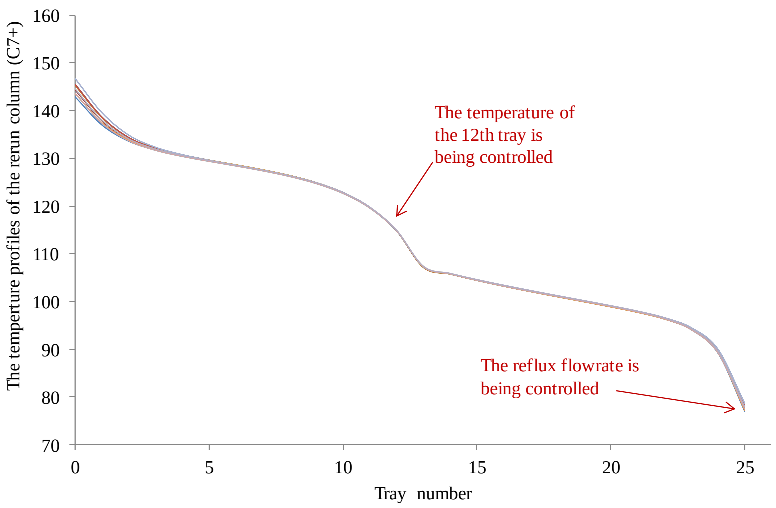

Figure 4.7c. The temperature profiles of rerun column for the base-case control structure

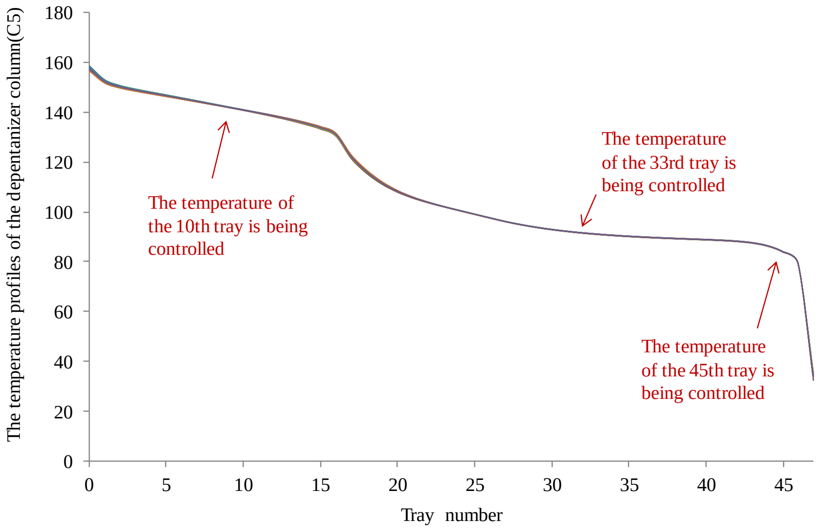

Figure 4.8a. The temperature profiles of depentanizer column for 5% disturbances

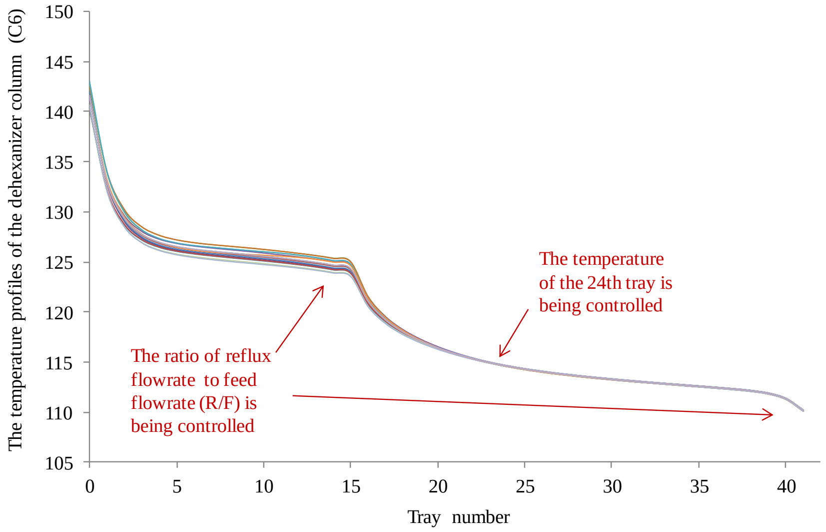

Figure 4.8b. The temperature profiles of dehexanizer column for 5% disturbances

Figure 4.8c. The temperature profiles of rerun column for 5% disturbances

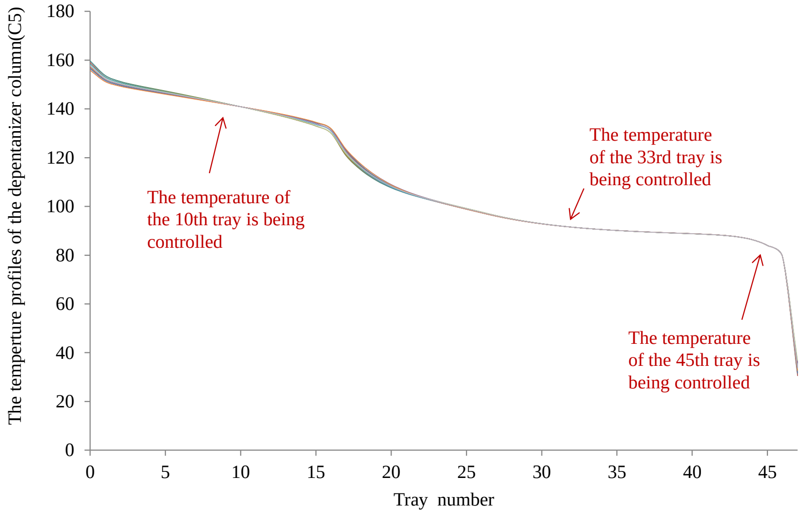

Figure 4.9a. The temperature profiles of depentanizer column for 10% disturbances

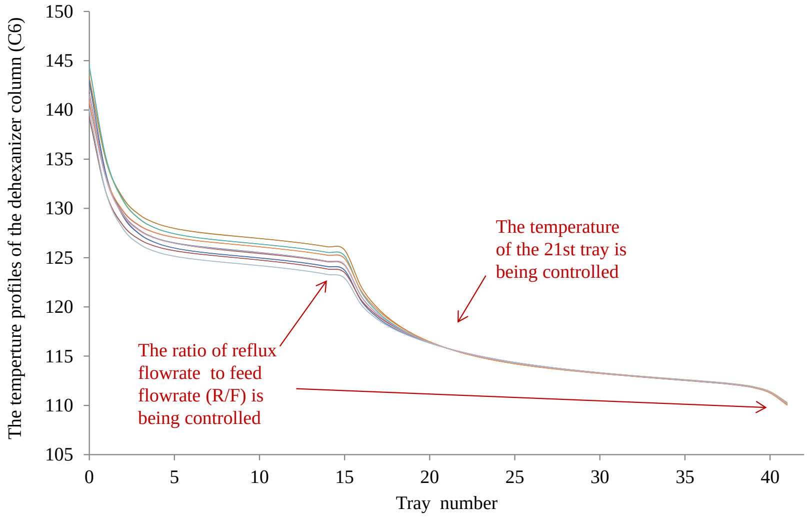

Figure 4.9b. The temperature profiles of dehexanizer column for 10% disturbances

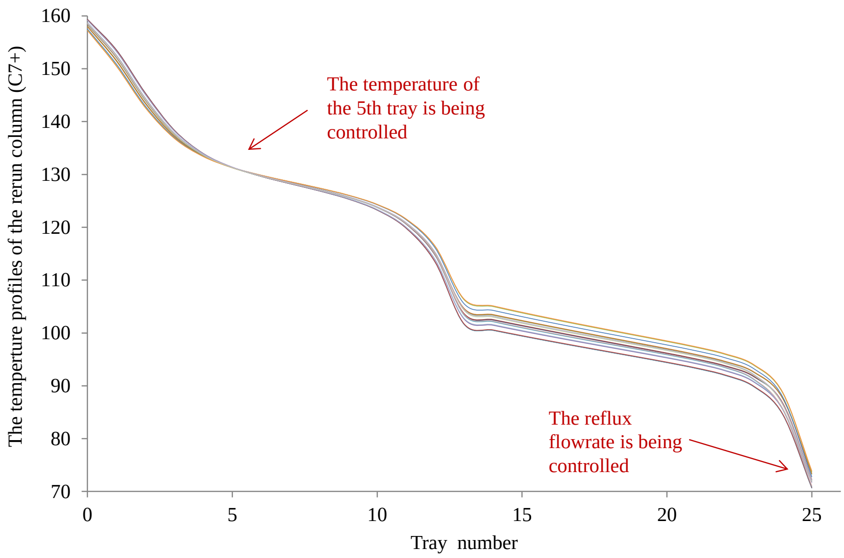

Figure 4.9c. The temperature profiles of rerun column for 10% disturbances

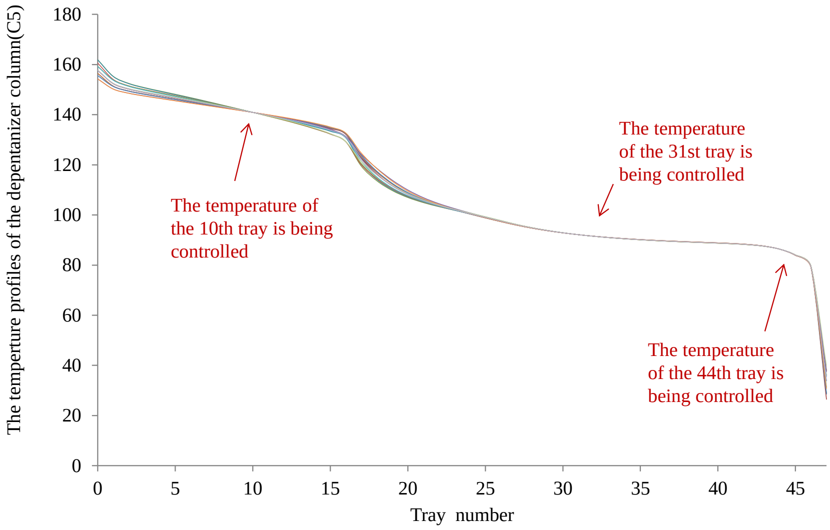

Figure 4.10a. The temperature profiles of depentanizer column for 20% disturbances

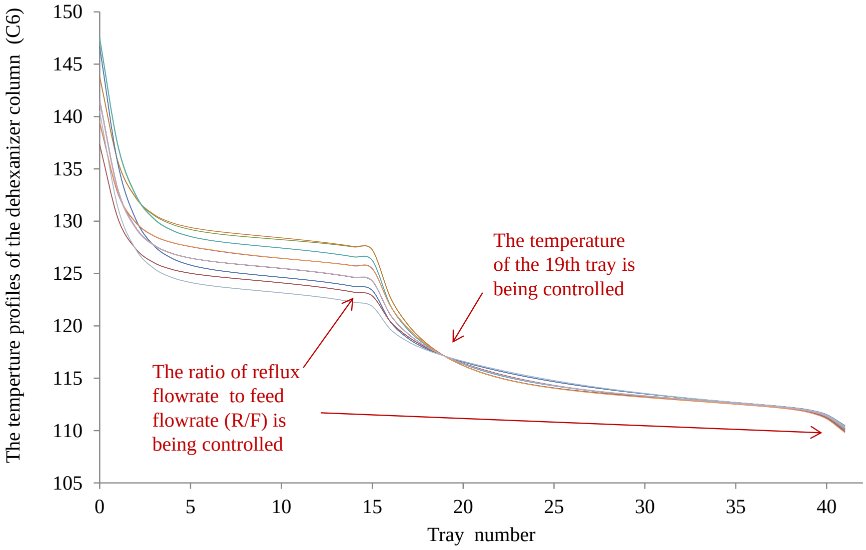

Figure 4.10b. The temperature profiles of dehexanizer column for 20% disturbances

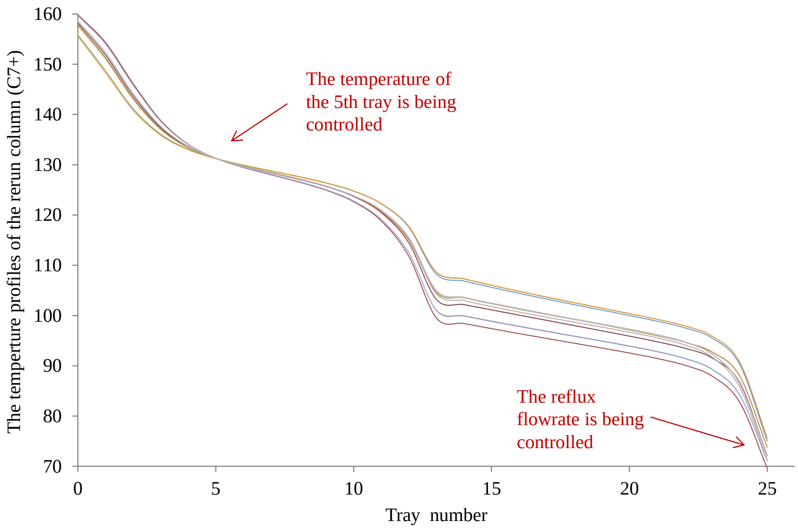

Figure 4.10c. The temperature profiles of rerun column for 20% disturbances

4.7. Discussions

This section discusses the results. In the first part of the discussions, the optimized control structure is compared to the base-case control structure. Then, in the second part of the discussions, the results of the sensitivity analyses are evaluated and discussed.

4.7.1. Optimized control structure versus base-case control structure

Table 4.7 showed the values of the objective functions for the optimized control structure (with respect to the 5% disturbance scenarios) and the base-case (unoptimized) control structure. The targets for optimization were that all the deviations should be ideally zero. Although the objective functions are competing and conflicting, the optimal solution exhibits the desirable properties. For the expected disturbance scenarios, the economic losses are minimized, while the manipulated variables are preserved from excessive movements. In addition, the product specifications are met and the minor changes in the average temperatures indicate short trajectories between different steady states and hence the process is insensitive to disturbances. These results demonstrate a good trade-off between different competing objective functions. This table also showed improvements over the base-case. For instance, less economic losses are incurred in the optimized control structure (-0.041% compared to -0.223%) and the quality of the products (in terms of the changes in the average densities and molecular weights) are inferentially controlled better. The average value of the changes in the temperature profiles is also less in the optimized control structure. However, the manipulated variables are varied more in the optimized control structure.

Table 4.8 presents the selected manipulated and controlled variables. The controlled variables associated with inventory designs are presented in the top three rows and are the same for all the control structures. The rows immediately after the inventory controls are the control structure for the base-case design. Then, the results of optimization with respect to the 5% disturbance scenarios are presented. The rest of results report sensitivity analyses and will be discussed later.

The base-case control structure was reported earlier in Figure 4.3, and where the base case design was reported. Figure 4.5 reports the results of optimization with respect to the 5% disturbance scenarios. In this figure, the available manipulated variables are shown using control valve symbols. The controlled variables selected by the optimization algorithm are shown using dotted circles. The liquid (level) and vapour (pressure) inventory controlled variables are shown using the solid squares. These are the results of the optimization framework in conjunction with the heuristics for inventory control.

As discussed earlier, in the proposed framework, the detailed control design is delegated to process control practitioners. The optimized control structure in this case study could be directly used in a multivariable control system. However, if a multi-loop control system is being designed, an appropriate pairing method such as RGA or process insights (Skogestad 2007; Luyben 2006) can be employed. An example of a possible multi-loop control structure is shown in Figure 4.6. Here, the controlled variables and the available manipulated variables are paired using the process insights.

Figure 4.8a shows the temperature profiles of the first distillation column for the sixteen disturbance scenarios. Since three temperature controlled variables are selected in this column, the temperature profiles are very similar in this column. The temperature profiles in the second and third distillation columns are shown in Figures 4.8b and c, which demonstrate a satisfactory control of temperature (and inferentially compositions) over the range of the expected disturbances.

The comparisons between the optimized control structure and the base-case control structure reveals the benefits that can be gained by the proposed optimization framework. The key differences are in the first column, as the heat duty of condenser, the temperature of the side stream and the temperature of the reboiler are being controlled in the base-case control structure. By contrast, three inside temperatures corresponding to three columns trays are being controlled in the optimized control structure. This strategy resulted in significant improvements of the performance of the optimized control structure, which can be investigated by comparing Figure 4.7a and Figure 4.8a. The main advantage of the optimized control structure is that it minimizes the losses of the products from the overhead purge stream, in the first column. In addition, the optimized control structure remains operable while the base-case control structure would lose its control action in some certain disturbance scenarios. It is shown in Figure 4.7a that for some disturbance scenarios, the base-case design requires such a low temperatures that is not achievable using cooling water. This would show itself as saturation of the control valve of the condenser (i.e., fully open) and the loss of the valuable products from overhead stream.

The difference between the two structures is less pronounced in the second and third columns. The optimized control structure of the second column uses the reflux/feed ratio compared to the reflux flowrate in the base-case control structure. In addition, the temperature of a tray is controlled in the optimized control structure, but the reboiler temperature is controlled in the base case. A comparison of Figure 4.7b with Figure 4.8b demonstrates the superior performance of the optimized control structure because the product is withdrawn from the column overhead and this part of column is less affected by disturbances in the optimized control structure. The control structures of the last column only differ in the number of the temperature tray and both control structures address the disturbances very well.

The values of the objective functions of the base-case control structure are compared to the optimized control structure in Table 4.7. In all objectives, the optimized control structure performs better. However, the optimized control structure manipulates the input variables more.

4.7.2. Sensitivity analyses

In this research, two sets of sensitivity analyses were performed, as discussed in the following. The first set of sensitivity analyses was with respect to the 5% disturbance scenarios. The second set of sensitivity analyses was with respect to the 10% and 20% disturbance scenarios.

4.7.2.1. Sensitivity analyses with respect to the 5% disturbance scenarios

It was explained earlier that the optimizer chose to fix a manipulated variable (i.e., the reflux flowrate) in the last column. In the first sensitivity analysis, the option of the reflux flowrate was excluded and the control structure was re-optimized. Table 4.8 shows that the solution of re-optimization was very similar as the ratio of the reflux flowrate to the feed flowrate was selected in the new optimization. The temperature tray also has moved down to the fifth tray. The values of the objective functions are slightly larger, but acceptable. The other sensitivity analyses were to move only the temperature controlled variables, one tray up and down. The results are reported in Table 4.7, which suggest that the solution is not very sensitive. In all these sensitivity analyses, the values of the multi-objective function remained acceptably in the 5% vicinity of the optimal solution. Furthermore, all the new solutions showed significant improvements over the base-case control structure. The temperature profiles of these analyses were very similar to figures 4.8 and are not shown in this thesis.

4.7.2.2. Sensitivity analyses with respect to the 10% and 20% disturbance scenarios

In the second part of the sensitivity analyses, the optimization was performed with respect to the 10% and 20% disturbance scenarios. The results of these analyses are reported in Tables 4.7 and 4.8, and are shown graphically in Figures 4.9 and 4.10. A comparison between the objective values of these scenarios with the previous results (i.e., with respect to the 5% disturbance scenarios) suggests that the economic objective function has strong functionality of the disturbances. In addition, the manipulated variables are varied more to reject the larger disturbances. Likewise, the variations in the intermediate states (chosen to be the column temperature profiles) are significantly more in these scenarios, as shown in Figures 4.9 and 4.10. However, Table 4.7 suggests that the optimizer was successful in controlling the quality of the products in terms of the average molecular weights and densities.

Table 4.8 shows that the control structures of the first column are the same in the 5% and 10% disturbance scenarios. However, the temperature trays in the second and third columns have changed slightly. The changes in the optimal control structure with respect to the 20% disturbance scenarios are more significant and most of the temperature trays are moved a few trays away. The most sensitive controlled variable is the temperature tray in the second column and as can be seen from Table 4.8, this temperature tray has moved more than others, when the system encountered larger disturbances. However, the product of this column is extracted from the top, and as shown in Figures 4.8b, 4.9b and 4.10b, the top part of the column is controlled tightly in all scenarios. In summary, these observations suggest that the optimal control structures and their corresponding profitability strongly depend on the considered disturbance scenarios.

4.8. Conclusion

This chapter presented a new optimization framework for optimal selection of control structures. It makes use of the notions of perfect control and inversion of the process model. The advantage of this optimization framework is that it postpones the design of controllers and reduces the size of the problem significantly, thus the proposed methodology is scalable and practical for larger industrial cases. The proposed framework decomposes the problem into two subproblems. One subproblem concerns steady-state control structure. The other subproblem addresses the design of inventory control systems.

The proposed optimization framework was demonstrated for a distillation train. The optimization framework was programmed using simulation-optimization. The optimization variables and constraints were presented and the applied software tools were explained. The results showed a very good trade-off between the objectives. The comparisons of the optimized and the base-case control structures showed that the optimized control structure performed better in terms of profitability and control objectives. Finally, the results of sensitivity analyses suggested that the optimal control structure and its profitability strongly depend on the considered disturbance scenarios.

5 | Integrated design and control using a steady-state inversely controlled process model

5.1. Introduction

The current industrial practice is to design a chemical process and its control system in sequence. However, the sequential approach is unfortunate because when the process design is fixed, there is little room left to improve the control performance. Therefore, design and control should be integrated. Nevertheless, the integrated problem is highly complex.

This chapter extends the method of the last chapter by applying the proposed steady-state optimization framework for integrated design and control. In the new framework, the complexities associated with controllers are removed from the problem formulation, but the process and its control structure are still optimized simultaneously.

The problem statement and the mathematical formulation of the proposed framework were presented in Chapter 3. In the subsequent sections, firstly similar to the last chapter, a goal-driven multi-objective function is proposed in order to establish the trade-off between process and control objectives. Similarly, it is also discussed that inventory control systems do not appear in a steady-state model and should be addressed separately. Then, the proposed optimization framework is demonstrated for an ETBE reactive distillation column. The process description is presented. In addition, the optimization variables and constraints are discussed. Optimization programming and the employed software tools are explained and the results are presented and discussed. As will be seen, the proposed optimization framework is successful in establishing the trade-off between control and process objectives.

5.2. Multi-objective function and goal programming

As discussed earlier, the problem of integrated design and control involves competing and conflicting objectives which require multi-criteria decision-making. In this section, a goal programming multi-objective function is proposed for integrated design and control. The implications of the objective functions are explained and the choices of the target values for these objectives are justified.

The objective functions proposed for the case study of this chapter are shown in Table 5.1. They are similar to the objectives considered in the last chapter (Table 4.1), as discussed in the following.

Table 5.1.
Objective functions for steady-state integrated design and control

Obj_1 = the deviations in the quality and quantity of products
Obj_2 = the deviations in the manipulated variables
Obj_3 = the deviations in the state variables
Obj_4 = the economic losses due to disturbances

The first objective, Obj_1, concerns the quality and quantity of products that are inferentially controlled. The second objective, Obj_2, concerns the movements of manipulated variables. Excessive and frequent changes in manipulated variables are not desirable because they may invoke interactions between control loops and exhaust control valves. The third objective, Obj_3, concerns the intermediate state variables, in order to make them insensitive to disturbances. The fourth objective, Obj_4, ensures that the economic losses associated with disturbances will be minimized. The instances of the proposed objective functions for the case of an ETBE reactive distillation will be discussed later in this chapter.

The difficulty associated with multi-objective optimization of integrated design and control is that the different economic and control performance objectives are incommensurable, i.e. it is difficult to aggregate their values as a single objective value. This chapter applies the goal programming method, as discussed earlier in Chapter 2.

In goal programming, each objective function is given a goal or target value. The deviations from these target values are used to construct an aggregated objective value as follows:

$$J_s = \left(\frac{1}{4}\sum_{w=1}^{4} \alpha_w\left(Obj_{w,s} - Obj_w{}^{target}\right) + Maximum\{\alpha_w\left(Obj_{w,s} - Obj_w{}^{target}\right)\}\right)$$

$$w = 1 \dots 4 \qquad (5-1)$$

where s is the index of disturbances. α_w is the weighting factor of each objective function. This is because, the four objective functions of Table 5.1 are not equally important, and a higher weight should be given to the first and fourth objectives. The actual values of α_w depends on the problem and sometimes it is needed to retune them during the optimization.

Goal programming of the first three objectives in Table 5.1 pose no difficulty because ideally the deviations in the quality and quantity of products, the changes in manipulated variables and the deviations in the state variables must be minimized toward zero. These targets will ensure tight control of the process. However, for the fourth objective in Table 5.1, minimizing the economic losses from a nominal operational point does not necessarily ensure optimal profitability. The reason is that in an integrated design and control framework, the nominal operating point is to be optimized itself. This suggests that a target is needed for optimal profitability. This target can be determined by maximizing $\text{Total Annual Profitability}$, as will be explained later. The deviations of all objective functions from their target values are minimized toward zero:

$$Obj_{w,s} - Obj_w{}^{target} \rightarrow 0 \qquad w = 1 \dots 4 \qquad (5-2)$$

Then, the expected value of the aggregated objective values for different disturbance scenarios must be minimized. In this research, it is assumed that the disturbances are known in advance. This expected value can be constructed by summing up the objective values weighted by the likelihood of each disturbance scenario, L_s , (Sahinidis, 2004):

$$\min \sum_{s=1}^{n_s} L_s \, J_s[\boldsymbol{Y_p}, \boldsymbol{Y_{cv}}, \boldsymbol{Y_{mv}}, \boldsymbol{p}, \boldsymbol{y_{i,setpoint}}, \boldsymbol{u_{j,nominal}}] \qquad \text{Problem 2.stst.gp}$$

subject to:

$$\boldsymbol{h}'[\boldsymbol{z}, \boldsymbol{x}, \boldsymbol{u}, \boldsymbol{y}, \boldsymbol{\mu}] = 0$$

$$\boldsymbol{g}[\boldsymbol{z}, \boldsymbol{x}, \boldsymbol{u}, \boldsymbol{y}, \boldsymbol{\mu}] \leq 0$$

$$\Omega_s[\boldsymbol{\mu}] = 0$$

$$\boldsymbol{Y_{cv,i}}\left(\boldsymbol{y_i} - \boldsymbol{y_{i,setpoint}}\right) = 0 \qquad i \in I_{kcv}$$

$$(\boldsymbol{1} - \boldsymbol{Y_{mv,j}})\left(\boldsymbol{u_j} - \boldsymbol{u_{j,nominal}}\right) = 0 \qquad j \in I_{kmv}$$

$$\boldsymbol{\Psi}(\boldsymbol{Y_{cv,i}}, \boldsymbol{Y_{mv,j}}) \geq 0$$

The notation Problem 2.stst.gp refers to the steady-state formulation of the proposed integrated design and control framework using a goal driven multi-objective function. Other mathematical notations were explained in Chapter 3. Addressing Problem 2.stst.gp, using simulation-optimization programming will be demonstrated for a reactive distillation column, later in this chapter.

5.3. Engineering insights and heuristics: dynamic degrees of freedom and design of inventory control systems

In the last chapter, it was explained that since dynamic degrees of freedom do not appear in a steady-state model, design of inventory control systems is not included in the proposed steady-state optimization framework and need to be considered separately. The task of designing inventory control systems can be addressed using heuristics and engineering insights developed over the decades of engineering practice. The implications of dynamic degrees of freedom for the case of the reactive distillation column are discussed later in this chapter.

5.4. Case study: Integrated design and control of an ETBE reactive distillation column

Reactive distillations are the leading technologies for process intensification. The application of these processes is motivated by significant reductions in the required capital and operating costs compared to the conventional reaction-separation processes. Furthermore, reactive distillations have significant advantages when conversion is thermodynamically limited by chemical equilibrium. The reason is that continuous removal of the products drives the overall conversion to completion. Other benefits include reduced downstream processing and higher energy efficiency due to utilization of reaction heat for evaporation of the liquid phase, (Sharma, 2010).

To date, a variety of methods for process design and control of reactive distillations has been proposed, which can be classified mainly into two categories, i.e., they have either a sequential approach or an integrated approach.

In the first category, sequential approach, the process is designed first, and then its control structure and controllers are decided. Similar to non-reactive distillation columns, several research activities have focused on developing graphical tools and short-cut methods in order to decide the number of stages in different sections of a reactive distillation column, optimal feed tray, and reflux ratio, (Barbosa and Doherty, 1988; Dragomir and Jobson, 2005; Carrera-Rodríguez, et al. 2011). These methods assume equilibrium conditions and mostly concern single-feed columns.

A more rigorous approach, however, is based on optimization. Cardoso, et al. (2000) proposed a variant of simulated annealing (SA) algorithm for optimization of an ethylene glycol reactive distillation. Jackson and Grossmann (2001) proposed a method based on disjunctive programming for two case studies: metathesis reaction of 2-pentene and production of ethylene glycol. Disjunctive programming provides a unique logic-based formulation of the problem, which can be translated to an MINLP formulation using several methods (e.g., big M or variable disaggregation) with different implications for convexity of the problem formulation, (see also Biegler, et al. 1997).

Lee, et al. (2010) studied heat integration of hydrolysis of methyl acetate. They concluded that a multi-effect distillation (in which feed is split between two smaller reactive distillation columns with different pressures) improves process economy compared to a design without heat integration, while the internally integrated design is less attractive due to high costs of compression.

Ramzan, et al. (2010) studied steady-state multiplicity of an ETBE reactive distillation using simulation and a lab-scale fixed bed column. They used steady-state analysis to identify input and output multiplicities and the optimal operating region.

Sneesby, et al. (1999) studied the design of a nine-tray single-feed ETBE reactive distillation column. They assumed equilibrium reactions for each tray. Later, Al-Arfaj and Luyben (2002) and Luyben and Yu (2008) extended the case study of Sneesby, et al. (1999) by considering a double-feed configuration, and modelling the reaction kinetics. They studied the dynamic performances of several control structures in the presence of different disturbances.

Researchers have reported difficulties in finding constant tuning parameters of proportional integral controllers for controlling ETBE reactive distillation columns. Sneesby, et al. (2000) proposed a multi-objective controller which allows online tracking of different operational modes (the constraints on the purity of the products or the constraints on the reaction conversion). Researchers have also proposed a model gain-scheduling controller (Bisowarno, et al. 2003) and a pattern-based predictive controller, (Tian, et al. 2003). Khaledi and Young (2005) studied the control of ETBE reactive distillation using a 2×2 model predictive controller. The purity of the product and conversion were being controlled. They assumed chemical equilibrium conditions. All the above methods are examples of the sequential approach in which firstly, the process is designed and then, its control structure and controllers are designed.

Recently, a new approach, integrated design and control, has gained the interests of researchers. Georgiadis, et al. (2002) applied dynamic optimization for an MTBE reactive distillation. They compared sequential and integrated approaches and demonstrated strong interactions between process design and control. Panjwani, et al. (2005) considered integrated design and control of an ethyl acetate reactive distillation column. They developed two superstructures; a superstructure for the process, which determines the optimal process design, and a superstructure for the control design, in which control structure and tuning parameters of proportional integral (PI) controllers were optimized. Miranda, et al. (2008) proposed dynamic optimization of an ETBE reactive distillation column. They considered only continuous variables. They took an optimal control approach in which instead of considering controllers, the (open loop) time trajectories of manipulated variables were optimized in order to reject disturbances. Although their proposed method ensures that process constraints are not violated during transient condition, selection of the control structure and designing the controllers were not included in their formulation.

In this chapter, the proposed optimization framework for integrated design and control using a steady-state inversely controlled process model is applied to the case of an ETBE reactive distillation column. In the subsequent sections, firstly the process description is presented. Then. the optimization variables and constraints are explained and the instances of the goal programming objectives and their target values for the case of an ETBE reactive distillation column are discussed. Later, the implemented software tools for simulation-optimization are explained. In this case study, a comparison is also made between the modelling approaches based on the kinetic correlations and assuming chemical equilibrium conditions. That part of the study will take the opportunity to sort out a problem identified by other authors (Al-Arfaj and Luyben 2002) for the sake of completeness. Finally, the results are presented and discussed.

5.4.1. Process description

There is an increasing demand for Ethyl Tert-Butyl Ether (ETBE), as a gasoline oxygenate and octane enhancer, and it is replacing Methyl Tert-Butyl Ether (MTBE) due to environmental concerns of the latter. In addition, ETBE is produced from reaction of isobutene and ethanol, and hence is semi-renewable:

$$C_4H_8\,(isobutene) + C_2H_6O\,(ethanol) \leftrightarrow C_6H_{14}O\,(ETBE) \qquad (5-3)$$

This reaction is equilibrium limited (only 84.7% at 70^oC) and the application of reactive distillations offers significant advantages because continuous removal of the product drives the overall conversion to completion, (Al-Arfaj and Luyben, 2002). The process flow diagram of an ETBE reactive distillation column is shown in Figure 5.1. The C4s feed stream is a mixture of isobutene and n-butene. N-butene is an inert and does not participate in the reaction. The distillate is mainly n-butene and the bottom stream is mainly ETBE. If the reactants are not fed according to the stoichiometry of the reaction, the excess ethanol leaves the column in the bottom stream.

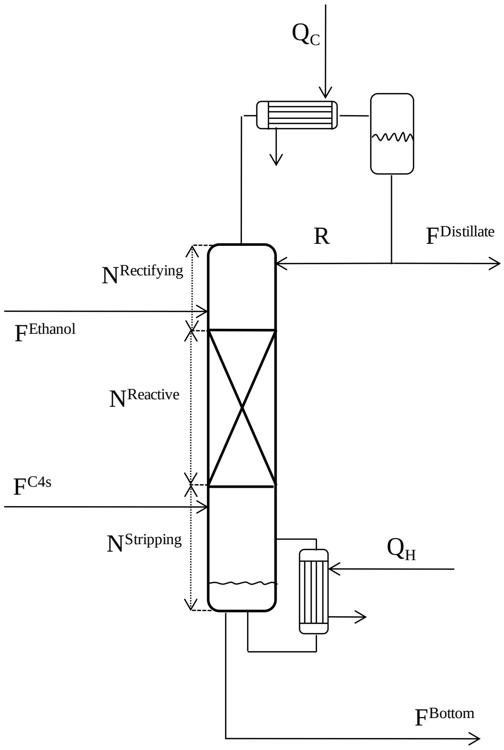

Figure 5.1. Process flow diagram of ETBE reactive distillation column.

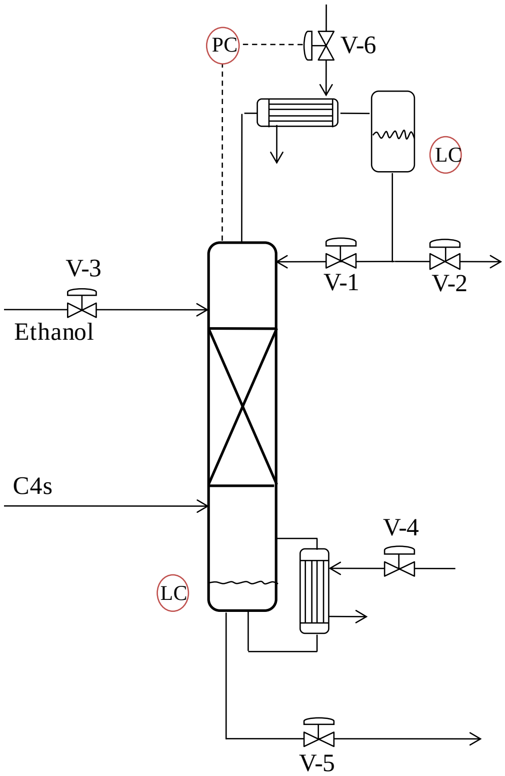

Figure 5.2. The manipulated variables in an ETBE reactive distillation shown by control valves

5.4.2. Optimization constraints

Optimization constraints can be classified into the constraints regarding (1) degrees of freedom, (2) disturbance scenarios, (3) perfect control, and (4) first principles modelling. These constraints are discussed in the following.

5.4.2.1. Available degrees of freedom and the implications of inventory control systems

In Chapter 2, based on the flowsheet-oriented method of Konda, et al. (2006), it was explained that a distillation column with total reflux has six degrees of freedom. In ETBE reactive distillation column, there are two feed streams, and the control degree of freedom is:

$$\mathrm{CDOF} = 13 - 3 - 3 = 7 \qquad (5-4)$$

However, one of these degrees of freedom is consumed by the C4s feed which is the throughput manipulation point, and is dictated by the upstream process. Therefore, the remaining control degree of freedom is six. These degrees of freedom are shown by control valves in Figure 5.2.

It was explained earlier that the application of a steady-state inversely controlled process model decomposes the subproblem of control structure selection into two smaller sub-problems. One sub-problem concerns inventory control systems, and the other sub-problem is addressed using steady-state optimization. The aim of the following analysis is to establish the available degrees of freedom for the steady-state optimization.

There are three material inventories, i.e., two liquid inventories at the column ends, in addition to the column vapour inventory. These inventories consume three degrees of freedom. The engineering practice is to control the column pressure (representing the vapour inventory) using the cooling duty of the condenser. The overhead liquid inventory can be controlled using either the reflux flowrate or the distillate flowrate. The bottom liquid inventory can be controlled using either the reboiler duty or the bottom flowrate. In order to incorporate these insights into the proposed optimization framework, the following constraints are considered:

$$Y_D + Y_R \leq 1 \qquad (5-5a)$$

$$Y_B + Y_V \leq 1 \qquad (5-5b)$$

where, Y_D, Y_R, Y_B, Y_V are the structural variables for selection of distillation flowrate, reflux flowrate, boil-up flowrate, and bottom rate as the manipulated variables, respectively.

5.4.2.2. Constraints regarding disturbance scenarios

In this research, it is assumed that disturbances are known in advance. The C4s feed stream to the ETBE reactive distillation column is the source of disturbances. As mentioned by Al-Arfaj and Luyben (2002), it is less likely to have control over the flowrate or composition of the C4s feed. However, the ethanol feed is delivered from storage and its flowrate can be adjusted as a manipulated variable.

The C4s feed is a mixture of isobutene and n-butene. Luyben and Yu, (2008) considered two disturbance scenarios, 1) changes in the flowrate or 2) changes in the composition. They mentioned that the latter is a more difficult scenario. In the present case study, both disturbances in the flowrate of the C4s feed and its composition are considered simultaneously. In each disturbance scenario, the mass flowrate of each of the components in the feed stream is changed by $\pm 10\%$. The combinations of these changes result in nine disturbance scenarios which represent the operational conditions (Table 5.2). These disturbance scenarios are equally likely.

Table 5.2.
Disturbance scenarios: $\pm$10% changes in molar fractions of isobutene and n-butene

Disturbance Scenario	Isobutene (molar fraction)	Isobutene (kmol.h^{-1})	N-butene (molar fraction)	N-butene (kmol.h^{-1})
1st	0.9	636.12	0.9	954.18
2nd	0.9	636.12	1	1060.20
3th	0.9	636.12	1.1	1166.22
4th	1	706.80	0.9	954.180
5th	1	706.80	1	1060.20
6th	1	706.80	1.1	1166.22
7th	1.1	777.48	0.9	954.18
8th	1.1	777.48	1	1060.20
9th	1.1	777.48	1.1	1166.22

5.4.2.3. Constraints regarding perfect control

The proposed integrated design and control framework, Problem 2.stst.gp, includes two sets of perfect control equality constraints for selection of controlled and manipulated variables:

$$\boldsymbol{Y_{cv,k}}(\boldsymbol{y_i} - \boldsymbol{y_{desired}}) = 0 \qquad (5-6a)$$

$$(\boldsymbol{1} - \boldsymbol{Y_{mv,k}})(\boldsymbol{u_i} - \boldsymbol{u_{nominal}}) = 0 \qquad (5-6b)$$

$$\boldsymbol{\Psi}(\boldsymbol{Y_{cv,k}}, \boldsymbol{Y_{mv,k}}) \geq 0 \qquad k \in K \qquad (5-6c)$$

$\boldsymbol{Y_{cv,i}}$ and $\boldsymbol{Y_{mv,j}}$ are binary variables, which indicate whether a controlled variable or a manipulated variable is selected respectively. $\boldsymbol{\Psi}(\,)$ ensures that the selected controlled variables and manipulated variables are consistent.

Here, two strategies are possible in order to satisfy these constraints. One is to meet these constraints in each iteration of optimization. This strategy was chosen in the last chapter. An alternative strategy is to relax the perfect control constraints during the optimization and the objective function of Problem $2.\mathrm{stst.gp}$ is penalized according to the violations of these constraints as follows:

$$\text{Penalty function} = \sum_{i=1}^{N_{cv}} \text{minimum}(wt_i \sum_{s=1}^{N_s} \frac{|y_{i,s} - y_{i,desired}|}{y_{i,desired}}) +$$

$$\sum_{j=1}^{N_{mv}} \text{minimum}(\ wt_j \sum_{s=1}^{N_s} \frac{|u_{j,s} - u_{nominal}|}{u_{nominal}}) \qquad (5-7a)$$

$$N_{CV} + N_{MV} = DOF \qquad (5-7b)$$

In above, N_s is the number of disturbance scenarios, N_{cv} is the number of the selected controlled variables and N_{mv} is the number of the selected manipulated variables. In this case study, the above penalty function was implemented by the *sortrows* command of MATLAB®. This command sorted the candidate controlled and manipulated variables according to the violations of their corresponding constraints. Then, the three candidates (because $DOF = 3$) with the minimum constraint violations were selected and the value of the penalty function was calculated according to them. By convergence of the optimization algorithm, the penalty function will approach to zero. The weighting factors of the penalty function were gradually and iterative increased until the variation in the selected controlled variables felt below 0.01 K for the temperature controlled variables and below 1 kg.h^{-1} for the flow controlled variables. The implication is that three perfect control constraints are satisfied by equation 5-7a. These constraints correspond to the selected manipulated and controlled variables.

In the new formulation, unlike the formulation of the last chapter, the choices of the simulation specifications are not limited to the selected controlled and manipulated variables. This formulation is advantageous especially when the convergence of the inversely controlled process model is poor or the total number of candidate controlled and manipulated variables is large. The reason is that in the new formulation, these variables appear in the objective function, while in the formulation of the last chapter, an optimization variable should be considered for each candidate controlled or manipulated variable and the size of the optimization problem grew sharply. Table 5.3 lists the candidate controlled and manipulated variables for the case of an ETBE distillation column. In Table 5.3, the notations R, D, V, B represent reflux, distillate, boil-up and bottom streams respectively. The notation T_i represents the temperature of the tray i and Q_H refers to the heat duty of the reboiler.

Table 5.3.
Candidate controlled and manipulated variables for the ETBE reactive distillation according to equations (5-6a, b).

Candidate variables to be selected as controlled variables ($\boldsymbol{y}_i$ equation 5-6a)	$T_1, \ldots, T_{Ntrays}$, $\frac{R}{D}, \frac{R}{B}, \frac{R}{V}, \frac{R}{F^{C4s}}, \frac{R}{F^{EtOH}}$, $\frac{D}{B}, \frac{D}{V}, \frac{D}{F^{C4s}}, \frac{D}{F^{EtOH}}$, $\frac{B}{V}, \frac{B}{F^{C4s}}, \frac{V}{F^{EtOH}}$
Candidate variables to be selected as manipulated variables ($\boldsymbol{u}_i$ in equation 5-6b)	R, D, V, B, Q_H

5.4.2.4. Constraints regarding first principles modelling

The first principles modelling was perform using Aspen Plus® and according to the guidelines by Luyben and Yu, (2008). The components were defined from the Aspen databank. The UNIFAC property package was used for liquid phase analysis and the Peng-Robinson property package was applied for vapour phase analysis. The Radfrac distillation model with total reflux was used and the option for the solver was set to *strongly non-ideal liquid*. The underlying equations of these models (i.e., Radfrac, Peng-Robinson, UNIFAC) can be found in Aspen-Plus document, (2009a,b).

Since the kinetic correlations (Al-Arfaj and Luyben, 2002; Luyben and Yu, 2008) include activity terms, it is not possible to use default forms, and the kinetic correlations were given to software using a Fortran subroutine. Luyben and Yu, (2008) provided the original FORTRAN code. Unfortunately, due to the changes in the way that Aspen Plus uses the memory, that code is outdated for Aspen Plus 2006 and later versions. The updated code, based on the guidelines from Solution (121621) by AspenTech support website, is provided in Appendix A. More detail about applied simulation-optimization programming will be presented later in this chapter.

5.4.3. Optimization variables

Optimization variables are listed in Table 5.4. They can be classified into 1) process parametric variables, 2) process structural variables, 3) control parametric variables, and 4) control structural variables. The numbers of the stages in each distillation section and the stage of the feeds are the process structural variables. The amount of the catalyst on each stage and the column pressure are process parametric variables. As will be discussed later in this chapter, due to difficulties with convergence of the solver, two new sets of optimization variables are introduced. They are $\alpha_{1,s}$ which represents the molar ratio of the ethanol feed flowrate to the bottom product flowrate, and $\alpha_{2,s}$ which represents the molar ratio of the ethanol feed flowrate to the isobutene flowrate in the C4s feed. Therefore, the control parametric variables are reflux ratios, $\alpha_{1,s}$ and $\alpha_{2,s}$. The control structural decisions are not shown in Table 5.4. They are implied in the penalty functions 5-5a, b. By convergence of the optimization algorithm, the values of three terms (equal to the number of steady-state degrees of freedom) in this penalty function will be very close to zero. These three terms correspond to three variables in Table 5.3 and determine which three candidate controlled or manipulated variables are selected. The process structural and parametric variables, as well as the control structural variables are the same for all disturbance scenarios. The control parametric variables are different for each disturbance scenario and are subscripted by the corresponding disturbance scenario, s in Table 5.4.

Table 5.4.

Optimization variables; $\alpha_{1,s}$ represents the ratio $F_s^{bottom}/F_s^{Ethanol-Feed}$ for disturbance scenario s. $\alpha_{2,s}$ represents the ratio $F_s^{Ethanol-feed}/F_s^{isobutene-Feed}$ for disturbance scenario s.

Optimization variable	Description	Optimization variable	Description
Number of rectifying stages*	Process structural variable	Reflux ratio$_{s=2}$	Control parametric variable
Number of reactive stages	Process structural variable	Reflux ratio$_{s=3}$	Control parametric variable
Number of stripping stages	Process structural variable	Reflux ratio$_{s=4}$	Control parametric variable
ethanol feed stage	Process structural variable	Reflux ratio$_{s=5}$	Control parametric variable
C4s feed stage	Process structural variable	Reflux ratio$_{s=6}$	Control parametric variable
Column Pressure (atm)	Process parametric variable	Reflux ratio$_{s=7}$	Control parametric variable
Catalyst hold-up (kg)	Process parametric variable	Reflux ratio$_{s=8}$	Control parametric variable
$\alpha_{1,s=1}$	Control parametric variable	Reflux ratio$_{s=9}$	Control parametric variable
$\alpha_{1,s=2}$	Control parametric variable	$\alpha_{2,s=1}$	Control parametric variable
$\alpha_{1,s=3}$	Control parametric variable	$\alpha_{2,s=2}$	Control parametric variable
$\alpha_{1,s=4}$	Control parametric variable	$\alpha_{2,s=3}$	Parametric control variable
$\alpha_{1,s=5}$	Control parametric variable	$\alpha_{2,s=4}$	Control parametric variable
$\alpha_{1,s=6}$	Control parametric variable	$\alpha_{2,s=5}$	Control parametric variable
$\alpha_{1,s=7}$	Control parametric variable	$\alpha_{2,s=6}$	Control parametric variable
$\alpha_{1,s=8}$	Control parametric variable	$\alpha_{2,s=7}$	Control parametric variable
$\alpha_{1,s=9}$	Control parametric variable	$\alpha_{2,s=8}$	Control parametric variable
Reflux ratio$_{s=1}$	Control parametric variable	$\alpha_{2,s=9}$	Control parametric variable

* In this Chapter, the first stage is condenser, and the last stage is reboiler. For example, the thirteenth stage is the twelfth tray.

5.4.4. Multi-objective function for integrated design and control of an ETBE reactive distillation column

Section 5.2 explained goal programming for multi-objective optimization of integrated design and control. This section explains the instances of the objective functions in Table 5.1 for the ETBE reactive distillation column. All these objectives are measured in terms of their deviations from their target values due to disturbance scenarios, which should ideally be zero.

The instances of the first objective are the purity of the ETBE (bottom) product stream (99% mass fraction of ETBE) and the purity of the overhead product stream (less than 2% mass fraction of isobutene). The target of 99% was chosen for ETBE in order to ensure that the solution will have at least the purity of 98% for all disturbances and the product will be marketable.

There are six manipulated variables in the ETBE reactive distillation, as shown in Figure 5.2. Since in this case study, disturbances included the changes in the feed flowrate, three of these manipulated variables (i.e., the ethanol feed, the overhead product and the bottom product) must change to be consistent with the stoichiometry of the reaction and hence their changes are necessary for perfect control and are not penalized. Therefore, the variations of the remaining manipulated variables, (i.e., the reboiler and condenser duties and the reflux flowrate) are the instances of the second objective function.

The variations in the composition of all four components (i.e., isobutene, n-butene, ethanol, and ETBE) all through the distillation column are the instances of the third objective.

As mentioned earlier, in order to generate a goal for the economic objective, TotalAnnual Profit (TAP) was maximized in advance:

$$\text{Total Annual Profit} = \text{TotalAnnualRevenue} - \text{TotalAnnualCosts} \qquad (5-8a)$$

$$\text{Total Annual Costs} = \text{Capital costs/payback period} + \text{annual energy costs} + \cdots$$
$$+\text{annual feedstock costs} \qquad (5-8b)$$

The economic losses are defined as the decrease in Maximum Total Annual Profit (TAP^{max}). Therefore, the decrease in Total Annual Profit compared to TAP^{max} is the instance of the fourth objective value in Table 5.1.

In order to evaluate TAP^{max} , an initial optimization was performed. In this optimization, the economic objective function (5-8a) was maximized. This optimization was performed with respect to the nine disturbances in Table 5.2. The results of this optimization showed that $\mathrm{TAP}^{\max} = 2.9 \times 10^{8}$ \$.yr^{-1}. This optimization does not consider the second and third objectives of Table 5.1. Therefore, a comparison of this optimization and the main optimization can demonstrate the effects of the second and third objectives, as will be discussed in the results.

The aim of the above optimization was to generate a target for the fourth objective function (Table 5.1) in the main optimization framework. However, during the main optimization, the author noticed that this target is not strong enough and economic losses, due to disturbances, are unreasonable. Furthermore, as discussed in Chapter 2, optimistic targets for goals are preferred to the pessimistic targets, because the later may result in an inferior solution. In addition, the case study has a nonlinear and nonconvex formulation which increases the likelihood of a local solution. For these reasons, the target value of the fourth objective was set optimistically to the value of 3.3×10^{8} \$.yr^{-1} which gave a higher priority to the economic objective and enhanced the likelihood of achieving a Pareto optimal solution.

The values of α_w, the weighting factors of the goal programming objective function (5-1) were selected to be $\alpha_1 = 100$, $\alpha_2 = 1$, $\alpha_3 = 0.1$, $\alpha_4 = 10$ for Obj_w $w = 1 \ldots 4$ in Table 5.1.

Table 5.5 lists the economic parameters and the sizing correlations used in this case study. Required information for the prices of the products, utilities and feedstocks were from ICIS pricing (2011), Ulrich (2006) and Al-Arfaj and Luyben (2002). The required capital costs were calculated by sizing the distillation column and its heat exchangers. The required energy costs were calculated from the heating and cooling duties of the reactive distillation column. The reference year was 2010, and prices from Ulrich, (2006) and Al-Arfaj and Luyben, (2002) were updated using Chemical Engineering Plant Cost Index (CE PCI) and Marshall & Swift Equipment Cost Index (M&S ECI) from Chemical Engineering magazine, (2011).

Different disturbances require different operating and capital costs. Since the disturbances are assumed equally likely, the average of the operating costs are considered. However, because equipment should remain operable at all disturbances, the highest capital costs are considered.

Table 5.5.
Economic data for calculating Total Annual Profit (Equations 5-8a and b)

	Economic parameters	**Reference**
C4 Feed ($\$.kmol^{-1}$)	29.65	ICIS pricing (2011)
ethanol ($\$.kmol^{-1}$)	39.67	ICIS pricing (2011)
ETBE ($\$.kmol^{-1}$)	118.25	ICIS pricing (2011)
Amberlyst 15 (Catalyst) ($\$.kg^{-1}$)	10.16	Al-Arfaj and Luyben (2002)
Low Pressure (LP) Steam (P=9.4 bar, T=451.7 K) ($\$.kg^{-1}$)	0.0019	Ulrich (2006)
Cooling Water (P=7 bar, Tsupply=30 ^oC) ($\$.m^{-3}$)	0.0414	Ulrich (2006)
	Sizing correlations and parameters	**Reference**
Capital costs of heat exchangers ($Area$ in m^2)	$7296Area^{0.65}$	Al-Arfaj and Luyben (2002)
Heat transfer coefficient (condenser) ($kW.K^{-1}m^{-2}$)	0.852	Al-Arfaj and Luyben (2002)
Heat transfer coefficient (reboiler) ($kW.K^{-1}m^{-2}$)	0.568	Al-Arfaj and Luyben (2002)
Capital cost of column Vessel ([D]=m; [L]=m)	$17640D^{1.066}L^{0.802}$	Al-Arfaj and Luyben (2002)
Payback period (years)	3	Al-Arfaj and Luyben (2002)

5.5. Implementation software tools

In Chapter 2, it was discussed that the simulation program acts as the implicit constraints of optimization. In the case study of this chapter, simulation was performed using Aspen-Plus® and optimization was performed by Genetic Algorithm (GA) Toolbox of MATLAB. Unfortunately, due to technical difficulties it was not possible to link MATLAB® directly to Aspen-Plus®. Therefore, MATLAB® was firstly linked to Microsoft Excel VBA® and then VBA® was linked to Aspen-Plus®. All integrations were based on Microsoft COM® automation interface. The optimization algorithm was the Genetic Algorithm (GA) Toolbox of MATLAB. The GA's settings were set to defaults. The details of optimization software can be found in the MATLAB documentation (2012).

Figure 5.3 shows the information flow of simulation-optimization program. The left-hand side block and the right-hand side block are Genetic Algorithm (GA) Toolbox of MATLAB and Aspen-Plus® simulator respectively. The middle block comprises of an m.file coded in MATLAB and an Excel VBA code, which integrates the two software tools.

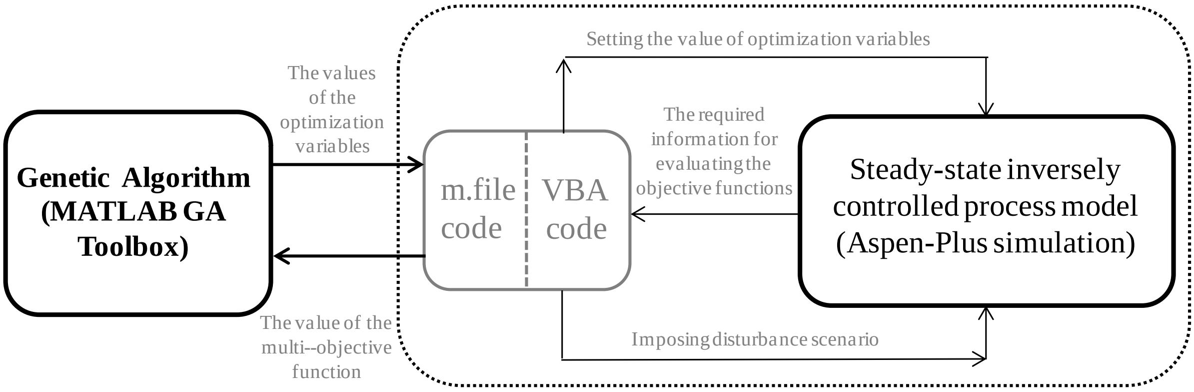

Figure 5.3. Information flow of the simulation-optimization programming.

The steps in each optimization iteration are as follows:

Step 1. The GA decides on the values of the optimization variables, (Table 5.4).

Step 2. The integrating code receives the values of the optimization variables, and set them in the simulation program.

Step 3. The integrating code evaluates the performance of the trial values of the optimization variables against the expected disturbance scenarios. These disturbances are imposed by changing the flowrate and the composition of the C4s feed, as described earlier.

Step 4. For each disturbance scenario, the corresponding values of the objective functions (Table 5.1) are evaluated. Then, the aggregated value of the multi-objective function (5-1) is constructed and penalized by the penalty functions (5-7). Since the disturbances are assumed equally likely, the expected value of the aggregated objective values is their average value which is reported to the GA.

Step 5. The GA evaluates the termination criteria and decides on improving the optimization variables.

In each simulation run, a simulation file was opened, run, and closed without saving. Since nine disturbance scenarios were considered, for each function recall (i.e., one evaluation of the objective function) the simulation was run nine times. The required time for each function recall was 4-5 minutes, which in the problematic cases when the solver had problems with convergence was significantly more. Each generation of the optimization algorithm had twenty individuals, and the optimization needed up to fifty generations. Therefore, each optimization run needed about one week. In addition, in order to refine the penalty functions and weighting factors, the optimization procedure needed to be interrupted and/or reiterated a few times. The results should be reproducible if the same version of the solver (i.e., Aspen V7.1) with exactly the same specifications (reported in Section 5.4.2.4.) is used. However, the genetic algorithm as a stochastic optimization method does not construct any proof for global optimality of the solution.

5.6. Treatment of the convergence failure of the equation solver

It was explained previously that the formulation of integrated design and control, using a steady-state inversely controlled process model, consists of algebraic equations (AEs), only. The AEs system is shown by inversely controlled process model (right hand-side inner block) in Figure 5.3 and was simulated using Aspen Plus®. If the values of a sufficient number of variables (equal to the difference between the number of unknown variables and the number of equations) for an AEs system are known, the values of the rest of the variables can be calculated. As discussed earlier, the advantage of including perfect control equations in the penalty functions (5-7) is that there is no need to consider an optimization variable for each candidate controlled or manipulated variable. Therefore, this formulation provides the opportunity to choose those simulation specifications which are more likely to ensure convergence of the simulation program, as discussed in the following.

The author encountered difficulties in simulation-optimization of the case study as the simulation was frequently diverging. Failure of the simulator solver was also reported by Luyben and Yu, (2008), when they were investigating the effects of the design parameters:

"Convergence issues and frequent Fortran system errors severely limited this investigation."

In the present study, the author's observations suggested that there were two types of solver failures. Since the solver is principally a nonlinear equation solver, its success depends on a close starting point. Strategies such as setting the solver for the maximum possible iterations, or automated re-initialization of the solver greatly improved this type of failure. However, the second type of failure was be due to infeasible trial values for the optimization variables. Unfortunately, this type of failure is not informative and the solver does not inform the optimizer about the degree of infeasibility. One resolution is to cruelly penalize the objective function for simulation failure. The risk is that the optimizer may converge to an easy local optimum. In this study, two instances for the second type of failure were identified and resolved, as discussed in the following.

The first instance was due to a reflux value that is not appropriate to remove products and introduce fresh feeds to the reactive stages. In that instance, reflux was changed by $+25\%$, -25% and $+50\%$. At the same time, a penalty value was added to the objective function. This strategy ensured that the value of the objective function reflected some fitness of the diverging solution, while the ultimate solution was feasible and converging.

The second instance of simulation failure was due to inconsistency with the reaction stoichiometry. Equation 5-3 suggests that for a kmol of isobutene in the feed, only a kmol of ethanol participate in the reaction and any extra ethanol would degrade the purity of the ETBE product. This analysis suggests that the value of $\alpha_{1,s}$ and $\alpha_{2,s}$ (in equations 5-7a, b below) should be tightly bounded around unity in order to maintain molar balance of the column:

$$F_s^{\text{bottom}} = \alpha_{1,s} F_s^{\text{ethanol feed}} \qquad (5-9a)$$

$$F_s^{\text{ethanol feed}} = \alpha_{2,s} F_s^{\text{isobutene Feed}} \qquad (5-9b)$$

where $F_s^{\text{isobutene Feed}}$ is molar flowrate of isobutene in the C4s feed for disturbance s, $F_s^{\text{ethanl}-\text{feed}}$ is the molar flowrate of the ethanol feed for disturbance s, F_s^{bottom} is the molar flowrate of the bottom stream for disturbance s. In this research, the above constraints were added to the simulation-optimization framework. $F_s^{\text{ethanl}-\text{feed}}$and F_s^{bottom}, were selected as the column specifications, and their values were calculated using the trial values of $\alpha_{1,s}$ and $\alpha_{2,s}$ from the optimization algorithm. The bounds on these variables were ($0.95 < \alpha_{i,s} < 1.05,\ i = 1,2$). This strategy ensured that eighteen optimization variables in Table 5.4 are almost near their optimal values and the solver would not diverge due to inconsistency with the reaction stoichiometry.

In the present study, the application of the abovementioned strategies brought all simulations into convergence. In each iteration of the inner-loop simulation, the status of the solver was checked and the objective functions were only evaluated after simulation convergence.

5.7. Comparisons between modelling approaches based on kinetic correlations and the assumption of equilibrium reaction

As mentioned earlier, researchers considered two approaches for modelling ETBE reactive distillation columns. These are modelling based on kinetic correlations (applied by Luyben and Yu, 2008; Bisowarno, et al. 2003; Miranda, et al. 2008) and modelling based on the assumption of chemical equilibrium (Sneesby 2000; Khaledi and Young, 2005). Since assuming chemical equilibrium implies that the residence time is large enough to maximize the conversion, it is expected that the results of the second modelling approach feature a higher overall conversion. However, Luyben and Yu (2008) (Page 236, top paragraph) reported an unexpected result when they compared the above two models. They reported that:

"*the conversion dropped to less than 50%, and the concentration of the both reactants in the entire reaction zone were quite high. We are at a loss to explain these results.*"

This study took the opportunity to sort out a problem identified by these authors for the sake of completeness. Fortunately, the updated code presented in Appendix A is able to provide the comparison accurately. The discussion of the comparison between the two modelling approaches will be provided later in Discussion Section. In this comparison, the number of rectifying stages was 2; the number of reactive stages was 18; the number of stripping stages was 4; the ethanol feed stage was 7; the C4s feed stage was 20; the reflux ratio was 7; the column pressure was 7.5 atm and the pressure drop was 0.01 $atm.tray^{-1}$; the catalyst holdup of each tray was 1000 kg; the ethanol feed flowrate was 716 ($kmol.h^{-1}$); the bottom product flowrate was 714 ($kmol.h^{-1}$); the C4s feed consisted of 706.8 ($kmol.h^{-1}$) isobutene and 1060.2 ($kmol.h^{-1}$) n-butene. The calculation of the equilibrium reaction was based on minimization of Gibbs free energies.

5.8. Results of the case study

This section reports the results. They are:

- Table 5.6 reports the optimal values of the objective functions.
- Table 5.7 reports the optimal values of the structural and parametric process and control variables.
- Table 5.8 reports the results of optimization of TotalAnnualProfit (TAP).
- Figure 5.4 presents the optimized process and control structures.
- Figures 5.5a, b, c, d and e present the results of the proposed optimization framework. These are the profiles of the temperature, ETBE, ethanol, isobutene, and n-butene composition respectively. Each figure presents the profiles corresponding to the nine disturbance scenarios, shown in Table 5.2.
- Figures 5.6a, b, c, d and e present the results of maximization of Total Annual Profit (TAP). These are the profiles of the temperature, ETBE, ethanol, isobutene, and n-butene composition respectively. Each figure presents the profiles corresponding to the nine disturbance scenarios, shown in Table 5.2.
- Figures 5.7a, b, c, d and e present the comparisons of the two modelling approaches based on the kinetic correlations and chemical equilibrium respectively. The method for this comparison was described in Section 5.7. These parts of the results are not a part of optimization.

The abovementioned figures and tables are explained in Discussion Section.

Table 5.6.
The value of objective functions

	Average purity of the ETBE product (mass fraction)	Average changes in manipulated variables	Average changes in intermediate compositions	Total Annual Profit(TAP) [$.yr^{-1}]
Proposed optimization framework	0.9866	4.37%	13.52%	2.864×10^{8}
TAP maximization	0.9878	6.14%	16.11%	2.9×10^{8}

Table 5.7.
Optimal values of the optimization variables using the proposed optimization framework.

Optimization variables	Optimal value	Optimization variables	Optimal value
Number of rectifying stages	2	Reflux ratio$_{s=1}$ [-]	6.88
Number of reactive stages	16	Reflux ratio$_{s=2}$ [-]	6.23
Number of stripping stages	4	Reflux ratio$_{s=3}$ [-]	6.35
ethanol feed stage	7	Reflux ratio$_{s=4}$ [-]	6.12
C4s feed stage	20	Reflux ratio$_{s=5}$ [-]	6.23
Column Pressure (atm)	6.44	Reflux ratio$_{s=6}$ [-]	5.75
Catalyst hold-up (kg)	1078.5	Reflux ratio$_{s=7}$ [-]	6.51
		Reflux ratio$_{s=8}$ [-]	6.51
$F_{s=1}^{\text{bottom}}$ (kmol.h^{-1})	626.81	Reflux ratio$_{s=9}$ [-]	6.56
$F_{s=2}^{\text{bottom}}$ (kmol.h^{-1})	627.74	$F_{s=1}^{\text{ethanol feed}}$ (kmol.h^{-1})	640.56
$F_{s=3}^{\text{bottom}}$ (kmol.h^{-1})	618.02	$F_{s=2}^{\text{ethanol feed}}$ (kmol.h^{-1})	638.89
$F_{s=4}^{\text{bottom}}$ (kmol.h^{-1})	703.20	$F_{s=3}^{\text{ethanol feed}}$ (kmol.h^{-1})	628.79
$F_{s=5}^{\text{bottom}}$ (kmol.h^{-1})	697.86	$F_{s=4}^{\text{ethanol feed}}$ (kmol.h^{-1})	717.56
$F_{s=6}^{\text{bottom}}$ (kmol.h^{-1})	693.44	$F_{s=5}^{\text{ethanol feed}}$ (kmol.h^{-1})	712.14
$F_{s=7}^{\text{bottom}}$ (kmol.h^{-1})	776.78	$F_{s=6}^{\text{ethanol feed}}$ (kmol.h^{-1})	706.78
$F_{s=8}^{\text{bottom}}$ (kmol.h^{-1})	765.24	$F_{s=7}^{\text{ethanol feed}}$ (kmol.h^{-1})	787.83
$F_{s=9}^{\text{bottom}}$ (kmol.h^{-1})	755.13	$F_{s=8}^{\text{ethanol feed}}$ (kmol.h^{-1})	780.91
		$F_{s=9}^{\text{ethanol feed}}$ (kmol.h^{-1})	771.18
Controlled variable (1)	Stage 2 temperature	Setpoint (1) (K)	332.8
Controlled variable (2)	Stage 13 temperature	Setpoint (2) (K)	335.6
Controlled variable (3)	The ratio of ethanol feed and ETBE product	Setpoint (3) [-] = (kg.s^{-1}).(kg.s^{-1})$^{-1}$	2.15

Table 5.8.
Optimal values of the optimization variables for maximization of TOTAL Annual Profit (TAP) discussed in Section 5.4.4.

Optimization variables	Optimal value	Optimization variables	Optimal value
Number of rectifying stages	2	Reflux ratio$_{s=1}$ [-]	5.6905
Number of reactive stages	15	Reflux ratio$_{s=2}$ [-]	4.5109
Number of stripping stages	4	Reflux ratio$_{s=3}$ [-]	5.0095
ethanol feed stage	7	Reflux ratio$_{s=4}$ [-]	4.7982
C4s feed stage	17	Reflux ratio$_{s=5}$ [-]	4.5517
Column Pressure (atm)	6.75	Reflux ratio$_{s=6}$ [-]	4.2993
Catalyst hold-up (kg)	1101	Reflux ratio$_{s=7}$ [-]	5.1610
		Reflux ratio$_{s=8}$ [-]	4.7358
$F_{s=1}^{bottom}$ (kmol.h^{-1})	623.41	Reflux ratio$_{s=9}$ [-]	4.4798
$F_{s=2}^{bottom}$ (kmol.h^{-1})	621.02	$F_{s=1}^{ethanol\ feed}$ (kmol.h^{-1})	630.98
$F_{s=3}^{bottom}$ (kmol.h^{-1})	620.94	$F_{s=2}^{ethanol\ feed}$ (kmol.h^{-1})	628.56
$F_{s=4}^{bottom}$ (kmol.h^{-1})	697.94	$F_{s=3}^{ethanol\ feed}$ (kmol.h^{-1})	628.49
$F_{s=5}^{bottom}$ (kmol.h^{-1})	702.69	$F_{s=4}^{ethanol\ feed}$ (kmol.h^{-1})	700.34
$F_{s=6}^{bottom}$ (kmol.h^{-1})	690.17	$F_{s=5}^{ethanol\ feed}$ (kmol.h^{-1})	709.22
$F_{s=7}^{bottom}$ (kmol.h^{-1})	771.78	$F_{s=6}^{ethanol\ feed}$ (kmol.h^{-1})	698.32
$F_{s=8}^{bottom}$ (kmol.h^{-1})	771.34	$F_{s=7}^{ethanol\ feed}$ (kmol.h^{-1})	781.16
$F_{s=9}^{bottom}$ (kmol.h^{-1})	770.68	$F_{s=8}^{ethanol\ feed}$ (kmol.h^{-1})	780.71
		$F_{s=9}^{ethanol\ feed}$ (kmol.h^{-1})	771.98

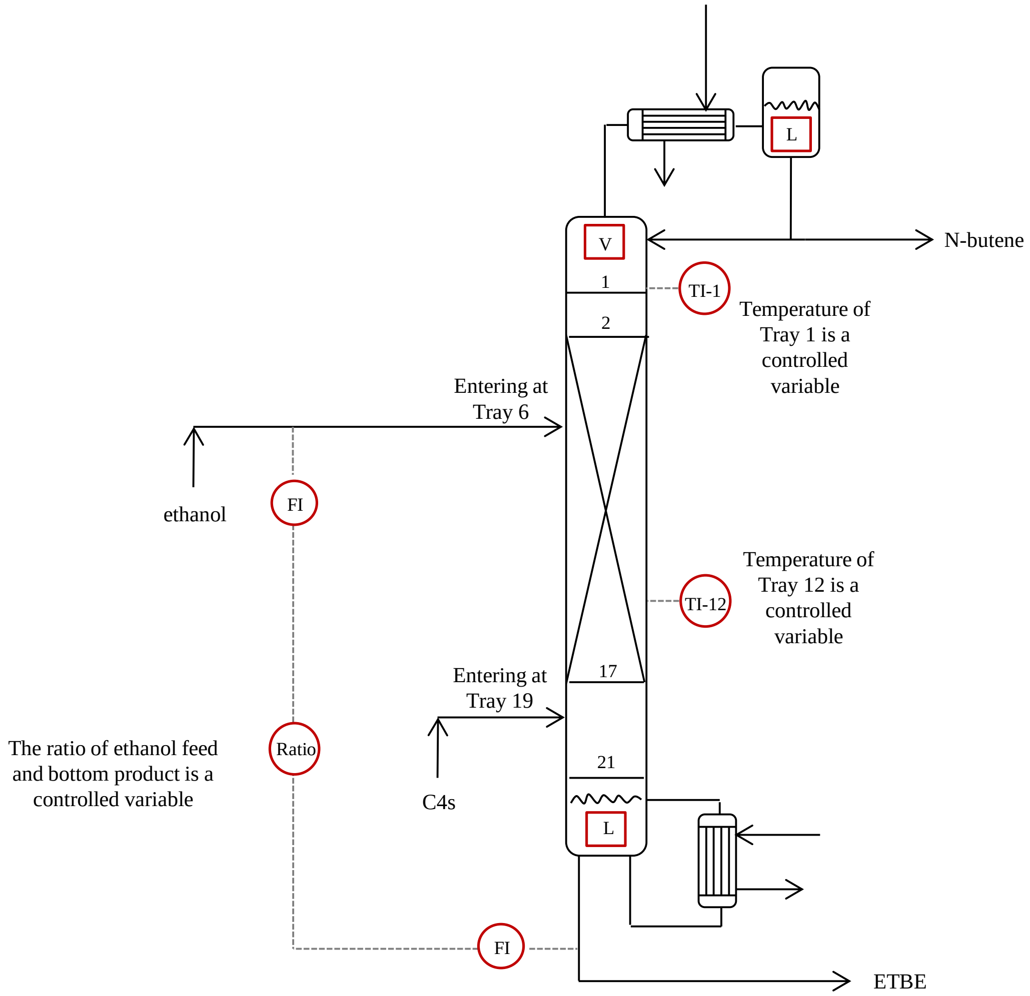

Figure 5.4. Optimized process and control structures of the ETBE reactive distillation column

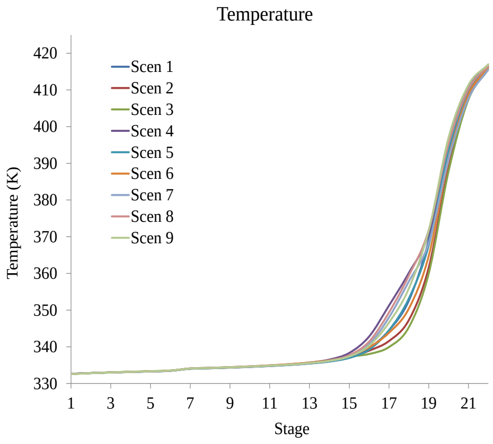

Figure 5.5a. Temperature profiles of the ETBE reactive distillation column for nine disturbance scenarios. This figure is the result of the proposed integrated design and control.

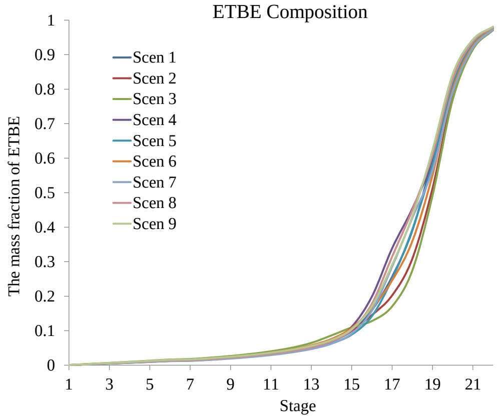

Figure 5.5b. ETBE composition profiles of the ETBE reactive distillation column for nine disturbance scenarios. This figure is the result of the proposed integrated design and control.

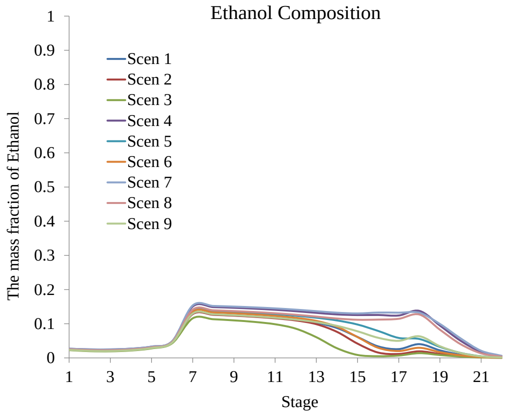

Figure 5.5c. Ethanol composition profiles of the ETBE reactive distillation column for nine disturbance scenarios. This figure is the result of the proposed integrated design and control.

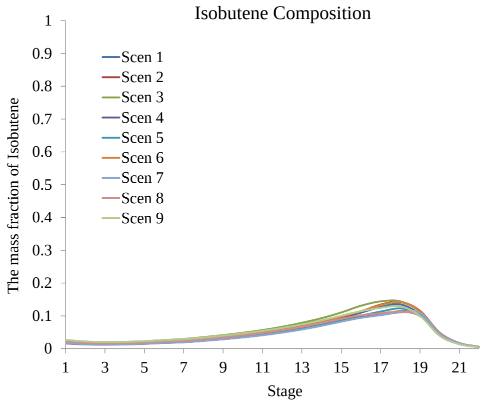

Figure 5.5d. Isobutene composition profiles of the ETBE reactive distillation column for nine disturbance scenarios. This figure is the result of the proposed integrated design and control.

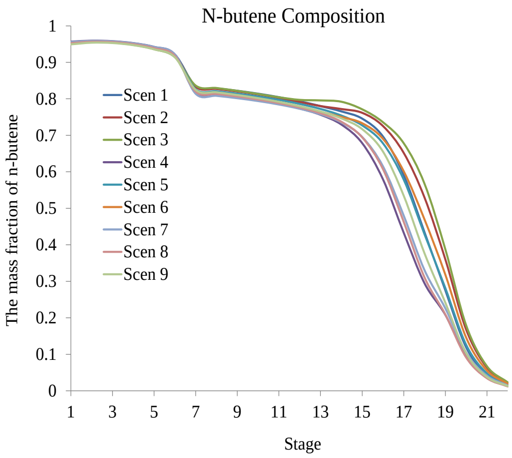

Figure 5.5e. N-butene composition profiles of the ETBE reactive distillation column for nine disturbance scenarios. This figure is the result of the proposed integrated design and control.

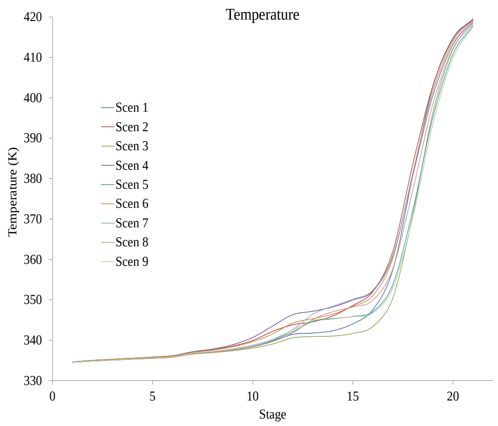

Figure 5.6a. Temperature profiles of the ETBE reactive distillation column for nine disturbance scenarios. This figure is the result of TAP maximization.

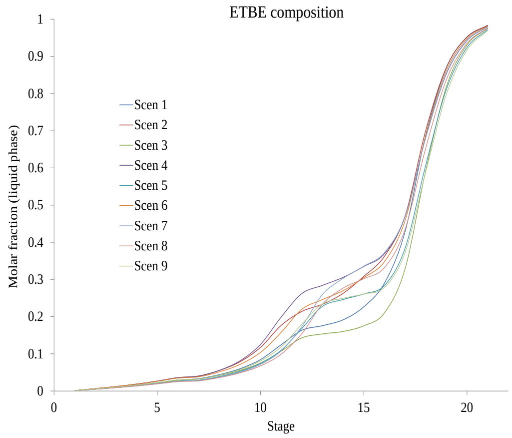

Figure 5.6b. ETBE composition profiles of the ETBE reactive distillation column for nine disturbance scenarios. This figure is the result of TAP maximization.

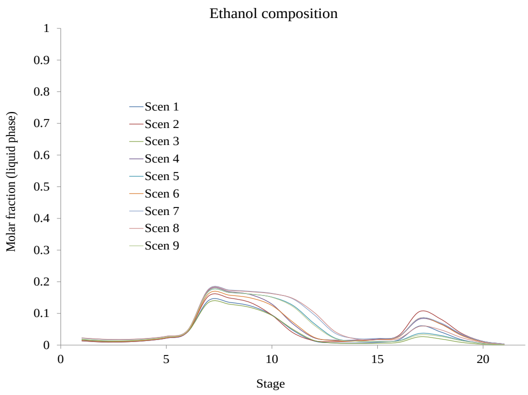

Figure 5.6c. Ethanol composition profiles of the ETBE reactive distillation column for nine disturbance scenarios. This figure is the result of TAP maximization.

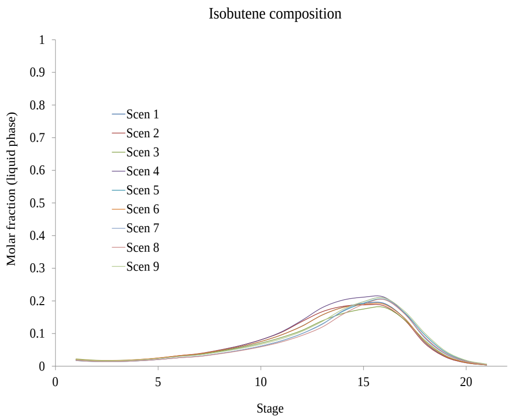

Figure 5.6d. Isobutene composition profiles of the ETBE reactive distillation column for nine disturbance scenarios. This figure is the result of TAP maximization.

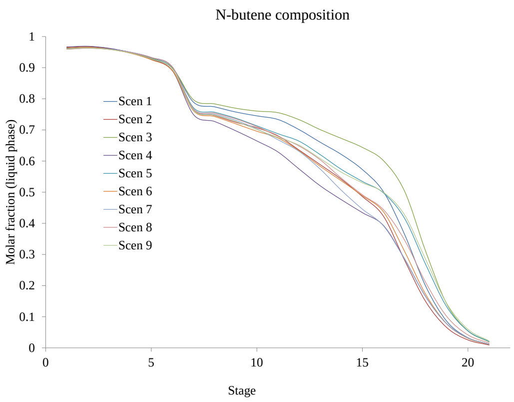

Figure 5.6e. N-butene composition profiles of the ETBE reactive distillation column for nine disturbance scenarios. This figure is the result of TAP maximization.

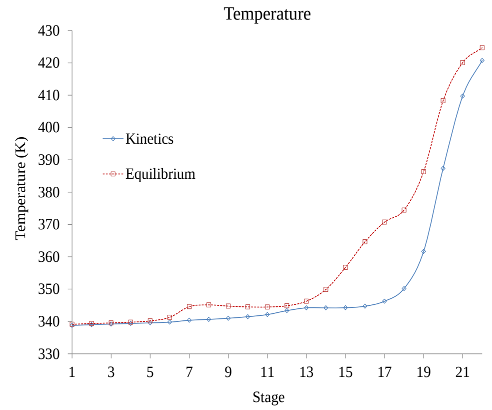

Figure 5.7a. The temperature profiles calculated based on the kinetic correlations (blue circles) and the equilibrium reaction assumption (red squares).

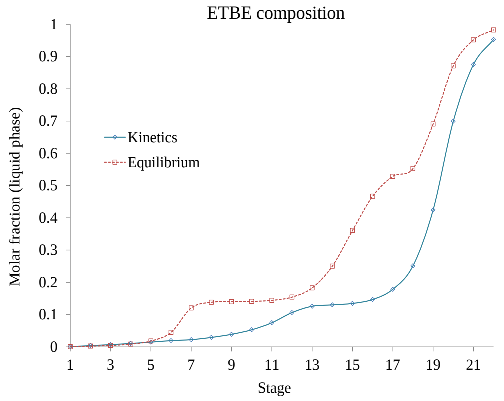

Figure 5.7b. The composition profiles of ETBE calculated based on the kinetic correlations (blue circles) and the equilibrium reaction assumption (red squares).

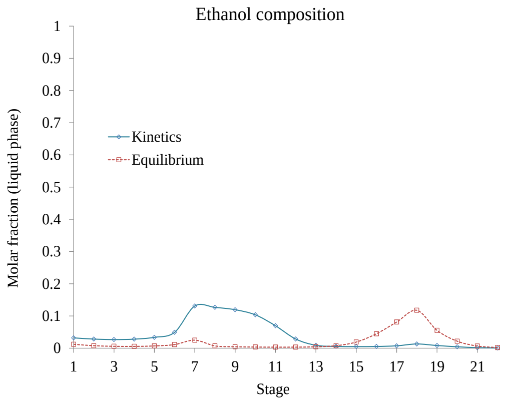

Figure 5.7c. The composition profiles of ethanol calculated based on the kinetic correlations (blue circles) and the equilibrium reaction assumption (red squares).

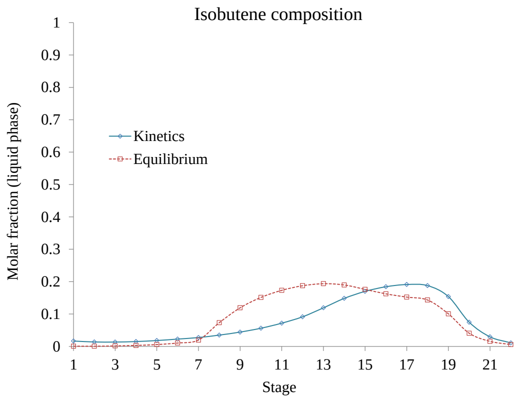

Figure 5.7d. The composition profiles of isobutene calculated based on the kinetic correlations (blue circles) and the equilibrium reaction assumption (red squares).

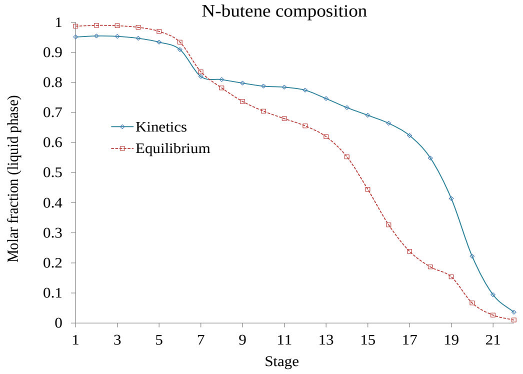

Figure 5.7e. The composition profiles of n-butene calculated based on the kinetic correlations (blue circles) and the equilibrium reaction assumption (red squares).

5.9. Discussions

This section presents the discussions of the optimization results and the comparisons between two modelling approaches based on the kinetic correlations and the assumption of chemical equilibrium.

5.9.1. Discussion of the optimization results

Table 5.6 reported the optimal values of the objective functions. It illustrates that a good trade-off is established between the different objective functions. The optimized process and its control structure were successful in maintaining the purity of the products while the economic losses are minimized. In addition, the changes in the manipulated variables are suppressed. Although the value of 13.5% is reported for the variations of the internal states, as shown in Figure 5.5c, most of these variations are related to ethanol and are limited to the area of C4s feed entrance where disturbances were imposed to the column. The rest of the process remains controlled tightly.

Figure 5.4 presented the optimized process and control structural variables. In a double-feed reactive distillation, the common practice is to feed the heavy (i.e., ethanol) and the light reactants (i.e., isobutene) above and below the reactive section respectively (e.g., Figure 5.1). Then, as the heavy reactant travels to the bottom and the light reactant travels to the top, they react and are converted to the product. However, in the optimized process, the optimizer chose to expand the reactive section and to feed the heavy reactant in the middle of the reactive section. Therefore, the reactive trays above the light feed entrance are responsible for both separation and reaction and these two phenomena are highly integrated. In addition, the optimizer chose to feed the C4s in the stripping section. This decision has a stripping effect in that the light components (isobutene and n-butene) carry the heavy unreacted component (ethanol) back to the reactive section. As shown in Table 5.7, the optimizer also chose high reflux ratios. This decision implies increasing the liquid hold-ups in the overhead and bottom accumulators and on the trays. Therefore, the optimized reactive distillation column is insensitive to disturbances.

The structural control decisions are to select (1) the temperature of the first tray, (2) the temperature of the twelve tray and (3) the ratio of the ethanol feed to the ETBE product as the controlled variables. The first two controlled variables are responsible for the quality of the ETBE and C4s products. Figures 5.5b, c, d and e show that the control structure was successful in tightly controlling the compositions of the components. However, in addition to quality control, a controlled variable should ensure that the ethanol and the C4s feed are supplied according to the reaction stoichiometry (equation 5-3). For this requirement, Luyben and Yu, (2008) suggested a cascade control structure in which the ratio of the two feeds was controlled and a composition analyser calculates the setpoint of this ratio controller. In the present study, the optimizer chose an alternative control structure which does not need a composition analyser. In the optimized control structure, the ratio of the mass flowrates of the ethanol feed to the ETBE product is controlled. This structure is consistent with the stoichiometry, because in order to produce one kmol of the ETBE product, one kmol of the ethanol feed should be consumed. Therefore, for a desired purity of the ETBE product the ratio of the mass flowrates of the ethanol feed and the ETBE product remains almost constant.

5.9.2. Discussion of Total Annual Profit (TAP) maximization

The aim of TAP maximization was to estimate the target of the fourth objective function in Table 5.1, which is economic. However, it is interesting to compare the result of this optimization with the result of the proposed integrated design and control framework.

A comparison between Table 5.8 and 5.7 suggest that the main difference between the two design is that the result of the proposed integrated design and control framework has one more reactive tray and the feed entry is three trays lower. In the solution of integrated design and control, higher reflux ratios are applied to increase the holdup of the materials and make the process less sensitive to the disturbances. In addition, the comparisons between the compositions and temperature profiles of the two solutions (Figures 5.5 and 5.6) suggest that the integrated design and control was more successful in regulating the compositions and the temperature of the internal trays. This should be attributed to the third objective in Table 5.1. Furthermore, as shown in Table 5.6, the result of the proposed optimization framework varies the manipulated variables 29% less than the solution of TAP maximization. This suggests that the excessive variations of the manipulated variables can be constrained without compromising the control quality.

5.9.3. The results for the comparisons between modelling approaches based on the kinetic correlations and the assumption of chemical equilibrium

Figures 5.6a- e provide the opportunity for the comparisons between modelling based on the kinetic correlations and modelling based on the assumption of chemical equilibrium. It is expected that the overall conversion will be higher for the chemical equilibrium assumption, because in this case it is assumed that the residence times are large enough that the reaction conversions are maximized.

Figures 5.6b to e show that, for the same operating conditions, the purity of the products at the column ends are about 3% higher for the model based on chemical equilibrium. Since the reaction is exothermic and the model based on chemical equilibrium predicts higher conversions, the temperature profile of this model is also higher than the temperature profile of the model based on the kinetic correlations, as shown in Figure 5.6a. These observations suggest that simplifying the reaction model by assuming chemical equilibrium may result in too optimistic design decisions.

5.10. Conclusion

This chapter demonstrated the application of the proposed integrated design and control framework using a steady-state inversely controlled process model. This framework contributes to the aim of complexity reduction by removing controller design from the problem. Moreover, it ensures that the solution features steady-state operability. A multi-objective function based on goal programming is applied to establish the trade-off between process and control objectives.

The proposed optimization framework was demonstrated for the case of an ETBE reactive distillation column. The instances of the process and control objectives for this case study were explained and their target values were justified. The optimization constraints regarding first principles modelling, disturbances and perfect control equations were explained and the insights about the reaction stoichiometry were applied in order to improve the convergence of the simulator solver. The implementation software tools were also explained.

The results demonstrated that the proposed optimization framework was able to establish a trade-off between the process and control objectives. The optimized solution addressed the disturbances efficiently while the economic losses were minimized.

6 | Integrated design and control using a dynamic inversely controlled process model

6.1. Introduction

Ignoring the interactions between process design and process control may result in economic penalties as well as safety and environmental concerns. Therefore, it is recommended that design and control should be integrated.

In Chapter 1, it was discussed that integrated design and control benefits, if controller design is separated from the problem formulation. With the aim of complexity reduction and based on the perfect control assumption, several optimization frameworks were developed in Chapter 3. In these frameworks, the combined controller-process model was replaced by an inversely controlled process model. The steady-state versions of the new optimization framework were applied in Chapters 4 and 5. The present chapter extends the steady-state methods of the last two chapters by applying a *dynamic* inversely controlled process model. In applying a steady-state inversely controlled process model, it was assumed that control is instantaneous and therefore, the effects of transient conditions were not considered. While a steady-state inversely controlled process model only ensures steady-state operability, more information can be gained as the proposed dynamic framework also ensures functional controllability.

The problem statement and mathematical formulations of the proposed framework using a dynamic inversely controlled process model were presented in Chapters 1 and 3. In the subsequent sections, firstly, a multi-objective function is formulated. Then, the proposed optimization framework for integrated design and control is demonstrated for two heat-integrated series reactors. The mathematical formulation of the original case study is presented and modified in order to construct the corresponding dynamic inversely controlled process model. Two solution strategies are applied for the optimization. They are dynamic optimization based on sequential integration and dynamic optimization base on full discretization. While the first solution strategy is more appropriate for problems with a small number of integer variables, in the second solution strategy, time-dependent variables are discretized and the problem formulation is translated into a mixed integer nonlinear formulation. Finally, the results are presented and discussed.

6.2. Multi-objective function and weighting factors

As suggested by other researchers (Luyben 2004; Alhammadi and Romagnoli 2004), the problem of integrated design and control involves competing and conflicting objectives. The concept of multi-criteria decision–making was discussed in Chapter 2. It was explained that the solutions of multi-objective optimization form a Pareto front which can be constructed by assigning weights, w'_i , to different objectives, as follows:

$$J_s(\,) = w'_1 \text{Process Objectives}_s(\,) + w'_2 \text{Control Objectives}_s(\,) \qquad (6-1)$$

where J_s is the aggregated objective value for disturbance s . In addition, $\text{Process Objectives}\,(\,)$ and $\text{Control Objectives}\,(\,)$ are the measures of the fitness of process and control designs respectively. Instances of these measures are given later in this chapter. In this research, it is assumed that the expected disturbance scenarios are known in advance and the stochastic optimization Problem 2.dyn is addressed as multi-period optimization. The value of the objective function is constructed by adding individual objective functions for different disturbance scenarios weighted by the likelihood of each disturbance scenario, (Sahinidis 2004).

$$E\{J_s(\,)\} = \sum_{s=1}^{n_s} L_s\, J_s(\,) \qquad (6-2)$$

where $E\{\,\}$ represents the expected value of the objective function $J_s(\,)$ and L_s is the likelihood of the disturbance scenario s.

6.3. Solution strategies for dynamic optimization

The solution strategies for dynamic optimization were reviewed in Chapter 2. This section applies two parallel solution strategies to address Problem 2.dyn. The first solution strategy is based on sequential integration. This strategy is the classic method for dynamic optimization and is appropriate for problems with a small number of integer variables. The second solution strategy is based on full discretization of time-dependent variables. In this approach, the problem is transformed to mixed integer nonlinear optimization.

6.3.1. Dynamic optimization based on the sequential integration strategy

Sequential integration is the classic strategy for dynamic optimization. If the sequential integration strategy is applied to the conventional integrated design and control framework (Problem 1), then input variables, $\boldsymbol{u}(t)$, are discretized by the parameters that determine the optimal time trajectories. However in the proposed optimization framework, due to process model inversion, the controlled variables, $\boldsymbol{y}(t)$, (outputs of the conventional problem) are discretized instead based on the desired setpoints, i.e., $\boldsymbol{y}_{i,setpoint}$. Similarly, if a manipulated variable, $\boldsymbol{u}(t)$, is not selected, this variable is discretized using its nominal value, $\boldsymbol{u}_{j,nominal}$. By these discretizations, Problem 2.dyn can be represented as the following nonlinear dynamic optimization problem:

$$\min \sum_{s=1}^{n_s} L_s J_s\left(\boldsymbol{Y}_{\boldsymbol{p}}, \boldsymbol{Y}_{\boldsymbol{cv},}, \boldsymbol{Y}_{\boldsymbol{mv}}, \boldsymbol{p}, \boldsymbol{y}_{\boldsymbol{i,setpoint}}, \boldsymbol{u}_{\boldsymbol{j,nominal}}\right) \qquad \text{Problem 2. dyn. si}$$

subject to:

$$\boldsymbol{f}[\dot{\boldsymbol{z}}(t), \boldsymbol{z}(t), \boldsymbol{x}(t), \boldsymbol{u}(t), \boldsymbol{y}(t), \boldsymbol{Y}_{\boldsymbol{p}}, \boldsymbol{p}, \boldsymbol{\mu}(t)] = 0$$

$$\boldsymbol{h}[\boldsymbol{z}(t), \boldsymbol{x}(t), \boldsymbol{u}(t), \boldsymbol{y}(t), \boldsymbol{Y}_{\boldsymbol{p}}, \boldsymbol{p}, \boldsymbol{\mu}(t)] = 0$$

$$\boldsymbol{g}[\boldsymbol{z}(t), \boldsymbol{x}(t), \boldsymbol{u}(t), \boldsymbol{y}(t), \boldsymbol{Y}_{\boldsymbol{p}}, \boldsymbol{p}, \boldsymbol{\mu}(t)] \leq 0$$

$$\Omega_s[\boldsymbol{\mu}(t)] = 0$$

$$\boldsymbol{Y}_{\boldsymbol{cv,i}}\left(\boldsymbol{y}_{\boldsymbol{i}}(t) - \boldsymbol{y}_{\boldsymbol{i,setpoint}}\right) = 0$$

$$(\boldsymbol{1} - \boldsymbol{Y}_{\boldsymbol{mv,j}})\left(\boldsymbol{u}_{\boldsymbol{j}}(t) - \boldsymbol{u}_{\boldsymbol{j,nominal}}\right) = 0$$

$$\boldsymbol{\Psi}(\boldsymbol{Y}_{\boldsymbol{cv,i}}, \boldsymbol{Y}_{\boldsymbol{mv,j}}) \geq 0$$

The notation Problem 2.dyn.si refers to the dynamic formulation of the proposed integrated design and control using the sequential integration strategy. In Problem 2.dyn.si, the optimization variables (i.e., the arguments of the objective function) are all time-independent. The structural variables ($\boldsymbol{Y_p}$, $\boldsymbol{Y_{cv,i}}$, $\boldsymbol{Y_{mv,j}}$) are enumerated and the corresponding continuous optimization subproblems are solved by a nonlinear optimization solver in the outer loop and a differential algebraic equation (DAE) solver in the inner loop.

Without loss of generality, it is assumed that Problem 2.dyn.si represents an index-1 DAE system (if not, then index reduction should be performed). The consistent initial conditions of this problem are calculated by solving the following set of algebraic equations which effectively represents the equivalent steady-state inversely controlled process model:

$$\boldsymbol{f}\left[\dot{\boldsymbol{z}}(t_0), \boldsymbol{z}(t_0), \boldsymbol{x}(t_0), \boldsymbol{u}(t_0), \boldsymbol{y}(t_0), \boldsymbol{Y_p}, \boldsymbol{p}, \boldsymbol{\mu}(t_0)\right] = 0 \qquad \text{Initialization Subproblem}$$

$$\boldsymbol{h}[\boldsymbol{z}(t_0), \boldsymbol{x}(t_0), \boldsymbol{u}(t_0), \boldsymbol{y}(t_0), \boldsymbol{Y_p}, \boldsymbol{p}, \boldsymbol{\mu}(t_0)] = 0$$

$$\boldsymbol{g}[\boldsymbol{z}(t_0), \boldsymbol{x}(t_0), \boldsymbol{u}(t_0), \boldsymbol{y}(t_0), \boldsymbol{Y_p}, \boldsymbol{p}, \boldsymbol{\mu}(t_0)] \leq 0$$

$$\Omega_{\boldsymbol{s}}[\boldsymbol{\mu}(t_0)] = 0$$

$$\boldsymbol{Y_{cv,i}}\left(\boldsymbol{y_i}(t_0) - \boldsymbol{y_{i,setpoint}}\right) = 0$$

$$(\boldsymbol{1} - \boldsymbol{Y_{mv,j}})\left(\boldsymbol{u_j}(t_0) - \boldsymbol{u_{j,nominal}}\right) = 0$$

$$\boldsymbol{\Psi}\left(\boldsymbol{Y_{cv,i}}, \boldsymbol{Y_{mv,j}}\right) \geq 0$$

$$\dot{\boldsymbol{z}}(t_0) = 0$$

The last equation ensures that the initial state is steady. These equations are shown in the left-hand block in the bottom of Figure 6.1 and are explained in the following.

The concept is shown in Figure 6.1. In the sequential integration strategy, an embedded DAE solver provides objective function information to a nonlinear optimization solver. The integration of the DAE system must be initialized from a feasible steady-state condition. A steady-state inversely controlled process model (the lower left envelope in Figure 6.1) is used to determine the initial steady state for each disturbance scenario. The details of a steady-state inversely controlled process model were discussed in Chapter 3. If no feasible steady state can be found, the algebraic equation (AE) solver reports a failure to the nonlinear optimization algorithm in order to change the values of the optimization variables, either by reducing the step size or by adding an incremental random number to the current solution. The implication is that if the initial and/or final steady-states are not feasible for a trial solution, it is inevitably functionally uncontrollable, and need not to be considered for further evaluations.

The steps in each optimization iteration are as follows:

Step 1. The nonlinear optimization algorithm specifies the values of the optimization variables.

Step 2. The initial steady state is calculated by the algebraic equation solver (AE) using the steady-state inversely controlled process model. If the initial steady state is not feasible, return to Step 1.

Step 3. The values of the initial steady state and optimization variables are delivered to the dynamic inversely controlled process model. The disturbances are imposed and the sequential integration gives the time trajectories for the manipulated variables and the remaining state variables. The values of the objective functions are calculated and reported to the optimizer.

Step 4. Based on the values of the objective function and the violations of the constraints, the optimization algorithm makes decisions regarding termination of the optimization cycle or improving the values of the optimization variables.

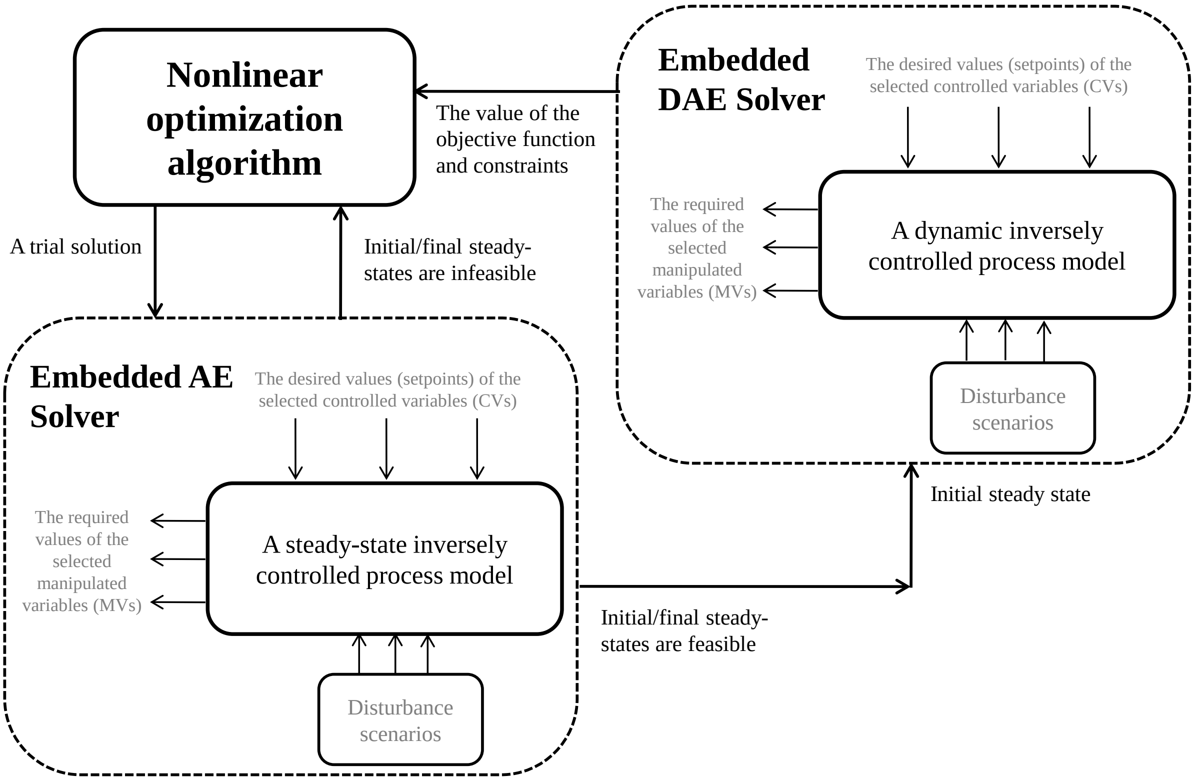

Figure 6.1. The sequential solution strategy for integrated design and control framework.

6.3.2. Dynamic optimization based on the full discretization strategy

The second solution strategy is based on full discretization using the Radau collocation method. In the full discretization strategy, the time horizon is divided into N_T finite elements. The time-dependent differential and algebraic variables are discretized and the DAE system is solved at the collocation points. The continuity of the time trajectories across the element boundaries are enforced by introducing continuity equations. After full discretization, the mixed integer (nonlinear) dynamic optimization (MIDO) problem is transformed into a large mixed integer nonlinear programming (MINLP) problem. The Details of the full discretization strategy can be found in (Biegler 2010). The discretized version of Problem 2.dyn is as follows:

$$\min \sum_{s=1}^{n_s} L_s\, J_s\left(\boldsymbol{z_{ij}}, \boldsymbol{x_{ij}}, \boldsymbol{u_{ij}}, \boldsymbol{y_{ij}}, \boldsymbol{\mu_{ij,s}}, \boldsymbol{Y_p}, \boldsymbol{Y_{cv}}, \boldsymbol{Y_{mv}}, \boldsymbol{p}, \boldsymbol{y_{i,setpoint}}, \boldsymbol{u_{nominal}}\right) \quad \text{Problem 2.dyn.fd}$$

Subject to:

$$\boldsymbol{f}[\boldsymbol{z_{ij}}, \boldsymbol{x_{ij}}, \boldsymbol{u_{ij}}, \boldsymbol{y_{ij}}, \boldsymbol{Y_p}, \boldsymbol{p}, \boldsymbol{\mu_{ij}}] = 0$$

$$\boldsymbol{h}[\boldsymbol{z_{ij}}, \boldsymbol{x_{ij}}, \boldsymbol{u_{ij}}, \boldsymbol{y_{ij}}, \boldsymbol{Y_p}, \boldsymbol{p}, \boldsymbol{\mu_{ij}}] = 0$$

$$\boldsymbol{g}[\boldsymbol{z_{ij}}, \boldsymbol{x_{ij}}, \boldsymbol{u_{ij}}, \boldsymbol{y_{ij}}, \boldsymbol{Y_p}, \boldsymbol{p}, \boldsymbol{\mu_{ij}}] \le 0$$

$$\Omega_s[\boldsymbol{\mu_{ij}}] = 0$$

$$\boldsymbol{Y_{cv,i}}\left(\boldsymbol{y_{ij}} - \boldsymbol{y_{setpoint}}\right) = 0$$

$$(\boldsymbol{1} - \boldsymbol{Y_{mv,j}})\left(\boldsymbol{u_{ij}} - \boldsymbol{u_{nominal}}\right) = 0$$

$$\boldsymbol{\Psi}(\boldsymbol{Y_{cv,i}}, \boldsymbol{Y_{mv,j}}) \ge 0$$

where $\boldsymbol{z_{ij}}, \boldsymbol{x_{ij}}, \boldsymbol{u_{ij}}, \boldsymbol{y_{ij}}$ and $\boldsymbol{\mu_{ij}}$ are the collocation optimization variables. The notation Problem 2.dyn.fd refers to the dynamic formulation of the proposed integrated design and control framework based on the full discretization strategy. The other notations are similar to Problem 2.dyn and were explained in Chapter 3. In Problem 2.dyn.fd, the optimizer estimates the time trajectories of the time-dependent variables, by determining the optimal values of the collocation variables. In this solution strategy, the continuity equations in addition to the differential and algebraic equations at the initial steady state ensure consistent initialization of the integrated design and control framework. The model inversion is performed by including perfect control equations in the optimization constraints.

Table 6.1 compares the two solution strategies and summarizes the discussions. The sequential integration solution strategy is based on enumeration of the structural variables and is limited to the cases in which the number of alternative structural decisions is small. For instance, it was efficiently applied to the case study of Section 6.4, in which there are only three binary variables (eight alternative structures). However, full discretization solution strategy is significantly more powerful when the number of alternative structural decisions is large or the problem needs to be solved several times (e.g., for constructing a Pareto front). In this chapter, the full discretization strategy was applied to study the trade-off between different competing objectives in the multi-objective function (6-23).

Table 6.1.

Comparison of the characteristics of two solution strategies for dynamic optimization.

Solution strategy	Sequential integration	Full discretization
Intermediate optimization path	Feasible	Infeasible
Optimization variables	Structural and parametric process variables, structural control variables, the nominal values of the manipulated variables which are not selected and the setpoints of controlled variables	Structural and parametric process variables, structural control variables, the setpoints of controlled variables, the nominal values of the manipulated variables which are not selected and the collocation variables
Number of optimization variables	small	large
Optimization algorithm	Each structure is enumerated as an NLP problem. The DAE solver provides the values of the objective function and constraint violations to the NLP optimizer	The dynamic optimization problem is discretized and translated to a large-scale MINLP problem.
Method for model inversion	Discretization of output (controlled) variables rather than input (manipulated) variables	Adding perfect control constraints to the problem formulation
Initialization method	Initial states are calculated using a steady-state inversely controlled process model.	Continuity equations at initial points ensure consistent initialization

6.4. Case study for the conventional integrated design and control optimization framework

Flores-Tlacuahuac and Biegler (2007) studied integrated design and control of two series reactors. The alternative process structures for these series reactors are shown in Figures 6.2a and b. The cooling media may flow in either co-current or counter-current configurations. Their study is an example of the conventional optimization framework for integrated design and control in which a combined process-controller model is optimized. The mathematical formulation of their study is presented in this section. In the next section, this mathematical formulation will be modified and adapted to the new optimization framework using a dynamic inversely controlled process model. In this chapter, any mention of *the original case study* refers to the work of Flores-Tlacuahuac and Biegler (2007).

Figure 6.2a Figure 6.2b

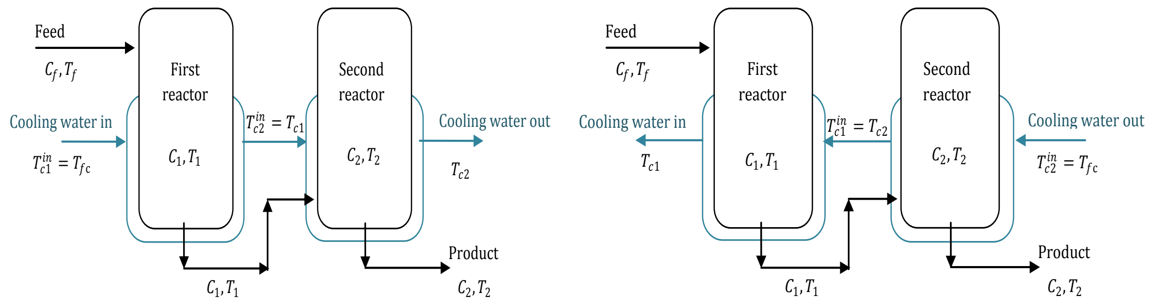

Figures 6.2. Different process structures: a) co-current heat exchange b) counter-current heat exchange.

The process model of the two series reactors is presented by equations (6-3) to (6-12). The model of the controllers is presented by equations (6-13) to (6-16). The definitions of the variables and their values at the base-case design are reported in Table 6.2, from (Flores-Tlacuahuac and Biegler 2007). The mass and energy balances for the first reactor are:

$$\frac{dC_1}{dt} = \frac{C_f - C_1}{\theta_1} + r_{A1} \qquad (6-3)$$

$$\frac{dT_1}{dt} = \frac{T_f - T_1}{\theta_1} + \beta r_{A1} - \alpha_1 (T_1 - T_{c1}) \qquad (6-4)$$

The energy balance for the cooling jacket of the first reactor is:

$$\frac{dT_{c1}}{dt} = \frac{T_{C1}^{in} - T_{C1}}{\theta_{c1}} + \alpha_{c1} (T_1 - T_{c1}) \qquad (6-5)$$

The mass and energy balances for the second reactor are:

$$\frac{dC_2}{dt} = \frac{C_1 - C_2}{\theta_2} + r_{A2} \qquad (6-6)$$

$$\frac{dT_2}{dt} = \frac{T_1 - T_2}{\theta_2} + \beta r_{A2} - \alpha_2 (T_2 - T_{c2}) \qquad (6-7)$$

The energy balance for the cooling jacket of the second reactor is:

$$\frac{dT_{c2}}{dt} = \frac{T_{c2}^{in} - T_{c2}}{\theta_{c2}} + \alpha_{c2}(T_2 - T_{c2}) \qquad (6-8)$$

The parameters in equations (6-3) to (6-8) are:

$$\theta_1 = \frac{V_1}{Q}, \quad \theta_2 = \frac{V_2}{Q}, \qquad \alpha_1 = \frac{UA_1}{\rho V_1 C_p}, \qquad \alpha_2 = \frac{UA_2}{\rho V_2 C_p}$$

$$\theta_{c1} = \frac{V_{c1}}{Q_c}, \quad \theta_{c2} = \frac{V_{c2}}{Q_c}, \qquad \alpha_{c1} = \frac{UA_1}{\rho_c V_{c1} C_{pc}}, \qquad \alpha_{c2} = \frac{UA_2}{\rho_c V_{c2} C_{pc}},$$

$$\beta = \frac{\Delta Hr}{\rho C_p}$$

The following kinetic correlations represent the reaction rates:

$$r_{A1} = -K_0 e^{-E/RT_1} C_1 \qquad (6-9)$$

$$r_{A2} = -K_0 e^{-E/RT_2} C_2 \qquad (6-10)$$

The decision regarding the process structure is represented by the binary variable Y_p in the equations (6-11) and (6-12):

$$T_{c1}^{in} = Y_p T_{fc} + (1 - Y_p) T_{c2} \qquad (6-11)$$

$$T_{c2}^{in} = Y_p T_{c1} + (1 - Y_p) T_{fc} \qquad (6-12)$$

$$\begin{cases} Y_p = 1 & co-current\ configuration \\ Y_p = 0 & countercurrent\ configuration \end{cases}$$

The equations for the controller model are:

$$T_f = T_{f,nominial} + (1 - Y_{mv})(K_P P(t) + K_i I(t)) \qquad (6-13)$$

$$Q_c = Q_{c,nominial} - Y_{mv}(K_P P(t) + K_i I(t)) \qquad (6-14)$$

$$P(t) = Y_{cv}(T_{1,setpoint} - T_1) + (1 - Y_{cv})(T_{2,setpoint} - T_2) \qquad (6-15)$$

$$\frac{dI(t)}{dt} = P(t), \qquad I(0) = 0 \qquad (6-16)$$

The controller equations will be replaced in the new optimization framework by perfect control equations in Section 6.5.2. The tuning parameters of the controller, K_P and K_i , are optimization variables in the conventional framework. Binary variable Y_{mv} selects between candidate manipulated variables, which are the flowrate of the cooling water, Q_c , or the temperature of the feed, T_f. Binary variable Y_{cv} selects between the candidate controlled variables, which are the temperature of the first reactor, T_1, or the temperature of the second reactor, T_2. In the original case study presented by Flores-Tlacuahuac and Biegler (2007), the following objective function based on an integral-square-error measure, was applied:

$$ISE = \min \frac{1}{t_{final}} \int_0^{t_{final}} \left(T_i - T_{i,setpiont}\right)^2 dt \quad , \qquad i\epsilon\{1,2\} \qquad (6-17)$$

where i is the index of the selected controlled variable.

Table 6.2
The parameters and the values of the variables at the base case scenario

Parameter	Description	Value*	Unit *	Value	SI Unit
Q	Volumetric feed flowrate	2.5	$L.s^{-1}$	2.5×10^{-3}	$m^3.s^{-1}$
T_f	Feed stream temperature	29	^oC	302	K
C_f	Feed Stream concentration	0.6	$mol.L^{-1}$	0.6	$kmol.m^{-3}$
V_1	Volume of the first reactor	900	L	0.9	m^3
V_2	Volume of the second reactor	900	L	0.9	m^3
Q_c	Cooling water flowrate	2	$L.s^{-1}$	2×10^{-3}	$m^3.s^{-1}$
T_{fc}	Cooling water feed stream temperature	25	^oC	298	K
V_{c1}	Volume of the cooling jacket of the first reactor	100	L	0.1	m^3
V_{c2}	Volume of the cooling jacket of the second reactor	100	L	0.1	m^3
E	Activation energy	10.1	$kcal.mol^{-1}$	4.2×10^7	$J.kmol^{-1}$
K_0	Pre-exponential factor	2000	s^{-1}	2000	s^{-1}
R	Ideal gas constant	0.00198	$kcal.mol^{-1}.K^{-1}$	8.32×10^3	$J.kmol^{-1}.K^{-1}$
ρ	Products density	850	$g.L^{-1}$	850	$kg.m^{-3}$
C_p	Product heat capacity	0.000135	$kcal.g^{-1}.C^{-1}$	564.84	$J.kg^{-1}.C^{-1}$
ΔH_r	Heat of reaction	-35	$kcal.mol^{-1}$	-1.46×10^8	$J.kmol^{-1}$
ρ_c	Cooling water density	1000	$g.L^{-1}$	1000	$kg.m^{-3}$
C_{pc}	Cooling water heat capacity	0.001	$kcal.g^{-1}.C^{-1}$	4.2×10^3	$J.kg^{-1}.K^{-1}$
A	Heat transfer area	900	cm^2	0.09	m^2
U	Heat transfer coefficient	0.00004	$kcal.s^{-1}.cm^{-2}.C^{-1}$	1.7×10^3	$J.s^{-1}.m^{-2}.K^{-1}$

* Values by Flores-Tlacuahuac and Biegler (2007).

6.5. Application of the proposed integrated design and control framework using a dynamic inversely controlled process model

This section applies the proposed integrated design and control framework to the case study. It gives some necessary extensions to the case study, and formulates the corresponding dynamic inversely controlled process model. Other topics include explaining feasibility constraints, a method for making comparison between the combined process-controller model and the inversely controlled process model, a discussion about the multi-objective function and explanation of the implementation software tools.

6.5.1. Amendments to the original case study

Flores-Tlacuahuac and Biegler (2007) considered a fixed value for the heat transfer area A_i , $i = 1,2$ of each cooling jacket. However, it is usual to scale the heat transfer area of a cooling jacket with reactor volume by:

$$A_i = \omega(V_i)^{2/3} \qquad (6-18)$$

Therefore, equation (6-18) is added to the original case study and its coefficient is calculated from the base-case design shown in Table 6.2, resulting in $\omega = 9.655$ $cm^2.L^{(-2/3)}$. The base case design requires a heat transfer area that is much smaller than the surface area of the reactor. Such a configuration would have to be realized in practice by a jacket that makes only partial contact with the reactor walls.

Flores-Tlacuahuac and Biegler (2007) suggested 50% and 200% of the base case design as the lower and upper bounds for the optimization values. The upper and lower bounds for the optimization variables in this research were 50% and 300%. The reason is that for some specific structures the heat transfer is thermodynamically limited by the maximum allowable temperature of the cooling water exiting the process, which is 80^{o}C. The bound on the optimization variables are shown in Table 6.3.

Table 6.3
The correspondence of the two solution strategies with case study formulation

Lower bound	Variable	Upper bound	Lower bound	Variable	Upper bound
0.900	V_1, V_2(m^3)	2.700	400	T_1, T_2 (K)	500
0.050	V_{c1}, V_{c2} (m^3)	0.300	298.15	T_f(K)	450
400	$T_{i,setpoint}$ (K)	500	298.15	$T_{c1}, T_{c2}, T_{c1}^{in}, T_{c2}^{in}$, (K)	380
0.55	C_f (kmol.m^{-3})	0.65	-0.01	r_{A1}, r_{A2} (kmol.s^{-1})	0
0	C_1, C_2 (kmol.m^{-3})	0.65	0	Q_c (m^3.s^{-1})	0.01

Flores-Tlacuahuac and Biegler (2007) assumed that the two series reactors and their cooling jackets are identical. This restrictive assumption is relaxed in the present study in order to provide extra degrees of freedom for integrated design and control.

Flores-Tlacuahuac and Biegler (2007) assumed the disturbance to be the feed composition. They evaluated several disturbances in the range $C_f = 0.55$ kmol.m^{-3} to $C_f = 0.65$ kmol.m^{-3} with different time constants. In this research a step disturbance from $C_f = 0.55$ kmol.m^{-3} to $C_f = 0.65$ kmol.m^{-3} is considered. This disturbance covers all the operational regions explored by the disturbances in the original case study (Flores-Tlacuahuac and Biegler 2007). However, due to nonlinearity of the process, the direction of the disturbance is also important. Therefore, another disturbance with the same magnitude but the reverse direction from $C_f = 0.65$ kmol.m^{-3} to $C_f = 0.55$ kmol.m^{-3} is also considered. It is assumed that these disturbances are equally likely.

6.5.2. Inversely controlled process model for the case of two series reactors

This section discusses replacement of the controller model with the perfect control equations and inverting the process model. Here, the perfect control equations (6-20) and (6-21) will replace the controller model equations (6-12) to (6-16) of the conventional integrated design and control framework.

The structural control decision regarding selection of the controlled variable is represented by the binary variable Y_{cv} as follows:

$$Y_{cv}T_1 + (1 - Y_{cv})T_2 = Y_{cv}T_{1,setpoint} + (1 - Y_{cv})T_{2,setpoint} \qquad (6-19)$$

$$\begin{cases} Y_{cv} = 1 & T_1 \ is\ selected\ as\ controlled\ variable \\ Y_{cv} = 0 & T_2 \ is\ selected\ as\ controlled\ variable \end{cases}$$

The structural control decision regarding selection of the manipulated variable is represented by the binary variable Y_{mv} as follows:

$$Y_{mv}T_f + (1 - Y_{mv})Q_c = Y_{mv}T_{f,nominial} + (1 - Y_{mv})Q_{c,nominial} \qquad (6-20)$$

$$\begin{cases} Y_{mv} = 1 & Q_c \ is\ selected\ as\ manipulated\ variable \\ Y_{mv} = 0 & T_f \ is\ selected\ as\ manipulated\ variable \end{cases}$$

These equations ensure that when a manipulated variable is not selected, it is left constant at its nominal value. However, the selected manipulated variable is free and its required value for disturbance rejection is calculated by the dynamic inversely controlled process model.

The author checked the index of the above DAE formulation of the dynamic inversely controlled process model, consisting of equations (6-3) to (6-12), (6-19), and (6-20), with Aspen Custom Modeller and it is 2. However as discussed by Pantelides (1988), consistent initialization of a DAE system requires the index of the DAE system to be one. In order to reduce the index of this DAE set, equation (6-19) is differentiated and replaced by:

$$Y_{cv}\frac{dT_1}{dt} + (1 - Y_{cv})\frac{dT_2}{dt} = 0 \qquad (6-21)$$

$$\begin{cases} T_1(t_{initial}) = T_{1,setpoint} \\ T_2(t_{initial}) = T_{2,setpoint} \end{cases}$$

$$\begin{cases} Y_{cv} = 1 & T_1 \ is\ selected\ as\ controlled\ variable \\ Y_{cv} = 0 & T_2 \ is\ selected\ as\ controlled\ variable \end{cases}$$

The author checked the index of the new formulation with Aspen Custom Modeller and it is one. Furthermore, in Chapter 3, the functional controllability conditions were discussed and it was explained that these conditions always hold for disturbance rejection in which setpoints are constant.

In conclusion, the mathematical formulation of the proposed optimization framework consists of equations (6-3) to (6-12), (6-20), and (6-21). Table 6.4 matches the case study formulation with the problem formulations 2.dyn.si and 2.dyn.fd.

Table 6.4

The correspondence of the two solution strategies with case study formulation

Solution strategy	Sequential integration	Full discretization
Enumeration variables	Y_p, Y_{cv}, Y_{mv}	none
Time-independent optimization variables	$V_1, V_2, V_{c1}, V_{c2}, T_{i,setpoint}$	Y_p, Y_{cv}, Y_{mv} , $V_1, V_2, V_{c1}, V_{c2}, T_{i,setpoint}$
Time-dependent optimization variables	DAE solver variables: C_1, C_2, C_f T_1, T_2, T_f, $T_{c1}, T_{c2}, T_{c1}^{in}, T_{c2}^{in}$, r_{A1}, r_{A2}, Q_c	Discretization variables: 1) differential collocation variables: $C_{1,ij}, C_{2,ij}, T_{1,ij}, T_{2,ij}, T_{c1,ij}, T_{c2,ij}$, 2) algebraic collocation variables: $C_{f,ij}, T_{f,ij}, T_{c1,ij}, T_{c2,ij}, T_{c1,ij}^{in}, T_{c2,ij}^{in}$, $r_{A1,ij}, r_{A2,ij}, Q_{c,ij}$
Differential constraints: $\boldsymbol{f}[]$	Equations (6-3) to (6-8)	Equations (6-3) to (6-8)
Algebraic constraints: $\boldsymbol{h}[]$	Equations (6-9) to (6-12), (6-20) and (6- 21)	Equations (6-9) to (6-12), (6-20) and (6- 21)

Note: The multi-objective function of the case study in the new framework is explained in Section 6.5.4.

6.5.3. Feasibility constraints

The concept of testing feasibility of initial and final steady states is illustrated in Figure 6.3 schematically. This graph shows the variations of a controlled variable (temperature of the second reactor) with the changes in a manipulated variable (cooling water flowrate) at different steady states. The lower profile represents the steady states before the disturbance occurrence ($C_f = 0.55$) and the upper profile represents the steady states after the disturbance occurrence ($C_f = 0.65$). For a given setpoint value, the length of the corresponding horizontal tie line (dashed line) represents the required change in the manipulated variable in order to maintain the controlled variable constant. A setpoint for the controlled variable is feasible if such a horizontal tie-line exists.

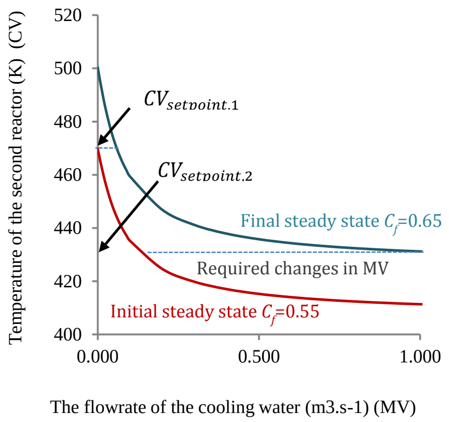

Figure 6.3. The variations of the controlled variable (T_2) with the manipulated variable (Q_c)

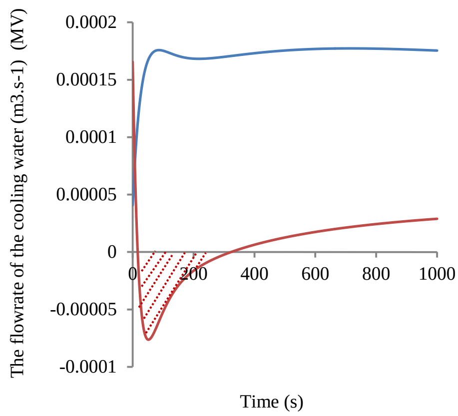

Figure 6.4. The time trajectories of the flowrate of the cooling water as the manipulated variable (Q_c) for two identical disturbances with reverse directions. The lower trajectory is infeasible.

The feasibility of initial and ultimate steady states does not ensure that the transient states are also feasible. Figure 6.4 shows the time trajectories of the cooling flowrate due to two step disturbances: (i) $C_f = 0.55$ kmol.m^{-3} to $C_f = 0.65$ kmol.m^{-3} and (ii) $C_f = 0.65$ kmol.m^{-3} to $C_f = 0.55$ kmol.m^{-3}. In this example, the volumes of the reactors were $V_i = 2.7$ m^3, and all other process variables are at their base-case values (Table 6.2). Figure 6.4 reveals that although the initial states and final states are feasible, the intermediate states can be infeasible, as shown by the shaded area. The physical reason is saturation of the control valve and the loss of control action. In this research, path constraints took care of such infeasibilities. Moreover, Figure 6.4 shows that due to the nonlinearities of the process model, two disturbances with opposite directions do not result in symmetrical time trajectories. This is the reason that another disturbance with the opposite direction is also considered in the case study.

6.5.4. Multi-objective function for integrated design and control of the two series reactors

In the original case study by Flores-Tlacuahuac and Biegler (2007), the objective function was equation (6-17). This objective function is not appropriate for the proposed integrated design and control framework for two reasons. Firstly, it does not include any term for process objectives (e.g., required capital investment). Therefore, this objective function contradicts with the aim of integrated design and control to establish a trade-off between control and process objectives. Secondly, minimizing the controller error (i.e., difference in the actual and desired values of the controlled variable) is not the concern of perfect control because due to satisfaction of perfect control equations, the integral of the square of controller errors (represented by ISE) is already equal to zero:

$$ISE = \min \frac{1}{t_{final}} \int_0^{t_{final}} \left(T_i - T_{i,setpiont}\right)^2 dt = 0 \ , \qquad i \in \{1,2\} \qquad (6-22)$$

where i is the index of the selected controlled variable. However, in the present case study, the temperature is being controlled to inferentially control the composition of the second reactor. The difference between the actual and desired compositions of the second reactor gives a rigorous measure of success of the inferential control strategy. This measure was included in the new multi-objective function, and is discussed in the following, along with other competing objectives. In this research, the following multi-objective function is considered in order to capture the trade-off between the involved control and process objectives:

$$\min \sum_{s=1,2} L_s \; J_s \qquad (6-23)$$

$$J_s(\mu_s) = w'_1 \text{ControlObjectives}_s + w'_2 \text{ProcessObjectives}_s$$

$$\text{ControlObjectives}_s = w_1 obj_{1,s} + w_2 obj_{2,s}$$

$$\text{ProcessObjectives}_s = w_3 obj_{3,s} + w_3 obj_{4,s}$$

$$obj_{1,s} = \int_{t0}^{tfinal} \left| C_2 - C_{2,desired} \right| dt, \qquad [obj_1] = \text{kmol.m}^{-3}.\text{s}$$

$$obj_{2,s} = \int_{t0}^{tfinal} \left(\frac{|MV - MV_{nominal}|}{MV_{nominal}} \right) dt, \qquad [obj_2] = \text{s}$$

$$obj_{3,s} = \sum_{i=1}^{2} V_i, \qquad [obj_3] = \text{m}^3$$

$$obj_{4,s} = \sum_{i=1}^{2} V_{c,i}, \qquad [obj_4] = \text{m}^3$$

where, s is the index for disturbance scenario. The terms of the multi-objective function (6-23) represent two different categories of the objectives for integrated design and control; the first category concerns the control objectives and the second category concerns the process objectives. In the first category, there are two control objectives. The first one, obj_1, measures the success in controlling the concentration of the second reactor inferentially by controlling the temperature of either the first or the second reactor. In the original case study, the aim of integrated design and control was to maximize the conversion. Therefore, $C_{2,desired}$ is set to be zero in this research to minimize the loss of the reactant. The weighting factor of the first objective, w_1, can be interpreted as the costs of the lost reactant over the simulation time. The second objective, obj_2, measures the costs of the control action. This variable is scaled by its nominal value because different manipulated variables may have different dimensions. The physical implication of this objective is that when the disturbances are imposed, maintaining the controlled variable at its setpoint should require minimum of the changes in the manipulated variable (Qin and Badgwell 2003; McAvoy 1999). The weighting factor of the second objective, w_2, can be interpreted as the cost of changing the manipulated variable over the simulation time. The third and the fourth objective functions obj_3 and obj_4 are the process objectives, and represent the required capital investment for purchasing the reactors and their cooling jackets. Their weighting factors have the dimension of cost per unit of volume.

Both categories of the process and control objectives have economic implications and their relative importance (i.e., w'_1/w'_2) depends on how frequently the process is subject to disturbance scenarios. If the process spends most of its time at relatively close steady states, the process objectives are dominant. However, if the process is prone to frequent and significant disturbances, the control objectives play a significant role in minimizing the losses associated with disturbances.

It is notable that the optimal values of the optimization variables depend on the ratios of the weighting factors which reflect the importance of the corresponding objectives. If all the weighting factors are multiplied by a constant positive value, the value of the multi-objective function will change but the optimal values of the optimization variables will remain unchanged. In the absence of any data for the case study, in order to explore the trade-off between the process and control objectives some simplifying assumptions are made and the weighting factors w_i are fixed and then the trade-off between the process and control objectives are explored by changing the ratio of w'_1 [-] and w'_2 [-].

In this research, $w_1 = 1$ kmol^{-1}.m^{3}.s^{-1} and $w_2 = 0.01$ s^{-1} give an estimate of the relative importance of the first and second control objectives. In addition, $w_3 = 1$ m^{-3} and $w_4 = 1.5$ m^{-3} suggest that the cooling jackets are 50% more expensive than the reactors, because they are more prone to thermal shocks, and have higher manufacturing costs due to their shape, size and hydraulic considerations. In order to explore the trade-off between the control objectives and the process objectives the ratio between their corresponding weighting factors, w'_1 and w'_2, are changed and optimization is performed for a variety of weighting factors $w'_1 \in \{1\}$, and $w'_2 \in \{10^{-6}, 10^{-3}, 3 \times 10^{-3}, 5 \times 10^{-3}, 10^{-2}\}$. These values correspond to a domain where the control objectives and the process objectives compete with each other. Outside this domain, one of the objectives is dominant, and there is no competition. The results of the multi-objective optimization are presented in Table 6.6. The Pareto front is constructed by plotting the competing process and control objectives against each other, and is shown in Figure 6.7. The physical implications of the trade-off between process and control objectives are discussed in Section 6.8.3.

The final time of the dynamic simulation, i.e., t_{final} in equation (6-23) can be included in the optimization variables, with the aim of minimizing the disturbance rejection time. In that case, additional constraints are needed to ensure that the final state of the system is steady ($^{d}/_{dt} = 0$). These constraints would add additional nonlinearity to the problem. In this research, the value of $t_{final} = 1000$ s was considered, which was large enough that most of intermediate solutions reached their final steady states. However, the integral terms in the objective function (6-23) encouraged minimization of the transition time between steady states and the effective time for the system to move from the initial steady state to the final steady state was significantly less than t_{final} as shown by the graphs in Results Section (i.e., Figure 6.5a-c). The choice of the number of time-intervals determines the precision of the simulation and was specified using pre-optimization analysis. The resolution of the time horizon for sequential integration was chosen using pre-optimization analyses. In these analyses, the resolution of the time horizon was reduced gradually, until the objective function become insensitive and only changes in the fourth decimal digit. Finer resolutions of the time horizon would increase computational expenses unreasonably. For sequential solution strategy, the integration step size was 10s. For the full discretization strategy, the length of the finite elements was 25sec. A Radau polynomial of order $K = 3$ was applied in this research. Since in full discretization strategy, the constraints are imposed at the collocation points, these choices imply that the constraints are satisfied about every 8sec. It was assumed that the disturbances have equal likelihood ($L_1 = L_2 = 0.5$). Both solution strategies were initialized from different starting points in order to avoid local minimums.

6.5.5. Post-optimization analysis: Designing actual controller

After integrated design and control of the case study using the proposed optimization framework, two sets of post-optimization analyses were performed. In these analyses, given the optimized process and its control structure, a PI controller was modelled and its tuning parameters were optimized. Such an optimization task has a significantly reduced size because the optimization variables only consist of continuous tuning parameters of the controller. The objective function of this optimization was equation (6-17) which concerns only the controller error.

In the first set of post-optimization studies, a PI controller is designed for the best solutions of the proposed framework (Structures 1, 2, 6 in Table 6.5). The aim was to investigate if including controllers would change the best structure.

In the second set of post-optimization studies, a PI controller is designed for the best solution of the proposed framework (Structures 6 in Table 6.5) against two disturbance scenarios corresponding to the fifth and sixth cases of the results of Flores-Tlacuahuac and Biegler (2007). In addition, similar bounds on the optimization variables were imposed (i.e., $0 < K_p < 500$ and $0 < K_i < 500$). The aim was to provide the opportunity to compare the results of the proposed optimization framework using the dynamic inversely controlled process model and the conventional optimization framework using the combined process-controller model.

The results of the abovementioned post-optimization studies are reported in Tables 6.8 and 6.9 and discussed in Discussions Section.

6.6. Implementation tools and considerations

As explained earlier, two solution strategies were implemented in this study. The first solution strategy was dynamic optimization based on sequential integration. The embedded algebraic equation (AE) solver and the embedded differential algebraic equation (DAE) solver in Figure 6.1 were both implemented in Aspen Custom Modeller (ACM®), which was invoked in the steady-state and dynamic modes respectively. The optimization algorithm was a nonlinear gradient-based solver which was coded in the Microsoft Excel VBA® environment. The two software tools were linked using Microsoft COM® automation interface. The required programming techniques can be found in the software documentation, (Aspen Custom Modeler documentation 2004). At each optimization iteration, the nonlinear optimization solver decided on the values of the optimization variables (V_1, V_{c1}, V_2, V_{c2}, and $T_{1,setpoint}$ or $T_{2,setpoint}$). These variables were exported to the AE solver which calculated the initial states required by DAE solver. Then, the DAE solver starts from the initial states and integrates through the time. The objective value for the current optimization variables was calculated from the results of the dynamic simulation and was reported to the nonlinear optimization solver in order to evaluate the termination criteria and to decide for improving the values of the optimization variables. The number of the optimization variables was five in addition to three enumeration variables. The simulation time of each optimization iteration was about 30 s and the execution time was in the order of hours for each enumeration. The sequential strategy was applied to the objective function (6-23) only for weighting factors $w'_1 = 1$, $w'_2 = 10^{-3}$ due to its long execution time.

The second solution strategy was a large MINLP optimization implemented in General Algebraic Modeling System (GAMS®). A comparison between different MINLP solvers is not the focus of this research but is presented by Flores-Tlacuahuac and Biegler (2007). In this research, the MINLP solvers were DICOPT and SBB (similar to Flores-Tlacuahuac and Biegler 2007). The total number of optimization variables for two disturbance scenarios was 7673 of which only three variables are binary and the rest are continuous. The bounds on the optimization variables were reported in Table 6.3. As discussed by Biegler (2010), the advantage of application of Radau polynomials is that the collocation variables can have the same bounds as the corresponding variables. The execution time depends on the starting point. The optimization algorithm was initialized from several different starting points to avoid local optimums. These starting points were the lower bounds, the upper bounds and the average of the lower and upper bounds of the optimization variables. As will be seen in Results Section, the optimal values of three optimization variables (i.e.,$V_{c1}, V_{c2}, T_{i,setpoint}$) are located at their bounds. The initializations from the opposite bounds often converged to a local solution or even did not converged at all. The execution time was less than one hour.

The execution time of the full discretization strategy was significantly lower compared to the sequential strategy for two reasons. Firstly, the optimization solver and dynamic model were implemented using the same program. Secondly, while the full discretization strategy traversed an infeasible optimization path, the sequential optimization strategy only examined feasible solutions. The execution time of full discretization provided the opportunity to examine the objective function (6-23) for a variety of weighting factors, w'_1 and w'_2, as shown in Table 6.6 and discussed in Section 6.8.3.

The post-optimization analyses (described in Section 6.5.5) were implemented using the built-in optimizer of gPROMS. There were only two optimization variables (i.e., the parameters of the PI controller) and the execution time was few minutes. The starting points were chosen from the upper bounds, lower bounds and the middle of the optimization bounds.

6.7. Results of the case study

This section presents the results. They are:

- Table 6.5 reports the enumeration results using the sequential integration strategy. Each column represents a specific process and control structure. All results are reported for the weighting factors $w'_1 = 1\,, w'_2 = 10^{-3}$ in the multi-objective function (6-23).
- Table 6.6 presents the results using the full discretization strategy with different combinations of weighting factors, w'_1 and w'_2, in the multi-objective function (6-23). This table provides the opportunity to explore the trade-off between the control objectives and the process objectives as will be explained in Discussion Section.
- Full discretization can also be used to enumerate different structures. The results of enumeration using this method is presented for a combination of weighting factors ($w'_1 = 1\,, w'_2 = 10^{-6}$) in Table 6.7.
- Table 6.8 reports the results of the first set of post-optimization studies. In this part of the analyses, a PI controller was designed for the best structures of Table 6.5.
- Table 6.9 reports the results of the second set of post-optimization studies. In this part of the analyses, a PI controller was designed for the best structure of Table 6.5 and its tuning parameters were optimized against the disturbance scenarios in the fifth and sixth cases studied by Flores-Tlacuahuac and Biegler (2007). The aim was to provide the opportunity for a comparison between the conventional framework and the proposed framework.
- Figures 6.5a-c are the time trajectories of the optimal solution, corresponding to structure 6 in Table 6.5.
- Figures 6.6a and b explain the uncontrollable structures in Table 6.5. These are the structures in which the flowrate of the cooling water was selected as the manipulated variable and the temperature of the first reactor was selected as the controlled variable.
- Figure 6.7 shows the Pareto front for the multi-objective function (6-23).
- Figure 6.8 shows the effects of the feed temperature on the product composition.

- Figures 6.9 are the time trajectories of the best solution in Table 6.8, regarding the first set of post-optimization studies.
- Figures 6.10 are the time trajectories of the best solutions in Table 6.9, regarding the second set of post-optimization studies.

Table 6.5.
The results of optimization for different process and control structures using the sequential integration strategy.

	Structure 1: Counter-current $T_2 - T_f$	Structure 2: Counter-current $T_1 - T_f$	Structure 3: Counter-current $T_2 - Q_c$	Structure 4: Counter-current $T_1 - Q_c$	Structure 5: Co-current $T_2 - T_f$	Structure 6: Co-current $T_1 - T_f$	Structure 7: Co-current $T_2 - Q_c$	Structure 8: Co-current $T_1 - Q_c$
Multi-objective value	3.9402	3.8650	-	-	5.3060	3.855	-	-
w'_1	1	1	1	1	1	1	1	1
w'_2	10^{-3}	10^{-3}	10^{-3}	10^{-3}	10^{-3}	10^{-3}	10^{-3}	10^{-3}
Constraints violation	No	No	Yes(2)	Yes(1)	No	No	Yes(2)	Yes(1)
Y_p	0	0	0	0	1	1	1	1
Y_{cv}	0	1	0	1	0	1	0	1
Y_{mv}	0	0	1	1	0	0	1	1
V_1 (m^3)	2.283	0.971	-	-	2.297	0.968	-	-
V_2 (m^3)	1.206	0.782	-	-	1.686	0.780	-	-
V_{c1} (m^3)	0.050	0.050	-	-	0.050	0.050	-	-
V_{c2} (m^3)	0.050	0.050	-	-	0.050	0.050	-	-
$CV_{setpoint}$ (K)	474.9	500	-	-	470.2	500	-	-

Y_p represents the structural decision for the process structure: $Y_p = 0$ counter-current and $Y_p = 1$ co-current. Y_{cv} represents the structural decision for controlled variable selection: $Y_{cv} = 0$, i.e., T_2 is CV and $Y_{cv} = 1$, i.e., T_1 is CV. Y_{mv} represents the structural decision for manipulated variable selection: $Y_{mv} = 0$, i.e., T_f is MV and $Y_{mv} = 1$, i.e., Q_c is MV. (1) Inversion of the process is not possible (See also Figures 6.6a and b.). (2) The maximum allowable temperature of the cooling water leaving the process is violated.

Table 6.6.
The results of optimization for different weighting factors (w'_1, w'_2) in the multi-objective function using the full discretization strategy.

	Structure: Co-current $T_1 - T_f$	Structure: Co-current $T_1 - T_f$	Structure: Co-current $T_1 - T_f$	Structure: Co-current $T_1 - T_f$	Structure: Co-current $T_1 - T_f$
Multi-objective value	1.0147	3.8553	6.8721	9.1727	14.4241
Control objectives	1.00915	1.9527	3.0588	3.8637	3.9241
Process objectives	5550	1902.6	1271.1	1061.8	1050
w'_1	1	1	1	1	1
w'_2	10^{-6}	10^{-3}	3×10^{-3}	5×10^{-3}	10^{-2}
Constraints violation	No	No	No	No	No
Y_p	1	1	1	1	1
Y_{cv}	1	1	1	1	1
Y_{mv}	0	0	0	0	0
V_1 (m^3)	2.700	0.970	0.571	0.450	0.450
V_2 (m^3)	2.700	0.783	0.551	0.462	0.450
V_{c1} (m^3)	0.050	0.050	0.050	0.050	0.050
V_{c2} (m^3)	0.050	0.050	0.050	0.050	0.050
$CV_{setpoint}$ (K)	500	500	500	500	500

Table 6.7.
The results of optimization for different process and control structures enumerated by full discretization strategy.

	Structure 1: Counter-current $T_2 - T_f$	Structure 2: Counter-current $T_1 - T_f$	Structure 3: Counter-current $T_2 - Q_c$	Structure 4: Counter-current $T_1 - Q_c$	Structure 5: Co-current $T_2 - T_f$	Structur 6: Co-current $T_1 - T_f$	Structure 7: Co-current $T_2 - Q_c$	Structure 8: Co-current $T_1 - Q_c$
Multi-objective value	1.0958	1.0251	-	-	1.0558	1.0147	-	-
w'_1	1	1	1	1	1	1	1	1
w'_2	10^{-6}	10^{-6}	10^{-6}	10^{-6}	10^{-6}	10^{-6}	10^{-6}	10^{-6}
Constraints violation	No	No	Yes(1)	Yes(1)	No	No	Yes(1)	Yes(1)
Y_p	0	0	0	0	1	1	1	1
Y_{cv}	0	1	0	1	0	1	0	1
Y_{mv}	0	0	1	1	0	0	1	1
V_1 (m^3)	2.700	2.700	-	-	2.694	2.700	-	-
V_2 (m^3)	2.700	2.700	-	-	2.700	2.700	-	-
V_{c1} (m^3)	0.050	0.050	-	-	0.050	0.050	-	-
V_{c2} (m^3)	0.050	0.050	-	-	0.050	0.050	-	-
$CV_{setpoint}$ (K)	458.086	500	-	-	461.421	500	-	-

(1) The optimization did not converge to a feasible solution

Table 6.8.
The results of the first set of post-optimization studies: designing a PI controller for the best structures of Table 6.5

Disturbance	Process and control structure	K_p	K_i	Objective function of Equation (6-17)
Described in Section 6.5.1	Structure 1 in Table 6.5	500	0	8.98×10^{-3}
Described in Section 6.5.1	Structure 2 in Table 6.5	500	500	2.6154×10^{-7}
Described in Section 6.5.1	Structure 6 in Table 6.5	500	500	2.6074×10^{-7}

Table 6.9.
The results of the second set of post-optimization studies: designing a PI controller for the best solution and comparison with the results of Flores-Tlacuahuac and Biegler (2007)

Disturbance	Process and control structure	K_p	K_i	Objective function of Equation (6-17)
Step function from C_f=0.6 to C_f=0.55	Structure 6 in Table 6.5	500	500	3.2489×10^{-8}
Step function from C_f=0.6 to C_f=0.55	Case 5 in Table 5 of (Flores-Tlacuahuac and Biegler 2007)	500	500	0.0009
Step function from C_f=0.6 to C_f=0.65	Structure 6 in Table 6.5	500	500	3.2491×10^{-8}
Step function from C_f=0.6 to C_f=0.65	Case 6 in Table 5 of (Flores-Tlacuahuac and Biegler 2007)	356	500	0.0025

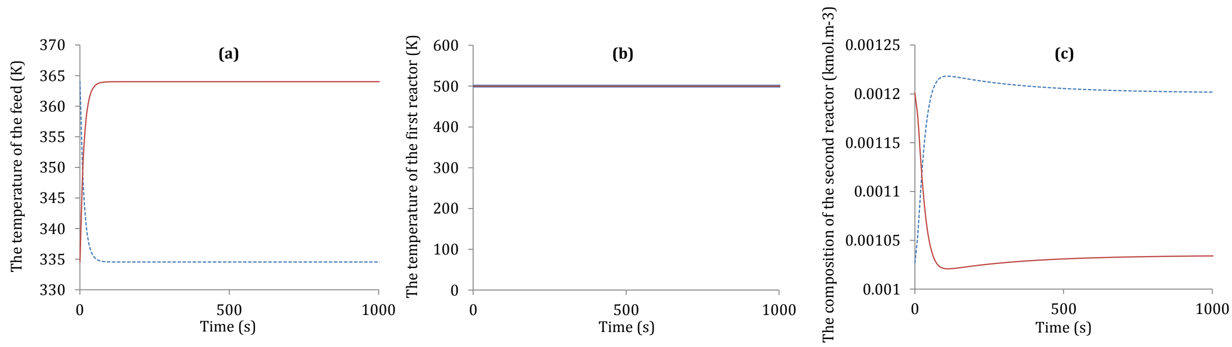

Figures 6.5. Results for the best solution (Structure 6 in Table 6.5) based on perfect control. The time trajectories of a) the feed temperature as the manipulated variable, b) the temperature of the first reactor as the controlled variable (overlaid on each other), c) the composition in the second reactor. Disturbance scenarios were described in Section 6.5.1.

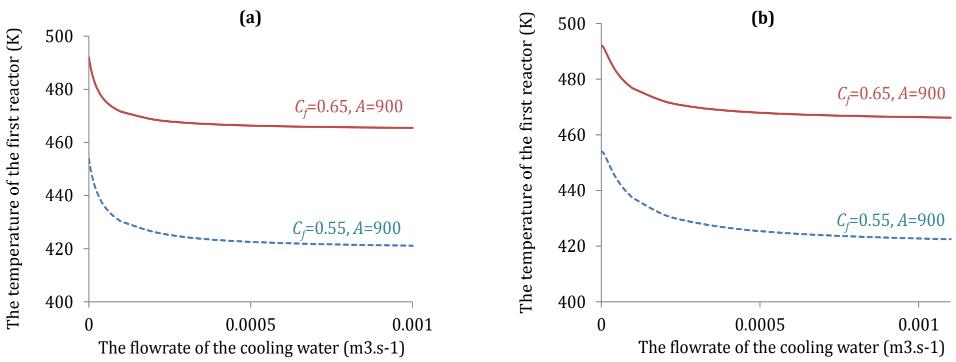

Figures 6.6. The variations of the temperature of the first reactor with the flowrate of the cooling water, for a) the co-current structure, b) the counter-current structure.

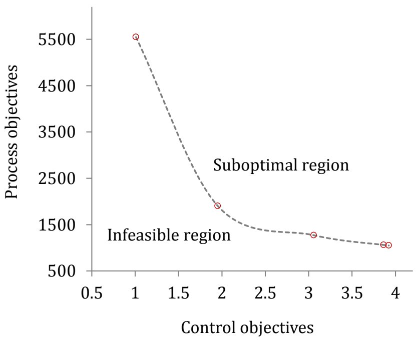

Figure 6.7. The Pareto front for the multi-objective function (6-23) based on the results in Table 6.6.

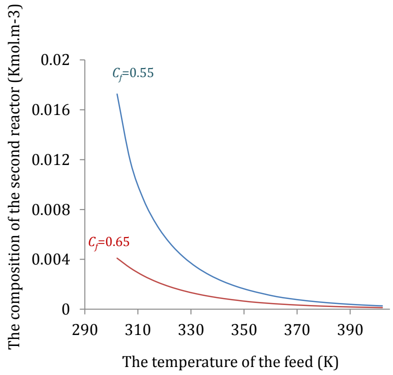

Figure 6.8. The variations of the composition of the second reactor with the feed temperature for the co-current structure.

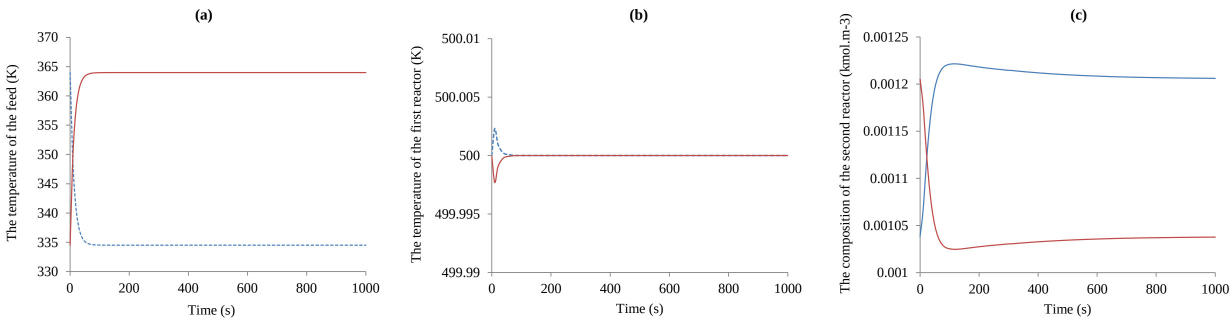

Figures. 6.9. Results of the first set of post-optimization studies. Trajectories of a) the feed temperature as the manipulated variable, b) the temperature of the first reactor as the controlled variable, c) the composition in the second reactor, for the best solution (Structure 6 in Table 6.5) using an optimized PI controller. Disturbances scenarios are described in Section 6.5.1.

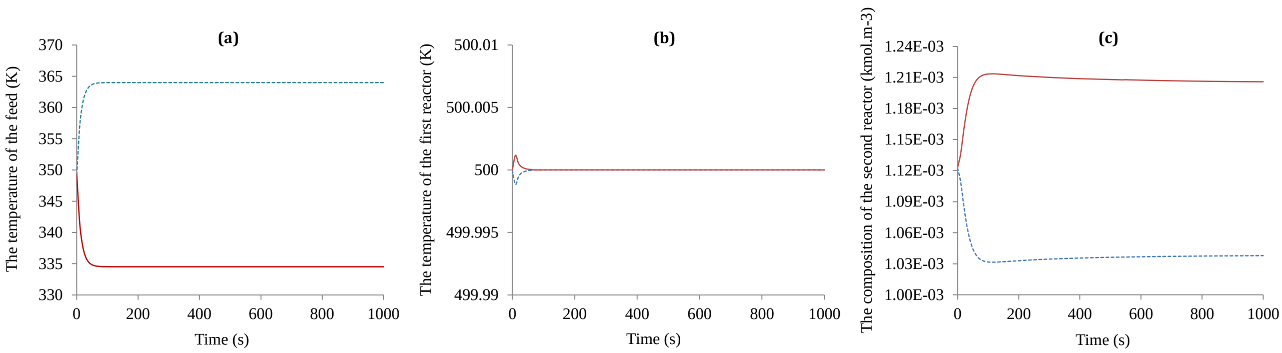

Figures. 6.10. Results of post-optimization analyses. Trajectories of a) the feed temperature as the manipulated variable, b) the temperature of the first reactor as the controlled variable, c) the composition in the second reactor, using an optimized PI controller. The disturbances are step functions from $C_f = 0.6$ to 0.55 (dotted line) and $C_f = 0.6$ to 0.65 (solid line) corresponding to case 5 and case 6 of (Flores-Tlacuahuac and Biegler 2007) respectively.

6.8. Discussions

In this section, the results of the proposed integrated design and control framework using the dynamic inversely controlled process model are explained and compared with the results of the conventional optimization from Flores-Tlacuahuac and Biegler (2007). The aim is to establish the advantages of the proposed method over the conventional one. The cases in which inversion of the process model was not possible (the blank columns in Table 6.5) are explained and justified. In addition, the trade-off between the process and control objective are discussed. The last part of this section discusses the results of post-optimization analyses.

6.8.1. The results of the proposed dynamic optimization framework

Table 6.5 and Table 6.6 show the results of the sequential integration and full discretization solution strategies respectively. The third column of Table 6.6 has the same combination of the weighting factors and is equivalent to Table 6.5. The results of the two solution strategies are in good agreement within the error tolerance of the two solution strategies. Table 6.6 is used for illustrating the relative importance of the control and process objectives and is discussed in Section 6.8.3.

Table 6.5 shows the enumeration results using the sequential strategy. The best process and control structure is the sixth structure in which the temperature of the first reactor, T_1 , is the controlled variable and the feed temperature, T_f, is the manipulated variable. The process structure is co-current. A close objective value is also achieved by the structure 2 which has a similar control structure but counter-current process structure. In general, counter-current heat-exchangers are preferred to co-current heat-exchangers. This is because in a counter-current structure the temperature difference which is the driving force for heat transfer, is kept alive. However, in the present case study, reaction heat enhances the temperature differences and maintains the driving force. Therefore, the counter-current structure is not necessarily dominant. In addition, the co-current structure has the desirable feature that the effects of the disturbances in the process side (reactor) and the utility side (cooling water) move in the same direction and leave the system together. However, in the counter-current structure, disturbances in the process and utility sides move in the opposite directions and remain in the process for a longer period.

The optimal trajectories of the feed temperature (i.e., the manipulated variable) are shown in Figure 6.5a. They show the fast and smooth responses to the disturbances. The optimal trajectories of the temperature of the first reactor (i.e. the controlled variable) are shown in Figure 6.5b. These temperature trajectories are two straight lines which are overlaid on each other and imply perfect control. The optimal trajectories of the composition of the second reactor are shown in Figure 6.5c. Features of the interest are high conversion and very small changes caused by the disturbances, as shown by the small scale of the vertical axis in Figure 6.5c.

A comparison between different structures reveals that the feed temperature is a more effective manipulated variable than the flowrate of the cooling water, although it is more difficult to be implemented. This is because several structures with cooling water as the manipulated variable (i.e., Structures 4 and 8) are uncontrollable. Table 6.5 also shows that in most structures the volumes of the cooling jackets are at their lower bounds because designing a large hold-up for the cooling jackets reduces their dynamic performances. The setpoints of the selected controlled variable in most cases are increased from the base-case design in order to make the process insensitive to the disturbances, which is explained in the next section.

It is notable that the full discretization strategy can also be used for enumeration of structures. Table 6.7 shows the results of enumeration using this method for a combination of weighting factors ($w'_1 = 1\, , w'_2 = 10^{-6}$). However, when the solver does not converge, the failure is not informative and it is not clear whether the process inversion is not possible or other constraints are violated. Notice that the weighting factors of the objective functions gave more priority to the control objectives and therefore, the upper bounds of the reactor volumes are active.

6.8.2. Uncontrollable process structures

During optimization, two uncontrollable structures were detected. In those structures, the flowrate of the cooling water was the manipulated variable and the temperature of the first reactor was the controlled variable. These uncontrollability issues manifested themselves as the failure of the integrator of the DAE solver. These observations can be explained by the test, presented in Section 6.5.3.

Figure 6.6a shows two steady-state analyses which demonstrate the variations of the temperature of the first reactor with the flowrate of the cooling water. The cooling water flows in a co-current structure. One profile is calculated for $C_f = 0.55$ kmol.m^{-3}, and the other profile is for $C_f = 0.65$ kmol.m^{-3}. Other process variables are at their nominal values (Table 6.2). A setpoint for the controlled variable is feasible if the corresponding horizontal tie-line connects the two profiles . Unfortunately, such a horizontal tie-line does not exist and the process inversion is not possible. Similar results are shown in Figure 6.6b for the counter-current process structure of the same control structure.

6.8.3. The implications of competing process and control objectives

Table 6.6 reports optimal solutions for a variety of the combinations of the weighting factors in the multi-objective functions (6-23). For simplicity, the first weighting factor is maintained constant at $w'_1 = 1$, while the second weighting factor, w_2, is changed from 10^{-6} to 10^{-2} which are the two extremes where the control objectives and the process objectives dominant respectively. For $w'_2 = 10^{-6}$ the upper bounds of the reactor volumes are active and the optimizer chose to use the largest possible reactors, because the large reactors are less sensible to the disturbances in the feed composition. On the other extreme, for $w'_2 = 10^{-2}$, the lower bounds of the reactor volumes are active and the control objectives are sacrificed in order to minimize the required capital investments. The optimal solutions for larger values of w'_2 are not shown because the objective functions become severely insensitive to control objectives and multiple solutions with a similar objective value were detected. The concept is shown in Figure 6.7. The horizontal axis and the vertical axis show the control objectives and the process objectives respectively. The designs corresponding to the points below the Pareto front are infeasible solutions. The designs corresponding to the points above the Pareto front are not optimal. The Pareto front illustrates the trade-off between the two objectives as improving the control objectives requires degrading the process objectives, and vice versa, which correspond to moving to left and right on the Pareto front respectively.

Table 6.6 also reveals that the process and the control objectives did not compete for the volume of the cooling jackets and the setpoint for the selected controlled variable. The lower bounds are active, because for smaller cooling jackets, less capital investment is required and at the same time, the response time of a cooling jacket with a smaller hold-up is shorter, hence the process and control objectives point to the same direction. In addition, as discussed earlier, a high temperature setpoint for the controlled variables makes the process insensitive to disturbances, while this does not impose any burden to the process objectives (as they are defined in this research) and therefore the upper bound for the temperature setpoint is active in all optimal solutions.

6.8.4. Discussions of post-optimization studies

As explained in Section 6.5.5, two sets of post-optimization studies were performed. In the first set of post-optimization studies, PI controllers are designed for the best structures of Table 6.5. The aim was to investigate if designing a controller changes the best solution. The results are reported in Table 6.8. This table shows that Structure 6 is still the best solution. The time trajectories of this structure are shown in Figures 6.9.The very small controller error in Table 6.8 and the small scale of Figure 6.9b suggest that for the present case study, the PI controller was able to closely approach the perfect control performance.

In the second set of post-optimization studies, in order to provide the opportunity for comparing the new optimization framework proposed in this research and the conventional framework studied by Flores-Tlacuahuac and Biegler (2007), an actual controller was designed for the best solution (Structure 6 in Table 6.5). Table 6.9 shows the results of the second set of post-optimization studies. These are equivalent to the fifth and sixth cases studied by Flores-Tlacuahuac and Biegler (2007). The results are also shown graphically in Figures 6.10. The small value of the objective function shows that perfect control is closely approached by the PI controller. Similar observations can be made from Fig. 9b which shows that the value of the controlled variable is maintained almost constant, (notice the very small scale of the vertical axis).

Another comparison can be made, based on the criteria of inferential control. Controlling the first reactor temperature inferentially aims at controlling the composition of the unconverted reactant in the second reactor and must indirectly attenuate its variations under disturbed conditions. In the conventional optimization framework, for a change of 0.05 kmol.m^{-3} in the feed composition, the composition of the second reactor varies in the range of 0.002 kmol.m^{-3} (Fig. 10 of Flores-Tlacuahuac and Biegler 2007). The variation in the product composition is 4% of the variation in the feed composition. However, in the new integrated design and control framework, for the same changes in the feed composition, the composition of the second reactor varies by 0.0001 kmol.m^{-3} (Shown in Fig. 6.10c). Here, the attenuation of the disturbances is about twenty times greater than the conventional method. However, the superior performance of the new integrated design and control framework should be attributed to the term,obj_1, in the objective function (6-23) which explicitly considers the task of inferential control. Figure 6.8 provides the explanation. This figure shows the variation of the second reactor composition with the feed temperature. The top profile is when the feed composition is $C_f = 0.55$ kmol.m^{-3} and the bottom profile is when the feed composition is $C_f = 0.65$ kmol.m^{-3}. Other process variables are at their nominal values (Table 6.2). The area between these two profiles is the operating region. This figure reveals that by increasing the feed temperature, the composition of the second reactor becomes insensitive to the disturbances in the feed composition, resulting in a tighter control and greater attenuation. Since the new framework was successful in recognizing the effects of the feed temperature (i.e., the nominal value of the manipulated variable), it chose a higher feed temperature (about 30 K higher than the results of Flores-Tlacuahuac and Biegler 2007). These observations suggest that the controller error (equation 6-17 considered by Flores-Tlacuahuac and Biegler 2007) may have misled the conventional optimization framework to a local solution.

Finally, as well as producing a well-optimized process and control structure, the new integrated design and control framework has achieved a reduction in the complexity of the problem because the differential and algebraic equations of the controller model are replaced by a set of explicit algebraic perfect control equations. Here, equations (6-13) to (6-16) are replaced by equations (6-20, 6-21), which reduces the number of equations. In addition, due to absence of the controller tuning parameters, the number of the optimization variables is less in the proposed framework (e.g., from 10 to 8 in the small example of this chapter), which in large-scale industrial problems can be an important advantage.

6.9. Conclusion

This chapter presented a dynamic optimization framework for integrated design and control based on perfect control. In this framework, instead of the combined model of the process and its controllers, the equivalent dynamic inversely controlled process model is applied. The treatment is based on the notion of functional controllability in which the process inputs (the required values of the manipulated variables) are generated from the process outputs (the desired values of the controlled variables) by inversion of the dynamic process model.

The proposed methodology was demonstrated using the case of two heat-integrated series reactors, which was previously studies by Flores-Tlacuahuac and Biegler (2007). Two solution strategies were applied for dynamic optimization. The first solution strategy was based on sequential integration. In this strategy, all alternative process and control structures were enumerated. Each enumeration was posed as a nonlinear dynamic optimization problem in which a differential algebraic equation (DAE) solver provided information of the objective function and constraints to the nonlinear optimizer. In the sequential integration strategy, model inversion was performed by discretizing the process outputs rather than the process inputs and initial states were calculated using the equivalent steady-state inversely controlled process model. The second solution strategy was based on full discretization of the time-dependent variables. In this solution strategy, the problem was posed as a large-scale MINLP problem. Model inversion was performed by including perfect control equations in the optimization constraints and initialization was performed using the continuity equations. Since the second solution strategy allowed the violations of the constraints in intermediate solutions, it was not limited to a feasible optimization path and its execution time was significantly shorter. In addition, the proposed framework utilized a multi-objective function to explore the trade-off between the involved process and control objectives.

The results demonstrated that the proposed optimization framework benefited from the conceptual as well as numerical complexity reductions. This framework was able to explain the implications of the competing process and control objectives and to establish the trade-off between them by constructing the corresponding Pareto front. Furthermore, while the proposed optimization framework did not make any assumption regarding controllers, it provided the benchmarks for the best performance that the controllers might achieve as the guidelines for control practitioners. The last part of this chapter performed two sets of post-optimization analyses. In these analyses, a PI controller was designed for the optimal process and control structure (i.e., the results of the proposed optimization framework). In the first set of the post-optimization analyses, a PI controller was designed for the best three solutions of the proposed framework. The results of these analyses showed that the optimal structure remains the same even after controller design. In the second set of post-optimization analyses, the controller parameters were optimized with respect to the disturbances scenarios considered in the fifth and sixth cases of (Tlacuahuac and Biegler 2007). The aim was to provide the opportunity for comparison between the proposed and conventional frameworks. The results of these analyses suggested that considering only the controller error might not be sufficient to establish the trade-off between process design and control.

7 | Summary, discussions and suggestions for future research

Introduction

In this chapter, the summary of the research is presented. In addition, for the case of a dynamic inversely controlled process model, the model inversion may result in a mathematical formulation which consists of high index differential algebraic equations (DAEs). The implications of the high index formulation for setpoint tracking and disturbance rejection are discussed in this chapter. This chapter also explains the causes of imperfect control. These are the inherent characteristics of the process, which limit controllability. Furthermore, this chapter provides the critical evaluations of the research achievements, and summarizes the advantages and disadvantages of the proposed methods. The discussion is based on the research aims and objectives proposed in the first chapter. The final section of this chapter suggests the future research directions for further contributions in the field of integrated design and control.

7.1. Research summary

Design and control of chemical processes share important decisions. If the process design is fixed there is little room left for improving the control performance. Furthermore, the process and control objectives are incommensurable and competing. A systematic framework is needed to integrate design and control. Such a framework should feature several desirable characteristics. It should be able to systematically generate and screen alternative process and control designs. In addition, it should be able to manage the problem complexities and ensure that the solution features the desirable properties such as operability or controllability. Finally, the proposed framework for integrated design and control should be able to establish direct links to the underlying chemical and physical phenomena based on first principles modelling.

The conventional approach for integrated design and control is to simultaneously optimize the process and its controllers. However, optimizing controllers poses conceptual as well as numerical difficulties. Firstly, the size of the problem is several orders of magnitude larger if controllers are included in the problem formulation. Secondly, controllability is the inherent property of the process and its control structure and does not depend on the design of controllers. Finally, the modern control systems are designed during commissioning stages and using commercial packages which may not be available when the process is being designed. Therefore, an important aim of this thesis was to disentangle the complexities of controllers from integrated design and control.

This research proposed an optimization framework for integrated design and control based on the concept of perfect control by introducing an *inversely controlled process model*. In an inversely controlled process model, the model of controllers is replaced by perfect control equations. The controlled variables are maintained constant at their setpoints by the perfect control equations and the required values of the manipulated variables are calculated for rejecting disturbances, hence, the process model is inverted. Then, by optimizing the structural and parametric variables of the inversely controlled process model, the alternative combinations of decisions for process and control design are generated and screened.

In addition, an inversely controlled process model is developed directly from the process model and therefore can be presented by first principles modelling and is not limited by any simplification such as linearization or input-output model reduction.

In the proposed optimization framework, although the process and its control structure are optimized simultaneously, the design of controllers is separated and delegated to a control practitioner. Furthermore, the proposed optimization framework provides the benchmarks for the best performance that can be achieved.

In the present research, the proposed optimization framework was presented in two versions using steady-state and dynamic formulations. The steady-state framework was applied for optimal control structure selection of a distillation train in Chapter 4 and for integrated design and control of a reactive distillation column in Chapter 5. In these case studies, the trade-offs between process and control objectives were established using goal programming. In Chapter 6, the proposed dynamic optimization framework was applied to the case of two series reactors. The trade-off between the process and control objective was established by constructing a Pareto front.

7.2. Physical implications of an inversely controlled process model

This section investigates the physical implications of the index of a dynamic inversely controlled process model and the causes of imperfect control for the proposed integrated design and control.

7.2.1. Index reduction

The following discussion about the index of differential algebraic equations (DAEs) concerns dynamic inversely controlled process models, only.

Inversion of a dynamic model may result in high index differential algebraic equations (DAEs). The index of a set of DAEs is defined as the number of differentiations that is required in order to convert that set of DAEs to the equivalent set of ordinary differential equations (ODEs). High index DAEs are not exclusive to inverse dynamic models and they appear frequently in the modelling of chemical processes. Examples of chemical processes with high index models include multiphase reactors, absorption/distillation columns with phase equilibrium, process networks with a negligible pressure drop, and reactors with slow and fast reactions, (Kumar and Daoutidis 1996). Furthermore, as discussed by Feehery and Barton (1996) activation/deactivation path constraints may cause fluctuations in the index over the time horizon.

Pantelides, (Pantelides, et al. 1988a; Pantelides 1988b) proposed an index reduction method which detects structurally high-index DAEs and returns the necessary set of equations for the consistent initialization. However, this method only provides a lower bound on the index, and the resulting system may be over determined. The method of dummy derivatives (Mattsson and Soderlind, 1993) uses the method of Pantelides as a pre-processing step and then makes the resulted over-determined system fully determined by introducing additional variables. In this method, for each additional equation derived by the pre-processing method, one time derivative is substituted by an algebraic variable. The resulting DAE system will have at most index of one. The index reduction does not pose any numerical limitation on the application of the proposed optimization framework because there are efficient index reduction algorithms, which are also built into commercial software tools. Aspen Custom Modeler (ACM) is able to detect high index formulations and provides assistance in index reduction. gPROMS is able to systematically generate the equivalent low index formulation. Furthermore, the full discretization strategy for dynamic optimization is robust to high-index DAEs (Flores-Tlacuahuac and Biegler 2007; Biegler 2010). A comparison between different methods for index reduction is not the focus of present research and this research makes use of the results of these methods and tools. However, it is pertinent to investigate the physical implications of the high index formulation, which is discussed in the following.

McLellan (1994) showed that the index of a nonlinear inversion problem is equal to $\alpha + 1$ where α is the relative order of the process. The relative order is defined as the minimum number of times that a controlled variable should be differentiated in order to generate an explicit relationship between that controlled variable and a manipulated variable. However, nonlinear inversion has physical implications as well, which are the hidden constraints that impose additional requirements for consistent initialization. As discussed in Chapter 3, the functional controllability conditions require that in a DAE system with relative order of α, the actual and desired values of the controlled variable and its first $\alpha - 1$ time derivatives must be equal at the initial condition. The physical implication is that there must be no jump in the process behaviour in order to match the perfect control trajectories. Explaining the implication of these requirements for consistent initialization benefits from differentiating between *setpoint tracking* and *disturbance rejection*. In the case of setpoint tracking, the value of a controlled variable is changed from the initial state to the final state. For a consistent initialization, the actual and desired values of the first $\alpha - 1$ time derivatives of the controlled variable have to be equal to some non-zero values. In practice, it is very difficult to measure the time derivative of a controlled variable accurately. Therefore, perfect setpoint tracking is of limited application. However, for disturbance rejection, the time derivatives of the controlled variables are all zero because the controlled variables are maintained constant, and therefore, index reduction poses no limitation on perfect disturbance rejection. The present thesis focused on the disturbance rejection in which the index of a dynamic inversely controlled process model does not limit its application.

7.2.2. Limiting factors of controllability

Chapter 2 discussed the causes of control imperfection. The limiting factors of controllability are the interactions between control loops, the constraints on the manipulated variables, model uncertainties, time delays, and right-half-plane zeros. Fortunately, none of these concerns limits the application of the proposed optimization frameworks, as discussed in the following.

The interactions between control loops are the concern of decentralized control systems. As explained earlier, the proposed steady-state and dynamic optimization frameworks do not make any presumption regarding the controllers and their pairing/partitioning. However, the best achievable control performance, determined by the proposed optimization frameworks, can be used later to decide on the degree of decentralization for the controllers.

Manipulated variables and their constraints are explicitly included in the optimization formulations and their multi-objective functions (Subproblem 2.stst, Problem 2.stst, and Problem 2.dyn, discussed in Chapter 4, 5, and 6 respectively) and are addressed systematically by the optimizer.

In this research, it was assumed that disturbances are known in advance. However, if it is not the case or there are uncertainties involved in the model parameters, the methods for steady-state flexibility analysis (Swaney and Grossmann 1985) and dynamic flexibility analysis (Dimitriadis and Pistikopoulos 1995) can be applied to explore the effects of uncertain parameters and identify the critical disturbance scenarios which can be combined with the proposed modelling approaches in this thesis.

The application of perfect control to processes with time delays needs more care, because handling time delays using process inversion requires prediction. For instance, Perkins and Wong (1985) showed that for a multi-variable linear system the period that must be waited before the time trajectories of the controlled variables can be specified independently, is bounded by the smallest and largest time delays in the process transfer function. The advantage of the proposed methodology is that it does not make any presumption regarding the controller type and the results of optimization can be applied in order to decide about the elements of the control law (i.e., predictive or feedforward) which should be included to approach perfect control. For example, a feedforward controller would achieve a higher performance in a system with long delays because it is informed earlier of the disturbances compared to a feedback controller.

Right-half-plane zeros in process inversion become poles. It is well understood that right-half-plane zeros cannot be moved by any feedback controller and similar to time delays, right-half-plane zeros are the characteristics of the process, (Yuan, et al. 2011). Unstable zero dynamics are the nonlinear analogues of right-half-plane zeros, and imply instability of the process inversion, called non-minimum phase behaviour (Slotine and Li 1991). The advantage of incorporating inversion of the process model in the optimization framework is that if inversion is not possible for a candidate solution, the constraints are violated which directs the optimization algorithm towards other candidates that do make the process controllable. Therefore, the optimal solution of the proposed integrated design and control framework features functional controllability for all expected disturbance scenarios.

7.3. Critical evaluation of research

Panel 7.1 recapitulates the research aims, the problem statement, and the proposed optimization framework based on perfect control. The aim of this research was to address the problem of integrated design and control (Problem 2) considering the criteria shown in this panel. The present research achieved these objectives by proposing an optimization framework based on perfect control. In the following potential advantages and disadvantages of the proposed method are discussed.

Panel 7.1.
The problem statement, the research aims and objectives (from Chapter 1) and the proposed framework for integrated design and control (from Chapter 3).

Problem 2: Integrated design and control (proposed)

Given the specifications of the feedstocks and the products, the desired throughputs and the expected disturbance scenarios, it is intended to design a process, and its control structure, which are optimal with respect to economic and control performance criteria and satisfy all technical, safety and environmental constraints. Furthermore, ensure that the designed process and its control structure are controllable.

The characteristic of the proposed framework for integrated design and control:

1. **A systematic approach**
   The developed framework systematically generates and screen alternative decisions regarding process and its control structure based on economic and control performance criteria.

2. **Complexity reduction**
   The developed framework reduces the problem complexities.

3. **Controllability**
   The developed framework should be able to ensure some desirable properties of the process and its control structure such as steady-state operability or functional controllability.

4. **First principles modelling**
   The developed framework can be implement using first principles models and is not necessarily limited to any simplifying assumption.

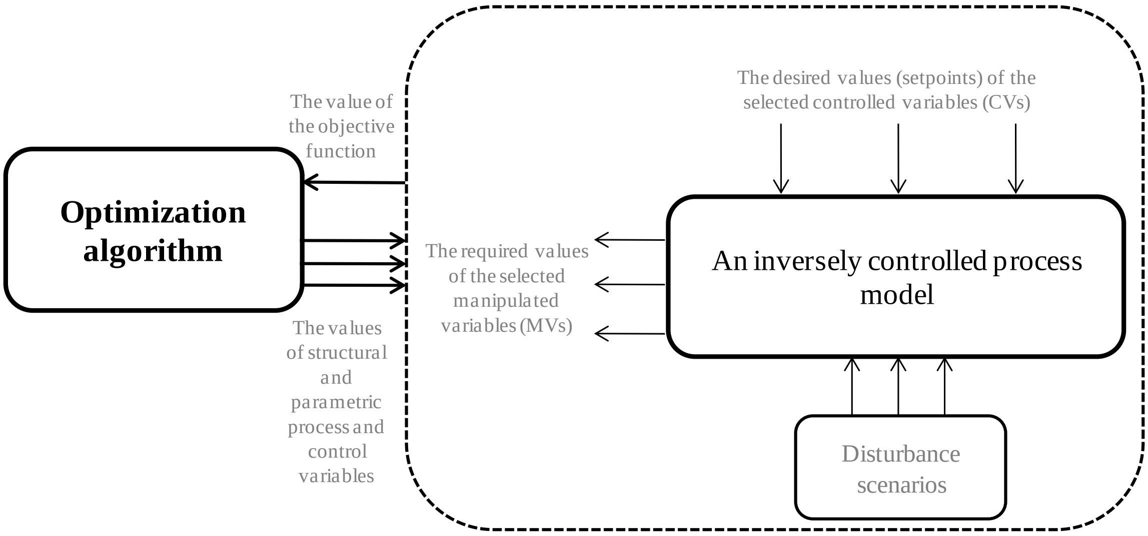

Figure 3.2. The proposed integrated design and control framework using the inversely controlled process model

The proposed optimization framework provides the opportunity for systematic decision-making regarding all alternative process designs and control structure selections. This is done by embedding an inversely controlled process model in the optimization framework, as shown in Panel 7.1. The decision-making regarding the structural and parametric process and control variables of the inversely controlled process model provides the opportunity to systematically generate alternative combinations of the decisions for process design and control structure selection and evaluate their performances against disturbance scenarios. In addition as discussed earlier, the present study contributes to the aim of numerical as well as conceptual complexity reduction by separating the design of controllers from the problem.

The justification for numerical complexity reduction is that the proposed optimization framework for integrated design and control (Problem 2, Section 1.2.5) is smaller and does not include the model of controllers. In addition, the required modelling efforts remain at the same level required for process modelling. However, in the proposed framework, the process and its control structure are still decided simultaneously and controllability of the solution is ensured. Furthermore, the proposed framework provides a benchmark for the best achievable control performance and delegates the detailed controller design (Subproblem 4, Section 1.2.4) to control practitioners.

In addition, the justification for conceptual complexity reduction is that often, modern control systems are designed during commissioning stages using commercial packages which may not be available when the process is being designed. Moreover, controllability is the inherent characteristic of the process and its control structure and does not depend on the design of controllers.

A high degree of numerical complexity reduction is achieved by the application of a steady-state inversely controlled process model (applied in Chapters 4, and 5), because its mathematical formulation consists of only algebraic equations. The steady-state assumption implies that control is instantaneous and the transient states are not considered. Therefore, the proposed steady-state framework ensures steady-state operability. However, at the price of higher modelling efforts, further information can be gained regarding functional controllability using a dynamic inversely controlled process model which also ensures that the solution stays controllable during the transition states.

Finally, the proposed optimization framework does not require simplifying the mathematical model of the process and can be applied based on first principles modelling.

Perfect control is an important approximation, which could lead to different strategies compared to the conventional integrated design and control framework. This is because in the proposed optimization framework, the problem of integrated design and control is divided into two subproblems, and therefore, the solution in principle could be *suboptimal* compared to the conventional framework where all the subproblems are addressed simultaneously. However, in the conventional optimization framework, the controller type is parameterized in advance and the type of controllers is pre-selected. By comparison, the solution of the proposed optimization framework is independent of the controller type and is based on the best control performance that can be achieved.

It is noteworthy, that the proposed optimization framework can also be used for analysis as well. In such an approach, the best solutions are screened by the proposed optimization framework and will be considered for controller design. Such an approach was demonstrated for the case of two heat-integrated series reactors in Chapter 6.

Finally, in some processes multiple inputs can stabilize the process at a given set-point. While this multiplicity is due to the nonlinearity of the process model (which in turn leads to nonconvex optimization problems), the fact that all candidate inputs will lead to different performance raises a number of issues. If the considered process features such a nonlinear behaviour, then the methods discussed in Section 2.13 should be applied to evaluate the nonlinear behaviour of the optimal solution. It is notable that input-output multiplicity is not the exclusive property of the proposed optimization framework and may happen in the conventional framework and other nonlinear methods as well.

7.4. Suggestions for future research directions

This thesis proposed a new optimization framework, based on the concept of perfect control. The author suggests five areas for further investigations.

7.4.1. Detailed design of controllers with emphasize on the cases with limited controllability

It was discussed earlier that the results of the proposed methodology provide a benchmark for design of the controllers. The author suggests detailed design of controllers using the provided benchmark as a potential area of further contribution. In particular, it should be investigated that in the presence of the limiting factors of controllability, which type of controllers (e.g., feedback, feedforward, or model-based) is more capable of approaching perfect control. It can be done by developing a superstructure of controllers which enables decisions regarding alternative control laws and their parameters. Such a superstructure has a reduced dimension as the process and its control structure are already designed by the proposed optimization framework. The outcome can be a set of qualitative guidelines that for example in the case of a process with some specific characteristics (e.g. delays) the controllers should employ some advantageous elements (e.g., feedforward) as well as quantification of the controller performance compared to perfect control. Therefore, it is predicted that the results of the proposed methodology will be helpful in deduction of the desirable properties of the controllers.

7.4.2. Degree of centralization

The temporal and spatial decentralization of controllers were discussed in Chapter 2. The author suggests that the proposed optimization based on the perfect control assumption can be extended for decision-making regarding the degree of centralization.

In principle, perfect control of the decentralized elements of a process does not ensure perfect control of the whole centralized system. This is because in the centralized control structure all the manipulated variables are employed simultaneously, while in the decentralized control system, fewer manipulated variables are available to each controller. Therefore, it is suggested that an inversely controlled process model is developed for the fully centralized scenario in which the whole process is perfectly controlled, as well as the decentralized scenarios in which individual sections of the process are controlled perfectly but are not controlled together. Such a method will be able to identify the best achievable control performance of a candidate set of decentralized controllers. Then a comparison between this performance and the ideal scenario in which all controllers are centralized, provides the opportunity for decision-making regarding the degree of decentralization and screening candidate configurations. Here the trade-off is between the performance deteriorations associated with decentralization and the costs of developing a fully centralized control system.

7.4.3. Inversely controlled process model within the context of self-optimizing control

In Chapter 2, the methods for self-optimizing control were discussed. In self-optimizing control, the economic objectives are translated to the task of maintaining a set of controlled variables at their setpoints. It was also discussed, that although maintaining the measurements constant is convenient, it does not ensure economic optimality in many cases. Therefore, it was suggested that a combination of the measurements could be controlled or even some researchers chose to directly control the gradient of the economic objective function. Similar approach can be applied using an inversely controlled process model. In such a framework, model inversion is performed with respect to a combination of the controlled variables or directly with respects to the economic objective function. The inputs of such a framework are the manipulated variables and the setpoints of the controlled variables. Another relevant perspective is to include the measurement noise and the effects of fast-acting disturbances which would require back-off from the active constraints.

7.4.4. Incorporating into commercial software tools

As discussed also by other researchers (e.g., Klatt and Marquardt, 2009), the evolving computational technologies have changed the perceptions of process systems engineers of their problem-solving capabilities. It is expected that if a problem (e.g., synthesis of a process or control system) is presented in its formal statement, the problem-solving strategy can be reformulated into an algorithmic procedure and solved by the means of computer programming tools. Such tools for computer-aided design assist designer to accelerate the process of decision-making and to enhance the fidelity of the results based on rigorous analysis. Examples of these programs are the simulation software tools by AspenTech[3] (e.g. Aspen Plus and Aspen HYSYS), PSE[4] (gPROMS) and MathWorks[5] (e.g. Simulink).

The author suggests that the modelling approach proposed in this research can be incorporated as a built-in module into these software tools. Then, after the process is modelled, the software tool provides the option to the designer to evaluate the control performance of the designed process using an automated procedure in which the corresponding inversely controlled process model is constructed. Then it is possible to evaluate the best achievable control performance against a portfolio of disturbances. Such a program may exploit the flowsheet interconnectivity to shortlist the candidate controlled and manipulated variables. However, the key step in automating the proposed methodology is to systematically consider the physical implications (discussed earlier in this chapter) of perfect control, and to translate them into programming procedures. Furthermore, ideally such a software tool should be able also to provide the option for optimization of the constructed inversely controlled process model, and to facilitate the application of the proposed framework for integrated design and control.

The abovementioned built-in modules would enhance the computational capabilities, available to the industrial practitioners, in order to efficiently consider the controllability characteristics of the process at the early stages of process design.

7.4.5. Developing surrogate inversely controlled process model from rigorous simulations

As mentioned in Chapter 2, since most of conventional optimization techniques require first and second derivatives, derivative free optimization algorithms need to be applied. Another similar area of potential contribution is developing surrogate models from simulations (Cozad, et al. 2011). In such a framework, a surrogate models is constructed and its parameters are optimized against the maximum error between the rigorous simulation and the lean surrogate model. The advantage is that the new surrogate model provides cheap evaluations of the gradients and can be optimized using standard optimization algorithms. The author suggests that surrogate model should be developed directly for the inversely controlled process model. Then, such a low complexity accurate model will provide

[3] Web address: http://www.aspentech.com/
[4] Web address: http://www.psenterprise.com/gproms/
[5] Web address: http://www.mathworks.co.uk/

opportunity to apply the methodology of this thesis to larger industrial examples.

Bibliography

Al-Arfaj, M. A., Luyben, W. L., (2002). Control study of ethyl tert-butyl ether reactive distillation. *Industrial Engineering and Chemistry Research*, 41 (16), 3784-3796.

Alhammadi, H., Romagnoli, J., (2004). Process Design and Operation: Incorporating Environmental, Profitability, Heat Integration and Controllability Considerations. In *The Integration of Process Design and Control*. Volume 17, Edited by Seferlis, P., Georgiadis, C. M., Elsevier Science, Amsterdam, 264-306.

Alstad, V., Skogestad, S., Hori, E. S., (2009). Optimal measurement combinations as controlled variables. *Journal of Process Control*, 19 (1), 138-148.

ANSI/ISA-95, (2000). *Enterprise-Control System Integration Part 1: Models and Terminology*. (Online: http://www.isa-95.com/subpages/technology/isa-95.php accessed March 2012).

ANSI/ISA-95, (2001). *Enterprise-Control System Integration Part 2:Object Model Attributes*. (Online: http://www.isa-95.com/subpages/technology/isa-95.php , accessed March 2012).

ANSI/ISA-95, (2005). *Enterprise Control System Integration Part 3: Activity Models of Manufacturing Operations Management*. (Online: http://www.isa-95.com/subpages/technology/isa-95.php accessed March 2012).

Antoulas, A. C., Sorensen, D. C., Gugercin, S., (2000). A survey of model reduction methods for large-scale systems. *Structured Matrices in Operator Theory, Numerical Analysis, Control, Signal and Image Processing, Contemporary Mathematics*, AMS publications, 280, 193-219.

Ariyur, K. B., Krstic, M., (2003). *Real-time optimization by extremum seeking*. John Wiley, New York.

Aske, E. M. B., Skogestad, S., (2009a). Dynamic degrees of freedom for tighter bottleneck control. *10th International Symposium on Process Systems Engineering*, Salvador-Bahia, Brazil, August 16-20.

Aske, E. M. B., Skogestad, S., (2009b). Consistent inventory control. *Industrial & Engineering Chemistry Research*, 48 (24), 10892-10902.

Aske, E. M. B., (2009c). *Design of Plantwide Control Systems with Focus on Maximizing*

Throughput. PhD Thesis. Department of Chemical Engineering, Norwegian University of Science and Technology.

Aspen Custom Modeler documentation, (2004). *Aspen Modeler Reference Guide*. Aspen Technology, (2004.1).

Aspen-HYSYS document, (2009a). *Operation Guide*. Aspen Technology, (V7.1).

Aspen-HYSYS document, (2009b). *Simulation Basis*. Aspen Technology, (V7.1).

Aspen-Plus document, (2009a). *Operation Guide*. Aspen Technology, (V7.1).

Aspen-Plus document, (2009b). *Physical Property Methods*. Aspen Technology, (V7.1).

Asteasuain, M., Bandoni, A., Sarmoria, C., Brandolin, A., (2006). Simultaneous process and control system design for grade transition in styrene polymerization. *Chemical Engineering Science*, 61 (10), 3362-3378.

Avraam, M.P., Shah, N., Pantelides, C.C., (1998). Modelling and optimisation of general hybrid systems in the continuous time domain. *Computers and Chemical Engineering*, 22 (Supplement), S221-S228.

Avraam, M.P., Shah, N., Pantelides, C.C., (1999). A decomposition algorithm for the optimisation of hybrid dynamic processes. *Computers and Chemical Engineering*, 23 (Supplement), S451-S454.

Bai, Z., (2002). Krylov subspace techniques for reduced-order modelling of large scale dynamical systems. *Applied Numerical Mathematics*, 43 (1-2), 9-44.

Bansal, V., Perkins, J. D., Pistikopoulos, E. N., Ross, R., van Schijndel, J. M. G., (2000a). Simultaneous design and control optimisation under uncertainty. *Computers & Chemical Engineering*, 24 (2-7), 261–266.

Bansal V., Ross R, Perkins J. D., Pistikopoulos E. N. (2000b). The interactions of design and control; double-effect distillation. *Journal of Process Control*, 10 (2-3), 219–227.

Bansal, V., Perkins, J. D., Pistikopoulos, E. N., (2002). A case study in simultaneous design and control using rigorous, mixed-integer dynamic optimization models. *Industrial & Engineering Chemistry Research*, 41 (4), 760–778.

Bansal, V., Sakizlis, V., Ross, R., Perkins, J.D., Pistikopoulos, E.N., (2003). New algorithms for mixed-integer dynamic optimization. *Computers and Chemical Engineering*, 27:647-668.

Bao J., Lee P. L., (2007). *Process Control: The Passive Systems Approach.* Advances in Industrial Control, Springer-Verlag, London.

Barbosa,, D., Doherty, M. F., (1988). Design and minimum-reflux calculations for single-feed multicomponent reactive distillation columns. *Chemical Engineering Science,* 43 (7), 1523-1537.

Barton, P.I., Lee, C.K., (2004). Design of process operations using hybrid dynamic optimization. *Computers and Chemical Engineering*, 28, 955-969.

Bauer, M., Cox, J. W., Caveness, M. H., Downs J. J., Thornhill, N. F., (2007). Finding the direction of disturbance propagation in a chemical process using transfer entropy. *IEEE Transactions on Control Systems Technology*, 15 (1), 12-21.

Bauer M., Thornhill N. F., Meaburn, A., (2004). Specifying the directionality of fault propagation paths using Transfer entropy. *7th international symposium on DYnamics and COntrol of Process Systems (DYCOPS 7)*, Boston, USA, July 1-4, 2004.

Biegler, L.T., Grossmann, I. E., Westerberg, A.W., (1997). *Systematic Methods for Chemical Process Design.* Prentice-Hall, London.

Biegler, L. T., Grossmann, I. E., (2004). Retrospective on optimization. *Computers & Chemical Engineering*, 28 (8), 1169-1192.

Biegler, L. T., (2010). *Nonlinear programming: concepts, algorithms, and applications to chemical processes.* Society for Industrial & Applied Mathematics, MOS-SIAM series on optimization, Philadelphia.

Bisowarno, B.H., Tian, Y.C., Tade, M.O., (2003). Model gain scheduling control of an ethyl tert-butyl ether reactive distillation column. *Industrial & Engineering Chemistry Research,* 42 (15), 3584–3591.

Brdys, M., Tatjewski, P., (2005). *Iterative algorithms for multilayer optimizing control*. Imperial College Press, London.

Bristol, E., (1966). On a new measure of interaction for multivariable process control. *IEEE Transactions on Automatic Control*, 11 (1), 133-134.

Buckley, P. S., (1964). *Techniques of Process Control*, Wiley, New York.

Caballero, J. A., Odjo, A., Grossmann, I. E., (2007). Flowsheet optimization with complex cost and size functions using process simulators. *AIChE Journal*, 53 (9), 2351–2366.

Cao, Y., Biss, D., Perkins, J. D., (1996). Assessment of input-output controllability in the presence of control constraints. *Computers & Chemical Engineering*, 20 (4), 337–346.

Cao Y., Yang Z., (2004). Multiobjective process controllability analysis. *Computers & Chemical Engineering*, 28 (1–2), 83–90.

Cao, Y., (2005). Direct and indirect gradient control for static optimisation. *International Journal of Automation and Computing*, 2 (1), 13—19.

Cao, Y., Kariwala, V., (2008). Bidirectional branch and bound for controlled variable selection Part I. Principles and minimum singular value criterion. *Computers & Chemical Engineering*, 32 (10), 2306–2319.

Cardoso, M. F., Salcedo, R. L., Feyo de Azevedo, S., Barbosa, D., (2000). Optimization of reactive distillation processes with simulated annealing. *Chemical Engineering Science*, 55 (21), 5059-5078.

Carrera-Rodríguez, M., Segovia-Hernández, J., G., Bonilla-Petriciolet, A., (2011). Short-cut method for the design of reactive distillation columns. *Industrial & Engineering Chemistry Research*, 50 (18), 10730–10743.

Cervantes, A.M., Biegler, L.T., (2000a). Optimization strategies for dynamic systems, in: Floudas, C., Pardalos, P., (Eds.), *Encyclopedia of Optimization*, Kluwer.

Cervantes, A.M., Biegler, L.T., (2000b). A stable elemental decomposition for dynamic process optimization. *Journal of Applied Mathematics and Computing*, 120 (1-2), 41–57.

Cervantes, A.M., Biegler, L.T., (2002). A reduced space interior point strategy for optimization of differential algebraic systems. *Computers & Chemical Engineering*, 24 (1), 39–51.

Chachuat, B., Singer, A.B., Barton, P.I., (2005). Global mixed-integer dynamic optimization. *AIChE Journal*, 51 (8), 2235–2253.

Chachuat, B., Singer, A.B., Barton, P.I., (2006). Global Methods for Dynamic Optimization and Mixed-Integer Dynamic Optimization. *Industrial & Engineering Chemistry Research*, 45 (25), 8373–8392.

Chachuat, B., Marchetti, A., Bonvin, D., (2008). Process optimization via constraints adaptation. *Journal of Process Control*, 18 (3-4), 244–257.

Chachuat, B., Srinivasan, B., Bonvin, D., (2009). Adaptation strategies for real-time optimization. *Computers & Chemical Engineering*, 33 (10), 1557–1567.

Chachuat, B., (2010). Introduction to the special issue on optimal process control. *Optimal Control Applications and Methods*, 31 (5), 391–392.

Chacon-mondragon, O. L., Himmelblau, D. M., (1996). Integration of flexibility and control in process design. *Computers & Chemical Engineering*, 20 (4), 447-452.

Chawanku, N., Budman, H., Douglas, P.L., (2005). The integration of design and control: IMC control and robustness. *Computers & Chemical Engineering*, 29 (2), 261–271.

Chemical Engineering magazine, (2011). Economic indicators. December, 2011, page 69, (Online: www.che.com, accessed March 2012).

Chen, C. Y., Joseph, B., (1987). On-line optimization using a two-phase approach: An application study. *Industrial & Engineering Chemistry Research*, 26 (9), 1924–1930.

Cozad, A., Sahinidis, N., Miller, D., (2011). A computational methodology for learning low-complexity surrogate models of process from experiments or simulations. *AIChE Annual Meeting*, Minneapolis, October 16-21, 2011. (Paper 679a).

Daoutidis P., Kravaris, C., (1991). Inversion and zero dynamics in nonlinear multivariable control. *AIChE Journal* 37 (4) 527-538.

DICOPT documentation, (2012). (Online: www.gams.com/dd/docs/solvers/dicopt.pdf, accessed April 2012).

Dimitriadis, V., Pistikopoulos, E. N., (1995). Flexibility analysis of dynamic systems. *Industrial & Engineering Chemistry Research*, 34 (12), 4451–4462.

Dixon, D.C., (1972). Degrees of Freedom in Dynamic and Static Systems. *Industrial & Engineering Chemistry Fundamentals*, 11 (2), 198–205.

Dormeanu B., Bildea C. S., Grievink J., (2009). On the application of model reduction to plantwide control. *Computers & Chemical Engineering*, 33 (3), 699–71.

Douglas, J., (1988). *Conceptual Design of Chemical Processes*. McGraw-Hill, New York.

Downs J. J., (1992). Distillation control in a plantwide control environment. In *Practical Distillation Control*. Edited by Luyben, W. L., Van Nostrand Reinhold, New York, 413–439.

Downs, J.J., Vogel, E.F., (1993). A plant-wide industrial process control problem. *Computers & Chemical Engineering*, 17 (3), 245–255.

Downs J. J., Skogestad S., (2011). An industrial and academic perspective on plantwide control. *Annual Reviews in Control*, 35 (1), 99–110.

Dragomir, R. M., Jobson, M. (2005). Conceptual design of single-feed hybrid reactive distillation columns. *Chemical Engineering Science*, 60 (16), 4377–4395.

Edgar, T. F., Himmelblau, D. M.,Lasdon , L. S., (2001). *Optimization of Chemical Processes*. McGraw-Hill, London.

Edgar, T. F., (2004). Control and operations: when does controllability equal profitability? *Computers & Chemical Engineering*, 29 (1) 41-49.

Engell S., (2007). Feedback control for optimal process operation. *Journal of Process Control*, 17, 203–219.

Exler, O., Antelo, L.T., Egea, J. A., Alonso, J A.A.,. Banga R., (2008). A Tabu search-based algorithm for mixed-integer nonlinear problems and its application to integrated process and control system design. *Computers and Chemical Engineering*, 32, (8), 1877-1891.

Feehery, W.F., Barton, P.I., (1996). A differentiation-based approach to dynamic simulation and optimization with high-index differential-algebraic equations, *Proc 2nd international workshop on Computational Differentiation, SIAM*, 239-253.

Flores-Tlacuahuac, A., Biegler, L.T., (2005). Dynamic optimization of HIPS open loop unstable polymerization reactors. *Industrial & Engineering Chemistry Research*, 44 (8), 2659–2674.

Flores-Tlacuahuac, A., Biegler, L.T., (2007). Simultaneous mixed-integrated dynamic optimization for integrated design and control. *Computers & Chemical Engineering*, 31 (5-6), 588–600.

Flores-Tlacuahuac A., Biegler L.T., (2008). Global optimization of highly nonlinear dynamic systems. *Industrial & Engineering Chemistry Research*, 47 (8), 2643–2655.

Floudas, C.A., Akrotirianakis, I.G., Caratzoulas, S., Meyer, C.A., Kallrath, J., (2005). Global optimization in the 21st century: Advances and challenges. *Computers and Chemical Engineering*, 29 1185–1202.

Forbes, J. F., Marlin, T. E., (1994). Model accuracy for economic optimizing controllers: The bias update case. *Industrial & Engineering Chemistry Research*, 33 (8), 1919–1929.

Francois, G., Srinivasan, B., Bonvin, D., (2005). Use of measurements for enforcing the necessary conditions of optimality in the presence of constraints and uncertainty. *Journal of Process Control*, 15 (6), 701–712.

Froisy, J. B., (1994). Model predictive control: Past, present and future. *ISA Transactions*, 33 (3), 235-243.

Gao, W., Engell, S., (2005). Iterative set-point optimization of batch chromatography. *Computers & Chemical Engineering*, 29 (6), 1401–1409.

Garcia, C. E., Morari, M., (1982). Internal model control. 1. A unifying review and some new results. *Industrial & Engineering Chemistry Process Design and Development*, 21 (2), 309-332.

Geoffrion, A.M., (1972). Generalized benders decomposition. *Journal of Optimization Theory and Application*, 10 (4), 237-260.

Georgakis, C., Uztürk, D., Subramanian, S., Vinson, D.R., (2003). On the operability of continuousprocesses. *Control Engineering Practice*, 11 (8), 859–869.

Georgakis, C., Vinson, D. R., Subramanian, S., Uztiirk, D., (2004). A geometric approach for process operability analysis. In *The Integration of Process Design and Control*. Volume 17, Edited by Seferlis, P., Georgiadis, C. M., Elsevier Science, Amsterdam, 96-126.

Georgakis, C., Li, L., (2010). On the calculation of operability sets of nonlinear high-dimensional processes. *Industrial & Engineering Chemistry Research*, 49 (17), 8035–8047.

Georgiadis, M. C., Schenk, M., Pistikopoulos, E. N., Gani, R., (2002). The interactions of design, control and operability in reactive distillation systems. *Computers & Chemical Engineering*, 26 (4-5), 735–746.

Gonzales-Pachon, J., Romero, C., (1999). Distance-based consensus methods: a goal programming Approach. *Omega*, 27 (3), 341-347.

Govatsmark, M. S., Skogestad, S., (2005). Selection of controlled variables and robust setpoints. *Industrial & Engineering Chemistry Research*, 44 (7), 2207–2217.

Grossmann, I. E., Floudas, C. A., (1987). Active constraint strategy for flexibility analysis in chemical processes. *Computers & Chemical Engineering*, 11 (6), 675–693.

Grossmann, I. E., (2002). Review of nonlinear mixed- integer and disjunctive programming techniques. *Optimization & Engineering*, 3, 227-252.

Grossmann, I. E., Biegler, L.T., (2004). Part II. Future perspective on optimization. *Computers and Chemical Engineering*, 28, 1193–1218

Guay, M., Zhang, T., (2003). Adaptive extremum seeking control of nonlinear dynamic systems with parametric uncertainty. *Automatica*, 39 (7), 1283–1294.

Halemane, K. P., Grossman, I. E., (1983). Optimal process design under uncertainty. *AIChE Journal*, 29 (3), 425–433.

Halvorsen, I. J., Skogestad, S., Morud, J. C., Alstad, V., (2003). Optimal selection of controlled variables. *Industrial & Engineering Chemistry Research*, 42 (14), 3273-3284.

Hangos, K. M., Tuza, Zs., (2001). Optimal control structure selection for process systems. *Computers & Chemical Engineering*, 25 (11-12), 1521-1536.

Hangos K.M., Bokor J., Szederkényi G., (2004). *Analysis and Control of Nonlinear Process Systems.* Springer-Verlag. London.

Harjunkoski, I., Nyström, R., Horch A., (2009). Integration of scheduling and control - Theory or practice? *Computers & Chemical Engineering*, 33 (12), 1909–1918.

Heath J. A., Kookos I. K., Perkins J. D., (2000). Process control structure selection based on economics. *AIChE Journal*, 46 (10), 1998-2016.

Hirschorn, R., (1979). Invertibility of nonlinear control systems. *IEEE Transactions on Automatic Control*, 24, (6), 855 – 865.

Holt, B. R., Morari, M., (1985). Design of resilient processing plants-V: The effect of deadtime on dynamic resilience. *Chemical Engineering Science*, 40 (7), 1229-1237.

Hori, E.S., Skogestad S., (2007). Selection of control structure and temperature location for two-product distillation columns. *Chemical Engineering Research and Design*, 85 (3), 293–306.

Hori, E. S., Skogestad, S., (2008). Selection of controlled variables: Maximum gain rule and combination of measurements. *Industrial & Engineering Chemistry Research*, 47

(23), 9465–9471.

ICIS pricing, (2011). (Online: www.icispricing.com , accessed Dec 2011).

Isidori, A., (1989*). Nonlinear Control Systems: An Introduction*. Second Edition, Springer Verlag, Berlin.

Jackson, J. R., Grossmann, I. E., (2001). Disjunctive programming approach for the optimal design of reactive distillation columns. *Computers & Chemical Engineering*, 25 (11-12), 1661-1673.

Jelali, M., (2006). An overview of control performance assessment technology and industrial applications. *Control Engineering Practice*, 14 (5), 441-466.

Jones, D., Tamiz, M., (2010). *Practical goal programming*. International series in operation research and management science, Volume 141, First Edition. Springer, New York.

Kalman, R. E., (1960). On the general theory of control systems. *In: Proceedings of First IFAC Congress*, Butterwoths, Moscow, 481–492.

Kariwala, V. (2007). Optimal measurement combination for local self-optimizing control. *Industrial & Engineering Chemistry Research*, 46 (11), 3629-3634.

Kariwala V., Cao, Y., Janardhanan. S., (2008). Local self-optimizing control with average loss minimization. *Industrial & Engineering Chemistry Research*, 47 (4), 1150-1158.

Kariwala, V., Cao, Y., (2009). Bidirectional branch and bound for controlled variable selection. Part II: Exact local method for self-optimizing control. *Computers & Chemical Engineering*, 33 (8), 1402–1412.

Kariwala V., Cao, Y., (2010a). Branch and bound method for multiobjective pairing selection. *Automatica*, 46 (5), 932-936.

Kariwala, V., Cao, Y., (2010b). Bidirectional branch and bound for controlled variable selection part iii: Local average loss minimization. *IEEE Transactions on Industrial Informatics*, 6 (1), 54 - 61.

Kiss, A.A., Bildea, C.S., Dimian, A.C., Iedema, P.D., (2002). State multiplicity in CSTR–separator–recycle polymerisation systems. *Chemical Engineering Science*, 57, (4), 535-546.

Kiss, A.A., Bildea, C.S., Dimian, A C., Iedema, P. D., (2003). State multiplicity in PFR–

separator–recycle polymerization systems. *Chemical Engineering Science,* 58, (13), 2973-2984.

Kiss, A.A., Bildea, C.S., Dimian, A.C., (2007). Design and control of recycle systems by non-linear analysis. *Computers & Chemical Engineering*, 31, (5–6), 601-611.

Khajuria, H., Pistikopoulos, E. N., (2011). Dynamic modeling and explicit/multi-parametric MPC control of pressure swing adsorption systems. *Journal of Process Control*, 21 (1), 151–163.

Khaledi, R., Young, B. R., (2005). Modeling and model predictive control of composition and conversion in an etbe reactive distillation column. *Industrial & Engineering Chemistry Research,* 44 (9), 3134-3145.

Klatt K.-U., Marquardt W., (2009). Perspectives for process systems engineering - Personal views from academia and industry. *Computers & Chemical Engineering*, 33 (3), 536–550.

Konda, N.V.S.N. M., Rangaiah, G.P., Krishnaswamy, P.R., (2006). A simple and effective procedure for control degrees of freedom. *Chemical Engineering Science,* 61, (4), 1184–1194.

Konda, N.V.S.N. M., Rangaiah, G.P., (2012) Control degree of freedom analysis for plantwide control of industrial processes. In *Plantwide Control: Recent Developments and Applications*. First Edition. Edited by Rangaiah, G.P., Kariwala, V., John Wiley, Chichester, 21-42.

Kookos, I. K., Perkins, J. D., (2001). An algorithm for simultaneous process design and control. *Industrial & Engineering Chemistry Research,* 40 (19), 4079-4088.

Kookos, I. K., (2001). *Control Structure Selection Based on Economics.* PhD thesis, Department of Chemical Engineering and Chemical Technology, Imperial College of Science, Technology and Medicine.

Kookos, I. K., Perkins, J. D., (2004). The back-off approach to simultaneous design and control. In *The Integration of Process Design and Control*. Volume 17, Edited by Seferlis, P., Georgiadis, C. M., Elsevier Science, Amsterdam, 216-238.

Kroschwitz J. I., Seidel A., (2004). *Kirk-Othmer Encyclopedia of Chemical Technology*. Wiley-Interscience. Hoboken.

Kuhlmann, A. Bogle, I. D. L., (2001). Controllability evaluation for nonminimum phase-processes with multiplicity. *AIChE Journal*, 47 (11), 2627-2632.

Kuhlmann, A. Bogle, I. D. L., (2004). Design of nonminimum phase processes for optimal switchability. *Chemical Engineering & Processing*, 43 (5), 655–662.

Kumar, A., Daoutidis, P., (1996). Feedback regularization and control of nonlinear differential-algebraic-equation systems. *AIChE Journal*, 42 (8), 2175-2198.

Larsson, T., Skogestad, S., (2000a). Plantwide control - A review and a new design procedure. *Modeling, Identification & Control*, 21 (4), 209-240.

Lee, H-Y., Lee, Y-C., Chien, I-L., Huang, H-P., (2010). Design and control of a heat-integrated reactive distillation system for the hydrolysis of methyl acetate. *Industrial & Engineering Chemistry Research*, 49 (16), 7398–7411.

Low K.H., Sorensen, E., (2003a). Simultaneous optimal design and operation of multivessel batch distillation. *AIChE Journal*, 49 (10), 2564–2576.

Low K.H., Sorensen, E., (2003b). Simultaneous optimal design and operation of multipurpose batch distillation. *Chemical Engineering and Processing*, 43 (3), 273–289.

Low, K.H., Sorensen, E., (2005). Simultaneous optimal configuration, design and operation of batch distillation. *AIChE Journal*,51 (6) 1700–1713.

Luyben, M. L., Floudas, C. A., (1994). Analyzing the interaction of design and Control - l . A multiobjective framework and application to binary distillation synthesis. *Computers & Chemical Engineering*, 18 (10), 933-969.

Luyben, M. L., Luyben, W. L., (1995). Design and control of a complex process involving two reaction steps, three distillation columns, and two recycle streams. *Industrial & Engineering Chemistry Research*, 34 (11), 3885-3898.

Luyben, M. L., Tyreus, B. D., Luyben, W. L., (1997). Plantwide control design procedure. *AIChE Journal*, 43 (12), 3161-3174.

Luyben W. L., (1993a). Dynamics and control of recycle systems. 1. Simple open-loop and closed-loop systems. *Industrial & Engineering Chemistry Research*, 32 (3), 466–475.

Luyben W. L., (1993b). Dynamics and control of recycle systems. 2. Comparison of alternative process designs. *Industrial & Engineering Chemistry Research*, 32 (3), 476-486.

Luyben W. L., (1993c). Dynamics and control of recycle systems. 3. Alternative process designs in a ternary system. *Industrial & Engineering Chemistry Research*, 32 (6), 1142–1153.

Luyben, W.L., (1994). Snowball effects in reactor/separator processes with recycle. *Industrial & Engineering Chemistry Research*, 33 (2), 299–305.

Luyben, W. L., (1996). Simple regulatory control of the Eastman process. *Industrial & Engineering Chemistry Research*, 35 (10), 3280-3289.

Luyben, W. L., Luyben, M. L., Tyreus B. D., (1999). *Plantwide Process Control.* McGraw-Hill, New York.

Luyben, W. L., (2004). The need for simultaneous design education. In *The Integration of Process Design and Control*. Volume 17, Edited by Seferlis, P., Georgiadis, C. M., Elsevier Science, Amsterdam, 10-41.

Luyben, W. L., (2005). Guides for the selection of control structures for ternary distillation columns. *Industrial & Engineering Chemistry Research*, 44 (18), 7113–7119.

Luyben, W. L., (2006). *Distillation Design and Control using Aspen Simulation*. John Wiley, Hoboken.

Luyben W. L., Yu. C, (2008). *Reactive distillation design and control.* John Wiley, Hoboken.

Lyman, P. R., Georgakis, C., (1995). Plant-wide control of the Tennessee Eastman problem. *Computers & Chemical Engineering*, 19 (3), 321-331.

Mäkilä, P. M., (1991). On identification of stable systems and optimal approximation. *Automatica*, 27 (4), 663-676.

Maarleveld, A., Rijnsdorp, J. E., (1970). Constraint control on distillation columns. *Automatica*, 6 (1), 51–58.

Malcolm, A., Polan, J., Zhang, L., Ogunnaike B. A., Linninger A. A., (2007). Integrating systems design and control using dynamic flexibility analysis. *AIChE Journal*, 53 (8), 2048–2061.

Manousiouthakis, V., Nikolau, M., (1989). Analysis of decentalised control structures for nonlinear systems. *AIChE Journal*, 35 (4), 549–558.

Marchetti, A., Chachuat, B., Bonvin D., (2009). Modifier-adaptation methodology for real-time optimization. *Industrial & Engineering Chemistry Research*, 48 (13), 6022–6033.

Marlin, T. E., Hrymak, A. N., (1997). Real-time operations optimization of continuous processes. *AIChE Symposium Series-CPC-V*, 93, 156–164.

Marquardt, W., (2001). Nonlinear model reduction for optimization based control of transient chemical processes. In *Proceedings of the 6th International Conference of Chemical Process Control*, *AIChE Symposium Series*, 326 (98), 12-42.

Marquardt, W., Mönnigmann, M., (2005). Constructive nonlinear dynamics in process systems engineering. *Computers & Chemical Engineering*, 29, (6), 1265-1275.

MATLAB documentation, (2012). *Optimization Toolbox User's Guide.* (Online: http://www.mathworks.co.uk/help/pdf_doc/optim/optim_tb.pdf , accessed March 2012).

Mattsson, S.E., Soderlind, G., (1993). Index reduction in differential-algebraic equations using dummy derivatives, *SIAM Journal on Scientific Computing*, 14 (3), 677-692.

Maurya, M. R., Rengaswamy, R., Venkatasubramanian V., (2003a). A systematic framework for the development and analysis of signed digraphs for chemical processes. 1. Algorithms and analysis. *Industrial & Engineering Chemistry Research*, 42 (20), 4789-4810.

Maurya, M. R., Rengaswamy, R., Venkatasubramanian V., (2003b). A systematic framework for the development and analysis of signed digraphs for chemical processes. 2. Control loops and flowsheet analysis. *Industrial & Engineering Chemistry Research*, 42 (20), 4811-4827.

Maurya, M. R., Rengaswamy, R., Venkatasubramanian V., (2004). Application of signed digraphs-based analysis for fault diagnosis of chemical process flowsheets. *Engineering Applications of Artificial Intelligence*, 17 (5), 501-518.

McAvoy, T. J., Ye, N., (1994). Base control for the Tennessee Eastman problem. *Computers & Chemical Engineering*, 18 (5), 383-413.

McAvoy, T. J., (1999). Synthesis of plantwide control systems using optimization. *Industrial & Engineering Chemistry Research*, 38 (8), 2984-2994.

McAvoy, T.J., Arkun, Y., Chen R., Robinson, D., Schnelle, P.D., (2003). A new approach to defining a dynamic relative gain. *Control Engineering Practice*, 11 (8), 907–914.

McLellan, P. J., (1994). A differential-algebraic perspective on nonlinear controller design methodologies. *Chemical Engineering Science*, 49 (10), l663-1679.

Miranda, M., Reneaume, J.M., Meyer, X., Meyer, M., Szigeti, F., (2008). Integrating process design and control: An application of optimal control to chemical processes. *Chemical Engineering & Processing*, 47 (11), 2004-2018**.**

Mitchell, M., (1998). *An introduction to genetic algorithms.* First Edition, MIT Press, Cambridge.

Moaveni, B., Khaki-Sedigh, A., (2009). *Control Configuration Selection for Multivariable Plants.* Springer, Berlin.

Mohideen, M.J., Perkins, J.D., Pistikopoulos, E.N., (1997). Towards an efficient numerical procedure for mixed integer optimal control. *Computers & Chemical Engineering*, 21 (Supplement), S457-S462.

Monnigmann, M., Marquardt, W., (2003). Steady-state process optimization with guaranteed robust stability and feasibility. *AIChE Journal*, 49 (2), 3110–3126.

Montgomery, D. C., (2005). *Design and Analysis of Experiments*. John Wiley, New York.

Moon J., Kim S., Linninger, A.A., (2011). Embedded control for optimizing flexible dynamic process performance. *Industrial & Engineering Chemistry Research*, 50 (9), 4993–5004.

Moore, C. F., (1992). Selection of controlled and manipulated variables. In *Practical Distillation Control*. Van Nostrand Reinhold, New York.

Morari, M., Y. Arkun, Stephanopoulos G., (1980a). Studies in the synthesis of control structures for chemical processes. Part I: Formulation of the problem. Process decomposition and the classification of the control tasks. Analysis of the optimizing control structures. *AIChE Journal*, 26 (2), 220-232.

Morari, M., Stephanopoulos G., (1980b). Studies in the synthesis of control structures for chemical processes. Part II: Structural aspects and the synthesis of alternative feasible control schemes. *AIChE Journal*, 26 (2), 232-246.

Morari, M., Stephanopoulos G., (1980c). Studies in the synthesis of control structures for chemical processes. Part III: Optimal selection of secondary measurements within the framework of state estimation in the presence of persistent unknown disturbances. *AIChE Journal,* 26 (2), 247-260.

Morari, M., (1983). Design of resilient processing plants-III: A general framework for the assessment of dynamic resilience. *Chemical Engineering Science,* 38 (2), 1881-1891.

Morari, M., Zafiriou, E., (1989). *Robust Process Control*. Prentice-Hall International, Englewood Cliffs.

Nagy Z. K., Braatz, R. D., (2007). Distributional uncertainty analysis using power series and polynomial chaos expansions. *Journal of Process Control*, 18 (9), 856-864.

Nagy Z. K., Richard D. Braatz, (2010). Distributional uncertainty analysis using polynomial chaos expansions. *IEEE International Symposium on Computer-Aided Control System Design* Part of *2010 IEEE Multi-Conference on Systems and Control*, Yokohama, Japan, September 8-10, 2010, 1103-1108.

Narraway L. T., Perkins, J. D., Barton, G. W., (1991), Interaction between process design and process control: economic analysis of process dynamics, *Journal of Process Control*, 1 (5), 243–250.

Narraway, L. T., Perkins, J. D., (1993). Selection of process control structure based on linear dynamic economics. *Industrial & Engineering Chemistry Research*, 32 (11), 2681–2692.

Ng, C., (1997). *A systematic approach to the design of plant-wide control strategies for chemical processes*. PhD thesis. Department of Chemical Engineering, Massachusetts Institute of Technology.

Niederlinskh A., (1971). A heuristic approach to the design of linear multivariable interacting control systems. *Automatica*, 7 (6), 691-701.

Odjo, A. O., Sammons, N. E., Jr., Yuan, W., Marcilla, A., Eden, M. R., & Caballero, J. A., (2011). Disjunctive-genetic programming approach to synthesis of process networks. *Industrial & Engineering Chemistry Research*, 50 (10), 6213–6228.

Ogunnaike, B. A., Ray, W. H., (1994). *Process Dynamics, Modeling, and Control*. Oxford University Press, New York.

Panjwani, P., Schenk, M., Georgiadis, M. C., Pistikopoulos,E. N., (2005). Optimal design and control of a reactive distillation system. *Engineering Optimization*, 37 (7), 733–753.

Pantelides, C. C., Gritsis, D., Morison, K.R., Sargent, R.W.H., (1988a). The mathematical modelling of transient systems using differential-algebraic equations, *Computers & Chemical Engineering*, 12 (5), 449-454.

Pantelides, C. C., (1988b). The consistent initialization of differential-algebraic systems. *SIAM Journal on Scientific Computing*, 9 (2), 213-231.

Patel, J., Uygun, K., Huang, Y., (2008). A path constrained method for integration of process design and control. *Computers and Chemical Engineering*, 32 (7) 1373-1384.

Pavan Kumar, M. V., Kaistha N., (2008a). Steady-state multiplicity and its implications on the control of an ideal reactive distillation column. *Industrial & Engineering Chemistry Research*, 2008, 47 (8), 2778–2787.

Pavan Kumar, M. V., Kaistha N., (2008b). Decentralized control of a kinetically controlled ideal reactive distillation column. *Chemical Engineering Science*, 63 (1), 228-243.

Pedersen K., Jørgensen S. B., Skogestad, S., (1999). A review on process controllability. Unpublished internal paper, (Online: http://130.203.133.150/viewdoc/download;jsessionid=71E5CA8CBC76B1E981251ACEB46ED923?doi=10.1.1.40.4192&rep=rep1&type=pdf , Accessed January 2012).

Penzl, T., (2006). Algorithms for model reduction of large dynamical systems. *Linear Algebra and its Applications*, 415 (2-3), 322-343.

Perkins, j. D., Wong, M. P. F., (1985). Assessing controllability of chemical plants. *Chemical Engineering Research and Design*, 63, 358-362.

Perkins J. D., Walsh S. P. K., (1996). Optimization as a tool for design/control integration. *Computers & Chemical Engineering*, 20 (4), 315-323.

Pham, Q.T., (1994). Degrees of freedom of equipment and processes. *Chemical Engineering Science*, 49 (15), 2507-2512.

Ponton J.W., (1994). Degrees of freedom analysis in process control. *Chemical Engineering Science*, 49 (13), 2089-2095.

Ponton, J., Laing, D. M., (1993). A hierarchical approach to the design of process control systems. *Transaction of IChemE*, 71, 181-188.

Poston, T.; Stewart, I. (1996). *Catastrophe Theory and Its Applications*; Dover, London.

Prasad, V., Bequette, B.W., (2003). Nonlinear system identification and model reduction using artificial neural networks. *Computers & Chemical Engineering*, 27 (12), 1741–1754.

Price R. M., Georgakis C., (1993). Plantwide regulatory control design procedure using a tiered framework. *Industrial & Engineering Chemistry Research*, 32 (11), 2693-2705.

Price R. M., Lyman P. R., Georgakis C., (1994). Throughput manipulation in plantwide control structures. *Industrial & Engineering Chemistry Research*, 33 (5), 1197-1207.

Qin, S.J., (1998). Control performance monitoring - A review and assessment. *Computers & Chemical Engineering*, 23 (2), 178-186.

Qin, S. J., Badgwell, T. A., (2003). A survey of industrial model predictive control technology. *Control Engineering Practice*, 11 (7), 733-764.

Ramzan, N., Faheem, M., Gani, R., Witt, W., (2010). Multiple steady states detection in a packed-bed reactive distillation column using bifurcation analysis. *Computers & Chemical Engineering*, 34 (4), 460–466.

Ranzi, M., Dente, M., Goldaniga, A., Bozzano, G., Faravelli T., (2001). Lumping procedures in detailed kinetic modeling of gasification, pyrolysis, partial oxidation and combustion of hydrocarbon mixtures. *Progress in Energy and Combustion Science*, 27 (1), 99–139.

Rathinam, M., Petzold, L., (2003). A new look at proper orthogonal decomposition. *SIAM Journal on Numerical Analysis*, 41 (5), 1893 -1925.

Rawlings J. B., (2000). Tutorial overview of model predictive control. *IEEE Control Systems Magazine*, 20 (3), 38-52.

Rawlings J. B., Mayne D. Q., (2008). *Model predictive control: theory and design*. Nob Hill Publication, Madison, Wisconsin.

Rawlings, J. B., Stewart, B. T., (2008). Coordinating multiple optimization-based controllers: New opportunities and challenges. *Journal of Process Control*, 18 (9), 839-845.

Ricardez-Sandoval, L. A., Budman, H. M., Douglas, P. L., (2008). Simultaneous design and control of processes under uncertainty: A robust modelling approach. *Journal of Process Control*, 18 (7-8), 735-752.

Ricardez-Sandoval, L. A., Budman, H. M., Douglas, P. L., (2009a). Integration of design and control for chemical processes: A review of the literature and some recent results *Annual Reviews in Control*, 33 (2), 158–171.

Ricardez-Sandoval, L. A., Budman H. M., Douglas P. L., (2009b). Simultaneous design and control of chemical processes with application to the Tennessee Eastman process. *Journal of Process Control*, 19 (8), 1377–1391.

Ricardez-Sandoval, L.A., Douglas, P.L., Budman, H.M., (2011). A methodology for the simultaneous design and control of large-scale systems under process parameter uncertainty. *Computers & Chemical Engineering*, 35 (2), 307–318.

Richalet, J., Rault, A., Testud, J. L., Papon, J., (1978). Model predictive heuristic control: Applications to industrial processes. *Automatica*, 14 (5), 413-428.

Ricker, N. L. (1996). Decentralized control of the Tennessee Eastman challenge process. *Journal of Process Control*, 6 (4), 205-221.

Roberts, P. D., (1979). An algorithm for steady-state system optimization and parameter estimation. *International Journal of Systems Science*, 10 (7), 719–734.

Rojas, O.J., Setiawan, R., Bao J., Lee, P.L., (2009). Dynamic operability analysis of nonlinear process networks based on dissipativity. *AIChE Journal*, 55 (4), 963–982.

Rosenbrock, H. H., (1970). *State-space and Multivariable Theory*. Nelson, London.

Ross R., Perkins, J. D., Pistikopoulos, E. N., Koot, G.L.M., van Schijndel, J.M.G., (2001). Optimal design and control of a high-purity industrial distillation system. *Computers & Chemical Engineering*, 25 (1), 141–150.

Russell, L.W., Perkins, J.D., (1987). Towards a method for diagnosis of controllability and operability problems in chemical-plants. *Chemical Engineering Research and Design*, 65 (6), 453-461.

Sahinidis, N. V., (1996). BARON: A general purpose global optimization software package. *Journal of Global Optimization*, 8 (2), 201–205.

Sahinidis, N., V., (2004). Optimization under uncertainty: state-of-the-art and opportunities. *Computers and Chemical Engineering*, 28 (6-7), 971–983.

Sakizlis, V., Perkins, J.D., Pistikopoulos E.N., (2003). Parametric controllers in simultaneous process and design optimization. *Industrial & Engineering Chemistry Research*, 42 (20), 4545–4563.

Sakizlis V., Perkins J. D., Pistikopoulos, E. N., (2004). Recent advances in optimization-based simultaneous process and control design. *Computers & Chemical Engineering*, 28 (10), 2069–2086.

Sakizlis V., Vakamudi K., Coward A. , Mermans I., (2010). Advanced process control in the plant engineering and construction phases. *Hydrocarbon Processing*, October 2010, 89 (10), 49-56.

Samsatli, N. J., Papageorgiou, L. G., Shah, N., (1998). Robustness metrics for dynamic optimization models under parameter uncertainty. *AIChE Journal*, 44(9), 1993-2006.

Seferlis P., Georgiadis M. C., (2004). *The Integration of Process Design and Control*, Elsevier Science, Amsterdam.

Seider, W.D., Seader, J.D., Lewin, D.R, Widagdo, S., (2010). *Product and Process Design Principles: Synthesis, Analysis and Design*, 3rd Edition, John Wiley & Sons, NJ.

Schweiger, C. A., Floudas, C. A., (1997). Interaction of design and control: Optimization with dynamic models. In *Optimal Control: Theory, Algorithms, and Applications*. Hager, W. W., Pardalos, P. M., Eds.; Kluwer Academic Publishers: Norwell, MA, 388-435.

Sharif, M., Shah, N., Pantelides, C.C., (1998). On the design of multicomponent batch distillation columns. *Computers and Chemical Engineering*, 22, S69-S76.

Sharifzadeh, M., Rashtchian, D., Pishvaie, M. R., Thornhill, N. F., (2011). Energy induced separation network synthesis of an olefin compression section: A case study. *Industrial & Engineering Chemistry Research*, 50 (3), 1610–1623.

Sharifzadeh, M., Thornhill, N.F., (2011). Optimal controlled variable selection using a nonlinear simulation-optimization framework. *21st European Symposium on Computer Aided Process Engineering, May 21- June 1, Porto Carras, Greece*. Book series: *Computer-Aided Chemical Engineering*, 29, 597-601.

Sharifzadeh, M., Thornhill, N.F., (2012). Optimal selection of control structures using a steady-state inversely controlled process model. *Computers & Chemical*

Engineering, 38, 126–138.

Sharma, N., Singh K., (2010), Control of reactive distillation column: A review. *International Journal of Chemical Reactor Engineering*, 8 (R5), 1-55.

Silva-Beard A., Flores-Tlacuahuac, A., (1999). Effect of Process Design/Operation on the Steady-State Operability of a Methyl Methacrylate Polymerization Reactor. *Industrial & Engineering Chemistry Research*, 4790–4804.

Singh, S. N., (1982a). Functional reproducibility of multivariable nonlinear systems. *IEEE Transactions on Automatic Control*, AC-27, 270-272.

Singh, S. N., (1982b). Reproducibility in nonlinear systems using dynamic compensation and output feedback. *IEEE Transactions on Automatic Control*, Control AC-27, 955-958.

Singh, S. N., (1982c). Generalized functional reproducibility condition for nonlinear systems. *IEEE Transactions on Automatic Control*, AC-27, 958-960.

Skogestad, S., Morari, M., (1987). Effect of disturbance directions on closed-loop performance. *Industrial & Engineering Chemistry Research*, 26 (10), 2029-2035.

Skogestad, S., Morari, M., (1988). Understanding the dynamic behavior of distillation columns. *Industrial & Engineering Chemistry Research*, 27(10), 1848-1862.

Skogestad, S., (2000a). Plantwide control: the search for the self-optimizing control structure. *Journal of Process Control*, 10 (5), 487-507.

Skogestad, S., (2000b). Self-optimizing control: the missing link between steady-state optimization and control. *Computers & Chemical Engineering*, 24 (2-7), 569-575.

Skogestad, S., (2004a). Control structure design for complete chemical plants. *Computers & Chemical Engineering*, 28 (1-2), 219-234.

Skogestad, S. (2004b). Near-optimal operation by self-optimizing control: from process control to marathon running and business systems. *Computers & Chemical Engineering*, 29 (1), 127-137.

Skogestad, S., Postlethwaite, I., (2005). *Multivariable Feedback Control: Analysis and Design*. Second Edition, John Wiley, Chichester.

Skogestad, S. (2007). The dos and don'ts of distillation column control. *Chemical Engineering Research and Design*, 85 (1), 13-23.

Skogestad, S. (2009). Feedback: still the simplest and best solution. *Modeling, Identification and Control*, 30 (3), 149-155.

Slotine, J. E., Li, W., (1991). *Applied Nonlinear Control.* Prentice-Hall, Englewood Cliffs.

Sneesby, M.G., Tade, M.O., Smith, T.N., (1999). Two-point control of a reactive distillation column for composition and conversion. *Journal of Process Control*, 9 (1), 19–31.

Sneesby, M.G., Tade, M.O., Smith, T.N., (2000). A multi-objective control scheme for an ETBE reactive distillation column. *Chemical Engineering Research and Design*, 78 (A2), 283-292.

Solution (121621). Call to DMS_IPOFF3() needs to be changed in Aspen Plus 2006 and higher. Aspen Technology, (Online: http://support.aspentech.com/ , accessed March 2012, a secured website).

Srinivasan, B., Primus, C. J., Bonvin, D., Ricker, N. L., (2001). Run-to-run optimization via constraint control. *Control Engineering Practice*, 9 (8), 911–919.

Srinivasan, B., Bonvin, D., (2002). Interplay between identification and optimization in run-to-run optimization schemes. In Proceeding of *American Control Conference (ACC).* Anchorage, USA, May8-10, 2174–2179.

Stephanopoulos, G., (2003). *Chemical Process Control: An Introduction to Theory and Practice*. Prentice-Hall, London.

Stephanopoulos, G., Ng, C., (2000). Perspectives on the synthesis of plant-wide control structures. *Journal of Process Control*, 10 (2-3), 97-111.

Subramanian, S., Georgakis, C., (2001). Steady-state operability characteristics of idealized reactors. *Chemical Engineering Science*, 56 (17), 5111–5130.

Swaney, E., Grossmann I. E., (1985). An index for operation flexibility in chemical process design. 1. Formulation and theory. *AIChE Journal*, 31 (4), 621–630.

Tatjewski, P., (2002). Iterative optimizing set-point control—The basic principle redesigned. In *Proceedings 15th World Congress of IFAC*, Volume 15 (Part 1), Barcelona, July 2002.

Tawarmalani M., Sahinidis N.V., (2004). Global optimization of mixed-integer nonlinear programms: a theoretical and practical study. *Mathematical Programming*, 99, 563–591.

Terrazas-Moreno, S., Flores-Tlacuahuac A., Grossmann, I. E., (2008). Simultaneous design, scheduling, and optimal control of a methyl-methacrylate continuous polymerization reactor. *AIChE Journal*, 54, (12) 3160–3170.

Thambirajah J., Benabbas L., Bauer M., Thornhill N. F., (2009). Cause-and-effect analysis in chemical processes utilizing XML, plant connectivity and quantitative process history. *Computers & Chemical Engineering*, 33 (2), 503-512.

Tian,Y., Zhao, F., Bisowarno, B.H., Tade, M.O., (2003). Pattern-based predictive control for ETBE reactive distillation. *Journal of Process Control*, 13 (1), 57–67.

Tyreus, B. D., Luyben, W. L., (1993). Dynamics and control of recycle systems. 4. Ternary systems with one or two recycle streams. *Industrial & Engineering Chemistry Research*, 32 (6), 1154-1162.

Ulrich G. D., Vasudevan P. T., (2006). How to estimate utility costs. *Chemical Engineering*, April, 2006, 66-69.

Umara, L. M., Hub, W., Cao, Y., Kariwala, V., (2012). Selection of controlled variables using self-optimizing control method. In *Plantwide Control: Recent Developments and Applications*. First Edition. Edited by Rangaiah, G.P., Kariwala, V., John Wiley, Chichester, 43-71.

Uztürk, D., Georgakis, C., (2002). Inherent dynamic operability of processes: general definitions and analysis of siso cases. *Industrial & Engineering Chemistry Research*, 41 (3), 421–432.

Vasudevan S., Konda, N.V.S.N. M., Rangaiah, G.P., (2008). Control degrees of freedom using the restraining number: further evaluation. *Asia-Pacific Journal of Chemical Engineering*, 3 638–647.

Vinson, D. R., Georgakis, C., (2000). A new measure of process output controllability. *Journal of Process Control*, 10 (2-3), 185-194.

Viswanathan, J., Grossmann, I. E., (1990). A combined penalty function and outer-approximation method for MINLP optimization. *Computers and Chemical Engineering*, 14 (7), 769-782.

Ward, J. D., Doherty, M. F., Yu, C.-C., (2007). Plantwide operation and control of processes with crystallization. *AIChE Journal*, 53 (11), 2885–2896.

Ward J. D., Yu C.-C., Doherty M. F., (2010). Plantwide dynamics and control of processes with crystallization. *Computers & Chemical Engineering*, 34 (1), 112–121.

Wongrat, W., Younes, A., (2011). Control vector optimization and genetic algorithms for mixed-integer dynamic optimization in the synthesis of rice drying processes. *Journal of the Franklin Institute*, 348 (7), 1318–1338.

Ydstie, B. E., (2010). *Process Control: The Passive Systems Approach* Review of, by Bao, J., Lee, P. L., *IEEE Control Systems Magazine*, Feb. 2010, 78-80.

Yim, S.Y., Ananthakumar, H.G., Benabbas, L., Horch A., Drath R., Thornhill, N. F., (2006). Using process topology in plant-wide control loop performance assessment. *Computers & Chemical Engineering*, 31 (2), 86-99.

Yuan, Z., Chen, B., Zhao, J., (2011). An overview on controllability analysis of chemical processes. *AIChE Journal*, 57 (5), 1185–1201.

Yuan, Z., Chen, B., Sin, G., Gani, R., (2012). State-of-the-art and progress in the optimization-based simultaneous design and control for chemical processes. *AIChE Journal*, 58, (6) 1640–1659.

Ziegler, J.G., Nichols, N. B., Rochester, N. Y., (1942). Optimum settings for automatic controllers. *Transactions of ASME*, 64, 759-768.

Appendix A. Fortran code (used in Chapter 5)

The original Fortran code was adapted from Luyben and Yu, (2008). In the following, blue highlights are the new codes added by the author and yellow highlights are the old codes removed in order to update the old FORTRAN code according to Solution (121621) by Aspen Technology.

New code:

```
    SUBROUTINE RAETBELB (NSTAGE, NCOMP,   NR,     NRL,     NRV,
                   T,      TLIQ,    TVAP,   P,       VF,
                   F,      X,       Y,      IDX,     NBOPST,
                   KDIAG,  STOIC,   IHLBAS, HLDLIQ,  TIMLIQ,
                   IHVBAS, HLDVAP,  TIMVAP, NINT,    INT,
                   NREAL,  REAL,    RATES,  RATEL,   RATEV,
                   NINTB,  INTB,    NREALB, REALB,   NIWORK,
                   IWORK,  NWORK,   WORK)
    IMPLICIT NONE
    INTEGER NCOMP,  NR,      NRL,     NRV,    NINT,
         NINTB,  NREALB,  NIWORK,  NWORK,  N_COMP
    INTEGER K_ETOH, K_IC4,   K_NC4,   K_ETBE
    PARAMETER (K_ETOH=1)
    PARAMETER (K_IC4=2)
    PARAMETER (K_NC4=3)
    PARAMETER (K_ETBE=4)
    PARAMETER (N_COMP=4)
    INTEGER IDX(NCOMP),  NBOPST(6),      INT(NINT),
         INTB(NINTB),  IWORK(NIWORK),  NSTAGE,
         KDIAG,      IHLBAS,      IHVBAS,     NREAL,  KPHI,
         KER,        L_GAMMA,       J
    REAL*8 X(NCOMP,3),      Y(NCOMP),
        STOIC(NCOMP,NR),  RATES(NCOMP),
        RATEL(NRL),       RATEV(NRV),
        REALB(NREALB),    WORK(NWORK),   B(1),   T,
        TLIQ,            TVAP,          P,      VF,   F
    REAL*8 HLDLIQ,    TIMLIQ,    HLDVAP,    TIMVAP,    TZERO,
        FT
    REAL*8 DLOG
    INTEGER IMISS, IDBG
    REAL*8 REAL(NREAL), RMISS, C1, C2, C3,
        C4,   C5,   C6,     DKA,    DKR,
        Q,    RATE, RATNET,  KETBE,  KA,  KRATE
        REAL*8 PHI(N_COMP)
        REAL*8 DPHI(N_COMP)
        REAL*8 ACTIV(N_COMP)
#include "ppexec_user.cmn"
    EQUIVALENCE (RMISS, USER_RUMISS)
    EQUIVALENCE (IMISS, USER_IUMISS)
```

```
#include "dms_maxwrt.cmn"
#include "dms_lclist.cmn"
      INTEGER DMS_ALIPOFF3
#include "dms_plex.cmn"
      EQUIVALENCE(B(1),IB(1))
      DATA IDBG/0/
 9010 FORMAT(1X,3(G13.6,1X))
 9000 FORMAT('fugly failed at T=',G12.5,'P=',G12.5,'ker=',I4)
 9020 FORMAT('compo',I3,'mole-frac',G12.5,'activity=',G12.5)
 9030 FORMAT('stage=',I4,'spec-rate=',G12.5,'net-rate=',G12.5)
C
C     BEGIN EXECUTABLE CODE
      KETBE=DEXP(10.387D0+4060.59D0/T-2.89055D0*DLOG(T)-0.0191544D0*T+
     5.28586D-5*T**2-5.32977D-8*T**3)
      KA=DEXP(-1.0707D0+1323.1D0/T)
      KRATE=(2.0606D12*DEXP(-60.4D3/8.314D0/T))
      IF(IDBG.GE.1)THEN
       WRITE(MAXWRT_MAXBUF(1),9010) FT,DKA,DKR
       CALL DMS_WRTTRM(1)
      ENDIF
      KPHI=1
C     fugacity coefficient of components in the mixture
      CALL PPMON_FUGLY(T,P,X(1,1)
     , Y, NCOMP, IDX, NBOPST, KDIAG, KPHI, PHI, DPHI, KER)
      IF(KER.NE.0)THEN
       WRITE(MAXWRT_MAXBUF(1),9000) T,P,KER
       CALL DMS_WRTTRM(1)
      ENDIF
C     NEW
      L_GAMMA=DMS_ALIPOFF3(24)
      DO J=1,NCOMP
       ACTIV(J)=dexp(B(L_GAMMA+LCLIST_LBLCLIST+J))*X(J,1)
      END DO
      IF(IDBG.GE.1)THEN
       DO J=1,NCOMP
        WRITE(MAXWRT_MAXBUF(1),9020) J,X(J,1),ACTIV(J)
        CALL DMS_WRTTRM(1)
       END DO
      ENDIF
      RATE=REALB(1)*KRATE*(ACTIV(K_ETOH))**2.d0*
     (ACTIV(K_IC4)-ACTIV(K_ETBE)/KETBE/ACTIV(K_ETOH))
      RATE=(RATE/(1.D0+KA*ACTIV(K_ETOH))**3.d0)/1.d3
      RATES(K_IC4)=-RATE
      RATES(K_ETOH)=-RATE
      RATES(K_ETBE)=RATE
      RATES(K_NC4)=0.D+00
      IF (IDBG.GE.1)THEN
        WRITE(MAXWRT_MAXBUF(1),9030) NSTAGE,RATE,RATNET
        CALL DMS_WRTTRM(1)
```

```
    ENDIF
    RETURN
#undef P_MAX3
    END
```

Outdated Fortran code by Luyben and Yu (2008):

```
    SUBROUTINE RAETBELB (NSTAGE, NCOMP,  NR,    NRL,    NRV,
                    T,     TLIQ,   TVAP,  P,      VF,
                    F,     X,      Y,     IDX,    NBOPST,
                    KDIAG,  STOIC,  IHLBAS, HLDLIQ,  TIMLIQ,
                    IHVBAS, HLDVAP,  TIMVAP, NINT,    INT,
                    NREAL,  REAL,    RATES,  RATEL,   RATEV,
                    NINTB,  INTB,    NREALB, REALB,   NIWORK,
                    IWORK,  NWORK,   WORK)
    IMPLICIT NONE
    INTEGER NCOMP,  NR,     NRL,    NRV,    NINT,
           NINTB,  NREALB,  NIWORK,  NWORK,  N_COMP
    INTEGER K_ETOH, K_IC4,   K_NC4,   K_ETBE
    PARAMETER (K_ETOH=1)
    PARAMETER (K_IC4=2)
    PARAMETER (K_NC4=3)
    PARAMETER (K_ETBE=4)
    PARAMETER (N_COMP=4)
    INTEGER IDX(NCOMP),   NBOPST(6),     INT(NINT),
           INTB(NINTB),  IWORK(NIWORK),  NSTAGE,
           KDIAG,       IHLBAS,       IHVBAS,    NREAL,  KPHI,
           KER,         L_GAMMA,       J
    REAL*8 X(NCOMP,3),      Y(NCOMP),
          STOIC(NCOMP,NR),  RATES(NCOMP),
          RATEL(NRL),       RATEV(NRV),
          REALB(NREALB),    WORK(NWORK),   B(1),   T,
          TLIQ,            TVAP,         P,     VF,   F
    REAL*8 HLDLIQ,   TIMLIQ,   HLDVAP,   TIMVAP,   TZERO,
          FT
    REAL*8 DLOG
    INTEGER IMISS, IDBG
    REAL*8 REAL(NREAL), RMISS, C1, C2, C3,
          C4,   C5,   C6,     DKA,    DKR,
          Q,    RATE, RATNET,  KETBE,  KA,  KRATE
       REAL*8 PHI(N_COMP)
       REAL*8 DPHI(N_COMP)
       REAL*8 ACTIV(N_COMP)
#include "ppexec_user.cmn"
    EQUIVALENCE (RMISS, USER_RUMISS)
    EQUIVALENCE (IMISS, USER_IUMISS)
#include "dms_maxwrt.cmn"
#include "dms_ipoff3.cmn"
#include "dms_plex.cmn"
    EQUIVALENCE (B(1),IB(1))
```

```
      DATA IDBG/0/
 9010 FORMAT(1X,3(G13.6,1X))
 9000 FORMAT('fugly failed at T=',G12.5,'P=',G12.5,'ker=',I4)
 9020 FORMAT('compo',I3,'mole-frac',G12.5,'activity=',G12.5)
 9030 FORMAT('stage=',I4,'spec-rate=',G12.5,'net-rate=',G12.5)
C
C    BEGIN EXECUTABLE CODE
      KETBE=DEXP(10.387D0+4060.59D0/T-2.89055D0*DLOG(T)-0.0191544D0*T+
         5.28586D-5*T**2-5.32977D-8*T**3)
      KA=DEXP(-1.0707D0+1323.1D0/T)
      KRATE=(2.0606D12*DEXP(-60.4D3/8.314D0/T))
      IF(IDBG.GE.1)THEN
       WRITE(MAXWRT_MAXBUF(1),9010) FT,DKA,DKR
       CALL DMS_WRTTRM(1)
      ENDIF
      KPHI=1
C    fugacity coefficient of components in the mixture
      CALL PPMON_FUGLY(T,P,X(1,1)
          , Y, NCOMP, IDX, NBOPST, KDIAG, KPHI, PHI, DPHI, KER)
      IF(KER.NE.0)THEN
       WRITE(MAXWRT_MAXBUF(1),9000) T,P,KER
       CALL DMS_WRTTRM(1)
      ENDIF
      L_GAMMA=IPOFF3_IPOFF3(24)
      DO J=1,NCOMP
       ACTIV(J)=DEXP(B(L_GAMMA+J))*X(J,1)
      END DO
      IF(IDBG.GE.1)THEN
       DO J=1,NCOMP
        WRITE(MAXWRT_MAXBUF(1),9020) J,X(J,1),ACTIV(J)
        CALL DMS_WRTTRM(1)
       END DO
      ENDIF
      RATE=REALB(1)*KRATE*(ACTIV(K_ETOH))**2.d0*
           (ACTIV(K_IC4)-ACTIV(K_ETBE)/KETBE/ACTIV(K_ETOH))
      RATE=(RATE/(1.D0+KA*ACTIV(K_ETOH))**3.d0)/1.d3
      RATES(K_IC4)=-RATE
      RATES(K_ETOH)=-RATE
      RATES(K_ETBE)=RATE
      RATES(K_NC4)=0.D+00
      IF (IDBG.GE.1)THEN
        WRITE(MAXWRT_MAXBUF(1),9030) NSTAGE,RATE,RATNET
        CALL DMS_WRTTRM(1)
      ENDIF
      RETURN
#undef P_MAX3
      END
```